

**PHYTOCHEMICAL AND BIOLOGICAL ACTIVITIES OF *PLECTRANTHUS  
MADAGASCARIENSIS***

**by**

**Kadidiatou Ndjoubi Ossamy**

**Thesis submitted in fulfilment of the requirements for the degree**

**Master of Applied Science: Chemistry**

**in the Faculty of Applied Science**

**at the Cape Peninsula University of Technology**

**Supervisor:** Prof Ahmed Mohammed

**Bellville Campus**

Date submitted: December 2019

**CPUT copyright information**

The dissertation/thesis may not be published either in part (in scholarly, scientific or technical journals), or as a whole (as a monograph), unless permission has been obtained from the University

## **DECLARATION**

I, Kadidiatou Ndjoubi Ossamy, declare that the contents of this dissertation/thesis represent my own unaided work, and that the dissertation/thesis has not previously been submitted for academic examination towards any qualification. Furthermore, it represents my own opinions and not necessarily those of the Cape Peninsula University of Technology.

---

**Signed**

**Date**

## ABSTRACT

Tuberculosis is the leading cause of mortality and morbidity in South Africa due to its association with several chronic illnesses such as psoriasis, diabetes mellitus, and HIV. These chronic diseases weaken the patients resulting in a high risk of progressing from latent to active tuberculosis. Because of side effects associated with synthetic drugs, the attention of the scientific community has shifted to natural products for their use as therapeutic agents to develop effective modern medicines with less adverse effects for treating infectious as well as chronic diseases. Less than 10% of medicinal plant species have been thoroughly investigated and therefore this project focused on exploring one such under-studied medicinal plant namely *Plectranthus madagascariensis*. Phytochemical investigation of *P. madagascariensis* have led to the isolation of five royleanones abietanes and a mixture of two abietane dimers. The five royleanones were identified as; 6 $\beta$ ,7 $\alpha$ -dihydroxyroyleanone (I), 7 $\alpha$ -acetoxy-6 $\beta$ -hydroxyroyleanone (II), horminone (III) and coleon U quinone (IV) and carnosolon (V) and the two the dimers as; grandidone A and 7-epimer grandidone A (VI & VII). All compounds were evaluated for their antitubercular, antidiabetic, antioxidant and cytotoxic activities. Compounds I-IV showed activity against the mycobacterial strain H<sub>37</sub>Rv in 7H9/CAS/Glu/Tx medium only except for compound II which showed activity in both 7H9/CAS/Glu/Tx and 7H9/ADC/Glu/Tw medium. Compound I, II, IV, and VI & VII displayed inhibitory effects against the intestinal enzyme  $\alpha$ -glucosidase with the mixture of VI & VII giving the most promising result as an IC<sub>50</sub> value twenty-one times lower than the positive control acarbose. All compounds exhibited cytotoxic effects against HacaT cell line with compound V being the most toxic. Furthermore, the compounds have antioxidant activity through single electron transfer and/or hydrogen atom transfer.

## ACKNOWLEDGEMENTS

**I wish to thank:**

- First and foremost, I would like to thank the Almighty God for being healthy and alive, without which I would not have been able to finish this research project.
- Secondly, I would like to thank my supervisor Professor Ahmed Mohammed. The guidance, constant encouragement, and support he gave me are priceless.
- I would also like to thank Dr. Badmus (Oxidative Stress Research Center, Cape Peninsula University of Technology) and Dr. Digby (Molecular Mycobacteriology Research Unit, Division of Medical Microbiology, University of Cape Town) for their input and technical assistance in the research project bioassays.
- I would like to extend my gratitude to Dr. Rajan Sharma for his advice, assistance, and availability throughout my studies.
- I would like to thank all my colleagues for their encouragement and intellectual support
- Finally, I would like to extend my heartfelt gratitude to my family and my friends for their incredible support, encouragements and prayers during these years of research.
- The financial assistance of the National Research Foundation towards this research is acknowledged. Opinions expressed in this thesis, and the conclusions arrived at are those of the author and are not necessarily to be attributed to the National Research Foundation.

**DEDICATION**

I dedicate this thesis to my parents. They have been the strength and the driving force that helped me to never give up through the challenges I have faced during my research studies. Their words of wisdom and encouragement were true motivation and inspiration to me. Thank you for believing in me and teaching me that success comes with hardships and challenges.

## TABLE OF CONTENTS

Declaration	ii
Abstract	iii
Acknowledgements	iv
Dedication	v
Glossary	xiii

### CHAPTER ONE: INTRODUCTION

1.1	General introduction	1
1.1.1	Tuberculosis	2
1.1.2	Diabetes	5
1.1.3	Psoriasis	6
1.2	The impact of medicinal plants in drug discovery	8
1.3	Justification of the study	9
1.4	Problem statement	10
1.5	Research questions	10
1.6	Aim of the research	11
1.7	Objectives of the research study	11
1.8	Hypotheses	11
1.9	Delimitations	11
1.10	Thesis outlines	11

### CHAPTER TWO: DITERPENES

2.1	Introduction	13
2.2	Biosynthesis of diterpenes	13
2.2.1	Biosynthesis of IPP and DMAPP	13
2.2.1.1	Mevalonate pathways	14
2.2.1.2	Methylerythritol phosphate pathway (MEP)	14
2.2.2	Biosynthesis of GGPP	15
2.2.3	Biosynthesis of monocyclic, bicyclic, tricyclic, and tetracyclic diterpenes	16
2.2.3.1	Biosynthesis of monocyclic diterpenes	16
2.2.3.2	Biosynthesis of bicyclic diterpenes	16
2.2.3.3	Biosynthesis of tricyclic diterpenes	17
2.2.3.4	Biosynthesis Tetracyclic diterpenes	18
2.3	Classification, characterization, and nomenclature of the abietane diterpenoids	19

### CHAPTER THREE: LITERATURE REVIEW

3.1	Introduction	21
3.2	<i>Plectranthus</i> genus	21
3.3	Botanical identification	22
3.3.1	General description	22
3.3.2	<i>Plectranthus madagascariensis</i>	23
3.4	Phytochemistry	23

3.4.1	Abietane diterpenoids isolated from Southern African <i>Plectranthus</i> species	23
3.4.2	Labdane diterpenoids isolated from Southern Africa <i>Plectranthus</i> species	31
3.4.3	Kaurane diterpenoids isolated from Southern Africa <i>Plectranthus</i> species	34
3.4.4	Clerodanes and halimane isolated from Southern Africa <i>Plectranthus</i> species	36
3.4.5	Pimaranes and beyranes isolated from Southern Africa <i>Plectranthus</i> species	37
3.4.6	Essential oils	38
3.5	Ethnobotanical uses of Southern African <i>Plectranthus</i> species	39
3.6	Ethnopharmacological and pharmacological uses of Southern African <i>Plectranthus</i> species	41
3.6.1	<i>Plectranthus amboinicus</i>	41
3.6.2	<i>Plectranthus barbatus</i>	42
3.6.3	<i>Plectranthus caninus</i>	42
3.6.4	<i>Plectranthus ecklonii</i>	42
3.6.5	<i>Plectranthus elegans</i>	43
3.6.6	<i>Plectranthus Ernstii</i>	43
3.6.7	<i>Plectranthus esculents</i>	43
3.6.8	<i>Plectranthus fruticosus</i>	43
3.6.9	<i>Plectranthus grandidentatus</i>	43
3.6.10	<i>Plectranthus hadiensis</i>	44
3.6.11	<i>Plectranthus hereroensis</i>	44
3.6.12	<i>Plectranthus laxiflorus</i>	44
3.6.13	<i>Plectranthus madagascariensis</i>	45
3.6.14	<i>Plectranthus Ornatus</i>	45
3.6.15	<i>Plectranthus porcatus</i>	45
3.6.16	<i>Plectranthus Saccatus</i>	45
3.6.17	<i>Plectranthus strigosus</i>	45
3.7	Other uses	46

## CHAPTER FOUR: EXTRACTION, ISOLATION AND CHARACTERISATION OF *PLECTRANTHUS MADAGASCARIENSIS* NATURAL PRODUCTS

4.1	Introduction	47
4.2	Materials and Methods	47
4.2.1	General Reagents	47
4.2.2	Chromatographic methods	48
4.2.2.1	Thin-layer chromatography (TLC)	48
4.2.2.2	Preparation of the spray reagent	48
4.2.2.3	Preparative thin-layer chromatography (prep-TLC)	49
4.2.2.4	Column chromatography	49
4.2.2.5	Semi-preparative high-performance liquid chromatography (semi-prep HPLC)	49
4.2.3	Spectroscopic methods	49
4.2.3.1	Nuclear Magnetic Resonance Spectroscopy (NMR)	49
4.2.3.2	Single crystal X-ray analysis	49
4.2.3.3	Fourier Transform Infrared Spectroscopy (FTIR)	50
4.2.3.4	Optical rotation measurements	50
4.2.3.5	Melting point	50
4.2.3.6	Ultraviolet (UV) Spectroscopy	50
4.3	Sample collection	50
4.4	Extraction of plant sample	50

4.5	Isolation of <i>P. madagascariensis</i> constituents	51
4.5.1	Column chromatography of the crude extract	51
4.5.2	Isolation of <i>P. madagascariensis</i> secondary metabolites	53
4.5.2.1	Processing of fraction K4-3-VIII and isolation of compound I	53
4.5.2.2	Processing of fraction K4-3- VI and isolation of compound II as well as the Compound VI &VII	54
4.5.2.3	Processing of fraction K4-3-III & IV and isolation of compound III	54
4.5.2.4	Processing of fraction K4-3-XI and Isolation of compound IV	55
4.5.2.5	Processing of fraction K4-3-XIII & XIV and isolation of compound V	56
4.6	Results and discussions	56
4.6.1	Compound I (6 $\beta$ ,7 $\alpha$ -dihydroxyroyleanone)	59
4.6.2	Compound II (7 $\alpha$ -acetoxy-6 $\beta$ -hydroxyroyleanone)	61
4.6.3	Compound III (horminone)	64
4.6.4	Compound IV (coleon U quinone)	66
4.6.5	Compound V (carnosolon)	68
4.6.6	Compounds VI (grandidone A) and VII (7-epimer grandidone A)	70
4.7	Spectroscopic data of the isolated compounds	74
4.8	Conclusion	75

## CHAPTER FIVE: BIOLOGICAL EVALUATION

5.1	Introduction	77
5.2	Chemicals	77
5.3	Antimycobacterial assay	78
5.3.1	Cells culture	78
5.3.2	Experimental procedure	79
5.3.3	Data analysis	79
5.3.4	Results and discussions	79
5.4	In vitro $\alpha$ -glucosidase assay	80
5.4.1	Phosphate buffer	81
5.4.2	Experimental procedure	81
5.4.3	Data analysis	81
5.4.4	Results and discussions	83
5.5	In vitro Cytotoxicity Assay	83
5.5.1	Cells Culture	83
5.5.2	Experimental procedure	83
5.5.3	Data analysis	84
5.5.4	Results and discussions	84
5.6	Antioxidant assay	86
5.6.1	FRAP assay	86
5.6.2	ORAC assay	86
5.6.3	TEAC assay	87
5.6.4	Results and discussions	87
5.7	Conclusion	88

## CHAPTER SIX: CONCLUSION AND RECOMMENDATION

6.1	Conclusions	89
6.2	Recommendations	90

<b>REFERENCES</b>	<b>91</b>
-------------------	-----------



## LIST OF FIGURES

(these are numbered according to the chapter in which they appear)

<b>Figure 1.1:</b> Estimated TB incidence in 2017, for countries with at least 100 000 incident cases	2
<b>Figure 1.2:</b> The lists for TB, TB/HIV, and MDR-TB high burden countries from 2016-2020 and their areas of overlap	4
<b>Figure 1.3:</b> Immunopathogenesis of psoriasis	7
<b>Figure 2.1:</b> Biosynthesis of IPP and DMAPP via the mevalonate pathway	14
<b>Figure 2.2:</b> Biosynthesis of IPP and DMAPP via the methylerythritol phosphate pathway	15
<b>Figure 2.3:</b> Biosynthesis of GGPP	16
<b>Figure 2.2:</b> Formation of monocyclic type diterpenes from GGPP	16
<b>Figure 2.5:</b> Formation of copalyl diphosphate stereoisomers (bicyclic diterpenes) from GGPP	17
<b>Figure 2.6:</b> Biosynthesis pathway of abietic acid	18
<b>Figure 2.7:</b> Biosynthesis pathways of <i>ent</i> -kaurane	19
<b>Figure 2.8:</b> Biosynthesis of beyerene	19
<b>Figure 2.9:</b> Numbering system of abietane diterpenes	20
<b>Figure 2.10:</b> Illustration of the uses of the terms “nor”, “abeo” and “seco”	21
<b>Figure 3.1:</b> Leaves of <i>P. argentatus</i> (A), <i>P. oertendali</i> (B) and <i>P. madagascariensis</i> (C)	22
<b>Figure 3.2:</b> Structures of compounds 7-18	24
<b>Figure 3.3:</b> Structures of compounds 19-30	25
<b>Figure 3.4:</b> Structures of compounds 31-35	26
<b>Figure 3.5:</b> Structures of compounds 36-43	27
<b>Figure 3.6:</b> Structures of compounds 44-51	28
<b>Figure 3.7:</b> Structures of compounds 52-58	29
<b>Figure 3.8:</b> Structures of compounds 59-63	30
<b>Figure 3.9:</b> Structures of compounds 64 and 65	31
<b>Figure 3.10:</b> Structures of compounds 66 and 67	31
<b>Figure 3.11:</b> Structures of compounds 68-99	33
<b>Figure 3.12:</b> Structures of compounds 100-120	35
<b>Figure 3.13:</b> Structures of compounds 121-127	36
<b>Figure 3.14:</b> Structures of compounds 128-136	37
<b>Figure 3.15:</b> Structures of compounds 137 and 138	38
<b>Figure 3.16:</b> Structures of compounds 139-141	38
<b>Figure 4.1:</b> TLC profile of K4-3-I to K4-3-IX fractions using solvent system B as mobile phase	52
<b>Figure 4.2:</b> TLC profile of K4-3-IX to K4-3-XVI fractions using solvent system B as mobile phase	52
<b>Figure 4.3:</b> TLC profile of K4-3-IX to K4-3-XVI fractions using solvent system E as mobile phase	53
<b>Figure 4.4:</b> TLC profile of compound I	53
<b>Figure 4.5:</b> TLC profile of subfraction K4-5, compound II and the mixture VI & VII	54
<b>Figure 4.6:</b> TLC profiles of subfraction K4-19 and compound III	55
<b>Figure 4.7:</b> semi-Prep HPLC profile of subfraction K4-55-1	55
<b>Figure 4.8:</b> TLC profile of subfractions K4-13-3, K4-9-2, and compound V	56
<b>Figure 4.9:</b> 3D structure of compound I (protons were omitted for clarity, generated by CHEM-DRAW (version 12))	59
<b>Figure 4.10:</b> <sup>1</sup> H NMR spectrum of 6β,7α-dihydroxyroyleanone (I)	59
<b>Figure 4.11:</b> <sup>13</sup> C NMR spectrum of 6β-7α-dihydroxyroyleanone (I)	60
<b>Figure 4.12:</b> DEPT-135 NMR spectrum of 6β-7α-dihydroxyroyleanone (I)	60
<b>Figure 4.13:</b> <sup>1</sup> H NMR spectrum of the 7α-acetoxy-6β-hydroxyroyleanone (II)	61
<b>Figure 4.14:</b> <sup>13</sup> C NMR spectrum of 7α-acetoxy-6β-hydroxyroyleanone (II)	62

<b>Figure 4.15:</b> DEPT-135 NMR spectrum of 7 $\alpha$ -acetoxy-6 $\beta$ -hydroxyroyleanone (II)	62
<b>Figure 4.16:</b> X-ray crystallographic structure of compound II. The hydrogens atoms have been omitted for the structure clarity purpose	63
<b>Figure 4.17:</b> Synthone motif of compound II	64
<b>Figure 4.18:</b> <sup>1</sup> H NMR spectrum of the royleanone horminone (III)	65
<b>Figure 4.19:</b> <sup>13</sup> C NMR spectrum of horminone (III)	65
<b>Figure 4.20:</b> DEPT-135 NMR spectrum of horminone (III)	66
<b>Figure 4.21:</b> <sup>1</sup> H NMR spectrum of coleon U quinone (IV)	67
<b>Figure 4.22:</b> <sup>13</sup> C NMR spectrum of coleon U quinone (IV)	67
<b>Figure 4.23:</b> DEPT-135 NMR spectrum of coleon U quinone (IV)	68
<b>Figure 4.24:</b> <sup>1</sup> H NMR spectrum of carnosolon (V)	68
<b>Figure 4.25:</b> <sup>13</sup> C NMR spectrum of carnosolon (V)	69
<b>Figure 4.26:</b> DEPT-135 NMR spectrum of carnosolon (V)	70
<b>Figure 4.27:</b> <sup>1</sup> H NMR spectrum of grandione A and 7-epimer grandidone A (VI & VII)	72
<b>Figure 4.28:</b> <sup>13</sup> C NMR spectrum of grandione A and 7-epimer grandidone A (VI & VII)	72
<b>Figure 4.29:</b> DEPT-135 NMR spectrum of grandione A and 7-epimer grandidone A (VI & VII)	73
<b>Figure 4.30:</b> COSY NMR spectrum of grandione A and 7-epimer grandidone A (VI & VII)	73
<b>Figure 4.31:</b> HMBC NMR spectrum of grandione A and 7-epimer grandidone A (VI & VII)	74
<b>Figure 4.32:</b> Methodology steps used in the isolation of bioactive compounds	76
<b>Figure 5.1:</b> $\alpha$ -glucosidase percentage inhibition of the grandidone A and 7-epimer grandidone A (VI & VII)	82
<b>Figure 5.2:</b> $\alpha$ -glucosidase percentage of inhibition of compounds I, II, and IV	83
<b>Figure 5.3:</b> Dose response curve of <i>P. madagascariensis</i> natural products and total extract	85

## LIST OF TABLES

(these are numbered according to the chapter in which they appear)

<b>Table 1.1:</b> Rifampin, pyrazinamide and isoniazid side effects	5
<b>Table 3.1:</b> Royleanones isolated from Southern Africa <i>Plectranthus</i> species	24
<b>Table 3.2:</b> Spirocoleons isolated from Southern Africa <i>Plectranthus</i> species	25
<b>Table 3.3:</b> Acylhydroquinones isolated from Southern Africa <i>Plectranthus</i> species	26
<b>Table 3.4:</b> Quinone methides abietanes isolated from Southern Africa <i>Plectranthus</i> species	27
<b>Table 3.5:</b> Vinylogous quinone abietanes isolated from Southern Africa <i>Plectranthus</i> species	28
<b>Table 3.6:</b> Dimers isolated from Southern Africa <i>Plectranthus</i> species	29
<b>Table 3.7:</b> Phenolic abietane isolated from Southern Africa <i>Plectranthus</i> species	30
<b>Table 3.8:</b> Seco-abietane isolated from Southern Africa <i>Plectranthus</i> species	31
<b>Table 3.9:</b> Dioxin quinone abietanes isolated from Southern Africa <i>Plectranthus</i> species	31
<b>Table 3.10:</b> Labdanes isolated from Southern Africa <i>Plectranthus</i> species	32
<b>Table 3.11:</b> <i>Ent</i> -kauranes isolated from Southern Africa <i>Plectranthus</i> species	34
<b>Table 3.12:</b> Phyllocladanes isolated from <i>Plectranthus</i> species	35
<b>Table 3.13:</b> Clerodanes and halimanes isolated from Southern Africa <i>Plectranthus</i> species	36
<b>Table 3.14:</b> Pimaranes isolated from Southern Africa <i>Plectranthus</i> species	37
<b>Table 3.15:</b> Beyeranes isolated from Southern Africa <i>Plectranthus</i> species	38
<b>Table 3.16:</b> Summary of Southern Africa <i>Plectranthus</i> species' medicinal uses and biological activities	40
<b>Table 3.17:</b> Others uses of Southern African <i>Plectranthus</i> species	46
<b>Table 4.1:</b> Solvent and reagents used in the research study	47
<b>Table 4.2:</b> TLC solvent system used in the study	48
<b>Table 4.3:</b> Summary of the studied plant extraction	51
<b>Table 4.4:</b> The solvent systems used during the total extract fractionation	51
<b>Table 4.5:</b> Conditions of the Prep HPLC	55
<b>Table 4.6:</b> NMR of compounds I–V in CDCl <sub>3</sub>	58
<b>Table 4.7:</b> Single-crystal X-ray parameters of 7 $\alpha$ -acetoxy, 6 $\beta$ -hydroxyroyleanone	64
<b>Table 4.8:</b> <sup>13</sup> C NMR data of compounds VI and VII in CDCl <sub>3</sub>	70
<b>Table 4.9:</b> Compounds isolated from main fractions (K4-3-III & IV, K4-3-VI, K4-3-VIII, K4-3-XI, and K4-3-XIII & XIV) and their weight	74
<b>Table 5.1:</b> Bioassays chemicals reagents	76
<b>Table 5.2:</b> The antimycobacterial activities of the isolated compounds, fraction, and total extract at 90% inhibition in 7H9/ADC/Glu/Tw and 7H9/CAS/Glu/Tx media	78
<b>Table 5.3:</b> Activity profile of the IC <sub>50</sub> values of <i>P. madagascariensis</i> isolated compounds and total extract against $\alpha$ -glucosidase	82
<b>Table 5.4:</b> The cytotoxicity activities of the <i>P. madagascariensis</i> isolated compounds and total extract against HaCaT cells	85
<b>Table 5.5:</b> Antioxidant activities of the isolated compounds	87

## APPENDICES

<b>Appendix A: IR and UV spectrums of <i>P. madagascariensis</i> Isolated natural products</b>	<b>103</b>
<b>Appendix B: Appendix B: GFP tagged <i>Mtb</i> Assay-10pt DR: Dose-response plot of <i>P. madagascariensis</i> isolated compounds, main fractions and total extract</b>	<b>109</b>

## GLOSSARY

Terms/Acronyms/Abbreviations	Definition/Explanation
IPP	Isopentenyl diphosphate
GPP	Geranyl pyrophosphate
FPP	Farnesyl pyrophosphate
DMAPP	Dimethylallyl diphosphate
TLC	Thin layer chromatography
Prep-TLC	Preparative thin layer chromatography
Semi-Prep HPLC	Semi-preparative high-performance liquid chromatography
NMR	Nuclear magnetic resonance
<sup>1</sup> H NMR	Proton nuclear magnetic resonance
<sup>13</sup> C NMR	Carbon-13 nuclear magnetic resonance
DEPT-135	Distortionless enhancement by polarization transfer
HMBC	Heteronuclear multiple bond coherence
COSY	Correlation nuclear magnetic spectroscopy
<i>J</i>	Coupling constant
<i>s</i>	Singlet
<i>d</i>	Doublet
<i>dd</i>	Doublet of doublets
<i>dt</i>	Doublet of triplets
<i>t</i>	Triplet
<i>td</i>	Triplet of doublet
<i>brs</i>	Broad singlet
<i>m</i>	Multiplet
IR	Infrared spectroscopy
UV	Ultra-violet spectroscopy
CDCl <sub>3</sub>	Deuterated chloroform
DCM	Dichloromethane
DMSO	Dimethyl sulphoxide
MeOH	Methanol
H <sub>2</sub> O	Deionised water
WHO	World Health Organisation
IUPAC	International union of pure and applied chemistry
<i>Mtb</i>	<i>Mycobacterium tuberculosis</i>
HaCaT	Immortalized human skin epithelial keratinocytes cells
DM	Diabetes mellitus
TEAC	Trolox equivalent absorbance capacity
ORAC	Automated oxygen radical absorbance capacity
FRAP	Ferric ion reducing antioxidant power
MIC	Minimum inhibitory concentration
IC	Inhibition Concentration
ADC/	Albumin-Dextrose complex
Glu	D-glucose
Tw	Tween 80
CAS	Casitone
Tx	tyloxapol
GFP	Green fluorescent protein
EDTA	Ethylene diamine tetra-acetic acid

DMEM	Dulbecco's Modified Eagle Medium
FBS	Fetal bovine serum
AAPH	2,2'-azobis(2-amidinopropane) dihydrochloride
ABTS	2,2'-azino-bis (3-ethylbenzothiazoline-6- sulfonic acid
<i>p</i> -NPG	<i>p</i> -nitrophenyl- $\alpha$ -glucopyranoside
N/A	Not applicable

# CHAPTER ONE

## INTRODUCTION

### 1.1 General introduction

Medicinal plants are plants that possess medicinal or biological properties, i.e., effects related to health, or which have been proven to be useful as drugs or contain organic constituents that are used in the development, discovery, and synthesis of drugs (Farnsworth & Soejarto, 1991). Medicinal plants have traditionally been used as teas, powders, poultices, poisons, spices, tinctures, hallucinogens, polymers, perfumes, waxes, narcotics, oil, fibers, and stimulants (Balick & Cox, 1997; Samuelsson, 2004; Duraipandiyar et al., 2006). Their applications and uses were passed down by healers and their apprentices to the next generation. According to literature, plants are the first medical treatment used by humankind, and about 50 % of modern clinically used drugs are derived from natural products (Matias et al., 2015).

These natural products are used as therapeutic agents to make a remarkable number of effective modern medicines with less adverse effects for treating infectious as well as chronic diseases. Infectious diseases are caused by pathogenic microorganisms namely fungi, bacteria, parasites or viruses (World Health Organization, 2017). These microorganisms are found in almost every habitat present in nature (60 % of the earth's biomass) and they are the main cause of mortality and morbidity, killing nearly 50,000 people per day (Ahmad & Beg, 2001; Silva & Fernandes, 2010).

Among the different infectious diseases present in South Africa, tuberculosis (Tb) is the leading cause of mortality and morbidity in the country. Additionally, due to TB association with several chronic illnesses such as psoriasis, diabetes mellitus (DM), and HIV which weaken the patients, there is an increase risk of progression from latent to active tuberculosis. About 15% of TB patients are likely to develop diabetes due to impaired glucose tolerance caused by TB (WHO, 2014).

Type 2 diabetes is also prevalent in patients with Psoriasis as the inflammatory nature of Psoriasis may affect organic systems, responsible for metabolic diseases (Holm & Thomsen, 2019). Additionally, the treatment of Psoriasis by anti-TNF agents increases the risk of TB infection as anti-TNF agents have the potential to reactivate TB in patients affected by Psoriasis in a period of less than a year (Shaikha, et al., 2012). Furthermore, Wakkeet, et al. (2010) showed that the risk of severe TB infection in patients affected by either diabetes mellitus or Psoriasis is twice as high as the risk for the normal population to contract either disease.

In the following sections, a brief introduction to tuberculosis, diabetes mellitus and psoriasis aetiology, epidemiology, and various chemotherapeutic agents will be detailed.

### 1.1.1 Tuberculosis

Tuberculosis (TB) is an airborne infectious disease (Yeon & Lee, 2008) caused by a slow-growing bacillus *Mycobacterium tuberculosis* (Njaria, 2017). The bacillus, *Mycobacterium tuberculosis* (*Mtb*), is present in the immune system of approximately 2 billion people (Quan et al., 2016). The majority of the infected people have latent TB infection (LTBI), which can quickly develop to active TB especially when they also suffer from diabetics, psoriasis, alcohol addiction, and human immunodeficiency virus (HIV) (WHO, 2018). Every year, around 10 million new cases of clinical TB encompassing 1.0 million children, 3.2 million women and 5.8 million men were registered (WHO, 2018). Generally, 90% of TB cases occur among adults (aged  $\geq 15$  years), with 9% being HIV-positive (72% in Africa). Additionally, 60% of TB cases were reported in South Africa (3%), Bangladesh (4%), Nigeria (4%), Pakistan (5%), Philippines (6%), Indonesia (8%), China (9%), and India (27%) (WHO, 2018) as illustrated in Figure 1.1.

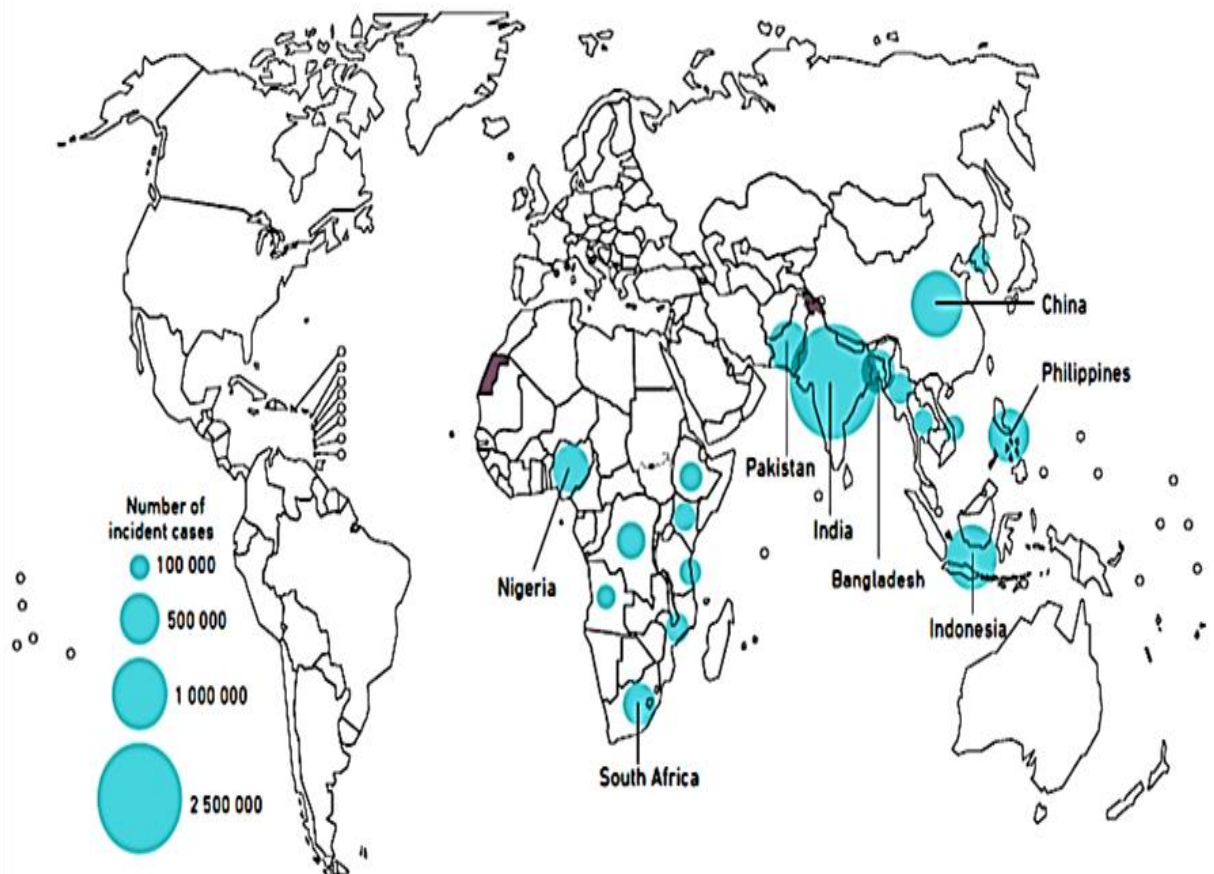


**Figure 1.1:** Countries with highest TB incident cases in 2017 (WHO, 2018)

The World Health Organisation (2018) and Bordignon et al. (2011) reports that 67% of HIV positive and 18% of psoriasis patients contracted TB while 15% (1.04 million) of TB patients contracted diabetes mellitus. The high prevalence of psoriasis-TB co-infection is due to the suppression of the immune system through psoriasis infection. Additionally, the



rate of TB-DM co-morbidity is becoming higher than TB-HIV co-infection as the percentage of TB-DM reaches at least 20% in TB-DM endemic countries like India and Mexico (Restrepo, 2017).

Worldwide, TB is the second leading cause of mortality and morbidity by infectious diseases, killing 1.3 million of HIV-negative people and 300 thousand of HIV positive patients annually (Srivastava et al., 2007; WHO, 2018). The African and South-East Asia region accounted for 82% of TB deaths in HIV-negative people and 85% of TB deaths in HIV-negative and HIV-positive patients. In South Africa, although the rate of TB cases and deaths has been declining since 2009, the airborne disease remains the primary cause of mortality. South Africa also ranks second highest on the list of reported TB incidence cases with 834 cases of TB per 100000 inhabitants (Churchyard et al., 2014; WHO, 2018).

From 1998 to 2015, The World Health Organisation has classified the high-burden countries (HBCs), which are responsible for 81% of TB incident cases into three categories namely TB, multidrug resistance TB (MDR-TB) and TB/HIV (co-infection) with some overlapping between two or all three groups. South Africa, Zimbabwe, Angola, Thailand, China, Ethiopia, India, Myanmar, Democratic Republic of Congo, Mozambique, Indonesia, Nigeria, Kenya, and Papua New Guinea, are the 14 African and Asiatic countries that appeared in all three categories as shown in Figure 1.1 (WHO, 2018). The highest TB-HIV co-infection incident cases were listed in African countries, with more than 50% of cases occurring in Southern Africa. Among the HBCs, South Africa has the highest number of TB/HIV co-infection incident cases. Furthermore, the second highest number of diagnosed MDR-TB cases as well as the third highest number of TB incident cases are ascribed to South Africa (Churchyard et al., 2014).

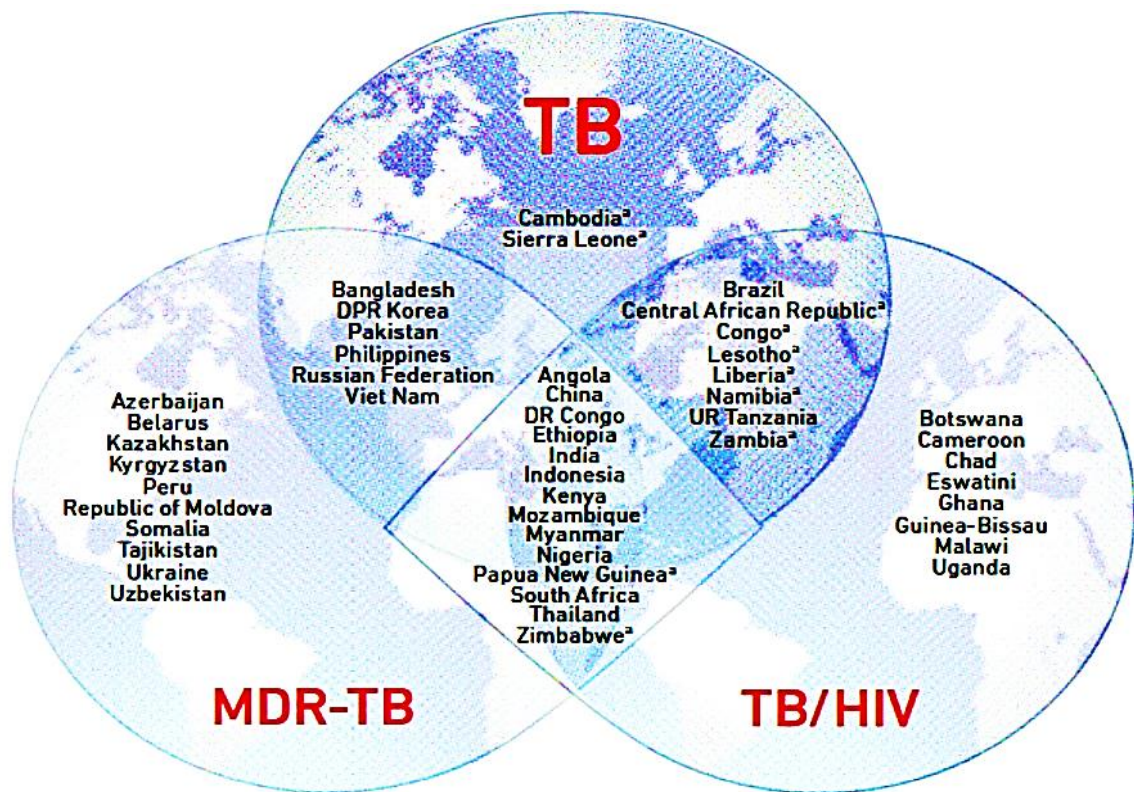


**Figure 3.2:** The lists for TB, TB/HIV, and MDR-TB high burden countries from 2016-2020 and their areas of overlap, as described in the global tuberculosis report updated by WHO in 2018. “a” shows countries that are included in the list of 30 most affected countries based on the severity of their TB burden as compared to the top 20.

Throughout the years, the spreading of multidrug resistance to almost every antimicrobial drug was observed, and TB strains are no exception. In 2012, about 450 thousand cases of MDR-TB was reported, with 10% of them being classified as extensively Drug-resistant (XDR) (Koch et al., 2014). Although drug resistance against the five frontline anti-tuberculosis drugs rifampin (RIF), streptomycin (SM), isoniazid (INH), ethambutol (EMB) and pyrazinamide (PZA) were reported before, the emergence of HIV have facilitated the transmission and spreading of MDR-TB and recently XDR-TB (Wade & Zhang, 2004). This is mostly due to the suppression of the immune system through HIV infection and the ability of *Mtb* to readily mutate (Kana & Churchyard, 2013). The XDR-TB which is expressed as MDR-TB with additional resistance to any fluoroquinolone and aminoglycosides antibiotics have severely limited possibility to eradicate TB leading to significant health problems as the number of MDR and XDR is growing every year (WHO, 2018; Kana & Churchyard, 2013). Additionally, the frontline antibiotics RIF, PZA, and INH, also causes painful and disagreeable side effects as tabulated in Table 1.1.

**Table 1.1:** Rifampin, pyrazinamide and isoniazid side effects

Drug (s)	Side effects
Rifampicin	Anorexia, nausea, abdominal pain, Orange/red-colored urine, Skin itching, rash
Pyrazinamide	Joint pains, Skin itching, rash
Isoniazid	Peripheral neuropathy, Skin itching, rash

### 1.1.2 Diabetes

Diabetes mellitus (DM) is a chronic disease characterised by hyperglycemia resulting from dysfunction in either insulin action or insulin secretion (Kharroubi & Darwish, 2015). This chronic disease is classified into type 1 and type 2 diabetes with most DM cases being type 2 diabetes (IDF, 2016). Type 1 diabetes which accounts for 5-10% of DM cases is caused by autoimmune destruction of the pancreatic  $\beta$  cells through T-cell mediated inflammatory response (insulinitis); in addition to a humoral (B cell) response (Devendra et al., 2004; Kharroubi & Darwish, 2015). Approximately, 80%-90% of insulin dependent DM cases (type1 DM) are juveniles (Kharroubi & Darwish, 2015; Okur et al., 2017). Type 2 diabetes which is a non-insulin-dependent diabetes resulting from a continuous defect in insulin secretion, accounts for 87-91% of diagnosed DM (Statistics South Africa, 2016; Okur et al., 2017). The number of diagnosed diabetic people has increased from 108 million to 451 million from 1980 to 2016 (WHO, 2016), leading to an estimated 54% (603 million) growth in diabetes cases by 2045 (International Diabetes Federation, 2017). This increase is mostly due to the increased sugar consumption, economic transition, obesity, aging population, genetic factors, autoimmune eradication of the pancreatic  $\beta$ -cells, and urbanization associated with nutrition transition (Okur et al., 2017: 61-65; Pheiffer et al., 2018). In South Africa, DM is ranked as the second most significant cause of mortality and morbidity, with 87% of diagnosed diabetics people (3.35 million) being obese or overweight (Joubert et al., 2007; IDF, 2016; Statistics South Africa, 2016). This is alarming as 69% of South African women and 38% of South African men are obese (Marie et al., 2014).

Glycaemic regulation in the bloodstream for type 2 DM patients is very crucial as it can lead to many macrovascular and microvascular complications such as blindness, renal failure, and stroke. In some cases, a defect in glycaemic regulation can result in an amputation of the lower limb depending on the severity of DM (Okur et al., 2017; Pheiffer et al., 2018). Thus, it is essential to reduce postprandial hyperglycemia which occurs when the blood glucose level is above 180 mg/mL, 1-2h after eating. This is possible by slowing down the rate of dietary carbohydrate or starch ingestion in the small intestine with the help of therapeutic or preventive natural antidiabetics drugs like  $\alpha$ -glucosidase inhibitors (Yilmazer-Musa et al., 2012). Moreover, many investigations on DM have shown that DM also caused an increased in free radicals' formation and a reduction in antioxidant capacity to scavenge free radicals. The oxidative stress caused by DM leads to the destruction of

the cell components as well as the genesis and development of many diseases like Alzheimer, cancer, Parkinson, or atherosclerosis (Moharram & Youssef, 2014; Ahmadi et al., 2018). Therefore, it is essential to have potent anti-diabetic drugs with antioxidant properties in order to increase the drug potency and reinforce the defence mechanisms of the organism against the pathologies associated to the attack of free radicals (Moharram & Youssef, 2014).

### **1.1.3 Psoriasis**

Psoriasis is a non-contagious, autoimmune, and incurable skin disease that harms the social and professional life of 2% of the world population (WHO, 2016; Declercq & Pouliot, 2013). This incurable disease is associated with several co-morbidities' illnesses such as Crohn's disease, lymphoma, arthritis, anxiety, diabetes, depression, and cardiovascular disorders (Takeshita et al., 2017). Psoriasis is characterized by symmetrical, sharply demarcated, red plaques, and papules covered with silver or white multi-layered scales (Huang et al., 2019; WHO, 2016). Psoriasis Lesions trigger pain, itching, stinging, and mostly occur on the scalp, trunk, knees, elbows, fingernail, and back with almost an equal distribution among men and women (Jayakar & Kumar, 2016). Chronic dermatosis is most common in Caucasians and Blacks' ethnic groups between 50-69 years old with a more severe form in men compared to women (Huang et al., 2019)

The aetiology of psoriasis is unknown, however the dysregulation of keratinocytes (primary cellular component of the skin) proliferation, differentiation, and death as well as the absence of granular layer results to the hyperproliferation and abnormal differentiation of epidermal keratinocytes (Udensi et al., 2011; Helwa et al., 2015). The hyperproliferation and abnormal differentiation of keratinocytes, which are histological characteristics to psoriasis take 7 to 10 days instead of 28-50 days to renew as compared to normal and healthy skin (Declercq & Pouliot, 2013). Keratinocytes (KCs) play a vital role in the skin permeability barrier, wound repair, as well as in the initiation and perpetuation of skin inflammatory (Corsini & Galli, 1998) and immunological responses, (Colombo et al., 2017; Hanel et al., 2013). The immune system is activated by many environmental factors including smoking, stress, drugs ( $\beta$ -receptor antagonists, non-steroidal anti-inflammatories (NSAIDs), antimalarials, lithium, and angiotensin-converting enzyme (ACE) inhibitors), trauma, excessive alcohol consumption, and streptococcal infection (Raboobee et al., 2010). The presentation of these exogenous antigens to innate natural killer T (NKT) cells, chemokines, cytokines, and dendritic cells and adaptive (CD4+ and CD8+ T lymphocytes) immunity, as well as the formation of the immunological synapse, leads to the differentiation of T cells into effector cells like Th1, Th2, and Th17 (Gaspari, 2006; Declercq & Pouliot, 2013; Engler et al., 2017). The effector Th1 cells which release tumour necrosis factor (TNF- $\alpha$ ) and interferon-gamma (IFN- $\gamma$ ) are predominant in psoriasis, whereas the

Th17 cells which release interleukins (IL)-17A, IL-17F and IL-22 play essential roles in psoriasis and vitiligo as it activates the keratinocytes and other cytokines of the innate immune system as shown in Figure 1.3 (Seo et al., 2012; Engler et al., 2017; Nedoszytko et al., 2014). The activation of the keratinocytes results in the upregulation of proinflammatory chemokines and cytokines that are found in psoriatic lesions (Engler et al., 2017; Nedoszytko et al., 2014).

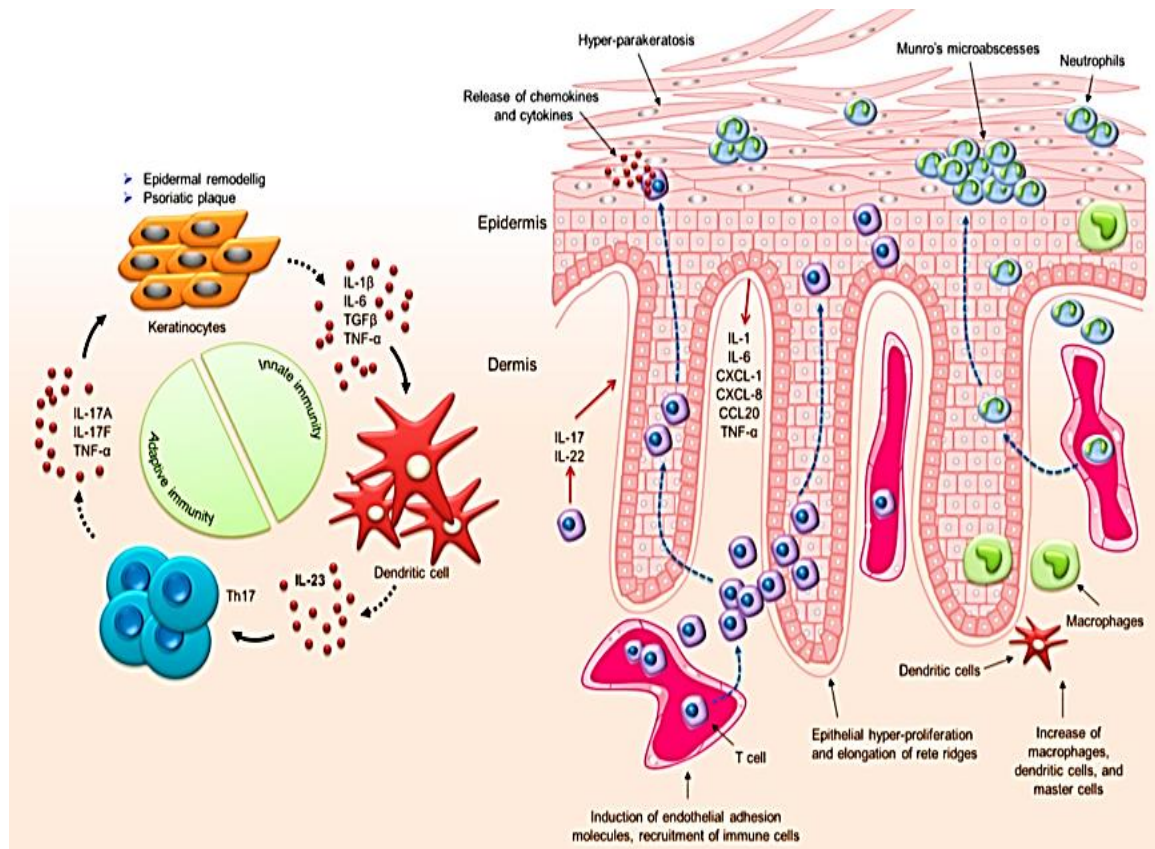


**Figure 1.3:** Immunopathogenesis of psoriasis (Huang et al., 2019).

Regarding the negative impact the disease has on affected people's lives, many clinical treatments have been in place to attenuate the symptoms of this incurable disease. However, these treatments have some adverse effects like organ toxicity, infection, atrophy, which result in the restriction of long term treatment (Huang et al., 2019). Thus, it is important to find potent anti-psoriatic and antiproliferative keratinocytes agents with less adverse effects.

#### 1.1.4 Rationale for *Plectranthus madagascariensis*' natural products as tuberculosis diabetes and psoriasis therapeutic agents.

The high cost of new chemotherapeutic agents, socioeconomic inequality, and substandard programme management with reference to inadequate case detection, diagnosis, and cure have made tuberculosis, diabetes and psoriasis high burden diseases.

Since these diseases beget significant economic and quality of life burdens, scientists have been looking for medicines from natural resources as they are reported to have fewer side effects compared to chemically synthesized or clinical drugs (Chartone-Souza, 1998; Sasidharan et al., 2011). According to the royal botanic gardens kew's there are only 391,000 medicinal plants around the world, only 35,000 of them have been thoroughly studied either chemically or for their physiologist activities. This implies that 356,000 plants with potential and interesting chemical entities could be decisive in the treatment of present and future diseases (Rasool, 2012). Among these under-studied plants, *Plectranthus madagascariensis* (Lamiaceae) has been selected for this research study according to the type of phytochemical constituents biosynthesized by *Plectranthus* species along with their pharmaceutical properties and traditional uses in respiratory and skin infections.

This chapter is divided into nine sections. The importance of medicinal plants in drug discovery, the justification of the study, and problem statement are discussed in sections 1.2, 1.3, and 1.4 respectively. Section 1.5 describes the research questions whereas section 1.6 focuses on the aim of the research. The objectives of the research study are provided in Section 1.7. The limitations of the thesis are presented in section 1.7, followed by the thesis outline in section 1.9.

## **1.2 The impact of medicinal plants in drug discovery**

Medicinal plants are fundamental components of research development in the pharmaceutical industry whose pharmacological properties were first discovered through traditional medicine and ethnomedicinal studies (Singh, 2015). From the ethnomedicinal studies done so far, natural products are the source in the discovery and development of many drugs. For example, nitisinone (**1**) known on the market as orfadin is the lead structure of medicines used to treat the rare inherited disease tyrosinemia (Balunas & Kinghorn, 2005). Moreover, Newman and Cragg (2016) reported that from 1<sup>st</sup> January 1981 to 31<sup>st</sup> December 2014, about 33-42 % of approved therapeutic agents were made of natural products and natural product-derived molecules. These natural products' functional groups and diversity have exhibited their impact on drug effectiveness, optimization, safety, and the ability to prevent a disease from spreading. This is mostly due to the natural products' smaller adverse effects, cultural acceptability, and excellent compatibility with the human body (Mustafa et al., 2017; Verma & Singh, 2008). Thus, enhancing the use of about 78 % of these new biological active constituents as a propitious alternative cure for infectious diseases (Lokhande et al., 2007). For instance, various groups of antifungal proteins like glucanase and chitinase used as protection for a developing embryo from many infections are found in the seeds of several medicinal plants (Mustafa et al., 2017).

Several drugs discovered and isolated from plants originated from different continents such as Africa, Australia, Asia, and South America, e.g., atropine (**2**) from *Atropa belladonna*, codeine (**3**) from *Papaver somniferum*, quinine (**4**) from *Cinchona cordifolia*, pilocarpine (**5**) from *Pilocarpus jaborandi* and theobromine (**6**) from *Theobroma cacao* (Figure 1.4, Salim et al., 2008: 1-20). The listed natural products have been used respectively as an anticholinergic, cough suppressant, antimalarial, parasympathomimetic, and anti-arteriosclerosis (Salim et al., 2008). Even though some have been retracted from the pharmaceutical industry due to their lack of efficacy, many of these chemical entities are still in use and possess a similar therapeutic purpose as their first ethnomedical use (Fabricant & Farnsworth, 2001).

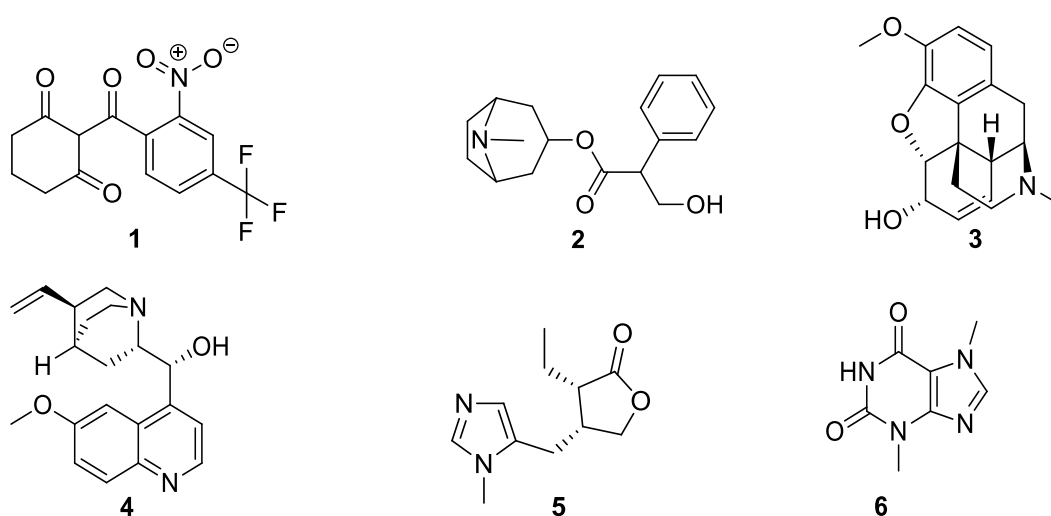


**Figure 1.4:** Structures of compounds 1-6.

### 1.3 Justification of the study

South Africa has an astonishing floral diversity used in both formal and informal systems of medicine. About 60-80% of South Africans use medicinal plants as their primary health care due to availability and affordability (Aston et al., 2018). Additionally, the phytoconstituents present in plants represent a significant source of new drugs. Many of the natural compounds have shown potency and usefulness in different industrial sectors such as the pharmaceutical, cosmeceutical, and nutraceutical industries. In the present work, among the phytochemical constituents present in *Plectranthus madagascariensis*, a pronounced interest has been shown towards the abietane diterpenoids due to their antimicrobial, antidiabetic and antiproliferative properties (Kubínová et al., 2014; Diogo et al., 2019).

Furthermore, the increase in multi and extensively *Mtb* resistance towards frontline TB drugs, as well as the different adverse effects caused by the clinically recommended cures,

greatly influence the emergence of tuberculosis and diabetes and psoriasis (Caulfield & Wengenack, 2016).

Regarding this matter, *P. madagascariensis* was chosen due to its history of use in the treatment of scabies, small wounds, colds, cancer, asthma, cough, diabetes, and chest complaints (Rabe & Staden, 1998; Kubínová et al., 2014; Diogo et al., 2019). Furthermore, integrating medicinal plants into modern medicines will stimulate research and might lead to discovery of various efficacious drugs.

#### **1.4 Problem statement**

Tuberculosis and diabetes are the top two leading causes of mortality and morbidity in South Africa, accounting for 6.5% and 5.5 % of natural deaths, respectively (Stats SA, 2018). Furthermore, the bacillus *Mtb* being able to adapt to the anti-tuberculosis drugs' mechanism of action results in the formation of *Mtb* multi-drug resistance and extensive drug resistance. Hence, challenging the country's public health as the inhibition or elimination of the bacteria becomes more arduous (Byarugaba, 2004; Chandra et al., 2017). The bad quality of life that comes with having the incurable disease psoriasis and the costly treatment related to the listed diseases is the reason why this study intends to contribute in finding more efficient natural-derived drugs to combat, control and reduce tuberculosis, diabetes and psoriasis pandemic.

#### **1.5 Research questions**

The research questions of this study are enumerated below.

- i. What are the active non-volatile secondary metabolites of *P. madagascariensis*?
- ii. What are the chemical structures of these metabolites?
- iii. Are *P. madagascariensis* secondary metabolites biologically active?
- iv. Specifically, can they be used to treat tuberculosis, diabetes, and psoriasis or developed into useful drugs?

#### **1.6 Aim of the research**

This research aims to isolate, characterize, and evaluate the anti-tuberculosis, antidiabetics, and cytotoxicity properties of the phytochemical constituents of the aerial parts of *P. madagascariensis*.

#### **1.7 Objectives of the research study**

The objectives of this study include:

- i. To collect and identify *P. madagascariensis*.
- ii. To extract of the aerial parts of *P. madagascariensis* metabolites



- iii. To isolate the bioactive chemical constituents of the total extract using chromatographic techniques such as column chromatography (CC), semi-preparative high performance liquid chromatography (semi-prep-HPLC) and preparative-TLC.
- iv. To characterize the isolated compounds using different spectroscopic techniques including 1D and 2D nuclear magnetic resonance (NMR) spectroscopy.
- v. To evaluate the biological activities and determine their MIC<sub>90</sub> and IC<sub>50</sub> of the isolated compounds.

## 1.8 Hypotheses

The ethnobotanical records of *Plectranthus* plants have shown that many species of this genera are used in traditional medicine to treat ailments such as Eye infections, diarrhoea, asthma, indigestion, , skin allergies, heart diseases, respiratory infections and fever (Waldiaa et al., 2011). Phytochemical studies of *P. madagascariensis* have revealed the abundant amount of terpenoids and phenolic compounds. Therefore, it is possible that *P. madagascariensis* contains bioactive terpenes or phenolic compounds that can be used in the treatment of tuberculosis, diabetes and psoriasis.

## 1.9 Delimitations

This research project will focus only on the extraction, isolation, and characterization of the biologically active constituents of *P. madagascariensis* aerial parts. Besides, the isolated secondary metabolites were evaluated for their biological activities.

## 1.10 Thesis outlines

This thesis is divided into six chapters as detailed below.

### CHAPTER ONE: INTRODUCTION

This chapter highlights the different problems and challenges faced by people suffering from tuberculosis, diabetes, and psoriasis in South Africa and worldwide. It also gives an insight into the impact of medicinal plants in drug discovery and development. This section includes the justification of the study, problem statement, aim, objectives, hypothesis, delimitations, and outlines of the research study.

### CHAPTER TWO: DITERPENES

This chapter introduces the various classes of diterpenes and their biosynthetic pathways. The abietane diterpenoids biosynthesis, classes and nomenclatures are the most pointed out in this part of the thesis.

### **CHAPTER THREE: LITERATURE REVIEW**

Chapter 3 gives a detailed literature review on the genus *Plectranthus* and in particular on the Southern African species. A meticulous review, on the phytochemistry, medicinal uses, and pharmacology of the Southern Africa *Plectranthus* species are presented in this chapter.

### **CHAPTER FOUR: EXTRACTION ISOLATION AND CHARACTERIZATION OF *PLECTRANTHUS MADAGASCARIENSIS* NATURAL PRODUCTS**

Chapter four presents the materials and methods used in the isolation and characterization of *P. madagascariensis* components as well as the different chromatography and spectroscopic methods and techniques used in the isolation of the chemical constituents. The structure elucidation of the isolated compounds is also elaborated in the chapter.

### **CHAPTER FIVE: BIOLOGICAL EVALUATION**

This chapter gives details of the efficiency of the isolated natural products as anti-tuberculosis, anti-diabetes, and anti-psoriasis agents.

### **CHAPTER SIX: CONCLUSION AND RECOMMENDATIONS**

This section summarized the outcomes of the investigations and gives some recommendations related to the research study.

## CHAPTER TWO

### DITERPENOIDS

#### 2.1 Introduction

Diterpenes are naturally occurring compounds of twenty carbon derived from the condensation of four isoprene units via the mevalonate and deoxy-xylulose phosphate pathways (De Sousa et al., 2018). Both pathways are the only route by which diterpenes can be naturally biosynthesized since both pathways produced the biochemical isoprene units, dimethylallyl diphosphate and isopentenyl diphosphate needed for the biosynthesis of diterpenes (Hemmelin et al., 2012; De Sousa et al., 2018). However, some authors stated that the deoxy-xylulose phosphate pathway is the most predominant pathway to naturally biosynthesized diterpenoids, although the mevalonate pathways can also supply different quantities of a molecule (Hemmelin et al., 2012; De Sousa et al., 2018). The condensation of these isoprene units leads to the formation of geranylgeranyl diphosphate GGPP which will undergo some cyclization reactions and produced monocyclic, bicyclic, tricyclic, tetracyclic, pentacyclic and macrocyclic diterpenes or diterpenoids (diterpene with functional groups attached to it) (Dewick, 2002)

In the genus *Plectranthus*, only bicyclic (labdanes), tricyclic (abietanes and pimaranes), and tetracyclic diterpenes (kauranes and beyeranes) diterpenoids have been identified so far. A more detailed description of their biosynthesis and cyclization reactions are discussed in section 2.2. The classification, characterization, and nomenclatures of the most diverse type of diterpenes (abietane diterpenoids) biosynthesized by Southern African *Plectranthus* species are given in Section 2.3.

#### 2.2 Biosynthesis of diterpenes

The occurrence, content, amount, and composition of diterpenoids in plants depend upon the plant species. This is due to the presence and activity of the enzymes responsible for their biosynthesis, which take place in three stages (Woźniak et al., 2015). The first stage is the biosynthesis of the activated isoprenes, isopentenyl diphosphate (IPP) and dimethylallyl diphosphate (DMAPP). The second stage is about the biosynthesis of geranylgeranyl diphosphate (GGPP), whereas the third stage consists of various cyclization reactions required for the biosynthesis of monocyclic, bicyclic, tricyclic and tetracyclic diterpenes from GGPP as described below.

##### 2.2.1 Biosynthesis of IPP and DMAPP

Plants produce IPP and DMAPP either via the mevalonate pathway (MVA) located in the plant's cytosol or the methylerythritol phosphate pathway (MEP), also known as the 1-deoxy-D-xylulose (DOX) pathways which occurs in the plant's chloroplast (Rijo, 2010).

Sometimes plants produced IPP and DMAPP using both paths simultaneously. These activated isoprenes are the introductory material for the biosynthesis of GGPP.

### 2.2.1.1 Mevalonate pathways

In this step, two molecules of acetyl-coenzyme A (acetyl-CoA) will react and be catalyzed by thiolase to yield acetoacetyl-CoA. The produced acetoacetyl-CoA reacts with another molecule of acetyl-CoA by Claisen condensation to produce  $\beta$ -hydroxy- $\beta$ -methylglutaryl-CoA (HMG-CoA). This is followed by the production of the intermediate mevalonic acid by reduction of HMG-CoA carbonyl groups to mevalonic acid with nicotinamide adenine dinucleotide phosphate (NADPH). Subsequently, the phosphate groups from two of adenosine triphosphate (ATP) molecules are transferred to mevalonic acid to produce 5-diphosphomevalonic acid. The 5-diphosphomevalonic acid is converted to IPP by diphosphomevalonic acid decarboxylase. Afterward, IPP is isomerized to yield DMAPP, as shown in Figure 2.1.

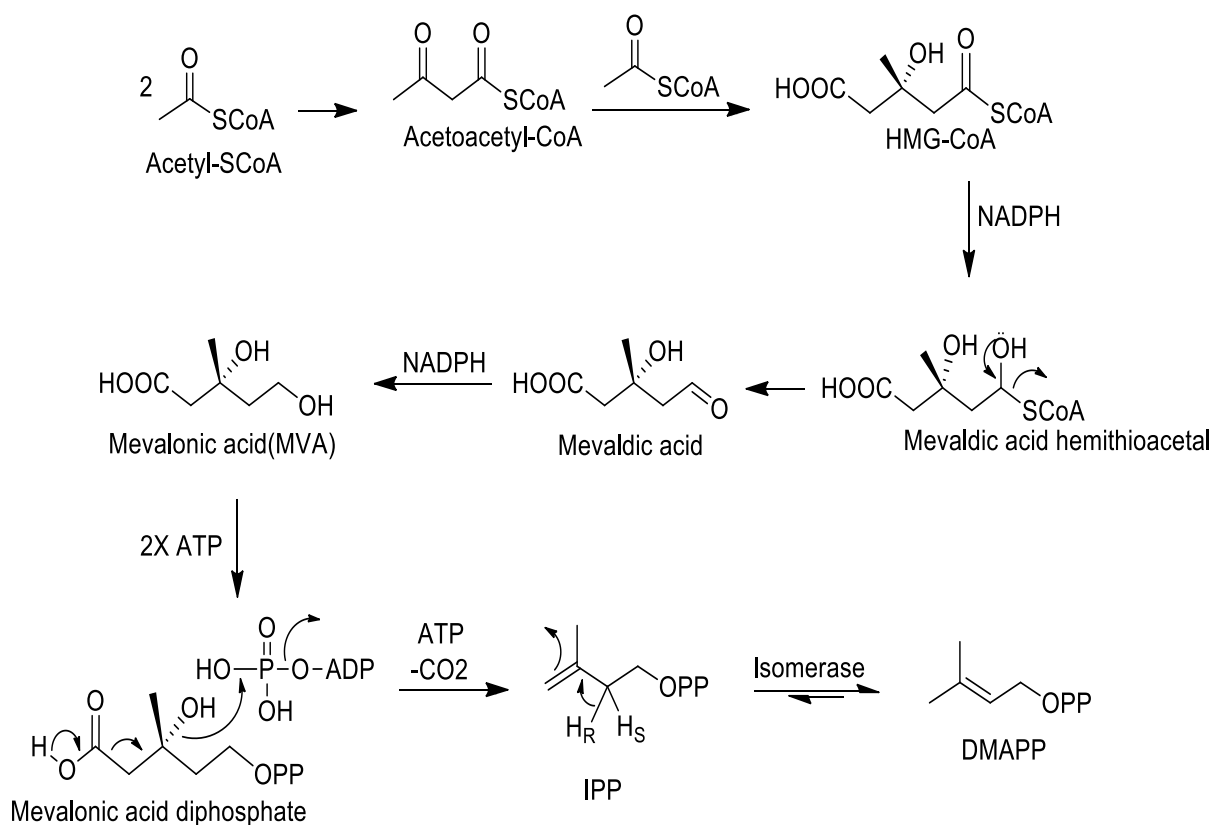


**Figure 2.1:** Biosynthesis of IPP and DMAPP via the mevalonate pathway (Dewick, 2002).

### 2.2.1.2 Methylerythritol phosphate pathway (MEP)

This step is initiated by the condensation of glyceraldehyde 3-phosphate and pyruvic acid (Figure 2.2). These two compounds undergo a condensation that leading to the decarboxylation of pyruvate to form 1-deoxy-D-xylulose 5-phosphate (DXP).

Intramolecular rearrangement of DXP is assumed to give a hypothetical rearranged intermediate, 2-C-methylerythrose 4-phosphate, which is then reduced to 2-C-methyl-D-erythritol-4-phosphate (MEP) by NADPH (Kuzuyama, 2002). MEP reacts with cytidine triphosphate (CTP) to form 4-diphosphocytidyl-2-C-methyl-D-erythritol (CDP-ME), which is phosphorylated with ATP and cyclase to yield 2-C-methyl-D-erythritol 2,4-cyclodiphosphate (MEcPP) which is reduced to IPP and DMAPP by an unspecified and unclear reduction process (Rijo, 2010).

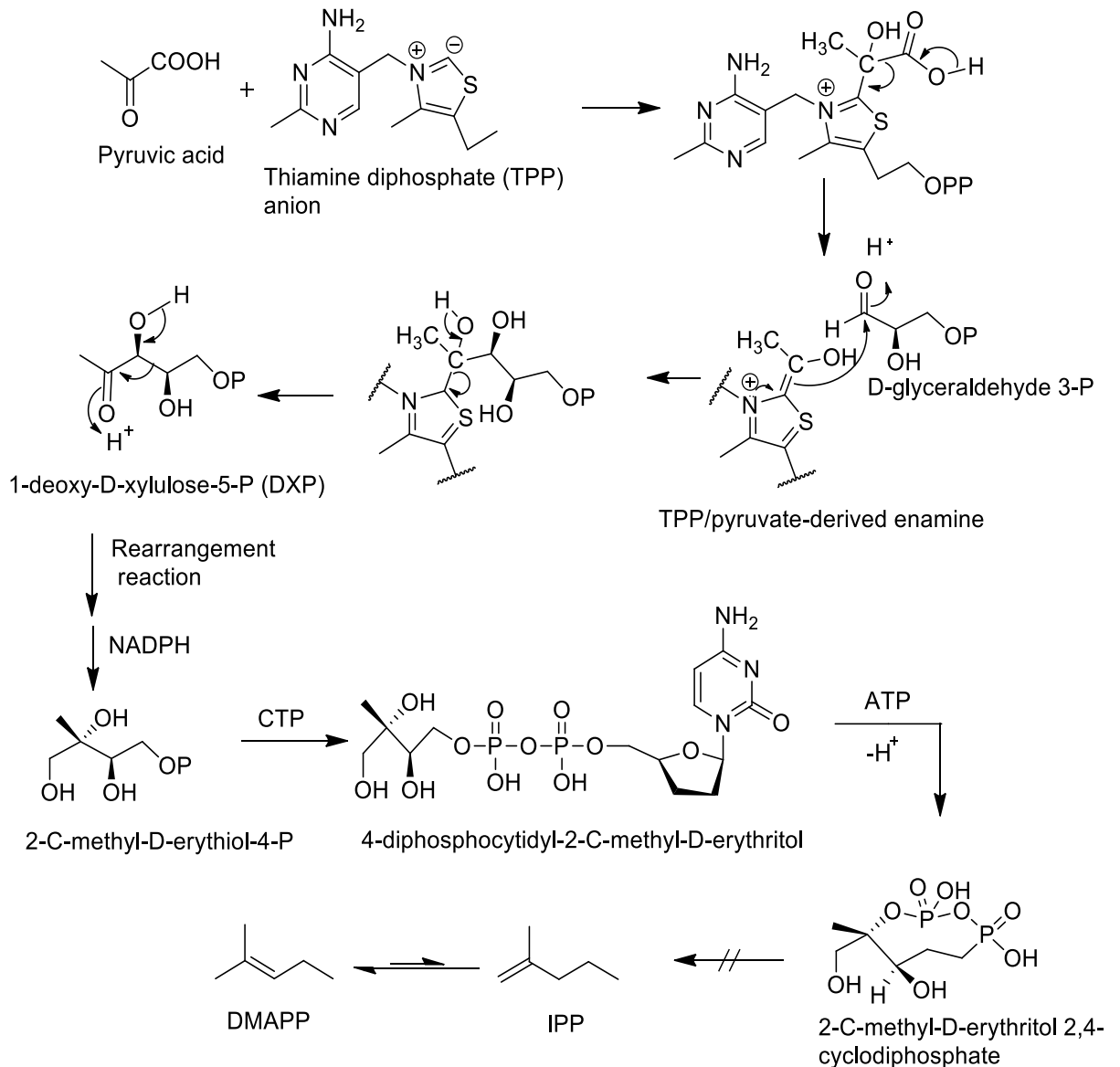


**Figure 2.2:** Biosynthesis of IPP and DMAPP via the methylerythritol phosphate pathway (Dewick, 2002).

### 2.2.2 Biosynthesis of GGPP

This stage involves a head to tail coupling of IPP with DMAPP to generate geranyl pyrophosphate (GPP). The tail of the geranyl pyrophosphate is condensed with the head of IPP to yield farnesyl pyrophosphate (FPP). Hereafter, IPP is added to FPP in a head to

tail arrangement that results in the formation of geranylgeranyl diphosphate (GGPP). Figure 2.3 shows the representation of the biosynthesis of GGPP.

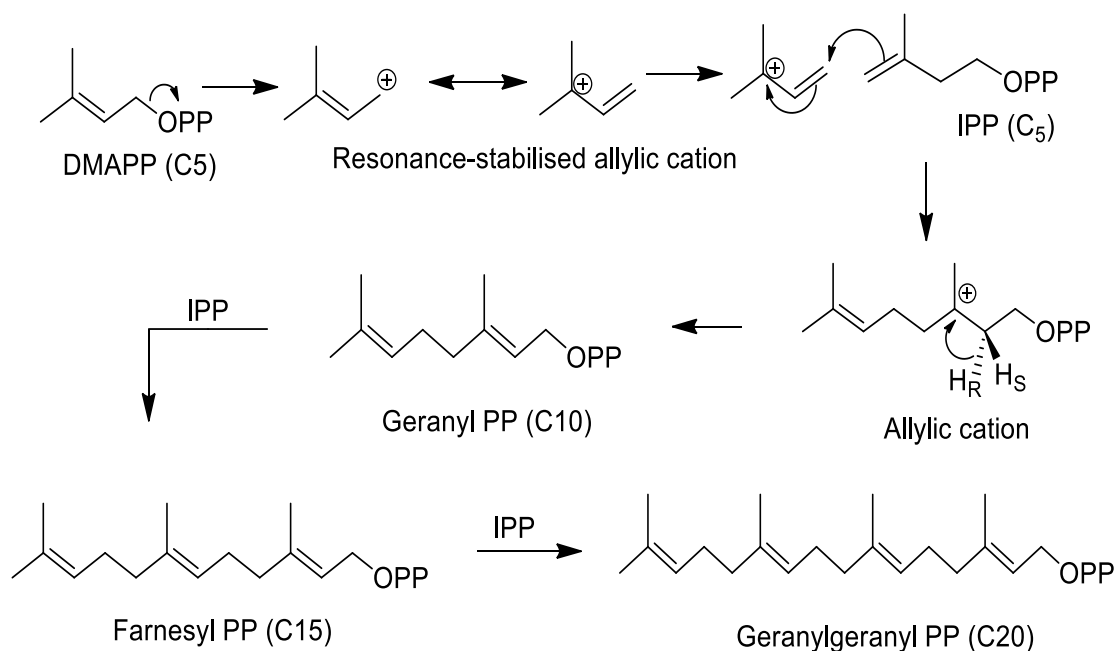


**Figure 2.3:** Biosynthesis of GGPP (Dewick, 2002).

## 2.2.3 Biosynthesis of monocyclic, bicyclic, tricyclic, and tetracyclic diterpenes

### 2.2.3.1 Biosynthesis of monocyclic diterpenes

After the biosynthesis of GGPP, the double bond on the isopropylidene unit located at the head of the GGPP chain is protonated to form the tertiary carbocation resulting in the first concerted cyclization and formation of monocyclic type diterpenes (Figure 2.4).

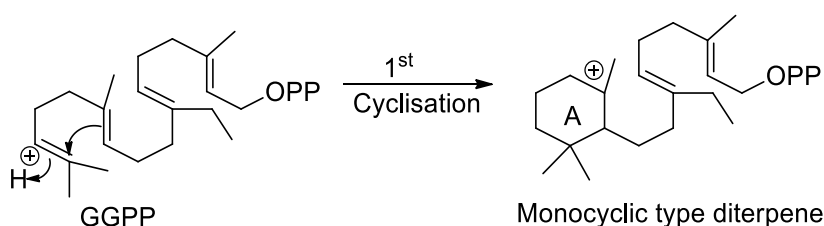


**Figure 2.4:** Formation of monocyclic type diterpenes from GGPP (reproduced from Dukhea, 2010).

### 2.2.3.2 Biosynthesis of bicyclic diterpenes

The sequential cyclization of GGPP in a chair-chair “normal” conformation followed by a loss of a proton from a methyl yields the bicyclic type diterpenes copalyl [(+)-copalyl PP], also known as labdadienyl PP. A rearrangement of GGPP in a chair-chair “antipodal”

conformation generates its stereoisomer ent-copalyl PP [(-)-copalyl PP]. The loss of PP from labdadienyl gives the labdane type diterpenes (Figure 2.5).

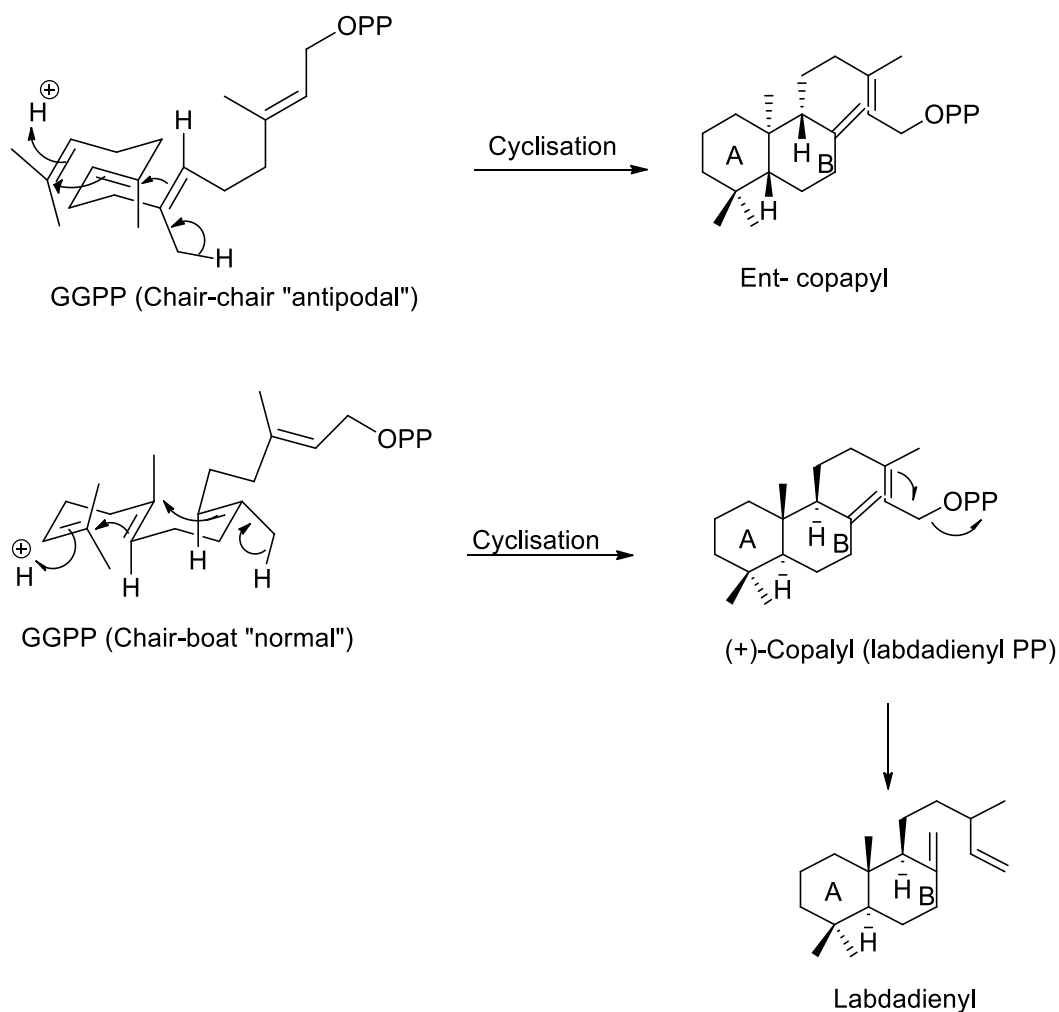


**Figure 2.5:** Formation of copalyl diphosphate stereoisomers (bicyclic diterpenes) from GGPP (De Sousa et al., 2018).

### 2.2.3.3 Biosynthesis of tricyclic diterpenes

The removal of the diphosphate from copalyl PP generates primary allylic cation, and further cyclization of labdadienyl leads to the formation of tricyclic type diterpenes like the intermediate sandaracopimarenyl cation. The gain of proton of sandaracopimarenyl cation from C-14 generates a double bond at ring C between C-8 and C-14, resulting in the formation of the second intermediate sandaracopimaradiene. The intermediate undergoes a methyl migration from C-17 to C-15, which yields an abietenyl cation. The loss of a proton at C-7 produces the diene abietadiene. Sequential oxidation of abietadiene 4 $\alpha$  methyl to carboxylic acid via alcohol and aldehyde yields abietic acid (Figure 2.6).

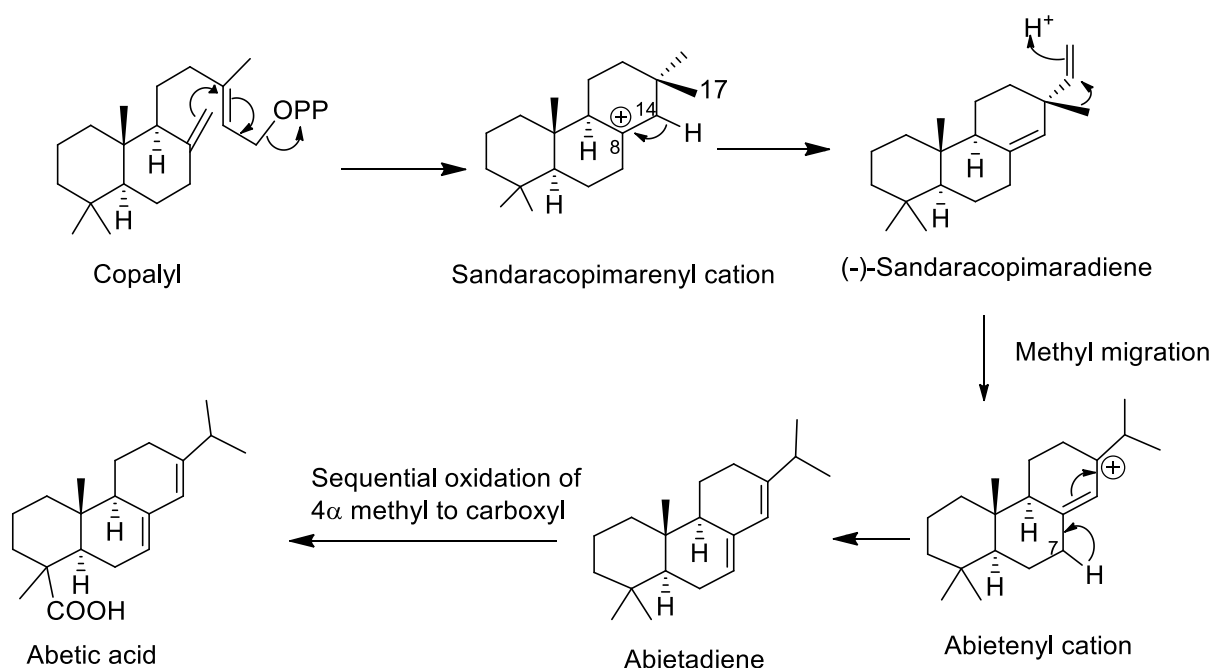


**Figure 2.6:** Biosynthesis pathway of abietic acid (Dewick, 2002).

#### 2.2.3.4 Biosynthesis Tetracyclic diterpenes

The tertiary carbocation on Sandaracopimarenyl obtained from ent-copalyl is attacked by the double bond to yield the fourth ring system and a secondary cation. The secondary cation on the fourth ring was stabilized by converting the secondary cation to a tertiary cation by 1,2 alkyl migration, which is followed by the loss of the proton from the methyl group results in the formation of ent-kauranes and its exocyclic double bonds. The sequential oxidation reactions of ent-kauranes results in the formation of various oxygenated kauranes like ent-kaurenoic acid (Figure 2.7).

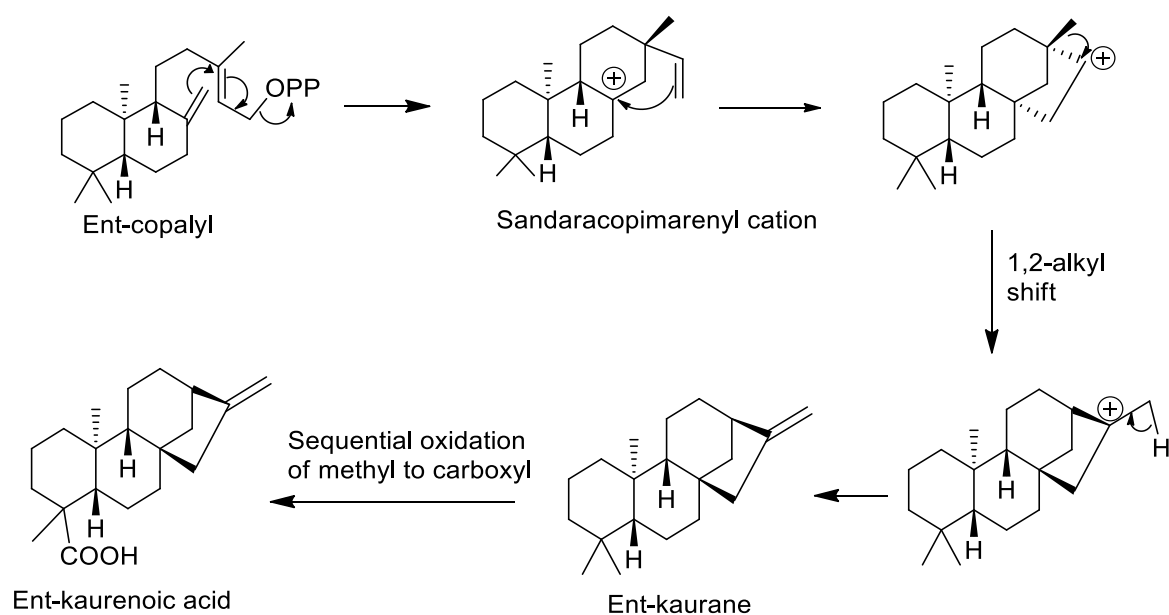


**Figure 2.7:** Biosynthesis pathways of ent-kaurane (Dewick, 2002).



The protonation of sandaracopimarenyl cation by the double bonds at C-16 with loss of the methyl at C-13 form the beyeranes type diterpenoids (Figure 2.8).

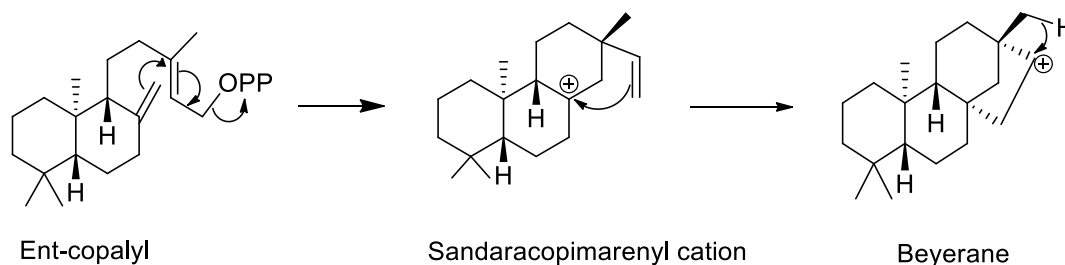


**Figure 2.8:** Biosynthesis of beyerene (Manito, 1981).

### 2.3 Classification, characterization, and nomenclature of the abietane diterpenoids

Among the different types of diterpenoids biosynthesized by *Plectranthus* species, Abietane diterpenoids are the most diverse type of diterpenoids found in the aerial parts and leaves of *Plectranthus* species. Abietane diterpenoids skeleton consists of two methyl groups at C-4, one methyl group at C-10, and one isopropyl group at C-13. The numbering system of this highly modified diterpenes was established in 1993 by the International Union of Pure and Applied Chemistry (IUPAC) as illustrated in Figure 2.9

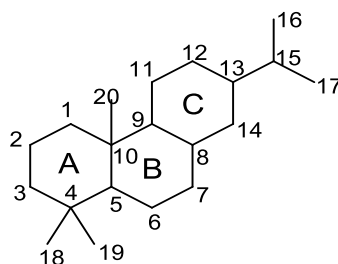


**Figure 2.9:** Numbering system of abietane diterpenes.

According to Abdel-Mogib et al. (2002), abietane diterpenoids can be classified into ten class, namely: phenolics abietanoids, dimeric abietanoids, royleanones, 1,4-phenanthraquinones, acylhydroquinones, spirocoleons, vinylogous quinones, seco-abietanoids, quinone methides, and abeo-acylhydroquinones. Each class of abietane diterpenoids exhibits a wide range of oxygenated groups allocated at different positions varying from one class to another. For example, the royleanones are characterized by a 12-hydroxy, 1,4-benzoquinone ring C, whereas the acylhydroquinones type abietane has a trihydroxybenzene ring C, a carbonyl group at C-7 and a double bond at C-5 - C-6. The spirocoleons have a cyclopropane attached at C-13, and 2-Cyclohexene-1,4-dione ring C. Vinylogous quinone is characterized by a tri- or di- hydroxycyclohexa-1,4-diene with double bonds at C-5 - C-6 and C-7 -C-8 or carbonyl groups at C-6 and C-7. In the case of vinylogous quinone with dihydroxycyclohexa-1,4-diene ring C, the carbon at position 12 is

attached to a carbonyl group. The 1,4-phenanthraquinones type abietane is characterized by aromatic ring A, B, and C. Quinone methides are bearing a p-quinone methide with a hydroxide group at C-11 and a cyclohexadiene ring corresponding to ring B. Furthermore, alkyl, alkenyl, carboxyl, cycloalkyl, hydroxyl and carbonyl, and hydroxyl groups can be substituted at position 2, 3, 6, 7, 16, 15 but rarely at position 20, 18 and 19 depending on the class of abietane diterpenoids.

The terms “nor”, “abeo” and “seco” are usually used in the nomenclature of some abietanes (Figure 2.10). The prefix “nor” is used when a methyl group is removed from a particular ring in the structure while the term “seco” is used to designate the removal of a side chain or broken bond within the parent structure. The prefix “abeo” or the prefix X(Y→ Z) abeo point out the migration of a single bond from its initial position in a fundamental parent structure to a new position; where, X is the locant of the position of the unchanged, end of the migrating bond; Y is the locant of the position of the moving end of the migrating bond and Z is the locant of the position of the moving end of the migrating bond in the final structure (IUPAC, 1999)

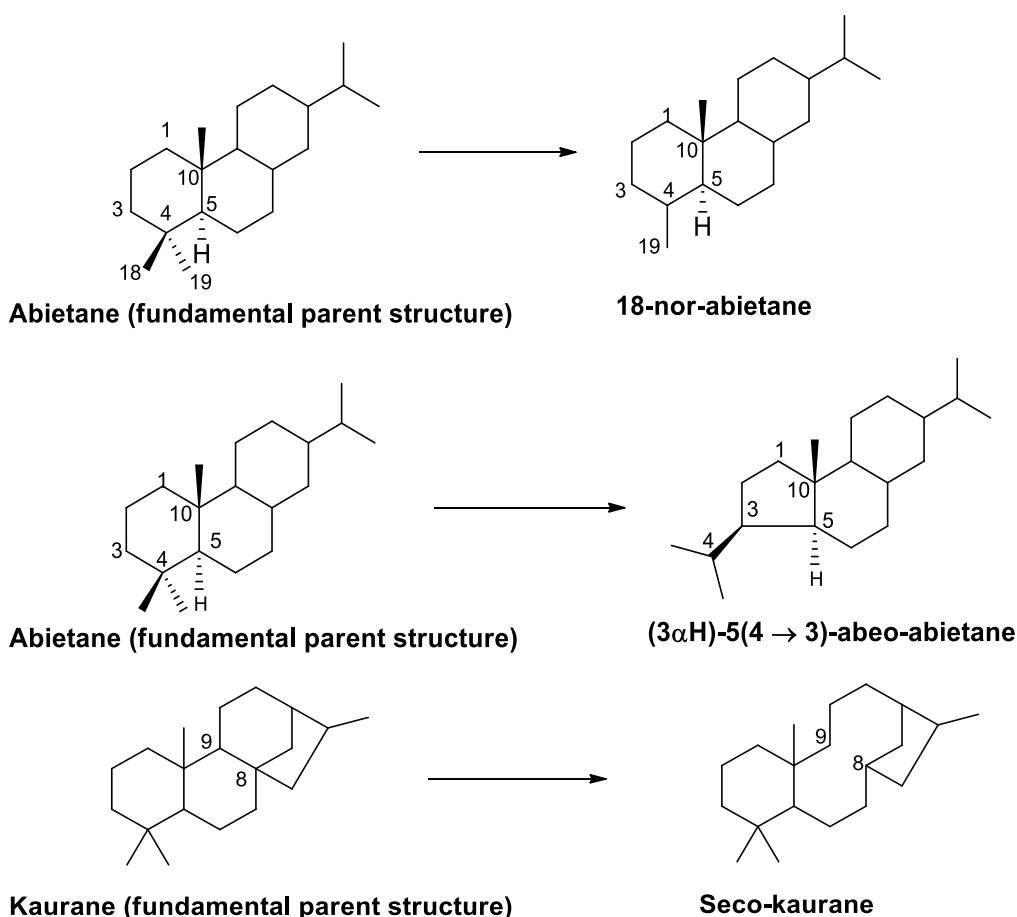


**Figure 2.10:** Illustration of the uses of the terms “nor”, “abeo” and “seco”.

## CHAPTER THREE

### LITERATURE REVIEW

#### 3.1 Introduction

Plants are abundant resources of secondary metabolites, which play a very crucial role in traditional and modern medicine. Secondary metabolites, also referred to as natural products are biologically active organic compounds that have been identified as therapeutic agents with economic and culinary importance. Among the various plant species belonging to the Cape flora of Southern Africa, the genus *Plectranthus* (section 3.2) and more specifically the Southern Africa *Plectranthus* species were selected and are being reviewed in this chapter. The botanical characteristics (section 3.3), phytochemistry (section 3.4), ethnobotanical uses, ethnopharmacological, pharmacological, and others uses (sections 3.5-3.7) of the Southern African *Plectranthus* species are described in detail. Regarding their phytochemistry, an emphasis is made on abietane diterpenoids since they are the most diverse type of bioactive compounds produced by *Plectranthus* species. Furthermore, the botanical identification of *P. madagascariensis* is given in section 3.3.2

#### 3.2 *Plectranthus* genus

The genus *Plectranthus* consists of 350 species of various sizes, foliage, and scent that belongs to the sage family Lamiaceae, subfamily Nepetoideae, and the tribe Ocimeae (Waldiaa et al., 2011). *Plectranthus* species are characterized by the two-lipped corolla and the aromatic leaves arranged in opposite pairs (Van Jaarsveld, 1987). Most of the 350 attractive and decorative *Plectranthus* species are semi-succulent to succulent shrubs or herbs growing in tropical and subtropical regions as well as in regions with warm weather like Africa, Australia, Asia and a few Pacific islands (Rice et al., 2011). In Southern Africa (South Africa, Lesotho, Namibia and Swaziland), over 53 species are reported to be endemic to the region with a few used to treat ailments and diseases like *P. ambiguus*, *P.amboinicus*, *P. barbatus*, *P. caninus*, *P. eckloni*, *P. elegans*, *P. ernstii*, *P. fruticosus*, *P. grandidentatus*, *P. herereonsis*, *P. madagascariensis*, *P. ornatus*, *P. porcatus*, *P. saccatus*, and *P. strigosus* (Codd 1985; Rabe & Staden 1998). In South Africa, the largest concentration of species is found in the Southern KwaZulu Natal and the North-Eastern coastal part of the Eastern Cape (Van Wyk & Smith, 2001). The genus *Plectranthus* has six subgenera, namely *Calceolanthus*, *Plectranthus*, *Burnatastrum*, *Coleus*, *Xerophilus*, and *Nodiflorus* and two significant clades, *coleus* and *Plectranthus* clades (Paton et al., 2004; Van Jaarsveld 2006). However, the *Plectranthus* clade which includes the genera *Aeollanthus*, *Tetradenia*, *Capitanopsis*, *Dauphinea*, *Thorncroftia*, and some species of the genus *Plectranthus* like *P. fruticosus* has below 50% of bootstrap support (Paton et al.,

2018). The *Coleus* clade which encompassed the remaining species of the genus *Plectranthus* (including the species that used to be called *Coleus*) and the genera *Anisochilus* and *Pycnostachys*, is the most recognised one (Paton et al., 2013). Paton et al. (2009; 2013) investigations on how to differentiate these two clades stated that *Plectranthus* species in the *Plectranthus* clade have more or less equal posterior and anterior corolla lobes and calyces with a centrally fixed pedicel (Paton et al., 2018). While those in the *Coleus* clade possess a wider anterior and shortened posterior corolla lip and calyces with a pedicel connecting the opposite posterior lip of the calyx (Paton et al., 2018).

### 3.3 Botanical identification

#### 3.3.1 General description

*Plectranthus* species are aromatic, annual or perennial shrub, well-branched herbs with different and attractive foliage and flowers like *P. argentatus*, *P. oertendali*, and *P. madagascariensis* (Figure 3.1, Rabe & Staden, 1998).

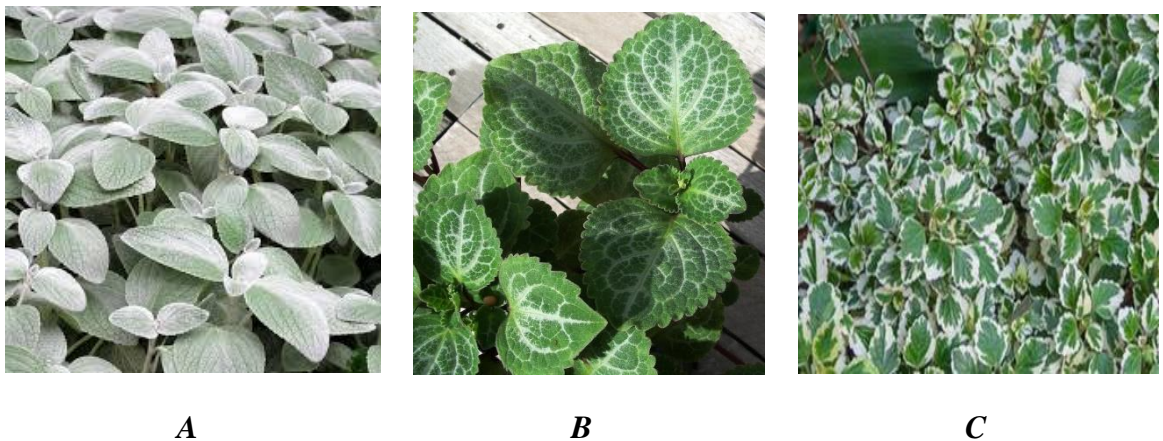


**Figure 3.1:** Leaves of *P. argentatus* (A), *P. oertendali* (B) and *P. madagascariensis* (C)

These evergreen herbaceous species are approximately 100 cm high and have opposite, oval leaves of length 4 cm and with 3-7 pairs of rounded teeth that are slightly hairy to the touch (Harrower, 2014). The roots of *Plectranthus* species are thick, tuberous, spindle-shaped, conical, and strongly aromatic (Soni & Singhai, 2012). The tubular flowers of 7-18 mm in length are either pale lavender, white, or light yellow. The inflorescence is a terminal, erect raceme, composed of 4 -6 flowers at each node (Harrower, 2014). The calyx is 2-4 mm long, elongating to 5 mm after the flower drops and holds the smooth, roundish, flattened, pale-brown seeds (nutlets) of 0.5-0.7 mm in diameter (Harrower, 2014). The flowers grow from February to May in Southern Africa. These botanical descriptions are common to the seventeen *Plectranthus* species that are endemics to Southern Africa regions. The differences between them lie in their foliage, size and local names. Thus, a

more detailed description of the research study plant *P. madagascariensis* is done in the next section.

### 3.3.2 *Plectranthus madagascariensis*

*P. madagascariensis* is commonly known as a thicket spurflower, candle plant, and Madagascar spurflower (Harrower, 2014). Locally the plant is named muishondblaar in Afrikaans and iboza lehlathi or ilozane in isiZulu (Harrower, 2014). The Madagascar spurflower is a hardy, small (54 cm) and fast-growing groundcover perennial herb. The plant has variegated evergreen leaves with whitish tooth edges. The creamy-white flowers appear from February to May. The general characteristics of *Plectranthus* species detailed in section 3.3.1 are also applied to *P. madagascariensis*.

## 3.4 Phytochemistry

Species of the genus *Plectranthus* are recognized as ornamental and medicinal plants with economic importance since they are rich sources of essential oil and diterpenoids with broad applications in pharmaceutical and cosmeceutical industries (Khan et al., 2016). The phytochemical analysis of *Plectranthus* constituents demonstrated the presence of many abietanes (**7-66**), labdanes (**67-99**), *ent*-kaurane (**100-120**), phyllocladane (**121-127**), neoclerodane (**128-135**), halimane (**136**), pimarane (**137-138**), and beyerene (**139-141**) diterpenoids (Rijo et al., 2007: 215-221). The diterpenoids isolated from the Southern African *Plectranthus* species are tabulated in Table 3.1 to 3.15.

### 3.4.1 Abietane diterpenoids isolated from Southern African *Plectranthus* species

In phytochemical studies, the highly oxidized abietane diterpenoids isolated from *Plectranthus* aerial parts, stem or roots are classified as royleanones (**7-18**), spirocoleons (**19-30**), acylhydroquinones (**31-35**), quinone methides (**36-43**), vinylogous quinones (**44-51**), dimeric abietanes (**52-58**), phenolics abietanes (**59-63**), seco abietanes (**64** and **65**), and dioxin quinone abietanes (**66** and **67**).

The paraquinone abietane, also known as royleanones are abundantly found in Southern Africa *Plectranthus* species. Furthermore, most of the royleanones isolated from Southern African *Plectranthus* species are 6,7 unsaturated compounds (**7-16**, and **18**). However, some of them are classified as 6,7 saturated molecules like compound **17** or 6,7-unsaturated compounds with external double bonds and some rearrangements like compounds **18** and **12**, which are also categorized as nor-abietane and bisabeo-abietane diterpenoids respectively (Figure 3.2, Table 3.1).

**Table 3.1:** Royleanones isolated from Southern Africa *Plectranthus* species

Plants	Isolated compounds	References
Common to <i>Plectranthus</i> genus	7 $\alpha$ -acetoxy-6 $\beta$ -hydroxy-7 $\alpha$ -acetoxy-royleanone (7) Horminone (8)	Teixeira et al., 1997; Yulianto et al., 2016.
<i>P. herereonsis</i>	6 $\beta$ -hydroxyroyleanone (9) 16-acetoxy-7 $\alpha$ , 12-dihydroxy-8, 12-abietadiene-11, 14-dione (10) 16-acetoxyhorminone (11) 3 $\beta$ -acetoxy-6 $\beta$ ,7 $\alpha$ , 12-trihydroxy-17(15 $\rightarrow$ 16) 18(4 $\rightarrow$ 3)-bisabeo-abieta-4(19),8,12,16-tetraene-11,14-dione (12)	Batista et al., 1995; Batista et al., 1996.
<i>P. madagascariensis</i>	6 $\beta$ ,7 $\alpha$ -dihydroxyroyleanone (13) 6 $\beta$ ,7 $\beta$ -dihydroxyroyleanone (14) 7 $\beta$ -acetoxy-6 $\beta$ -hydroxyroyleanone (15) 7 $\alpha$ -formyloxy-6 $\beta$ -hydroxyroyleanone (16) Coleon U quinone (17)	Kubínová et al., 2014; Diogo et al., 2019.
<i>P. barbatus</i>	Plectranthone J (18)	Alasbahi & Melzig, 2010.

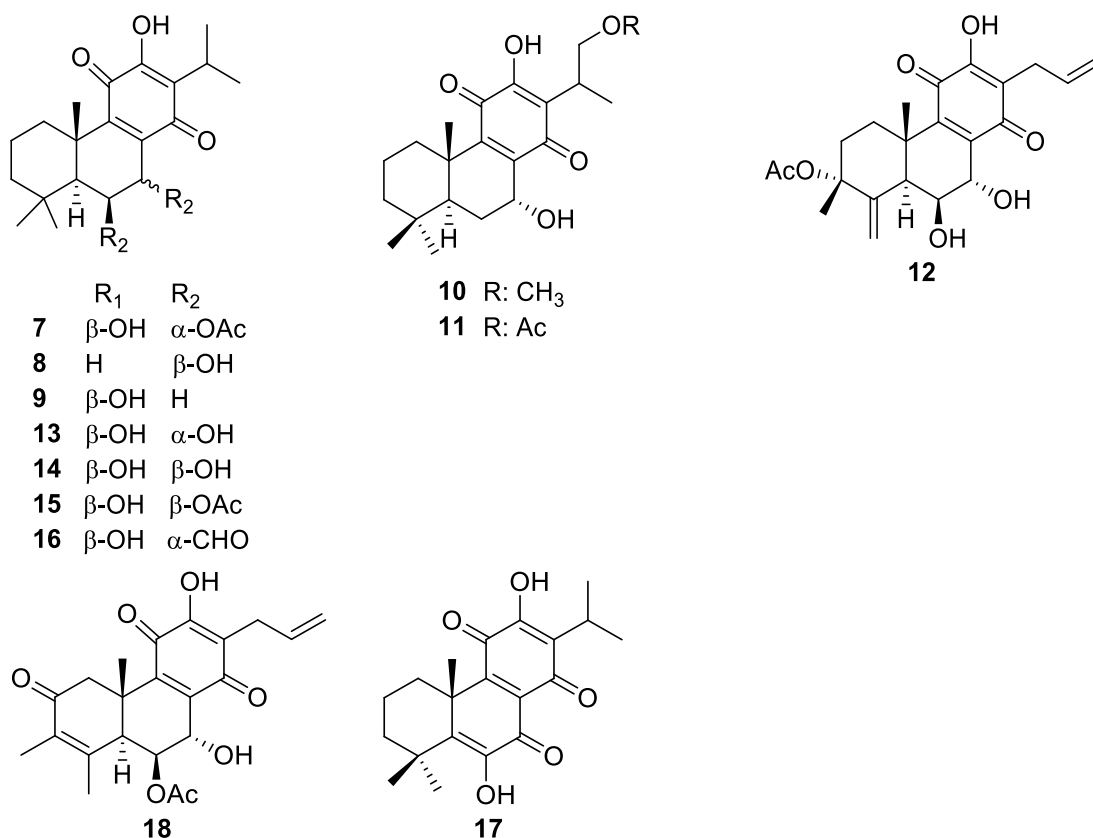
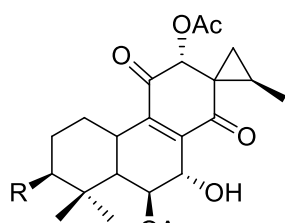


**Figure 3.2:** Structures of compounds 7-18

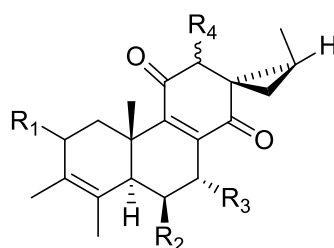
*P. caninus* and *P. barbatus* are the primary sources of spirocoleons from Southern Africa *Plectranthus* species as they account for ten out the twelve isolated compounds with compound **21** being common to both plants. *P. ambinoicus*, *P. ornatus*, and *P. porcatus* yielded one compound each. The isolated spirocoleons are characterized by a cyclopropyl ring at C-13 linked to a cyclohexene quinone or cyclohexane ring, as shown in Figure 3.3. Moreover, the alkyl, hydroxyl or acetate group attached at C-3, C-6, C-7, and C-12 of the isolated spirocoleons are either in  $\alpha$  or  $\beta$  position (Table 3.2, Figure 3.3).

**Table 3.2:** Spirocoleons isolated from Southern Africa *Plectranthus* species

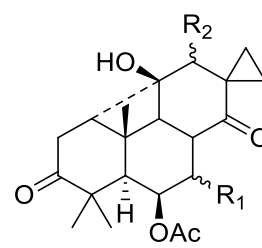
Plants	Isolated compounds	References
<i>P. ambinoicus</i> <i>P. ornatus</i>	3 $\beta$ -hydroxy-3-deoxybarbatusin ( <b>19</b> )	Silva et al., 2017.
<i>P. barbatus</i>	Coleon O ( <b>20</b> ) Coleon T ( <b>21</b> ) Cyclobutatusin ( <b>22</b> ) 7 $\beta$ -acetyl-12-deacetylcyclobutatusin ( <b>23</b> ) Plectrin ( <b>24</b> )	Alasbahi & Melzig, 2010.
<i>P. caninus</i>	7,12-diacetylcoleon J ( <b>25</b> ) Coleon M ( <b>26</b> ) Coleon N ( <b>27</b> ) Coleon R ( <b>28</b> ) Coleon T ( <b>21</b> ) Barbatusin ( <b>29</b> )	Arihara et al., 1977; Arihara et al., 1983.
<i>P. porcatus</i>	(13 <i>S</i> ,15 <i>S</i> )-6 $\beta$ ,7 $\alpha$ ,12 $\alpha$ ,19-tetrahydroxy-cyclo-8-abietene-11,14-dione ( <b>30</b> )	13 $\beta$ ,16- Simões et al., 2010.



**19** R: OH  
**28** R: OAc  
**29** R: =O



R<sub>1</sub> R<sub>2</sub> R<sub>3</sub> R<sub>4</sub>  
**20** H OH OAc  $\alpha$ -OH  
**21** H OH OH  $\beta$ -OH  
**24** =O OAc OH  $\alpha$ -OH  
**26** H OH OAc  $\alpha$ -OAc



R<sub>1</sub> R<sub>2</sub>  
**22**  $\alpha$ -OH  $\alpha$ -OAc  
**23**  $\beta$ -OAc  $\beta$ -OH

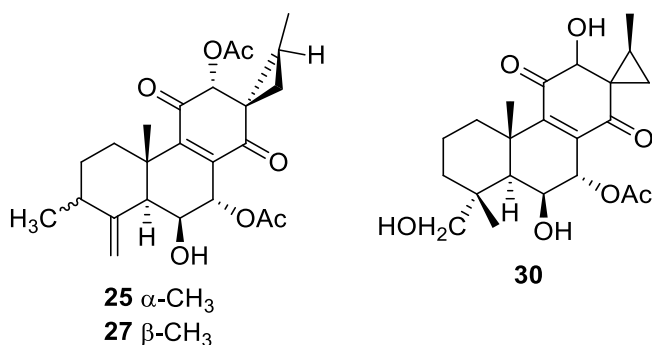
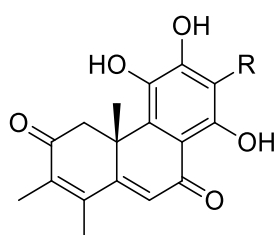


**Figure 3.3:** Structures of compounds **19-30**.

About five acylhydroquinones abietanes (**31-35**) were isolated from the Southern Africa *Plectranthus* specie *P. barbatus*. The isolated compounds are bearing one to two double bonds on C-3 and C-4 or C-5 and C-6 or both, in addition to the trihydroxy-benzene ring and the carbonyl group at C-7 as shown in Table 3.3 and Figure 3.4.

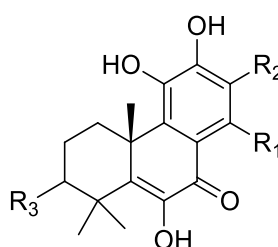
**Table 3.3:** Acylhydroquinones isolated from Southern Africa *Plectranthus* species

Plant	Isolated compounds	References
<i>P. barbatus</i>	(16 <i>R</i> )-Plectrinon A ( <b>31</b> ) Plectrinon B ( <b>32</b> ) Coleon C ( <b>33</b> ) Coleon S ( <b>34</b> ) 14-Deoxycoleon U ( <b>35</b> )	Alasbahi & Melzig, 2010.



**31** R: (*R*)-CH<sub>2</sub>CH(OH)CH<sub>3</sub>

**32** R: CH<sub>2</sub>CHCH<sub>2</sub>



	R <sub>1</sub>	R <sub>2</sub>	R <sub>3</sub>
<b>33</b>	OH	CH(CH <sub>3</sub> )CH <sub>2</sub> OH	H
<b>34</b>	OH	CH(CH <sub>3</sub> ) <sub>2</sub>	OH
<b>35</b>	H	CH(CH <sub>3</sub> ) <sub>2</sub>	H

**Figure 3.4:** Structures of compounds **31-35**.

Ten quinone methides abietanes (Table 3.4, Figure 3.5) were isolated from *P. ambiguus*, *P. eckloni*, and *P. strigosus*, with eight of them isolated from *P. strigosus*. Compounds **36-43** are bearing a p-quinone methide with a hydroxy group at C-11 and a cyclohexadiene ring corresponding to ring B. Compounds **36-43** have their substituents attached to C-1 (**39, 41**



and **42**) or C-18 (**37**, **38** and **40**) and sometimes to C-1 and C-18 like compounds **37** and **43**.

**Table 3.4:** Quinone methides abietanes isolated from Southern Africa *Plectranthus* species

Plants	Isolated compounds	References
<i>P. ambiguus</i> <i>P. strigosus</i>	Parviflorone A ( <b>36</b> )	Liu & Ruedi, 1995. Alder et al., 1984.
<i>P. strigosus</i>	Parviflorone B ( <b>37</b> ) Parviflorone C ( <b>38</b> ) Parviflorone D ( <b>39</b> ) Parviflorone E ( <b>40</b> ) Parviflorone F ( <b>41</b> ) Parviflorone G ( <b>42</b> ) Parviflorone H ( <b>43</b> )	Alder et al., 1984; Gaspar-Marques et al., 2008.
<i>P. eckloni</i> <i>P. strigosus</i>	Parviflorone D ( <b>39</b> ) Parviflorone F ( <b>41</b> )	Uchida et al., 1981; Van Zyl et al., 2008

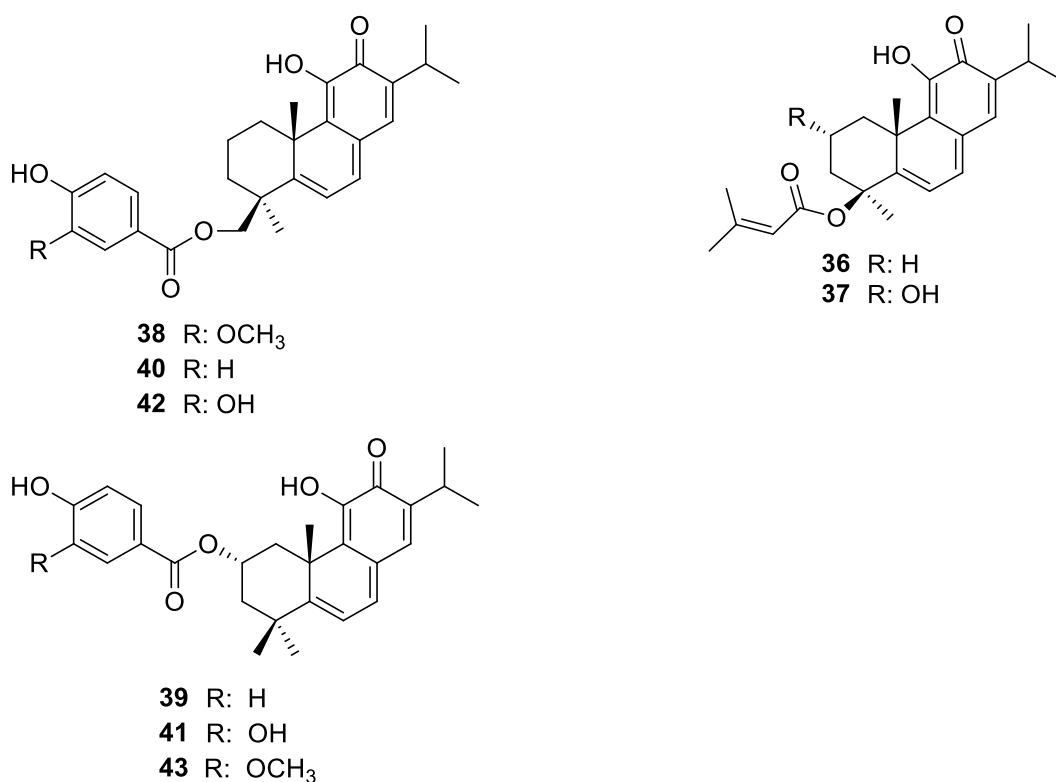


**Figure 3.5:** Structures of compounds **36-43**

A total of eight vinylogous quinone abietane (Table 3.5, Figure 3.6) were isolated from *P. grandidentatus* (**44-51**), two from *P. elegans* (**42** and **43**) and one each from *P. barbatus*

(39), *P. caninus* (40), and *P. ambinoicus* (41). The main differences between compounds 44-51 hinge on the substituents attached to C-6, C-13, and C14. For example, compound 48 has an oxolane group attached at C-13 and C-14, whereas compound 50 has an isopropyl group at C-13 and a hydroxy group at C-14. Compounds 44 and 45 showed similarity, except that compound 44 has a carbonyl group at C-6, while compound 45 has a hydroxy group attached to the quaternary carbon at position 6. Compounds 47 and 49 are the only compounds with one methyl group at C-4.

**Table 3.5:** Vinylogous quinone abietanes isolated from Southern Africa *Plectranthus* species

Plants	Isolated compounds	References
<i>P. grandidentatus</i>	Coleon V (44) Coleon U (45) 14-O-acetyl-coleon U (46)	Rijo et al., 2007.
<i>P. barbatus</i>	Coleon F (47)	Alasbahi & Melzig, 2010.
<i>P. caninus</i>	Coleon P (48)	Arihara et al., 1983.
<i>P. ambinoicus</i>	(16S)-coleon E (49)	Silva et al., 2017.
<i>P. elegans</i>	11-hydroxy-12-oxo-7,9 (11),13-abietatriene (50) 14-hydroxytaxodione (51)	Dellar et al., 1996.

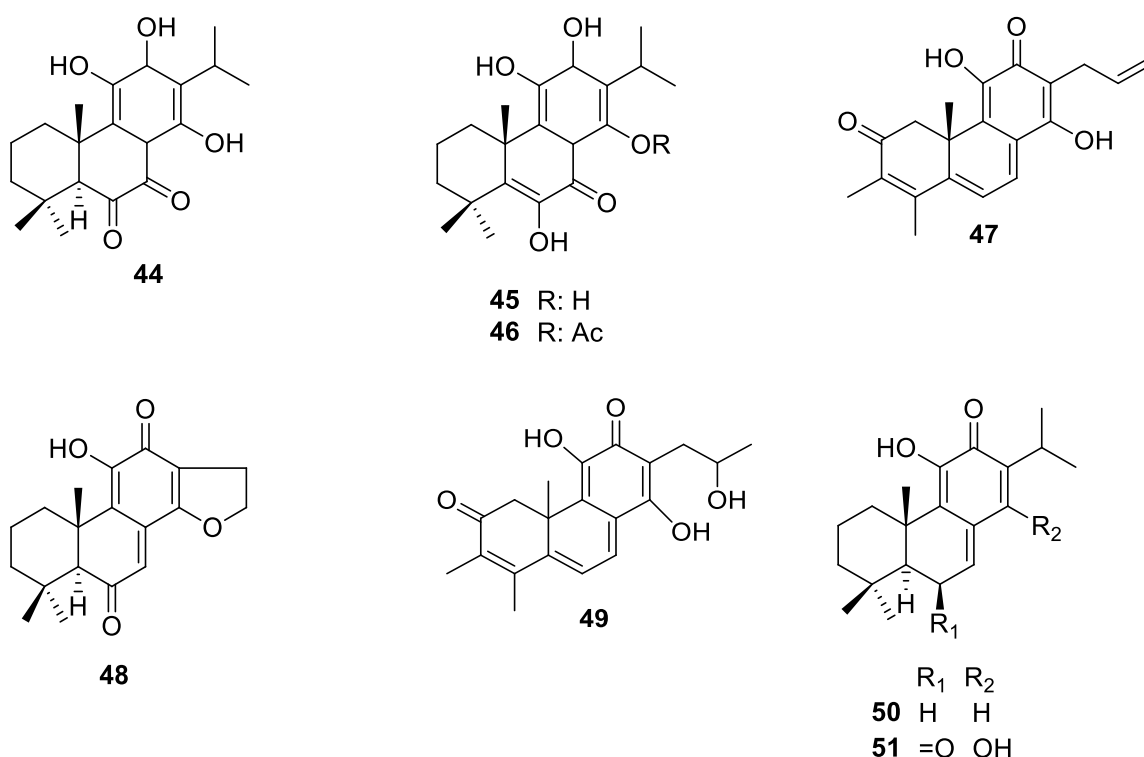
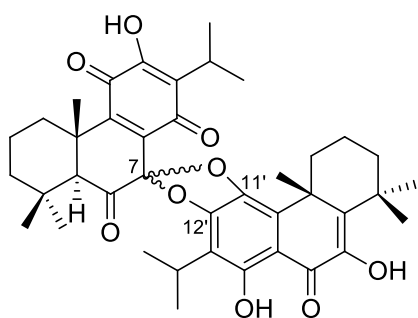


**Figure 3.6:** Structures of compounds 44-51

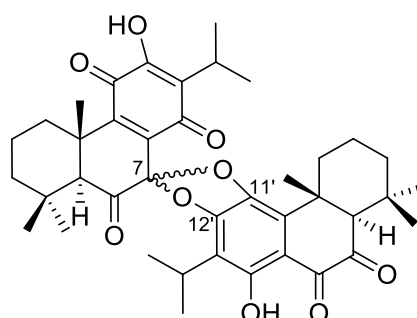
The seven royleanone type abietane dimers (**52-58**) isolated from *P. grandidentatus* consist of linking two abietanes either by carbon atoms (**54**) or oxygen atoms (**52, 53, 55, 56, 57** and **59**). The two molecules are linked from C-7 to C-7' (**54**), or C-7 to C11' and C-12' (**52, 53, 56** and **57**) or C-7 to C-14' (**55** and **58**). Additionally, compounds **56, 57**, and **58** are respectively epimers of compounds **52, 53**, and **55** as shown in Table 3.6 and Figure 3.7.

**Table 3.6:** Dimers isolated from Southern Africa *Plectranthus* species

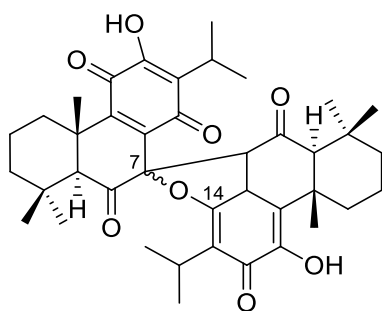
Plants	Isolated compounds	References
<i>P. grandidentatus</i>	Grandidone A ( <b>52</b> ) Grandidone B ( <b>53</b> ) Grandidone C ( <b>54</b> ) Grandidone D ( <b>55</b> ) 7-epigrandidone A ( <b>56</b> ) 7-epigrandidone B ( <b>57</b> ) 7-epigrandidone D ( <b>58</b> )	Teixeira et al., 1997.



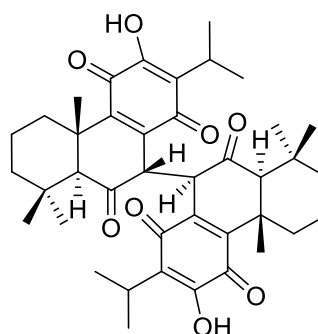
**52**  $\beta$ -C(7)-O-C(11')  
**56**  $\beta$ -C(7)-O-C(12')



**53**  $\beta$ -C(7)-O-C(11')  
**57**  $\beta$ -C(7)-O-C(12')



**55**  $\beta$ -C(7)-O-C(14)  
**58**  $\beta$ -C(7)-O-C(14)



**54**

**Figure 3.7:** Structures of compounds **52-58**

Six phenolic abietanes (**59-63**) were isolated from *P. elegans* (**59**) and *P. barbatus* (**60-63**). The abietatriene **59** bears a hydroxy group at C-6 and C-11 as well as a methoxy group at C-12. The difference between compounds **61** and **62** lies in the substitution at C-7 while the dissimilarity between the abietatriene bearing the 6, 20 epoxy group (**62** and **63**) lies on their substituents at C-6 and C-20 (Table 3.7, Figure 3.8).

**Table 3.7:** Phenolic abietane isolated from Southern Africa *Plectranthus* species

Plants	Isolated compounds	References
<i>P. elegans</i>	7 $\alpha$ ,11-dihydroxy-12-methoxy-8,11,13-abietatriene ( <b>59</b> )	Dellar et al., 1996
<i>P. barbatus</i>	Ferruginol ( <b>60</b> ) Sugiol ( <b>61</b> ) 20-deoxocarnosol ( <b>62</b> ) 6 $\beta$ -hydroxycarnosol ( <b>63</b> )	Alasbahi & Melzig, 2010.

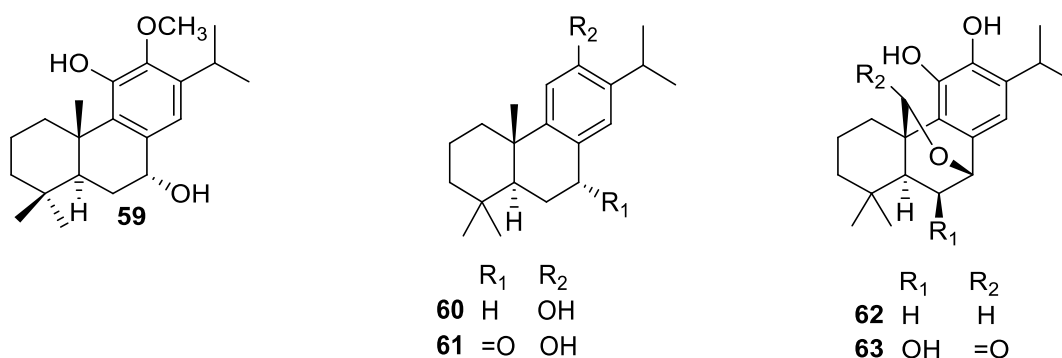


**Figure 3.8:** Structures of compounds **59-63**

From *P. barbatus*, two 6,7 seco-abietane diterpenoids (**64** and **65**) were isolated, as shown in Table 3.8 and Figure 3.9.

**Table 3.8:** Seco-abietane isolated from Southern Africa *Plectranthus* species

Plant	Isolated compounds	Reference
<i>P. barbatus</i>	6,7-secoabietane diterpene I ( <b>64</b> ) 6,7-secoabietane diterpene II ( <b>65</b> )	Alasbahi & Melzig, 2010.

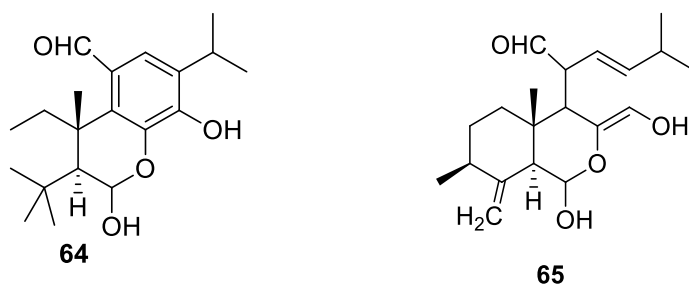


**Figure 3.9:** Structures of compounds **64** and **65**

Compounds **66** and **67** isolated from *P. ecklonii* are referred as dioxin quinone abietanes. Both compounds have a dibenzo-p-dioxin quinone ring, as well as an isopropanoate group at C-2, and alkyl groups at C1 and C-4 as substituents.

**Table 3.9:** Dioxin quinone abietanes isolated from Southern Africa *Plectranthus* species

Plants	Isolated compounds	References
<i>P. ecklonii</i>	Ecklonoquinone A ( <b>66</b> ) Ecklonoquinone B ( <b>67</b> )	Uchida et al., 1980.

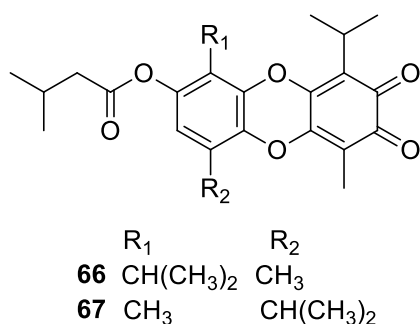


**Figure 3.10:** structures of compounds **66** and **67**

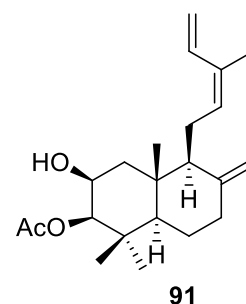
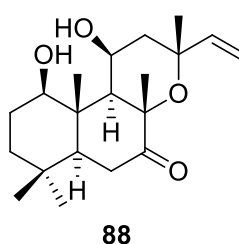
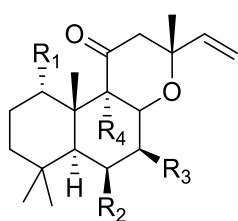
### 3.4.2 Labdane diterpenoids isolated from Southern Africa *Plectranthus* species

Thirty-two labdane diterpenoids (Table 3.10, Figure 3. 11) were isolated from four Southern Africa *Plectranthus* species, namely *P. barbatus* (**68-87**), *P. ernstii* (**70**), *P. fruticosus* (**73-79**) and *P. ornatus* (**117-120**). Compounds **68-87**, as well as compounds **118** and **119**, have a  $\delta$ -lactone group at C-8 and C-9 with an acetyl or a hydroxyl or an alkyl group at C-1, C-6, C-7, and C-9. The dissimilarity between these compounds lies in their stereochemistry, which is either *R* or *S*. Compounds **73-79** are differentiated by the orientation (*Z* or *E*) of the 3-methylpenta-1.3-diene at C-12. Compounds **117** and **120** are labdanes with a carboxylic group at C-15 and an olefinic group at C-13 and C-14.

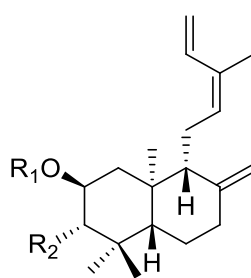
**Table 3.10:** Labdanes isolated from Southern Africa *Plectranthus* species

Plants	Isolated compounds	References
<i>P. barbatus</i>	Forskolin ( <b>68</b> ) 9-deoxyforskolin, ( <b>69</b> ) 1,9-dideoxyforskolin ( <b>70</b> ) 1,9 dideoxy-7-deacetylforskolin ( <b>71</b> ) Deacetyl-1-deoxyforskolin ( <b>72</b> ) 6-acetyl-1-deoxyforskolin ( <b>73</b> ) 6-acetyl-1,9-dideoxyforskolin ( <b>74</b> ) 1,6-di-O-acetyl-forskolin ( <b>75</b> ) Isoforskolin ( <b>76</b> ) 1,9-dideoxycoleonol B ( <b>77</b> ) 7-deacetyl-forskolin ( <b>78</b> ) Forskolin E ( <b>79</b> ) Forskolin F ( <b>80</b> ) Forskolin G ( <b>81</b> ) Forskolin H ( <b>82</b> ) Forskolin I ( <b>83</b> ) Forskolin J ( <b>84</b> ) Forskolin K ( <b>85</b> ) Forskolin L ( <b>86</b> ) Coleosol ( <b>87</b> )	Alasbahi & Melzig, 2010.
<i>P. ernstii</i>	1 <i>R</i> ,11 <i>S</i> -dihydroxy-8 <i>R</i> ,13 <i>R</i> -epoxylabd-14-ene ( <b>88</b> )	Stavri et al., 2009.
<i>P. fruticosus</i>	Ent-2 <i>α</i> -acetoxylabda-8(17),12 <i>Z</i> ,14-trien-3 <i>β</i> -ol ( <b>89</b> ) Ent-labda-8(17),12 <i>Z</i> ,14-trien-2 <i>α</i> -ol ( <b>90</b> ) 3 <i>β</i> -acetoxylabda-8(17),12 <i>E</i> ,14-trien-2 <i>α</i> -ol ( <b>91</b> ) Ent-2 <i>α</i> -acetoxylabda-8(17),12 <i>Z</i> ,14-triene ( <b>92</b> ) Ent-labda-8(17),12 <i>Z</i> ,14-triene-2 <i>α</i> ,3 <i>β</i> -diol ( <b>93</b> )	Gaspar-Marques et al., 2003; Gaspar-Marques et al., 2004.

	<i>Ent</i> -3 $\beta$ -acetoxylabda-8(17),12 <i>Z</i> ,14-trien-2 $\alpha$ -ol ( <b>94</b> )	
	<i>Ent</i> -labda-8(17),12 <i>Z</i> ,14-triene-2 $\alpha$ ,3 $\beta$ -dibenzoate ( <b>95</b> )	
<i>P. ornatus</i>	Labd-13-en-8 $\beta$ -hydroxy-15-oic acid ( <b>96</b> ) Plectornatin B ( <b>97</b> ) Plectornatin C ( <b>98</b> ) Rhinocerotinoic acid ( <b>99</b> )	Oliveira et al., 2005; Rijo et al., 2002; Rijo et al., 2007.



	R <sub>1</sub>	R <sub>2</sub>	R <sub>3</sub>	R <sub>4</sub>
<b>68</b>	OH	OH	OAc	OH
<b>69</b>	OH	OH	OAc	H
<b>70</b>	H	OH	OAc	H
<b>71</b>	H	OH	OH	H
<b>72</b>	H	OH	OH	OH
<b>73</b>	H	OAc	OAc	OH
<b>74</b>	H	OAc	OAc	H
<b>75</b>	OAc	OAc	OAc	OH
<b>76</b>	OAc	OH	OAc	OH
<b>77</b>	H	OAc	OH	H
<b>78</b>	OH	OH	OH	OH
<b>79</b>	OAc	OH	OAc	H
<b>80</b>	H	OH	OAc	OH
<b>81</b>	OH	OAc	OAc	H
<b>82</b>	OAc	OAc	H	H
<b>83</b>	OAc	OAc	OH	OH
<b>84</b>	OH	OAc	OAc	OH
<b>85</b>	OAc	OAc	OAc	H
<b>86</b>	H	OH	H	H
<b>87</b>	H	OH	H	OH



	R <sub>1</sub>	R <sub>2</sub>
<b>89</b>	Ac	OH
<b>90</b>	H	H
<b>92</b>	Ac	H
<b>93</b>	H	OH
<b>94</b>	H	OAc
<b>95</b>	COC <sub>6</sub> H <sub>5</sub>	COC <sub>6</sub> H <sub>5</sub>

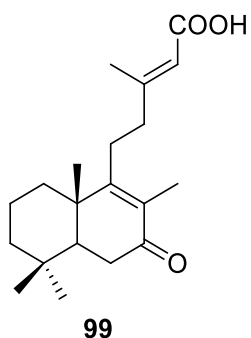
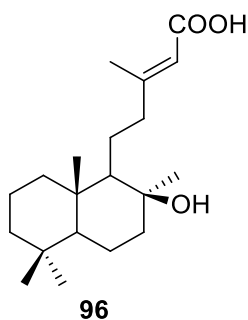
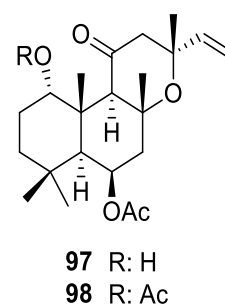


**Figure 3.11:** Structures of compounds **68-99**

### 3.4.3 Kaurane diterpenoids isolated from Southern Africa *Plectranthus* species

Twenty-one *ent*-kauranes diterpenes are isolated from *P. fruticosus* (100-116) and *P. strigosus* (117-120). The differences between these compounds lie on the substituents and functional group attached to the carbons at positions 15 and 16.

**Table 3.11:** Ent-kauranes isolated from Southern Africa *Plectranthus* species

Plants	Isolated compounds	References
<i>P. fruticosus</i>	<p><i>Ent</i>-15<math>\beta</math>,16<math>\beta</math>-epoxykauran-19-oic acid (100)</p> <p><i>Ent</i>-15<math>\beta</math>,16<math>\beta</math>-epoxykauran-19-ol (101)</p> <p><i>Ent</i>-12<math>\beta</math>-acetoxo-16-kauran-19-oic acid (102)</p> <p><i>Ent</i>-12<math>\beta</math>-acetoxo-15-kauran-19-oic acid (103)</p> <p>Methyl <i>ent</i>-12<math>\beta</math>-acetoxo-16-kauran-19-oate (104)</p> <p>Methyl <i>ent</i>-12<math>\beta</math>-acetoxo-15-kauran-19-oate (105)</p> <p>Methyl <i>ent</i>-15<math>\beta</math>,16<math>\beta</math>-epoxykauran-19-oate (106)</p> <p><i>Ent</i>-12<math>\beta</math>-acetoxo-15<math>\beta</math>-hydroxykaur-16-en-19-oic acid (107)</p> <p><i>Ent</i>-7<math>\beta</math>-hydroxykaur-15-en-19-oic acid (108)</p> <p><i>Ent</i>-12<math>\beta</math>-acetoxo-17-oxokaur-15-en-19-oic acid (109)</p> <p><i>Ent</i>-12<math>\beta</math>-acetoxo-7<math>\beta</math>-hydroxykaur-16-en-19-oic acid (110)</p> <p><i>Ent</i>-7<math>\beta</math>-Hydroxy-15<math>\beta</math>,16<math>\beta</math>-epoxykauran-19-oic acid (111)</p> <p>Ethyl <i>ent</i>-12<math>\beta</math>-hydroxykaur-16-en-19-oate (112)</p> <p>Methyl-<i>ent</i>-12<math>\beta</math>-acetoxo-7<math>\beta</math>-hydroxykaur-15-en-19-oate (113)</p> <p>Methyl-<i>ent</i>-12<math>\beta</math>-acetoxo-15<math>\beta</math>,16<math>\beta</math>-epoxykauran-19-oate (114)</p> <p>Methyl-<i>ent</i>-12<math>\beta</math>-acetoxo-15<math>\beta</math>-hydroxykaur-16-en-19-oate (115)</p> <p>Methyl <i>ent</i>-12<math>\beta</math>-acetoxo-17-oxokaur-15-en-19-oate (116)</p>	Gaspar-Marques et al., 2003; Gaspar-Marques et al., 2004.
<i>P. strigosus</i>	<p><i>Ent</i>-16-kauran-19-ol (117)</p> <p><i>Ent</i>-16-kauran-19-oic acid (118)</p> <p>Xylopic acid (119)</p> <p>Xylopinic acid (120)</p>	Gaspar-Marques et al., 2008.



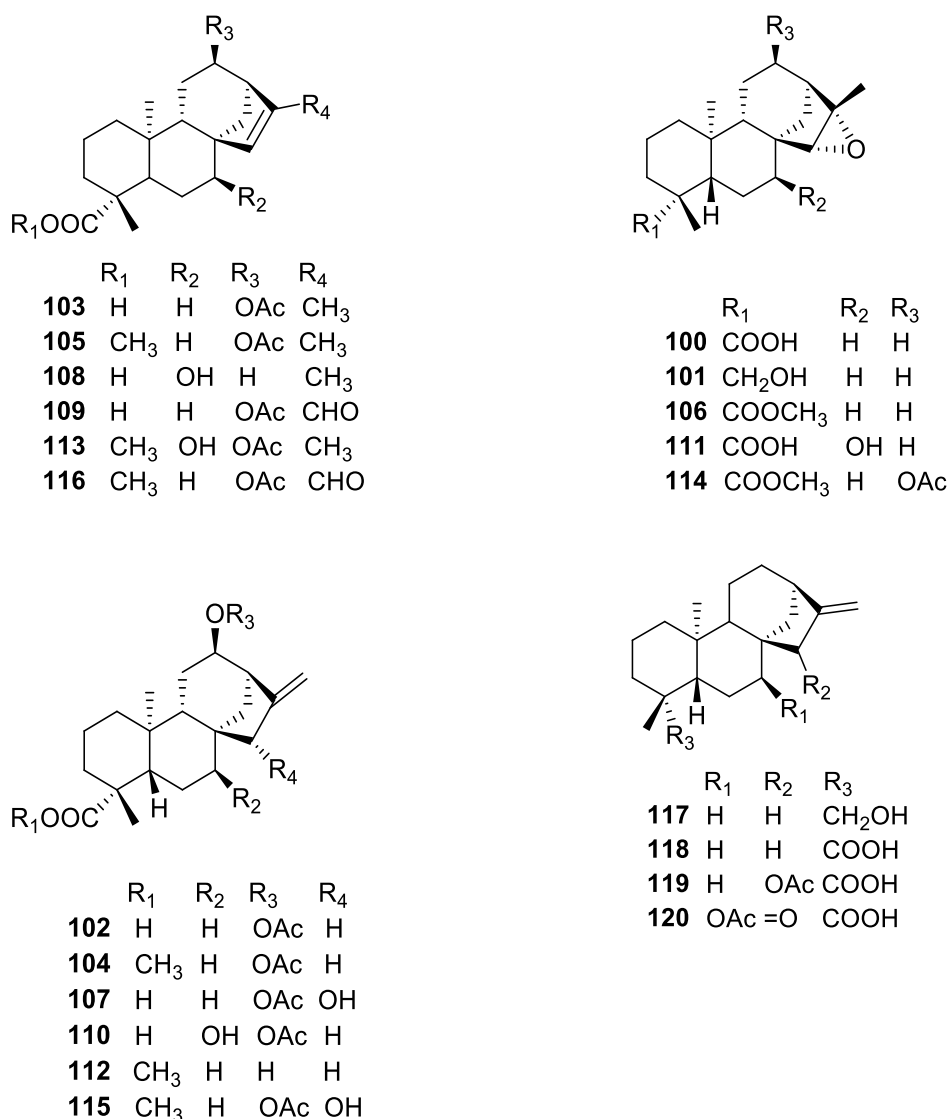


**Figure 3.12:** Structures of compounds 100-120

Seven phyllocladanes (13 $\beta$ -kauranes) were isolated from *P. ambiguus* (Table 3.12, Figure 3.13). Compounds **121-125** have esters group at C-2 and C-3 and sometimes at C-16 like compounds **122** and **124**. The only difference between compounds **126** and **127** is oriented to the substituent at C-2, which is an isobutanoate for compound **126** and a CH<sub>2</sub> for compound **127**.

**Table 3.12:** Phyllocladanes isolated from *Plectranthus* species

Plants	Isolated compounds	References
<i>P. ambiguus</i>	(16 <i>R</i> )-2 $\alpha$ -(3-methyl-2-butenoyloxy)-3 $\alpha$ -acetoxy-phylllocladane-16,17-diol ( <b>121</b> )	Liu & Ruedi, 1996: 1563-1568.
	(16 <i>R</i> )-2 $\alpha$ -(3-methyl-2-butenoyloxy)-3 $\alpha$ ,17-diacetoxy-16-hydroxyphylllocladane ( <b>122</b> )	
	(16 <i>R</i> )-2 $\alpha$ -(3-methylbutanoyloxy)-3 $\alpha$ -acetoxy-phylllocladane-16,17-diol ( <b>123</b> )	

	(16 <i>R</i> )-2 $\alpha$ -(3-methylbutanoyloxy)-3 $\beta$ ,17-diacetoxy-16-hydroxyphyllocladane ( <b>124</b> )	
	(16 <i>R</i> )-3 $\alpha$ -acetoxyphyllocladane-16,17-diol ( <b>125</b> )	
	(16 <i>R</i> )-2 $\alpha$ -(3-methyl-2-butenoyloxy)-16,17-dihydroxyphyllocladane-3-one ( <b>126</b> )	
	Calliterpenone ( <b>127</b> )	

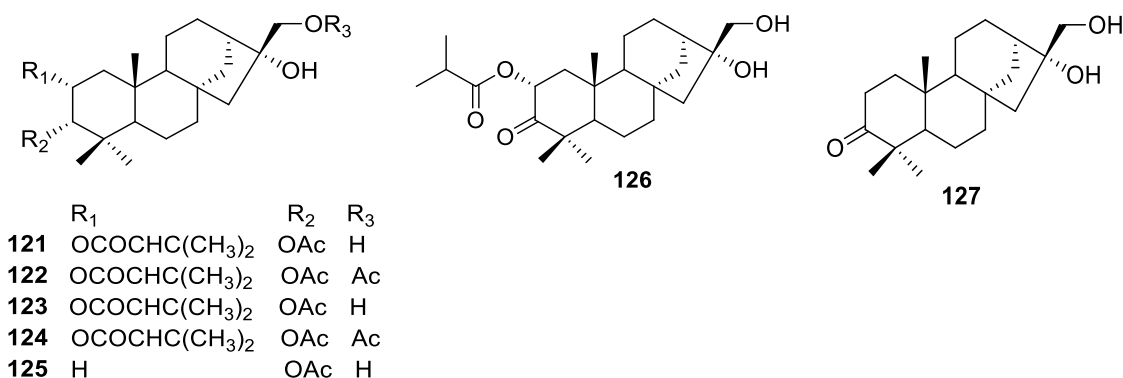


**Figure 3.13:** Structures of compounds **121-127**

#### 3.4.4 Clerodanes and halimane isolated from Southern Africa *Plectranthus* species

About Eight neoclerodane diterpenoids (**128-135**) and a halimane (**136**) diterpenoids were isolated from *P. ornatus* (Table 3.13, Figure 3.14). Compounds **128**, **130**, and **133** have the decalin skeleton while compounds **129**, **131**, and **135** have a cyclohexene skeleton as a ring A and cyclohexane as ring B. compound **132** and **134** are similar except that compound **132** has a cyclopentane skeleton as ring A whereas compound **134** has cyclopentene group as ring A.

**Table 3.13:** Clerodanes and halimanes isolated from Southern Africa *Plectranthus* species

Plants	Type of diterpenes	Isolated compounds	References
<i>P. ornatus</i>	Neoclerodanes	11 <i>R</i> -acetoxy-3 $\beta$ -hydroxycleroda-4(18), 13 <i>E</i> -dien-15-oic acid ( <b>128</b> ) 11-acetoxy-2-oxo-ent-cleroda-3,13 <i>E</i> -dien-15-oic acid ( <b>129</b> ) <i>Ent</i> -3 $\alpha$ -hydroxycleroda-4(18),13 <i>E</i> -dien-15-oic acid ( <b>130</b> ) Ornatins A ( <b>131</b> ) Ornatins B ( <b>132</b> ) Ornatins C ( <b>133</b> ) Ornatins D ( <b>134</b> )	Oliveira et al., 2005; Ávila et al., 2017.

		Ornatins E (135)	
	Halimane	11 <i>R</i> -acetoxyhalima-5,13 <i>E</i> -dien-15-oic acid (136)	Rijo et al., 2007.

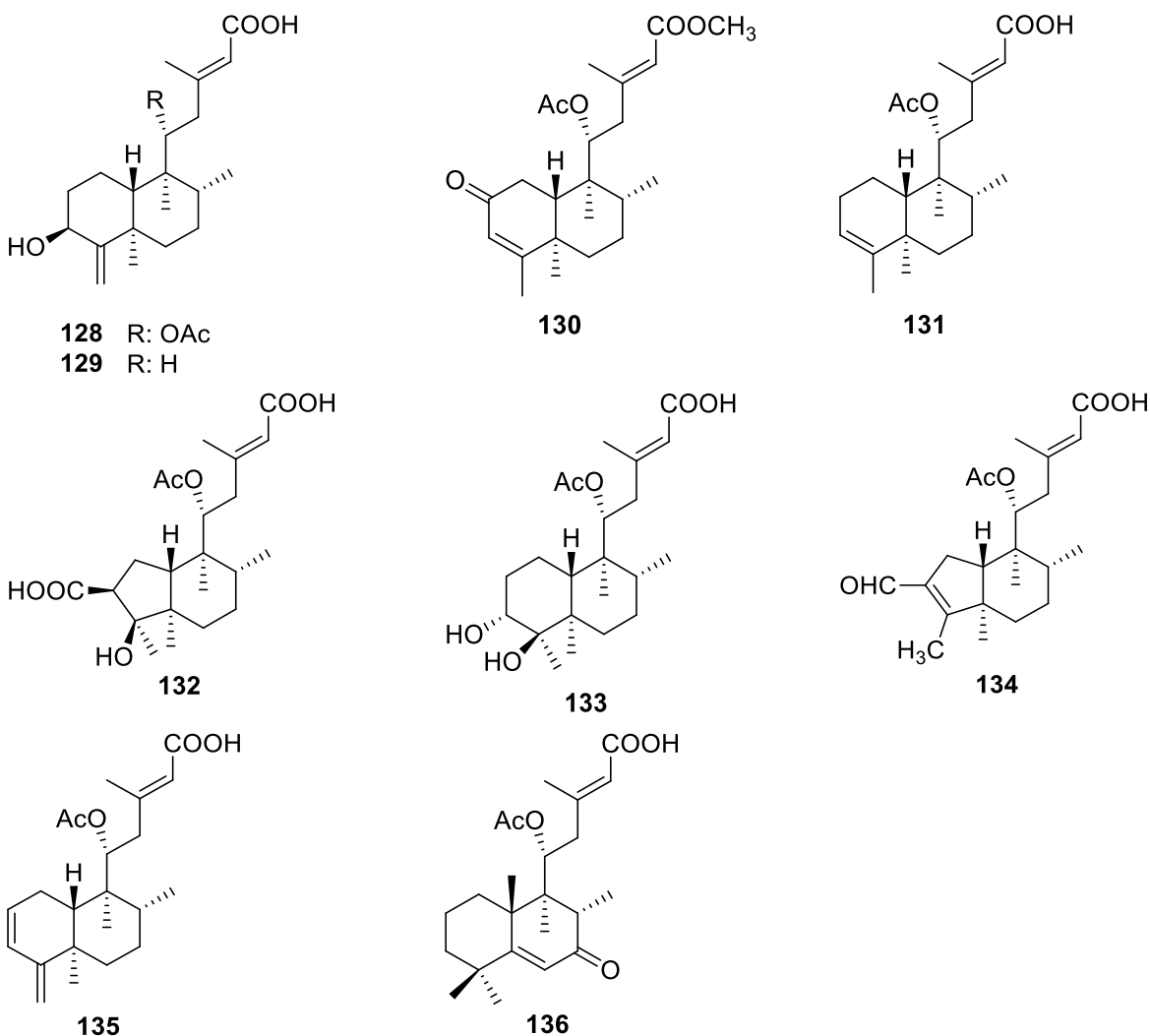


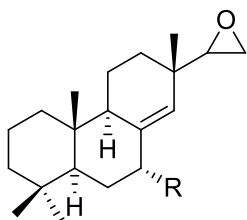
**Figure 3.14:** Structures of compounds **128-136**

### 3.4.5 Pimaranes and beyranes isolated from Southern Africa *Plectranthus* species

The pimarane diterpenoids **137** and **138** isolated from *P. ernstii* have an oxirane group attached to cyclohexene ring. Compound **137** has a hydroxy group at C-7, whereas compound **138** has a carbonyl group at that position (Table 3.14, Figure 3.15).

**Table 3.14:** Pimaranes isolated from Southern Africa *Plectranthus* species

Plants	Isolated compounds	Reference
<i>P. ernstii</i>	15( $\zeta$ ),16-epoxy-7 $\alpha$ -hydroxypimar-8,14-ene ( <b>137</b> ) -15( $\zeta$ ),16-epoxy-7-oxopimar-8,14-ene ( <b>138</b> )	Stavri et al., 2009.



137 R: OH

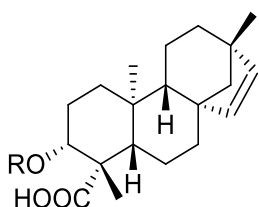
138 R: =O

**Figure 3.15:** Structures of compounds **137** and **138**

Three beyerane diterpenoids were isolated from *P. saccatus*. The compounds **139** and **140** have an ester group at C-3, and a carboxyl group at C-19, whereas compound **141** has a methanol group at C-18 (Table 3.15, Figure 3.16).

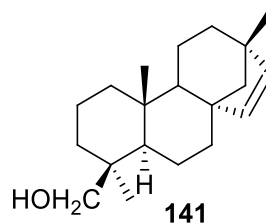
**Table 3.15:** Beyeranes isolated from Southern Africa species

Plants	Isolated compounds	References
<i>P. saccatus</i>	<i>Ent</i> -3 $\beta$ -(3-methyl-2-butenoyl)-oxy-15-beyeren-19-oic acid ( <b>139</b> ) <i>Ent</i> -3 $\beta$ -(3-methyl-butanoyl)-oxy-15-beyeren-19-oic acid ( <b>140</b> ) <i>Ent</i> -7 $\alpha$ -acetoxy-15-beyeren-18-oic acid ( <b>141</b> )	Wellsow et al., 2006; Simões et al., 2010.



139 R: COCHC(CH<sub>3</sub>)<sub>2</sub>

140 R: COCH<sub>2</sub>CH(CH<sub>3</sub>)<sub>2</sub>



141

**Figure 3.16:** Structures of compounds **139-141**

### 3.4.6 Essential oils

The genus *Plectranthus* is abundant in essential oils mainly made of monoterpenes and sesquiterpenes. Such volatile components are responsible for the herbaceous *Plectranthus* aromatic as well as therapeutic properties. For example, essential oils extracted from *Plectranthus* species are used in the making of perfume, shampoos, cream, soap, and deodorant due to their firm, pleasant and long-lasting smell, along with their antimicrobial, antioxidant and nematocidal properties (Ali et al., 2012; Marwah et al., 2007). The phytochemical analysis of *Plectranthus* essential oils via gas chromatography- flame-ionisation detectors (GC-FID) distinguished and identified the oil's major components or

types of terpenes present in them. Analysis of the essential oil of *P. amboinicus* collected in Crato and Fortaleza by Santos et al. (2016) showed that the composition of the plant oil differs from one region to another due to climate, type of soil, and the surrounding environment. For instance, the essential oil of *P. amboinicus* from Crato was mainly composed of germacrene (38.60%), *E*-caryophyllene (18.91%), and copaene (8.03%) whereas, the essential oil from the one collected in Fortaleza was rich in carvacrol (90.55%) and  $\beta$ -caryophyllene (3.09%).

Ascensao et al. (1998) investigations on *P. madagascariensis* essential oils extracted via distillation extraction and hydrodistillation from flowers and leaves revealed the presence of the orange-to-reddish crystalline diterpenoid 6,7-dehydroroyleanone. On the other hand, the essential oil of *P. fruticosus* is rich in sabinyl acetate (>50%), sabinene (20.28%) and bornyl acetate (12.81%) (Pages et al., 1991; Maistry, 2007).

Waldia et al. (2011) reviewed the volatile components and reported that  $\alpha$ -pinene, camphene, terpinen-4-ol,  $\alpha$ -cubebene, caryophyllene, germacrene D,  $\gamma$ -cadinene, thymol, ethyl salicylate, neral, chavicol, eugemol,  $\beta$ -phellandrene, geranyl acetate, farnesene, 1,8-cineole, isobornyl acetate, (*Z*)- $\beta$ -ocimene, carvacrol acetate, and piperitone epoxide are also present in other *Plectranthus* species. However, their abundance or presence in a plant depends on the genus plant's flowering and vegetative phases, as well as the parts harvested and provenance.

### 3.5 Ethnobotanical uses of Southern African *Plectranthus* species

A review on the ethnobotanical applications of the genus *Plectranthus* revealed that the stems, leaves, roots, and tubers of the *Plectranthus* species are used in folklore medicine in the treatment of wounds, skin infections, gastric disorders, infections and fever, genito-urinary conditions, muscular-skeletal conditions and pain as summarized in Table 3.18 (Maree et al., 2014; Lukhoba et al., 2006). The gastric disorders are the most common ailments healed by *Plectranthus* species as 21 out of the 62 studied *Plectranthus* species are used to treat gastric disorders (Brito et al., 2018).

*Plectranthus madagascariensis* is mostly used to treat respiratory and skin diseases, whereas the most widely used species of the genus *Plectranthus* are *P. barbatus* and *P. amboinicus*, which account for the 68% ethnobotanical usage of this genus. These two species have been used in thirteen categories as described in the Economic Botany Data Collection Standard (Rice et al., 2011; Cook, 1995). *P. laxiflorus* is used in the treatment of ten categories, while other Southern Africa *Plectranthus* species are applied in one to four groups as shown in Table 3.16 (Lukhoba et al., 2006).

**Table 3.16:** Summary of Southern Africa *Plectranthus* species' medicinal uses and biological activities.

<b>Species</b>	<b>Ethnomedicinal uses</b>	<b>Pharmacological properties</b>	<b>References</b>
<i>P. ambiguus</i>	Respiratory		Potgieter et al., 1999.
<i>P. amboinicus</i>	Respiratory veterinary	Antimicrobial Antiviral Anti-HIV inhibition Anti-tumour Anti-cancer Anti-expectorant	Rice et al., 2011; Lukhoba et al., 2006 Arumugam et al., 2016; Roshan et al., 2014.
<i>P. barbatus</i>	Digestive Liver complaints Skin Respiratory Infections/fevers Genito-urinary Pain Muscular-Skeletal Circulation and Blood Nervous Sensory Poison treatment Inflammation	Antibacterial Antiviral Antifungal Antiprotozoal Anti-tumour Anti-inflammatory Anti-feedant Anti-candida	Alasbahi & Melzig, 2010; Rice et al., 2011; Lukhoba et al., 2006.
<i>P. caninus</i>	Digestive Respiratory	Anti-tumour	Painuly & Tandon, 1983; Lukhoba et al., 2006.
<i>P. ecklonii</i>	Pain Fever Skin	Anti-bacterial Anti-fungal Anti-fever	Waldia et al., 2008; Rice et al., 2011.
<i>P. elegans</i>	Digestive Respiratory Urinary	Anti-bacterial Anti-fungal Anti-helminthic	Rice et al., 2011; Waldia et al., 2008.
<i>P. esculent</i>	Digestive Pain	Antibacterial	Lukhoba et al., 2006.
<i>P. fruticosus</i>	Skin	Antimicrobial	Gaspar-Marques et al., 2003.
<i>P. hadiensis</i>	Respiratory Digestive Skin Inflammatory	Antioxidant Antiplasmodial Anticancer	Hutchings et al., 1996; Muthukumarana & Dharmadasa, 2014; Laing et al., 2006; Van Zyl et al., 2008.
<i>P. hereroensis</i>	Digestive	Anti-viral Anti-bacterial	Batista et al., 1995.
<i>P. laxiflorus</i>	Digestive Skin Respiratory Infections/Fever Inflammation	Antimicrobial Antioxidant	Hutchings et al., 1996; Rabe & Van Staden, 1998; Lukhoba et al., 2006.

	Genito-urinary Pain Mouthwash Muscular-skeletal Nervous Sensory Veterinary (Cattle)		
<b><i>P. madagascariensis</i></b>	Respiratory Skin	Antibacterial Antioxidant	Rabe & Van Staden 1998; Lukhoba et al., 2006.
<b><i>P. Ornatus</i></b>	Skin	Antibacterial	Lukhoba et al., 2006.
<b><i>Saccatus</i></b>	N/A	Antifeedant	

### 3.6 Ethnopharmacological and pharmacological uses of Southern African *Plectranthus* species

#### 3.6.1 *Plectranthus amboinicus*

*P. amboinicus* is a medicinal plant known for its antioxidant, antiepileptic, diuretic, antimutagenic, antimicrobial, cytotoxic, radioprotective, anticlastogenic, anti-tumorigenic, antifeedant and antigenotoxic properties (Arumugam et al., 2016; Kazdan et al., 1981). An *in vivo* investigation done by Chiu et al. (2012) revealed that the plant possessed anti-inflammatory and analgesic properties while Gurgel et al. (2009) demonstrated that besides the anti-inflammatory activity, the plant possessed anti-tumor activity against Sarcoma-180 and Ehrlich ascites carcinoma. The *in vitro* work on this medicinal plant showed its antibacterial, antifungal, antioxidant, and antidandruff activities (Yulianto et al., 2016: 28-34). According to Yulinato et al. (2006), 7-acetoxy-6-hydroxyroyleanone is the compound responsible for the inhibition of MCF-7 cells leading to the cytotoxic activity. The essential oil extracted from the leaves was reported to have larvicidal inhibitory effect against *Anopheles gambiae* after 48 h (Prudent et al., 1995; Arumugam et al., 2016). Its ethyl acetate extract exhibited vigorous larvicidal activity against *Anopheles stephensi*, *Culex quinquefasciatus*, and *Aedes aegypti* (Baranitharan & Dhanasekaran, 2014). Whereas, the ethanolic extract showed antibacterial activity against *Proteus mirabilis*, *Escherichia coli*, *Klebsiella pneumonia*, *Staphylococcus aureus*, *Pseudomonas aeruginosa*, and *Proteus mirabilis*. In Cuba, a decoction of the leaves was used to inhibit the growth of *Mycobacterium tuberculosis* activity (Frame et al., 1998). Studies done on some of the *P. amboinicus* crude extracts have shown anti-HIV inhibition activity (Kusumoto et al., 1995) and antiviral activity against Herpes Simplex Virus-1 (Hattori et al., 1995).

### 3.6.2 *Plectranthus barbatus*

*P. barbatus* is the most studied and used *Plectranthus* species in both formal and informal medical system. This edible medicinal plant is used as food supplements, and the main components of its aqueous extracts viz rosmarinic acid, (16S)-Coleon E (**49**) and scutellarein 4'-methyl ether 7-O-glucuronide impact the crude antioxidant and antiacetylcholinesterase activities (Falé et al., 2009). Compound (**49**) is also known to prevent dental caries by inhibiting the glucosyltransferase activity and reduce biofilm formation of *Streptococcus mutans* and *Streptococcus sobrinus* that are the crucial factors for dental plaque formation or oral diseases (Figueiredo et al., 2010).

In Brazil, it is used as a substitute for *Peumus boldus* to treat gastritis and intestinal spasms as well as hepatic disorders (Alasbahi & Melzig, 2010). For instance, Silva et al. (2017) investigation on 3 $\beta$ -hydroxy-3-deoxybarbatusin (**19**) and barbatusol isolated from *P. barbatus* leaves showed their gastric effect in rats where oral administration (10mg/Kg) reduce the lesions by 96% and 76% respectively.

In Brazil, concoctions of *P. barbatus* leaves are used to treat the unpleasant psychological and physiological effects experienced by people in hangover state (Brito et al., 2018). In Central Africa, this plant is also used in the treatment of syphilis and as an emmenagogue, an aphrodisiac, and a contraceptive (Lukhoba et al., 2006).

### 3.6.3 *Plectranthus caninus*

The diterpenes and phenolic compounds isolated from the plant are responsible for the plant cytotoxic, diuretic, and antitumor properties (Painuly & Tandon, 1983; Aswal et al., 1984). Tadesse et al. (2011) investigations on *P. caninus* essentials oils showed the antibacterial, anti-inflammatory, anti-infective, and free radical scavenging activities of the volatile components of this medicinal plant.

### 3.6.4 *Plectranthus ecklonii*

The quinone methides abietane diterpenoids parvifloron D (**39**) and parvifloron F (**41**) isolated from *P. ecklonii* ethyl acetate extract displayed an inhibitory effect against *Listeria monocytogenes*, *Mycobacterium smegmatis*, *Mycobacterium tuberculosis*, *S. aureus*, *E. coli*, *E. faecalis* and *P. aeruginosa* (Nyila et al., 2009). Both compounds also demonstrated their anti-tyrosinase activity as well as their cytotoxic activity against Vero monkey kidney cell lines (Nyila et al., 2009). Compound (**41**) is also utilized as an antimalarial compound (Van Zyl et al., 2008). A study by Grayer et al. (2003) revealed the antifungal activities of the caffeic acid nepetoidin A and B against *Aspergillus niger*.



### 3.6.5 *Plectranthus elegans*

The chloroform crude extract of *P. elegans* reduces the growth of the spore germination of the fungus *Cladosporium cucumerinum* (Dellar et al., 1996). 11-hydroxy-12-oxo-7,9(II),13-abietatriene (**50**), and 7 $\alpha$ ,11-dihydroxy-12-methoxy-8,11,13-abietatriene (**59**) showed antibacterial activity against *B. subtilis*, *S. aureus*, and *Streptomyces scabies*.

### 3.6.6 *Plectranthus ernstii*

The pimarane 15( $\zeta$ ),16-epoxy-7 $\alpha$ -hydroxypimar-8,14-ene (**137**) showed moderate inhibition against methicillin-resistant and different multidrug-resistant strains of *S. aureus* (Stavri et al., 2009). Additionally, 1*R*,11*S*-dihydroxy-8*R*,13*R*-epoxylabd-14-ene (**88**), 15( $\zeta$ ),16-epoxy-7 $\alpha$ -hydroxypimar-8,14-ene (**137**) and *rel*-15( $\zeta$ ),16-epoxy-7-oxopimar-8,14-ene (**138**) exhibited antimycobacterial activity against *M. fortuitum*, *M. phlei*, and *M. smegmatis*.

### 3.6.7 *Plectranthus esculentus*

In Eastern and Southern Africa, *P. esculentus* is used to alleviate headaches and fever (Rice et al., 2011; Roshan et al., 2014). It is also stated to have anthelmintic activity (Kokwaro, 1993: 325-380).

### 3.6.8 *Plectranthus fruticosus*

*P. fruticosus* is used in Rome to treat burns (Lukhoba et al., 2006). Sabinyl acetate, being the main component of *P. fruticosus* essential oil, gives the rich oil a highly foetotoxic and teratogenic effect (Fournier et al., 1986). From all the kauranes isolated from the plant, only *ent*-15 $\beta$ ,16 $\beta$ -epoxykauran-19-oic acid (**100**), and methyl *ent*-12 $\beta$ -acetoxy-17-oxokaur-15-en-19-oate (**109**) showed moderate activity against *S. aureus* (Gaspar-marques et al., 2003).

### 3.6.9 *Plectranthus grandidentatus*

Review done by Cerqueira et al. (2004) on the genus *Plectranthus*, indicated that the coleon and royleanones abietane diterpenoid isolated from *P. grandidentatus* are responsible for the plant's antifungal, antibacterial, and antitumor activities. For example, coleon U (**45**), 7 $\alpha$ -acetoxy,6 $\beta$ -hydroxyroyleanone (**7**), and horminone (**8**) reduce the growth of vancomycin-resistant *Enterococcus faecalis* (VRE) and methicillin-resistant *S. aureus* (MRSA) bacteria (Gaspar-Marques et al., 2006). These abietane diterpenoids also isolated from the genus *Salvia* were proven to have antitumor, cytotoxic, antioxidant, and antibacterial activities (Kinouchi et al., 2000; Mei et al., 2002). Cerqueira et al. (2004) investigations on *P. grandidentatus*, demonstrated the high capacity of compounds (**45**)

and (7) to inhibit the spreading of B and T-lymphocytes induced by mitogens, inhibiting preferentially T-cell population.

#### **3.6.10 *Plectranthus hadiensis***

The hexane extract of *P. hadiensis* showed a good inhibitory effect against the fungus *Rhizoctonia solani* and *Sclerotinia sclerotiorum*, whereas the dichloromethane extract exhibited moderate activity against the fungi *S. sclerotiorum*, the bacteria *B. subtilis* and *Xanthomonas campestris* (Laing et al., 2006). The royleanones **7** and **13** isolated from the dichloromethane extract of the plant's aerial parts showed anticancer activity against MCF-7, NCI-H460, TK-10, UACC-62, and SF-268 cells lines (Gaspar-Marques et al., 2002). However, these two compounds were less potent than Cyclosporin A (Positive control). Compounds **7** and **16** were reported to possess antiplasmodial activity against FRC-3 with MIC of 3.11 $\mu$ M and 4.6 $\mu$ M respectively (Van Zyl et al., 2008; Bero & Fre, 2009; Amoa Onguéné et al., 2013).

#### **3.6.11 *Plectranthus hereroensis***

The royleanones 16-acetoxy-7 $\alpha$ ,12-dihydroxy-8,12-abietadiene-II,14-dione (**10**), exhibited bacterial inhibition effect against *Vibrio cholerae* and *S. aureus* (Batista et al., 1995: 167-169). Compound (**10**) was revealed to be an active antiviral agent against Herpes simplex type II (Batista et al., 1995). Compound **8** isolated from the acetone extract of the root of *P. hereroensis* was stated to be antimicrobial agents against *Candida albicans*, *P. aeruginosa*, *S. aureus*, and *V. cholerae*.

#### **3.6.12 *Plectranthus laxiflorus***

*P. laxiflorus* is rubbed onto the skin in the treatment of leprosy, rheumatism, and abdominal pain (Lukhoba et al., 2006: 1-24). In South Africa, tea made from the leaves is used to cure coughs and colds (Bhatt et al., 2010; Rabe & Van Staden, 1998). *P. laxiflorus* and *P. barbatus* are both used as laxatives and mouthwash for teeth and gum disorders (Bhatt et al., 2010; Alasbahi & Melzig, 2010). Traditionally, the Pokot people in Kenya applied it as an enema for the treatment of influenza (Lukhoba et al., 2006), abdominal pain, and feverishness (Rabe & Van Staden, 1998). Some local people used *P. laxiflorus* as a contraceptive (Lukhoba et al., 2006). Infusion of its crushed root is used to treat gall illness and as a mouthwash for loose and bleeding teeth (Rice et al., 2011; Hulme, 1954). Hutchings et al. (1996) investigations revealed that crushed leaves and stems of the plant are used to treat eye complaints and to repel mosquitoes. A combination of the bark and root concoction is used against redwater (Masika & Afolayan, 2003).

### 3.6.13 *Plectranthus madagascariensis*

In folklore medicine, *P. madagascariensis* is used for scabies and small wounds as well as in the treatment of colds, asthma, cough, and chest complaints (Rabe & Staden, 1998). Kubínová et al. (2014) reported that the plant extract was an effective inhibitor of  $\alpha$ -glucosidase and butyrylcholinesterase (BuChE) due to the presence of 7 $\beta$ -acetoxy, 6 $\beta$ -hydroxyroyleanone (**15**), and rosmarinic acid. The extract containing the compound (**15**) was stated to have antibacterial activity against *S. aureus* and *E. faecalis*, as well as antifeedant effects (Wellsow et al., 2006). Coleon U quinone (**17**) isolated from *P. madagascariensis* leaves was revealed to be efficacious against the gram-negative bacteria *Pseudomonas syringae* and the gram-positive bacteria *Bacillus subtilis* (Wellsow et al., 2006). Compounds (**7**) and (**13**) exhibited high selectivity for lung cancer cells (Diogo et al., 2019).

### 3.6.14 *Plectranthus Ornatus*

In Brazil, *P. ornatus* leaves were indigenously utilized to treat skin infections (Brasileiro et al., 2006). *Ent-3 $\alpha$ -hydroxycyclo-4(18),13E-dien-15-oic acid* (**130**), ornatin C (**133**), ornatin D (**134**), and coleon R (**28**) showed mild activity against *S. aureus* (Ávila et al., 2017). Ornatin E (**135**) inhibited *Staphylococcus epidermidis* (Ávila et al., 2017); whereas, Plectronatin B and C (**97 and 98**) moderately reduced the growth of the bacteria *Candida albicans* (Rijo et al., 2002). The halimane **136** possessed antibacterial activities against five *S. aureus* strains and two *E. faecalis* strains (Rijo et al., 2011). Compound **136** was also effective against *Enterococcus flavescens* and *enterococcus faecium* (Rijo et al., 2011), whereas the labdane rhinocerotinoic acid (**99**) is known as an anti-inflammatory compound (Dekker et al., 1988: 33-35).

### 3.6.15 *Plectranthus porcatus*

The cycloabietane isolated from *P. porcatus* (13S,15S)-6 $\beta$ ,7 $\alpha$ ,12 $\alpha$ ,19-tetrahydroxy-13 $\beta$ ,16-cyclo-8-abietene-11,14-dione (**30**) exhibited feeble antibacterial activity against *S. aureus* (Simões et al., 2010).

### 3.6.16 *Plectranthus Saccatus*

The beyerane diterpenoid *ent-3 $\beta$ -(3-methyl-2-butanoyl)-oxy-15-beyeren-19-oic acid* (**139**), was revealed to have antifeedant activity against *Spodoptera littoralis* (Wellsow et al., 2006).

### 3.6.17 *Plectranthus strigosus*

The kaurane *ent-16-kauren-19-ol* (**117**) and *ent-16-kauren-19-oic acid* (**118**), were revealed to have an antiherpetic property (Gasper-Marques et al., 2008).

### 3.7 Other uses

Some of the Southern African *Plectranthus* species have also been used as food, food additives, insect repellent, material to drive away evil spirits and for horticultural purposes, as presented in Table 3.17.

**Table 3.17:** Other uses of Southern African *Plectranthus* species

<i>Plectranthus</i> species	Uses	References
<i>P. amboinicus</i>	Food (Vegetables)  Food additives (Food stuffings; mask the odour of strong smells associated with fish, goat, and shellfish; and spices dishes containing tomato)  Insect repellent	Morton, 1992; Prudent et al., 1995; Lukhoba et al., 2006. .
<i>P. barbatus</i>	Horticulture  Food (vegetables)	Fleurentin et al., 1983; Lukhoba et al., 2006.
<i>P. ecklonii</i> <i>P. elegans</i> <i>P. madagascariensis</i>	Horticulture	Lukhoba et al., 2006.
<i>P. esculentus</i>	Food (starch, minerals and vitamin A)  Food additives (to sweeten porridge)	Lukhoba et al., 2006.
<i>P. fruticosus</i>	Fly repellent	Roberts, 1990.
<i>P. hadiensis</i>	Fodder (to feed rock rabbits in Tanzania)  Fish poison  Charm	Hutchings et al., 1996; Lukhoba et al., 2006.
<i>P. laxiflorus</i>	Food (vegetable)  Mosquito repellent  Materials (to drive away evil spirits in India, Kenya, and Tanzania)	

## CHAPTER FOUR

### EXTRACTION ISOLATION AND CHARACTERIZATION OF *PLECTRANTHUS MADAGASCARIENSIS* NATURAL PRODUCTS

#### 4.1 Introduction

The phytochemical study of *Plectranthus madagascariensis* extract was carried out using various chromatographic methods such as thin layer chromatography (TLC), Sephadex LH-20, Preparative TLC (prep-TLC), semi-preparative high performance liquid chromatography (semi-prep HPLC) as well as silica gel 60 column chromatography. The solvent system used for these chromatography techniques were determined according to the extracts constituent's migration over the TLC plates or on how the solvent and the solutes interact in the column in the case of semi-prep HPLC. The characterization and structure elucidation were conducted using spectroscopy techniques and methods such as nuclear magnetic resonances spectroscopy (NMR), infrared spectroscopy (IR), ultraviolet spectroscopy (UV), X-ray spectroscopy and optical rotation spectroscopy.

This chapter is organized into eight sections. The materials and methods used in the extraction, isolation, and characterization of the *P. madagascariensis* components are given in section 4.2. Section 4.3 details the sample collection parameters, while section 4.4 emphasizes the extraction of the bioactive compounds. Sections 4.5 and 4.6 focus respectively on the isolation and characterisation of *P. madagascariensis* natural products. The spectroscopic data characteristics of *P. madagascariensis* constituents are discussed in section 4.7. A brief conclusion of the chapter outcomes is given in section 4.8.

#### 4.2 Materials and Methods

##### 4.2.1 General Reagents

The solvents used in the research study were purified via distillation except for the deuterated and HPLC grade solvents (Table 4.1). Different solvents and reagents used are tabulated in the following Table.

**Table 4.1:** Solvent and reagents used in the research study

Solvents	Supplier
Hexane	Kimix, Cape Town, SA
Ethyl acetate	Kimix, Cape Town, SA
Methanol	Kimix, Cape Town, SA
HPLC acetonitrile	Sigma, Aldrich Cape Town, SA

HPLC methanol	Merck, Cape Town, SA
Methanol	Kimix, Cape Town, SA
Dichloromethane	Kimxi, Cape Town, SA
Deuterated chloroform	Merck, Cape Town, SA
Sulphuric acid	Sigma, Aldrich, Cape Town, SA
Vanillin	Sigma, Aldrich, Cape Town, SA
Deuterated methanol	Merck, Cape Town, SA

## 4.2.2 Chromatographic methods

### 4.2.2.1 Thin-layer chromatography (TLC)

TLC analysis was done on a precoated silica gel 60 F<sub>254</sub> aluminum plates (Merck, Germany). A small amount of each sample was diluted in methanol/dichloromethane (MeOH/DCM) and spotted on the TLC plate before their development in the mobile phase solvent system of different polarities (Table 4.2). Afterward, the plate was exposed to ultraviolet (UV, CAMAG) light at wavelengths 254 and 366 nm to detect the compounds with conjugated double bonds before spraying with vanillin/sulphuric acid reagent and heating at 100 °C for five minutes (Wagner et al., 1984). By heating the plate, the compounds with and without conjugated bonds were visualized and identified.

**Table 4.2:** TLC solvent systems used in the study

Solvent systems	Ratio	TLC Solvent system code
Hexane: Ethyl acetate	90:10	A
	85:15	B
	80:20	C
Dichloromethane (DCM): Methanol (MeOH)	99:1	D
	98:2	E
	95:5	F

### 4.2.2.2 Preparation of the spray reagent

The vanillin/sulphuric acid reagent spray was prepared by dissolving 15 g of vanillin in 250 mL of absolute ethanol, and 2.5 mL of concentrated sulphuric acid was carefully added.

### 4.2.2.3 Preparative thin-layer chromatography (prep-TLC)

Preparative TLC analysis was done by spotting the sample across a glass TLC plate coated with silica gel 60 F<sub>254</sub> (Merck, Germany). The target components were visualized

and identified under the UV lamp as bands, scraped from the TLC plates, and recovered from the silica using a MeOH and DCM mixture.

#### **4.2.2.4 Column chromatography**

Glass columns of different diameters and lengths were packed with either silica gel 60 [(0.040-0.063 $\mu$ m), (230-400 mesh)], or with Sephadex LH-20. The Sephadex LH-20 was used in the case of size exclusion chromatography, whereas the silica gel 60 was used for normal phase chromatography. Different solvent systems with different polarities were used as mobile phase "eluent". During the process, the volume of eluent collected depended on the quantity of the starting material.

#### **4.2.2.5 Semi-preparative high-performance liquid chromatography (semi-prep HPLC)**

A Shimadzu HPLC was used to profile crude extracts and purify their chemical constituents. The purification process was conducted by filtering the sample dissolved in 100% HPLC grade methanol with 0.2-micron Whatman GD/X syringe filters to remove insoluble residue or particles. 50  $\mu$ L of the dissolved sample was injected in an HPLC grade acetonitrile and deionized water of increasing polarity and pumped into a Supelco C18 column (25 x 1 cm, 5  $\mu$ m) by LC-20AB binary pump at a flow rate of 1.5 mL/min for an hour. For more proficient purification, the column temperature was regulated by the column oven CTO-10AD VP at approximately 40 °C. The target compounds were detected by the highly sensitive SPD-M20A UV/VIS detector that operated at wavelengths 254, 272, and 366 nm. The collection of the compound(s) peak(s) was done manually.

### **4.2.3 Spectroscopic methods**

#### **4.2.3.1 Nuclear Magnetic Resonance Spectroscopy (NMR)**

The NMR analysis was recorded on a Bruker 400 MHz FT-NMR spectrometer. The chemical shifts were reported in part per million (ppm) relative to tetramethylsilane (TMS) as standard. The splitting pattern of the isolated compounds protons are presented in terms of broad (*br*), singlet (*s*), doublet (*d*), triplet (*t*), quartet (*q*), multiplet (*m*), double of triplets (*dt*), etc. The coupling constants (*J*) are reported in Hz.

#### **4.2.3.2 Single crystal X-ray analysis**

The phi scan and omega scan techniques were used to generate the Single-crystal X-ray intensity data of compound **II** which was collected on a Bruker Kappa Duo Apex II diffractometer using graphite monochromated Mo K $\alpha$  radiation with a wavelength of 0.71073 Å at 173K (Bruker, 2005). An oxford cryostream cooling system with N<sub>2</sub> gas at a flowrate of 20 cm<sup>3</sup>/min, was used to control the temperature. The Bruker SAINT-Plus

Software (Madison , USA) was used to scale and reduce the data while the multi-scan method (SADABS) was used to correct data for absorption effects (Sheldrick, 1997). The Sheldrick (2008; 2015) software, namely SHELXS was operated within the X-seed interface (Barbour, 2001) and used to solve and refine the structure. The crystal system was established by observing the Laue symmetry of the diffraction pattern, while the space group was determined by utilizing the predetermined cell parameters and collected intensities as inputs to the program XPREP (Bruker, 1997). The hydrogen atoms were geometrically constrained except for those involved in hydrogen bonding, which were found in the electron density map and refined isotropically.

#### **4.2.3.3 Fourier Transform Infrared Spectroscopy (FTIR)**

A Perkin-elmer fourier Transform infrared spectrophotometer (UATR two) was used to support compound structures and confirm the absence or presence of specific functional groups in the studied extract.

#### **4.2.3.4 Optical rotation measurements**

Anton Paar MCP 200 Polarimeter was used to measure the optical activity of the isolated compounds (0.1 g/mL in DCM) with a wavelength of 589 nm at 25 °C.

#### **4.2.3.5 Melting point**

The melting point apparatus, analogue SMP 11, was used to measure the melting point of the isolated crystals. The samples were heated up to 10 °C/min to the samples melting temperatures which were measured with a thermometer ranging from 1-300 °C.

#### **4.2.3.6 Ultraviolet (UV) Spectroscopy**

A SPECTRO star Nano Absorbance Reader (BMG LABTECH) was used to determine the UV-visible absorbance maxima of each compound from wavelengths 200 to 950 nm.

### **4.3 Plant sample collection**

The aerial parts of *P. madagascariensis* were collected at the Cape Peninsula University of Technology (Bellville Campus) student center in January 2018 and identified by Prof. Christopher Cupido of Fort Hare University.

### **4.4 Extraction of plant sample**

The fresh aerial parts of *P. madagascariensis* (2448.3 g) were cut into pieces and macerated in about 2 L of a solution made of hexane, dichloromethane, and acetone (2:2:1) for one hour under frequent swirling at room temperature. The mixture underwent vacuum filtration using Whatman filter paper yielding the dark orange filtrate which was



concentrated to dryness using Buchi Rotavapor R-300 at 45 °C and 14 mbar. The dark orange solid (K4-1-Hex) was weighed (13 g) and transferred into a sample vial which was kept in the fridge to prevent decomposition of compounds until ready for further analysis.

#### 4.5 Isolation of *P. madagascariensis* constituents

##### 4.5.1 Column chromatography of the total extract

The total extract (13 g) was subjected to silica gel (Merck 60, 0.040-0.063 mm) column chromatography using hexane and ethyl acetate gradient of increasing polarity resulting in the collection of 61 fractions of 250 mL each (Table 4.3).

**Table 4.3:** The solvent systems used during the total extract fractionation

Volume of solvent	Solvent system	Fractions (250 mL)
1 L	Hexane 100	1-4
2 L	Hexane: Ethyl acetate 95:5	5-12
2 L	Hexane: Ethyl acetate 93:7	13-21
1.5 L	Hexane: Ethyl acetate 89:11	22-28
1.5 L	Hexane: Ethyl acetate 95:15	29-35
1.5 L	Hexane: Ethyl acetate 80:20	36-42
1 L	Hexane: Ethyl acetate 75:25	43-46
1 L	Hexane: Ethyl acetate 70:30	47-50
1 L	Hexane: Ethyl acetate 60:40	51-54
1 L	Hexane: Ethyl acetate 50:50	55-58
1 L	Methanol 100	59-61

The collected fractions were concentrated to 2 to 3 mL using rota evaporator and were monitored with TLC using solvent systems A, B, and C. Fractions with similar retention factors, color, and UV characteristics were combined and given codes with roman numbers. Thus, generating 16 combined fractions which were weighed and subjected to TLC using solvent systems B and E, as shown in Figures 4.1, 4.2, and 4.3 as well as in Table 4.4.

**Table 4.4:** Summary of the main fractions code, weights, and TLC solvent systems

Fractions (250 mL)	Combined fractions code	Weight of portions (g)	TLC Solvent systems
1-5	K4-3-I	0.0052	B
6-10	K4-3-II	0.1264	
11-14	K4-3-III	0.0908	

15-21	K4-3-IV	0.2099	B and E
22-24	K4-3-V	0.3097	
25-28	K4-3-VI	1.2397	
29-32	K4-3-VII	1.3729	
33-35	K4-3-VIII	0.9761	
36-39	K4-3-IX	0.4564	
40-42	K4-3-X	0.3693	
43-47	K4-3-XI	0.6221	
48-53	K4-3-XII	0.3772	
54-56	K4-3-XIII	0.1577	
57-59	K4-3-XIV	0.3799	
60	K4-3-XV	0.4963	
61	K4-3-XVI	0.8345	

Figures 4.1, 4.2, and 4.3 are representative of the main fractions TLC profile after spraying with vanillin/sulphuric acid under UV light at wavelength 254 nm and 366 nm.

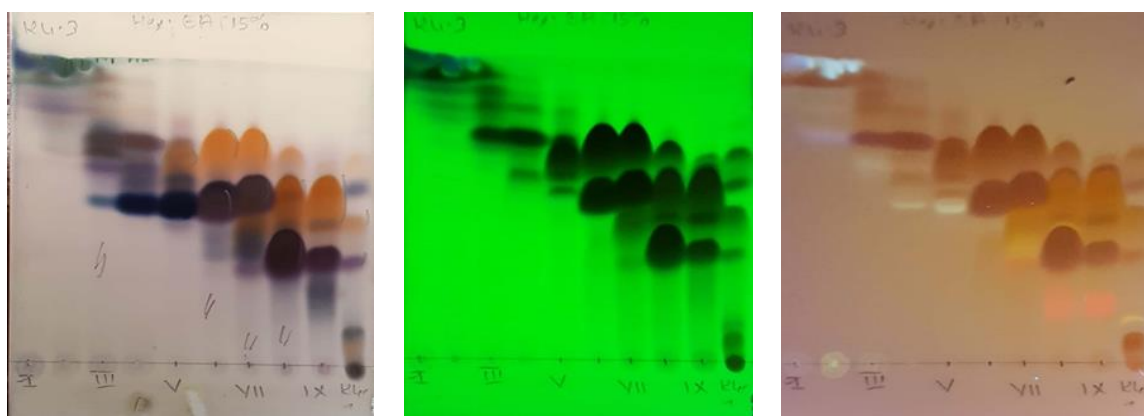


**Figure 4.1:** TLC profile of K4-3-I to K4-3-IX fractions using solvent system B as mobile phase

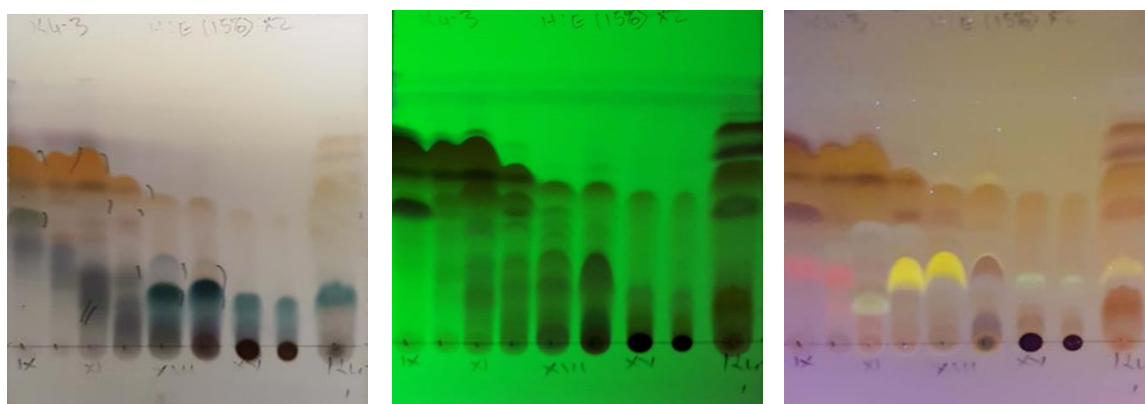


**Figure 4.2:** TLC profile of K4-3-IX to K4-3-XVI fractions using solvent system B as mobile phase

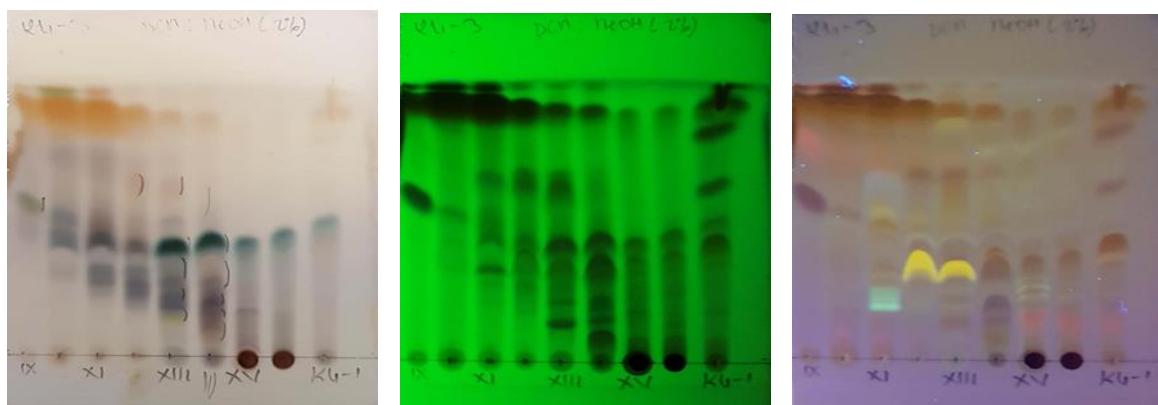


**Figure 4.3:** TLC profile of K4-3-IX to K4-3-XVI fractions using solvent system E as mobile phase

#### 4.5.2 Isolation of *P. madagascariensis* secondary metabolites

From the 16 main fractions, only fractions K4-3-III, K4-3-IV, K4-3-VI, K4-3-VIII, K4-3-XI, K4-3-XIII and K4-3-XIV were further purified. The remaining fractions were not considered due to their similarities with the selected subfractions except fractions K4-3-I and K4-3-II which did not show interesting bioassay results.

Most purifications were carried out with Sephadex LH-20 using 95% MeOH and 5% deionised water (H<sub>2</sub>O). However, the purification process of some fractions also required the use of prep-TLC, semi-prep-HPLC as well as deactivated silica gel 60 (prepared with silica gel and 10% w/v of H<sub>2</sub>O) column chromatography. All the chromatography methods used during the purification process of the isolated compounds were monitored with TLC.

##### 4.5.2.1 Processing of fraction K4-3-VIII and isolation of compound I

Fraction K4-3-VIII (97 mg) was subjected to Sephadex LH-20 and eluted with MeOH and H<sub>2</sub>O (95:5). The fractionation of K4-3-VIII produced seven subfractions (K4-7-1 to K4-7-7). Subfraction K4-7-3 (29.8 mg) was further purified by going through an isocratic silica gel column chromatography using Hexane and ethyl acetate (95:5). The column chromatography process results in the pure single compound (**I**, 25.7 mg) (Figure 4.4).

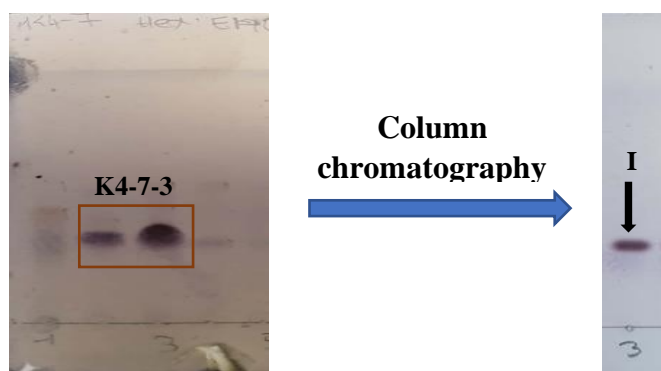


**Figure 4.4:** TLC profile of compound I

#### 4.5.2.2 Processing of fraction K4-3- VI and isolation of compound II as well as the Compound VI & VII

Fraction K4-3-VI (200 mg) was subjected to Sephadex LH-20 using 95% MeOH and 5% H<sub>2</sub>O producing in the process seven sub-fractions (K4-5-1 to K4-5-7). Subfractions K4-5-2 and K4-5-3 as well as subfractions K4-5-6 and K4-5-7 were combined and underwent isocratic silica gel column chromatography using hexane and ethyl acetate (98:2). The isocratic column chromatography of K4-5-2 & 3 (74 mg) resulted in the isolation of the pure compound II (61.9 mg). Whereas the isocratic column chromatography of K4-5-6 & 7 (64.2 mg) yielded the mixture (VI & VII) which appeared as a single spot on TLC (Figure 4.5).

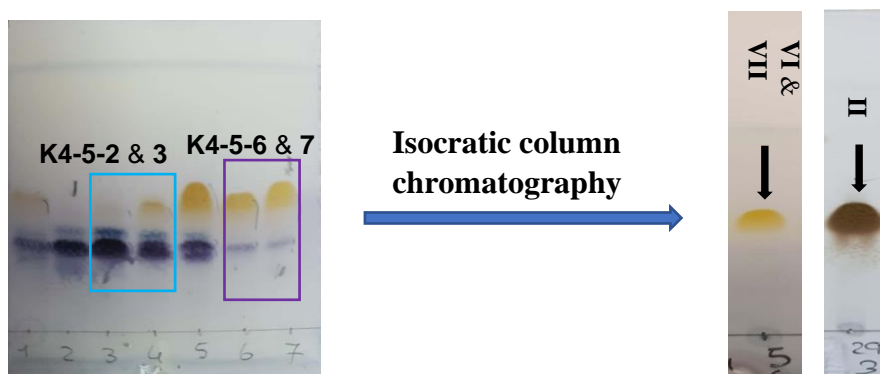


**Figure 4.5:** TLC profile of subfractions K4-5, compound II and the mixture VI & VII

#### 4.5.2.3 Processing of fraction K4-3-III & IV and isolation of compound III

Main fractions K4-3-III (0.0908 g) and K4-3-IV (0.01982 g) were merged (K3-3-III & IV) and subjected to isocratic column chromatography using deactivated silica gel 60 and Hexane: ethyl acetate (90:10) as eluent. The fractionation of the main fraction K4-3-III & IV (0.2890 g) yielded 38 sub-fractions which were collected (50 mL each) and pooled together according to their TLC profiles to finally generate six subfractions (K4-19-1 to K4-19-6) as pointed out in Figure 4.4. Sub-fraction K4-19-4 (60 mg) was applied to four prep-TLC plates and developed twice in Hexane: ethyl acetate (90:10) solvent system to yield compound III (Figure 4.6).

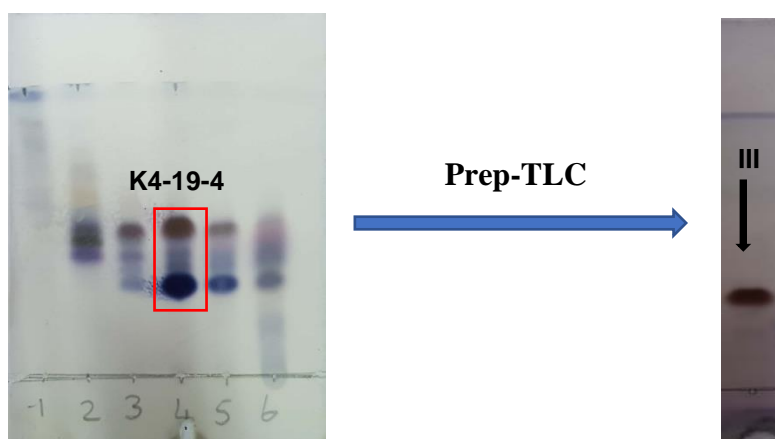


**Figure 4.6:** TLC profile of subfraction K4-19, and compound III

#### 4.5.2.4 Processing of fraction K4-3-XI and Isolation of compound IV

Fraction K4-3-XI (0.6221 g) was subjected to sequential Sephadex LH-20 using MeOH: H<sub>2</sub>O (95:5), which yielded nine subfractions (K4-55-1 to K4-55-9). Subfraction K4-55-1 was injected into the semi-prep HPLC and eluted to acetonitrile: deionized water of increasing polarity (60% to 80% acetonitrile in 30 minutes, then 80% to 100% acetonitrile for 15 minutes, Table 4.5). Two major peaks were observed at 28 min and 39.5 min (Figure 4.7). The peak at 39.5 minutes (Figure 4.7) was collected and found to be pure compound IV (6 mg), whereas the peak at 28 minutes was a mixture of compound IV and a derivative (not determined).

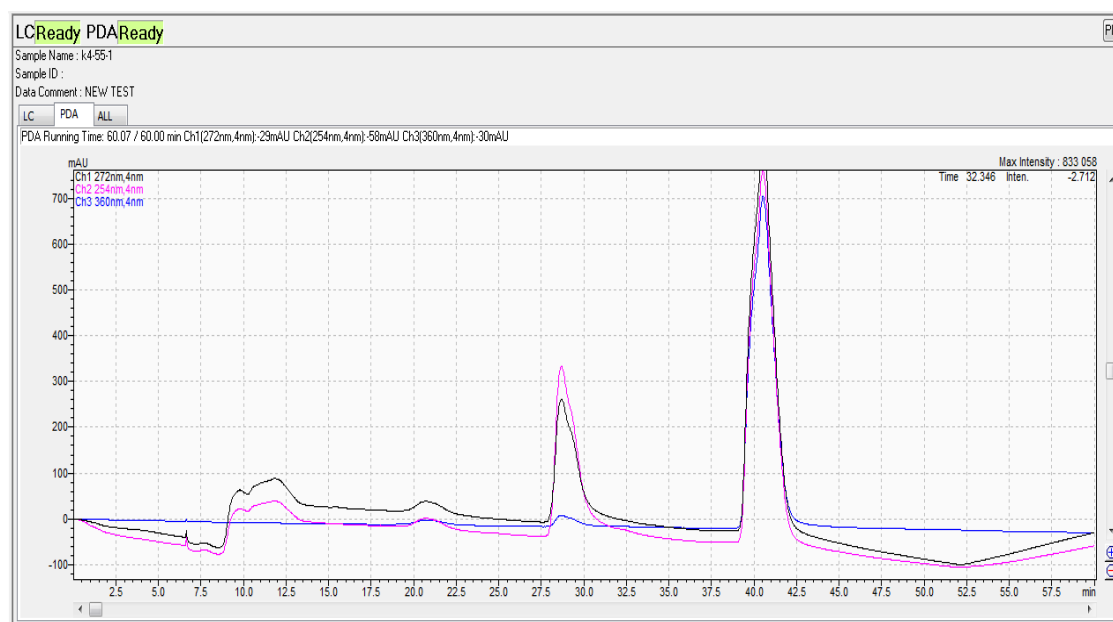


**Figure 4.7:** semi-prep HPLC profile of subfraction K4-55-1

**Table 4.5:** Conditions of the semi-prep HPLC

Solvent	Acetonitrile: deionised water (60 to 100% acetonitrile)
Column	SUPELCO, RP18 (25X2.1 cm)

Flow rate	1.5 mL/min
Detection	UV at $\lambda$ 272; 254 and 360 nm

#### 4.5.2.5 Processing of fraction K4-3-XIII & XIV and isolation of compound V

Fraction K4-3-XIII and XIV (400 mg) were combined and subjected to sequential Sephadex LH-20 using MeOH: H<sub>2</sub>O (95:5) to yield subfractions K4-9 and K4-13. The subfractions constituents were screened with TLC (Figure 4.8). From the TLC results, subfractions K4-9-2 (18.7 mg) and K4-13-3 (44.2 mg) were pooled together and purified with Sephadex LH-20 and elute with MeOH: H<sub>2</sub>O (95:5) which resulted in the isolation of compound V (26.7 mg).

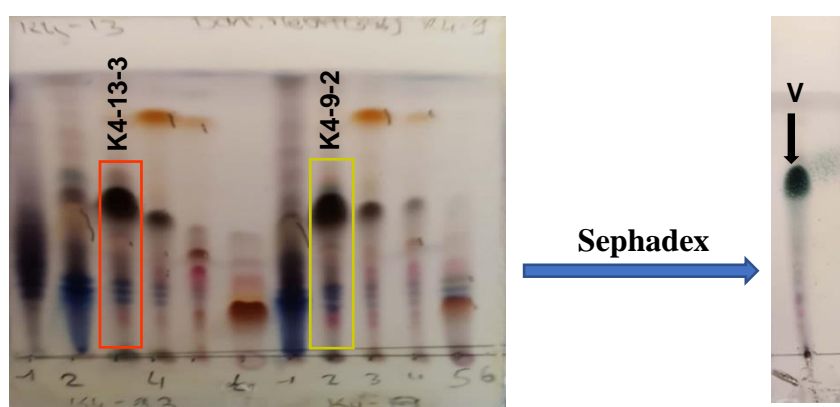


**Figure 4.8:** TLC profile of subfractions K4-13-3, K4-9-2, and compound V

## 4.6 Results and discussions

*P. madagascariensis* collected from the greenhouse of the University of Veterinary and Pharmaceutical Sciences, Brno, Czech Republic has been studied, and four compounds were identified *viz* rosmarinic acid, 6 $\beta$ ,7 $\beta$ -dihydroxyroyleanone (**14**), 7 $\beta$ -acetoxy-6 $\beta$ -hydroxyroyleanone (**15**) and coleon U quinone (**17**) (Kubínová et al., 2014).

To the best of our knowledge the isolated compounds **14** and **15** which contain 6 $\beta$ , 7 $\beta$  stereochemical configurations have not been identified before from Lamiaceae and especially *Plectranthus*, instead (and more common) 6 $\beta$ , 7 $\alpha$  orientations have been documented and identified. Additionally, a recent study was published by Diogo et al. (2019) on the bioactive compounds of the plant material collected from Portugal, and they identified rosmarinic acid, 6 $\beta$ ,7 $\alpha$ -dihydroxyroyleanone (**13**), 7 $\alpha$ -formyloxy-6 $\beta$ -hydroxyroyleanone (**16**), 7 $\alpha$ -acetoxy-6 $\beta$ -hydroxyroyleanone (**7**), and coleon U (**45**). This publication did not mention the isolation and/or identification of 6 $\beta$ , 7 $\beta$  related structures, but stated that compounds **14** and **15** have 6 $\beta$ , 7 $\alpha$  configurations without further explanations. The situation becomes unclear, as Kubínová et al. (2014) did not report the spectroscopic data of the two compounds in their study. This is the reason why it was

essential to conduct a careful study for the explicit identification of the secondary metabolites from these species and determined their biological activities.

*P. madagascariensis* aerial parts were collected from the Cape Peninsula University of Technology (Bellville campus) in January 2018 and extracted with dichloromethane hexane and acetone in a 2:2:1 ratio. The chromatographic isolation led to the isolation of five pure compounds (**I-V**) and the inseparable mixture of two epimeric dimers (**VI & VII**). The isolated compounds were identified using NMR. The <sup>1</sup>H and <sup>13</sup>C NMR results of compounds **I-V** are tabulated in Table 4.6, whereas the dimers **VI & VII** NMR results are summarized in Table 4.6.

**Table 4.6:** NMR data of compounds I-V in CDCl<sub>3</sub>

No (C)	I		II		III		IV		V	
	<sup>13</sup> C	<sup>1</sup> H, <i>m</i> , ( <i>J</i> = Hz)	<sup>13</sup> C	<sup>1</sup> H, <i>m</i> , ( <i>J</i> = Hz)	<sup>13</sup> C	<sup>1</sup> H, <i>m</i> , ( <i>J</i> = Hz)	<sup>13</sup> C	<sup>1</sup> H, <i>m</i> , ( <i>J</i> = Hz)	<sup>13</sup> C	<sup>1</sup> H, <i>m</i> , ( <i>J</i> = Hz)
1	38.4	2.59, <i>dt</i> (12.7, 3.0) 1.19*	38.3	2.58, <i>dt</i> (12.7, 3.0) 1.22*, <i>m</i>	35.8	1.16* 2.70, <i>dt</i> (12.7, 3.0)	30.8	2.66, <i>m</i> 1.60*	29.6	2.13, <i>td</i> (12.7, 3.0) 2.74*
2	19.0	1.61, <i>m</i> 1.83, <i>m</i>	18.9	1.59, <i>dt</i> (12.7, 3.0) 1.80, <i>m</i>	18.9	1.54, <i>m</i> 1.74, <i>m</i>	17.7	1.89, <i>m</i> 1.58, <i>m</i>	18.5	1.79* 1.69, <i>m</i>
3	42.3	1.25* 1.50*	42.3	1.40, <i>m</i> 1.24, <i>m</i>	41.1	1.46, <i>m</i> 1.25, <i>m</i>	36.3	1.99* 1.49*	41.3	1.26, <i>m</i> 1.43*, <i>m</i>
4	33.7		38.6		33.0		36.4		32.4	
5	49.5	1.47, <i>s</i>	49.7	1.27, <i>s</i>	45.8	1.60, <i>s</i>	143.3		58.2	1.63, <i>s</i>
6	69.3	4.46, <i>brs</i>	66.4	4.24, <i>s</i>	25.8	1.96, <i>d</i>	146.8		105.2	
7	69.1	4.53, <i>d</i> , (1.5)	69.0	5.60, <i>d</i> , (1.8)	63.2	4.73, <i>d</i> (1.5)	177.5		192.8	
8	140.9		137.0		143.2		126.8		121.4	
9	147.6		150.1		147.8		155.1		137.7	
10	38.6		33.5		39.1		41.4		51.5	
11	183.5		183.3		183.9		183.6		140.5	
12	151.2		151.2		151.3		150.7		148.3	
13	124.3		124.3		124.2		126.0		133.3	
14	189.1		186.0		189.1		184.3		120.1	7.65, <i>s</i>
15	24.0	3.18, <i>septet</i> (7.1)	24.1	3.09, <i>septet</i> (7.08)	24.0	3.16, <i>septet</i> (7.1)	24.4	3.22, <i>septet</i> (7.0)	27.1	3.02, <i>septet</i> (7.1)
16	19.8	1.23, <i>d</i> (7.1)	19.6	1.11, <i>d</i> (7.08)	19.9	1.20, <i>d</i> (7.1)	19.8	1.24, <i>d</i> (7.0)	22.4	1.16, <i>d</i> (7.1)
17	19.9	1.23, <i>d</i> (7.1)	19.8	1.13, <i>d</i> (7.08)	19.8	1.21, <i>d</i> (7.1)	19.8	1.25, <i>d</i> (7.0)	22.5	1.17, <i>d</i> (7.1)
18	33.5	1.06, <i>s</i>	33.5	0.92, <i>s</i>	33.2	0.98, <i>s</i>	27.2	1.43, <i>d</i> (3.9)	33.7	1.04, <i>s</i>
19	24.3	1.27, <i>s</i>	23.6	1.16, <i>s</i>	21.7	0.90, <i>s</i>	29.1	1.42, <i>d</i> (3.9)	22.2	1.31, <i>s</i>
20	21.6	1.62, <i>s</i>	21.3	1.55, <i>s</i>	18.4	1.22, <i>s</i>	27.5	1.64, <i>s</i>	72.3	3.37, <i>d</i> H <sub>a</sub> , (7.5) 4.29, <i>d</i> H <sub>b</sub> , (7.5)
7-OCOCH <sub>3</sub>			21.0	1.98, <i>s</i>						
7-O <sup>13</sup> COCOCH <sub>3</sub>			170.1							
6-OH		5.31, <i>s</i>					7.09			5.21, <i>s</i>
7-OH						3.03 <i>br</i>				
12-OH				7.23, <i>s</i>		7.26, <i>s</i>		7.08, <i>s</i>		7.23, <i>s</i>



#### 4.6.1 Compound I (6 $\beta$ ,7 $\alpha$ -dihydroxyroyleanone)

The  $^1\text{H}$  NMR spectrum (Figure 4.10) showed signals of five methyls at  $\delta_{\text{H}}$  1.62 (s, Me-20); 1.27 (s, Me-19); 1.06 (s, Me-18); 1.23 (d,  $J = 7.1$  Hz, Me-17); 1.23 (d,  $J = 7.1$  Hz, Me-16). The latter two methyl groups with the proton signal at  $\delta_{\text{H}}$  3.18 (septet,  $J = 7.1$  Hz, H-15) indicate the presence of an isopropyl group. Furthermore, the  $^1\text{H}$  NMR showed signals of two low field two protons attached to two oxygenated carbons at  $\delta_{\text{H}}$  4.53 (d,  $J = 1.5$  Hz, H-7) and 4.46 (brs, H-6); in addition to a cluster of proton signals between  $\delta_{\text{H}}$  1.20 to  $\delta_{\text{H}}$  1.50 (see Table 4.6 for more details). The fact that the two protons at C-6 $\beta$  and C-7 $\alpha$  have negligible coupling between them is directly reflected from the distortion chair form of ring B, as a result of the direct effect of the planar structure of ring C and affected the stereochemistry of all ring B proton directly (Figure 4.9) directly.

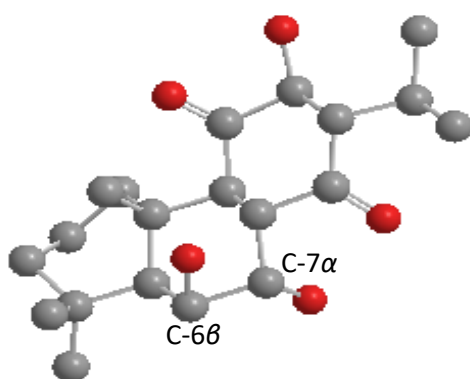


**Figure 4.9:** 3D structure of compound I (protons were omitted for clarity, generated by CHEM-DRAW (version 12))

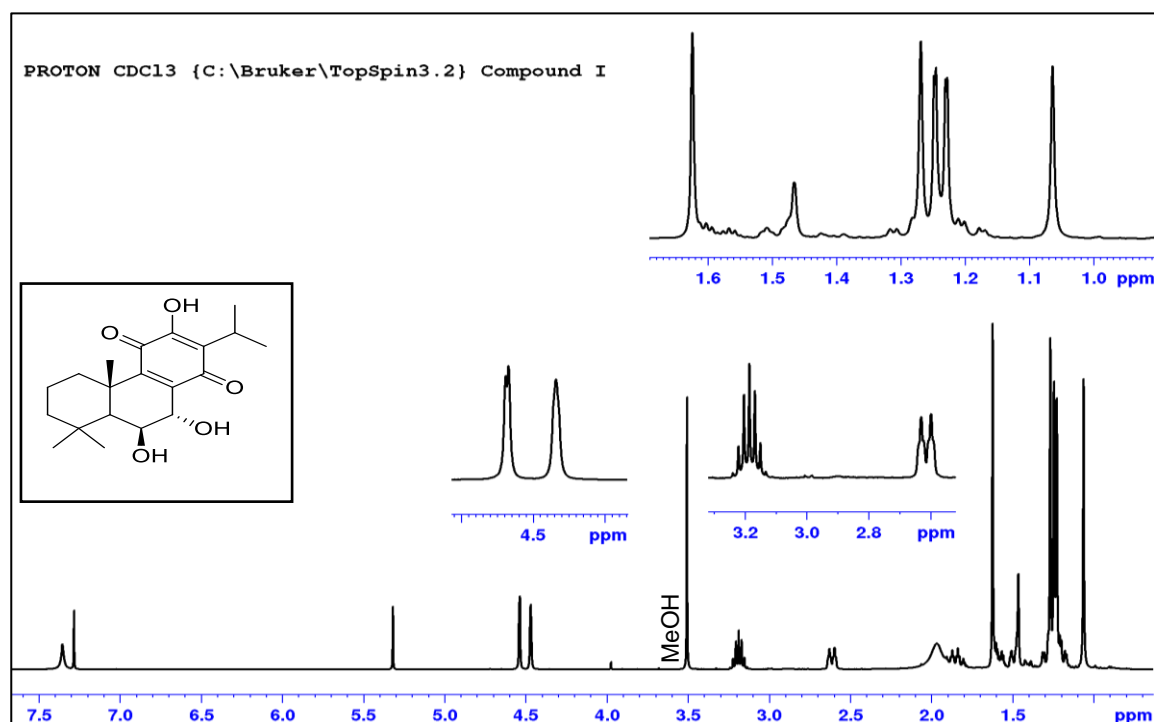


**Figure 4.10:**  $^1\text{H}$  NMR spectrum of the 6 $\beta$ ,7 $\alpha$ -dihydroxyroyleanone (I)

The  $^{13}\text{C}$  NMR spectrum (Figure 4.11) showed twenty signals which were classified according to DEPT-135 (Figure 4.12) to five methyls, three methylenes; four methines groups and eight quaternary carbons with six of them forming quinonoidal structure (ring C), at  $\delta_{\text{C}}$  140.9 (C-8), 147.6 (C-9), 183.5 (C-11), 151.2 (C-12), 124.3 (C-13), and 189.1 (C-14), in addition to the two oxygenated carbons at  $\delta_{\text{C}}$  69.3 (C-6), and 69.1 (C-7).

C13CPD CDC13 {C:\Bruker\TopSpin3.2} Compound I

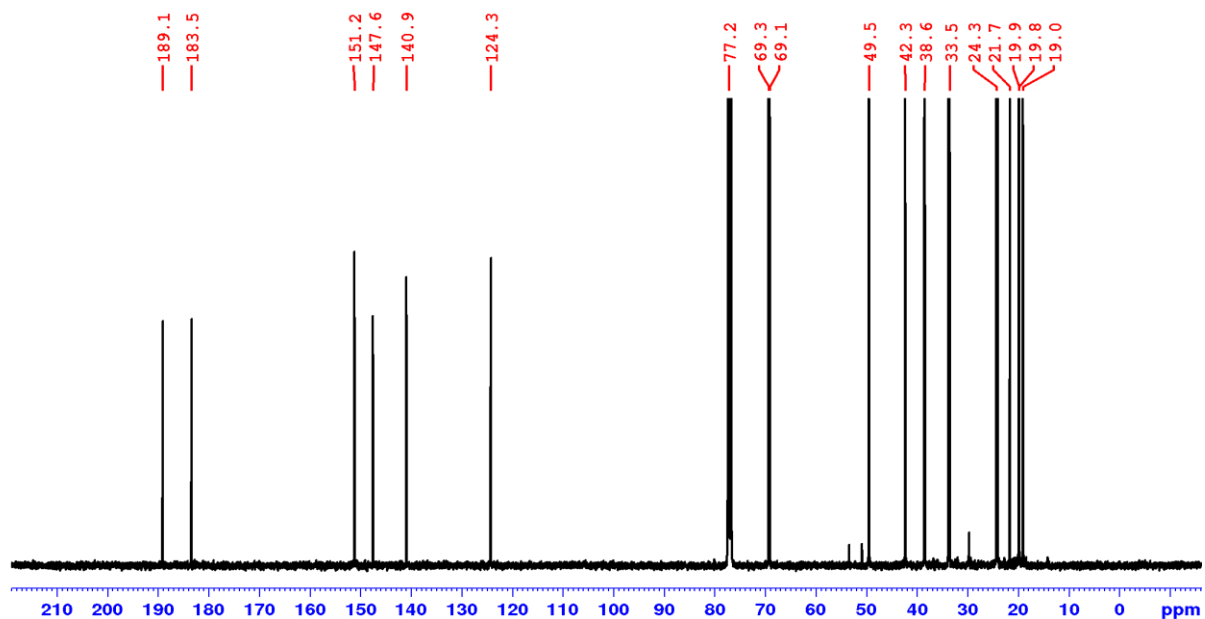


Figure 4.11:  $^{13}\text{C}$  NMR spectrum of  $6\beta,7\alpha$ -dihydroxyroyleanone (I)

C13DEPT135 CDC13 {C:\Bruker\TopSpin3.2} Compound I

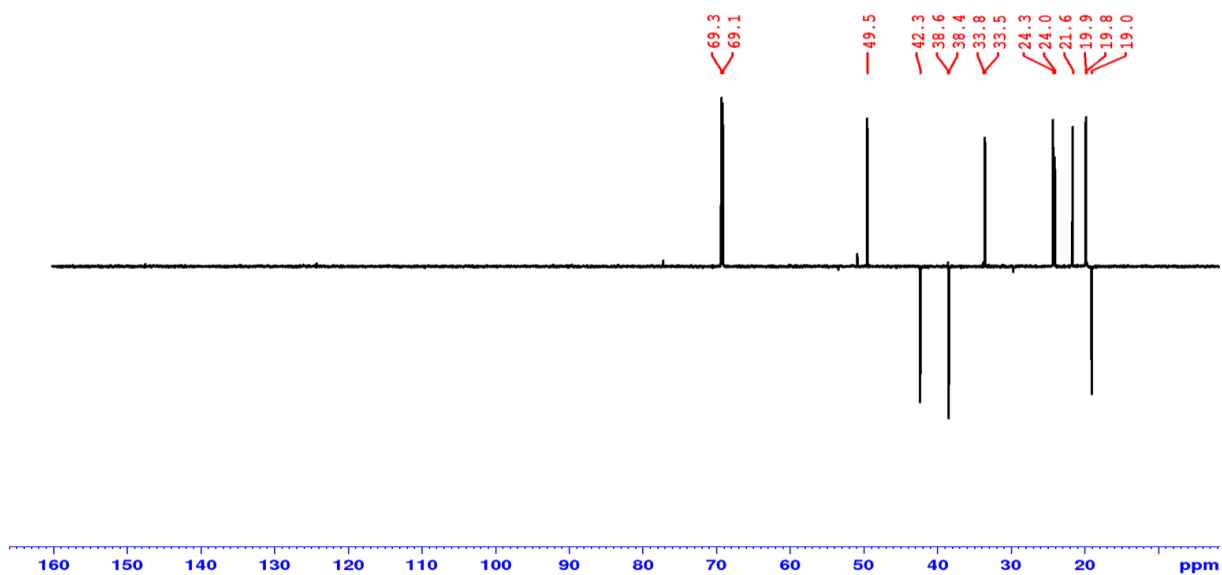
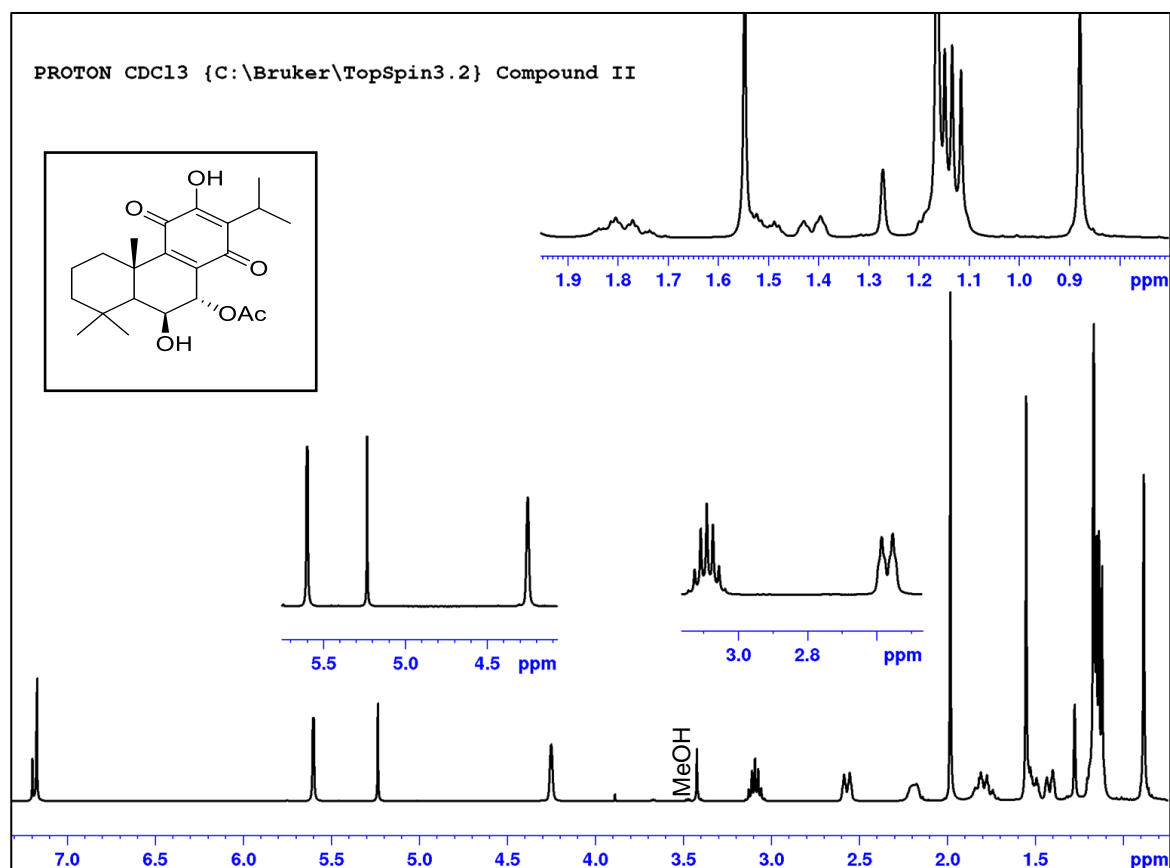


Figure 4.12: DEPT-135 NMR spectrum of  $6\beta,7\alpha$ -dihydroxyroyleanone (I)

The above mentioned data were identical to the royleanone 6 $\beta$ ,7 $\alpha$ -dihydroxyroyleanone isolated by Rasikari (2007), and Diogo et al. (2019) from *P. fasciculatus* and *P. madagascariensis*, respectively.

#### 4.6.2 Compound II (7 $\alpha$ -acetoxy-6 $\beta$ -hydroxyroyleanone)

The  $^1\text{H}$  NMR spectrum (Figure 4.13) showed signals of five upfield methyl groups at  $\delta_{\text{H}}$  1.55 (s, Me-20); 1.16 (s, Me-19); 0.92 (s, Me-18); 1.13 (d,  $J = 7.08$  Hz, Me-17); 1.11 (d,  $J = 7.08$  Hz, Me-16); as well as the signal of a downfield methyl attached to a carbonyl group at  $\delta_{\text{H}}$  1.98 (OCOCH $_3$ ). The  $^1\text{H}$  NMR showed signals of a downfield proton attached to the two methyls (Me-16 and Me-17) at  $\delta_{\text{H}}$  3.09 (septet,  $J = 7.08$  Hz, H-15). Two signals of deshielded protons attached to an oxygenated carbon were observed in the  $^1\text{H}$  NMR spectrum at  $\delta_{\text{H}}$  4.24 (H-6 $\alpha$ ) and 5.60 (H-7 $\beta$ ). Moreover, a cluster of protons signals between  $\delta_{\text{H}}$  1.10 to 1.70 was observed (see Table 4.6 for more details). The compound shows a similar  $^1\text{H}$  NMR profile like I, except the low field shift of H $_{7\alpha}$  (from 4.53 to 5.60) which indicates the link of an acetoxy group to this position.



**Figure 4.13:**  $^1\text{H}$  NMR spectrum of 7 $\alpha$ -acetoxy-6 $\beta$ -hydroxyroyleanone (II)

The  $^{13}\text{C}$  NMR spectrum (Figure 4.14) showed twenty-two signals which were classified according to DEPT-135 (Figure 4.15) to six methyls, three methylenes; four methines and

nine quaternary carbons with six of them forming quinonoidal structure (ring C), at 137.0 (C-8), 150.1 (C-9), 183.3 (C-11), 151.2 (C-12), 124.3 (C-13), and 186.0 (C-14). Moreover, two oxygenated carbons at  $\delta_C$  66.4 (C-6), and 69.0 (C-7) and an acetoxy group at  $\delta_C$  21.0 (7-OCOCH<sub>3</sub>) and 170.1 (7-O<sub>2</sub>CCH<sub>3</sub>) were identified.

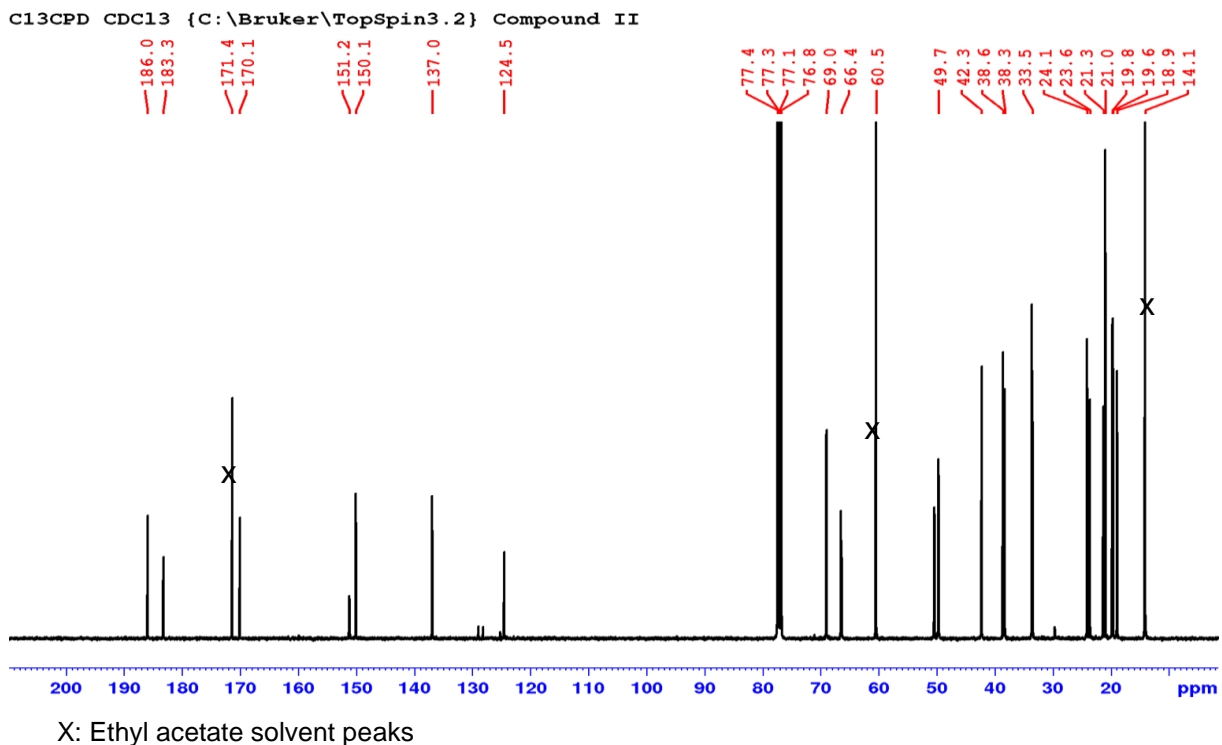


**Figure 4.14:** <sup>13</sup>C NMR spectrum of 7 $\alpha$ -acetoxy-6 $\beta$ -hydroxyroyleanone (II)

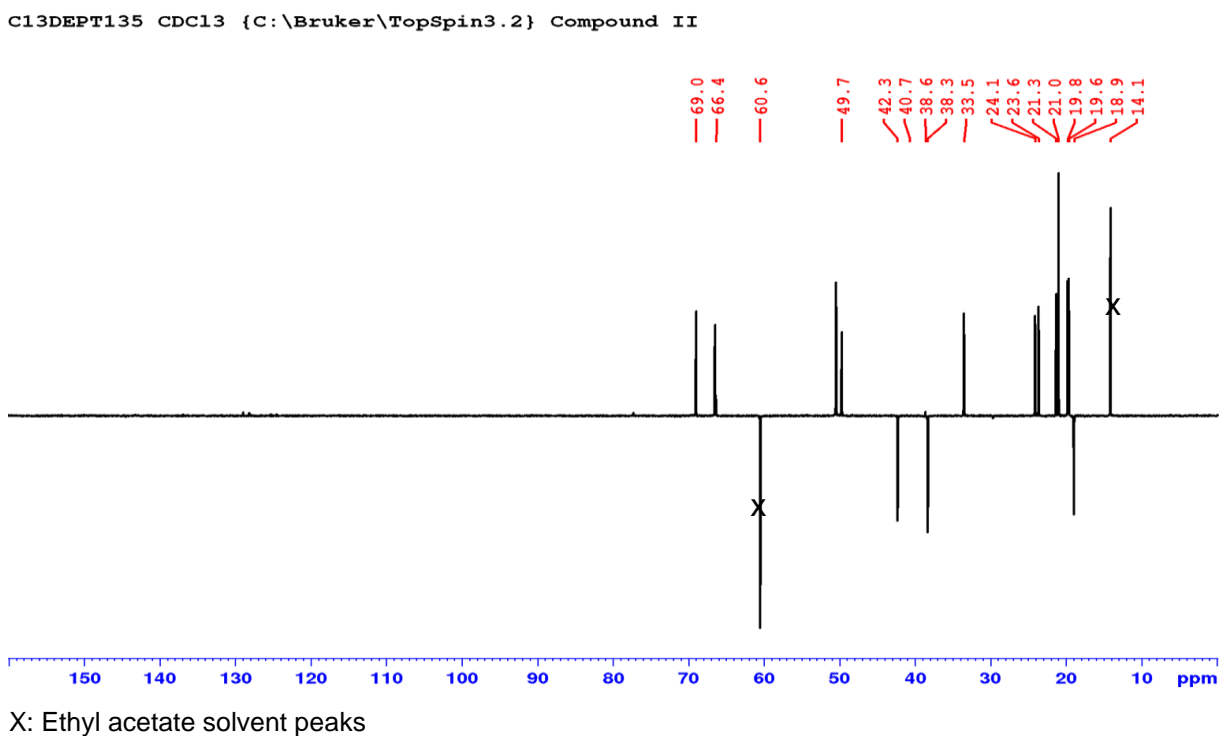


**Figure 4.15:** DEPT-135 NMR spectrum of 7 $\alpha$ -acetoxy-6 $\beta$ -hydroxyroyleanone (II)

The above-mentioned data are identical to the royleanone 7 $\alpha$ -acetoxy-6 $\beta$ -hydroxyroyleanone isolated by Rasikari (2007) and Diogo et al. (2019) from *P. actites* and *P. madagascariensis*, respectively. Compounds **I** and **II** isolated in this study correspond to compounds **13** and **7** isolated from *P. madagascariensis* by Diogo et al. (2019). From Diogo et al. (2019) publication, we assume that compounds **14** and **15** isolated by Kubínová et al. (2014) should correspond to compounds **13** and **7** which have different stereochemical orientation for C-6 and C-7. Thus, for clarification about the exact configuration of these compounds isolated from *P. madagascariensis*, the configuration of compound **II** was analyzed using X-ray spectroscopy as it formed an excellent crystal adequate for X-ray analysis. The results of the X-ray analysis (Figure 4.16) showed that compound **II** consists of the typical three fused cyclohexane rings with two of them are trans fused cyclohexane rings (C-5-C-10 and C-8-C-9/C-11-C-14) which is endemics to royleanone type abietane diterpenoids. Although the temperature of analysis (173K) of compound **II** is slightly higher than the one of Bernades et al., 2018 (165K, Table 4.7), it was noticed that the crystalline packing have similar R<sub>6</sub><sup>6</sup> synthon motif (Figure 4.17). This motif involved the intramolecular (O2-H(2O)...O1) and intermolecular (O2-H(2O)...O3 and O6-H(6O)...O5) hydrogen bonds. All these parameters confirmed that compound **II** is indeed a typical 6 $\beta$ , 7 $\alpha$  configuration as reported by Diogo et al. (2019).

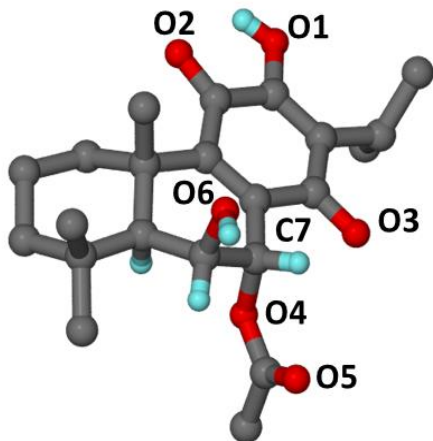


**Figure 4.16:** X-ray crystallographic structure of compound **II**. The hydrogens atoms have been omitted for the structure clarity purpose.

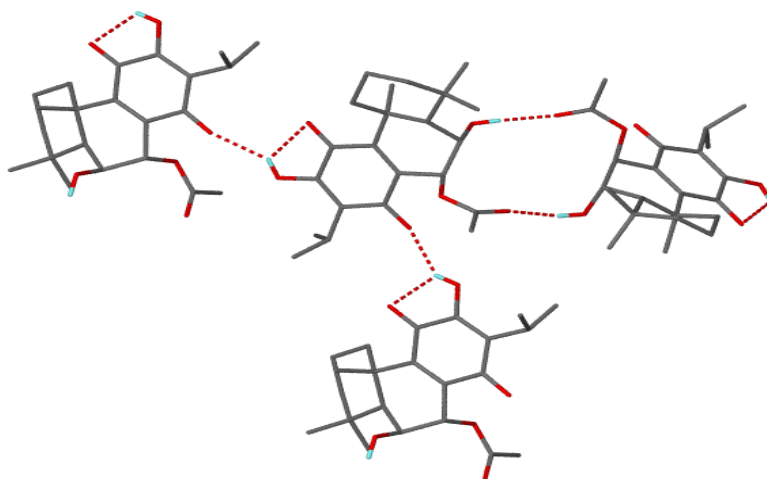


**Figure 4.17:** Synthon motif of compound **II**

**Table 4.7:** Single-crystal X-ray parameters of *7 $\alpha$ -acetoxy-6 $\beta$ -hydroxyroyleanone* (**II**)

Parameters	Values	
Identification code	<b>II</b>	Bernades et al., 2018
Molecular formula	C <sub>20</sub> H <sub>30</sub> O <sub>6</sub>	C <sub>20</sub> H <sub>30</sub> O <sub>6</sub>
Temperature	173 K	165 K
Crystal size	0.290 x 0.360 x 0.400 mm	0.25 X 0.20 X 0.500 mm
Crystal system	Orthorhombic	Orthorhombic
Unit cell dimensions		
A	7.3893(4) Å	7.3873(7) Å
B	14.1145(8) Å	14.0964 (12) Å
C	20.6199(12) Å	20.5705 (18) Å
Volume	2150.6(4) Å <sup>3</sup>	2142.1 (3) Å <sup>3</sup>
Reflections collected	32427	10019

#### 4.6.3 Compound III (horminone)

The <sup>1</sup>H NMR spectrum (Figure 4.17) showed signals of five methyls at  $\delta_{\text{H}}$  1.22 (s, Me-20); 0.90 (s, Me-19); 0.98 (s, Me-18); 1.21 (d,  $J = 1.7$  Hz, Me-17); 1.20 (d,  $J = 1.7$  Hz, Me-16). The <sup>1</sup>H NMR signal at  $\delta_{\text{H}}$  3.16 (*septet*,  $J = 7.1$  Hz, H-15) is representative of the presence of the isopropyl group. Whereas the low field <sup>1</sup>H NMR signal at  $\delta_{\text{H}}$  4.73 (d,  $J = 1.5$  Hz) indicates the presence of a proton attached to an oxygenated carbon. Several proton signals between  $\delta_{\text{H}}$  1.20 to 1.60 are also observed (see Table 4.6 for more details).

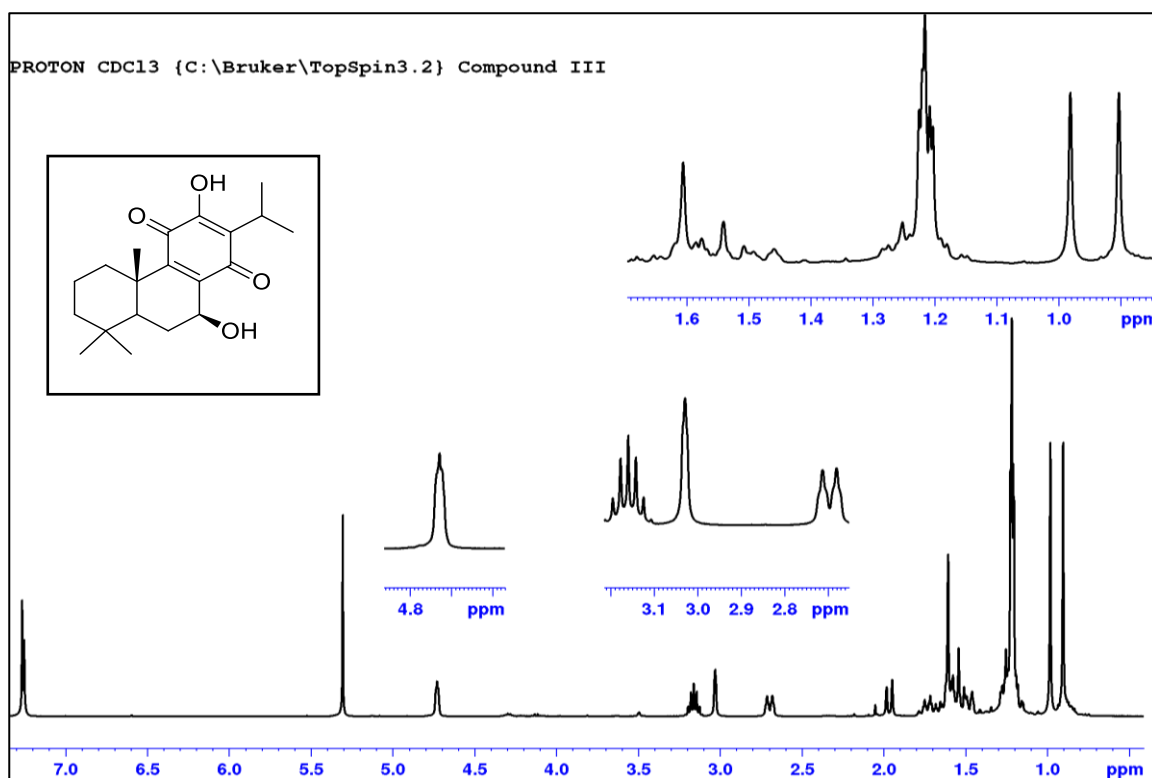


**Figure 4.18:** <sup>1</sup>H NMR spectrum of the horminone (III)

The <sup>13</sup>C NMR spectrum (Figure 4.18) showed twenty signals which were classified according to DEPT-135 (Figure 4.19) to five methyls, four methylenes; three methines and eight quaternary carbons with six of the quaternary carbons forming the quinonoid structure (ring C), at  $\delta_c$  140.9 (C-8), 147.5 (C-9), 183.1 (C-11), 151.2 (C-12), 124.3 (C-13), and 189.5 (C-14). Additionally, an oxygenated carbon at  $\delta_c$  63.2 (C-7 $\alpha$ ) was detected.

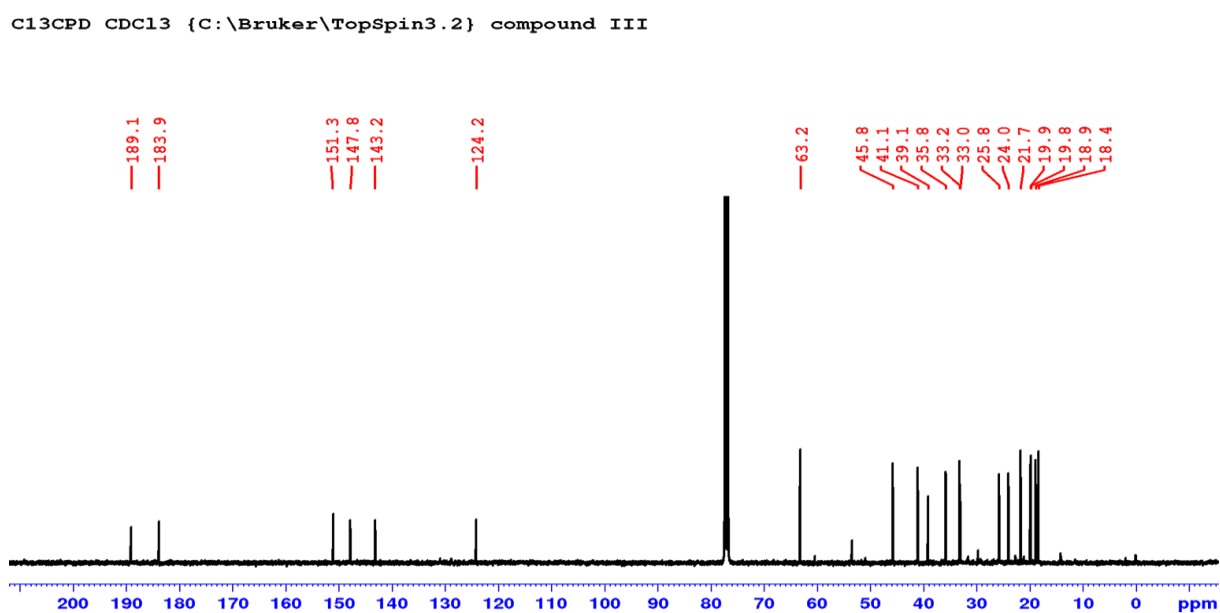


**Figure 4.19:** <sup>13</sup>C NMR spectrum of horminone (III)

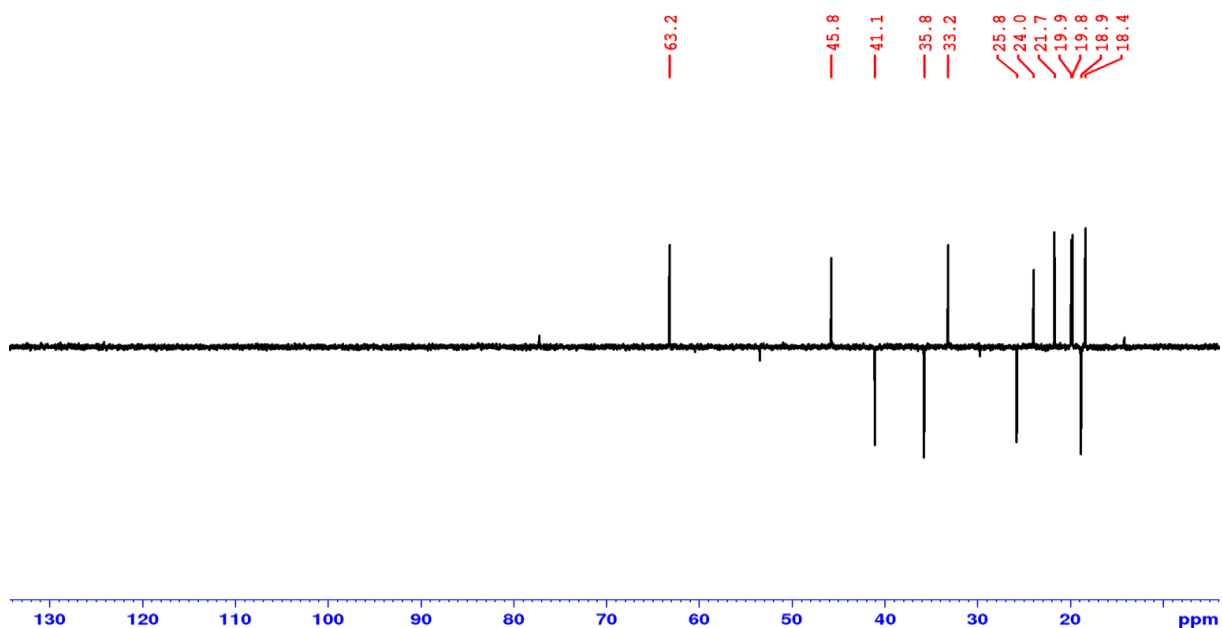


Figure 4.20: DEPT-135 NMR spectrum of horminone (III)

The above-mentioned data were identical to the royleanone 7 $\alpha$ -hydroxyroyleanone (Horminone) isolated by Naman (2015) from *Plectranthus species*.

#### 4.6.4 Compound IV (coleon U quinone)

The  $^1\text{H}$  NMR spectrum (Figure 4.20) showed signals of five methyls at  $\delta_{\text{H}}$  1.64 (s, Me-20); 1.42 (*d*,  $J = 3.9$  Hz, Me-19); 1.43 (*d*,  $J = 3.9$  Hz, Me-18); 1.25 (*d*,  $J = 6.8$  Hz, Me-17); 1.24 (*d*,  $J = 6.8$  Hz, Me-16). The proton signal at  $\delta_{\text{H}}$  3.22 (*septet*,  $J = 7.0$  Hz, H-15) indicate the presence of an isopropyl group, in addition to a cluster of proton signals between  $\delta_{\text{H}}$  1.22 to 1.80 (see Table 4.6 for more details).



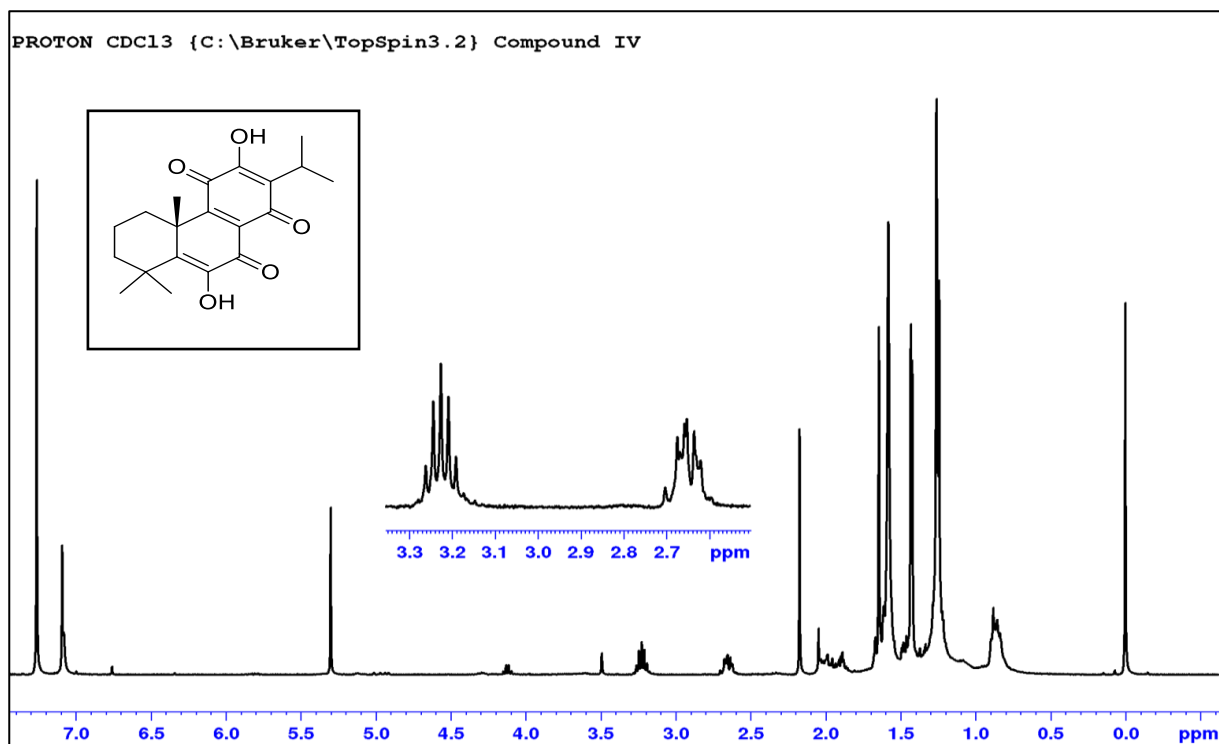


Figure 4.21:  $^1\text{H}$  NMR spectrum of coleon U quinone (IV)

The  $^{13}\text{C}$  NMR spectrum (Figure 4.22) showed 20 signals which were classified according to DEPT-135 (Figure 4.22) to five methyls, three methylenes; one methines and ten quaternary carbons with Six of them forming quinonoidal structure (ring C), at  $\delta_{\text{C}}$  126.8 (C-8), 155.1 (C-9), 183.6 (C-11), 150.7 (C-12), 126.0 (C-13) and 184.3 (C-14).

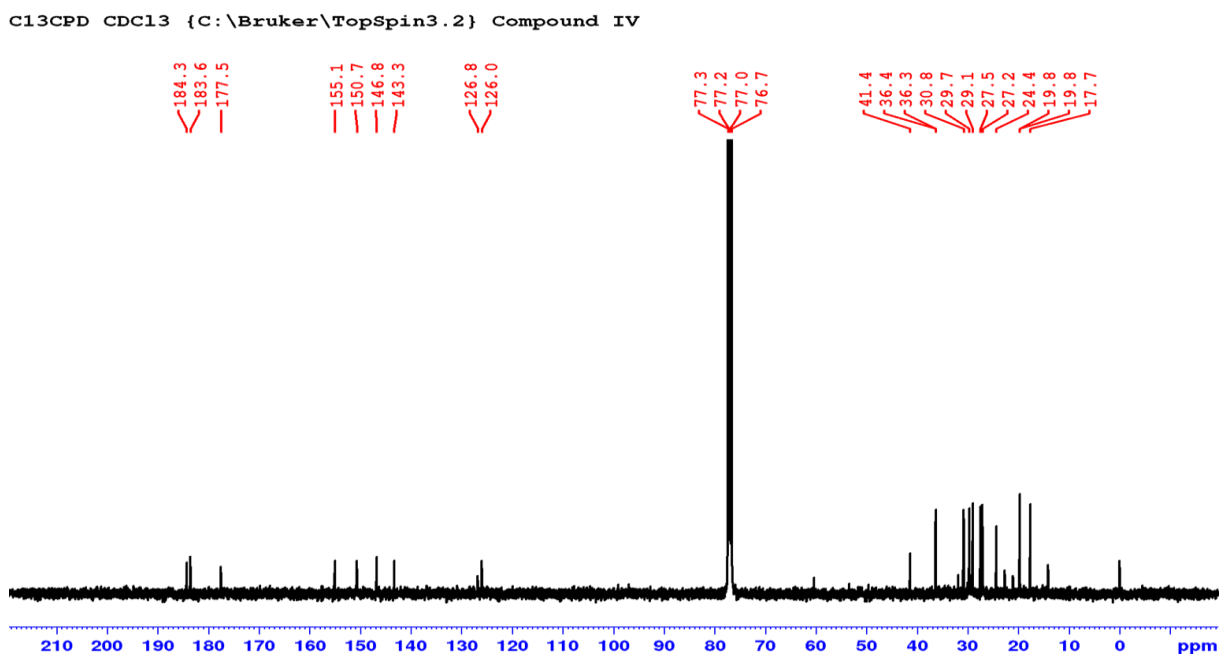
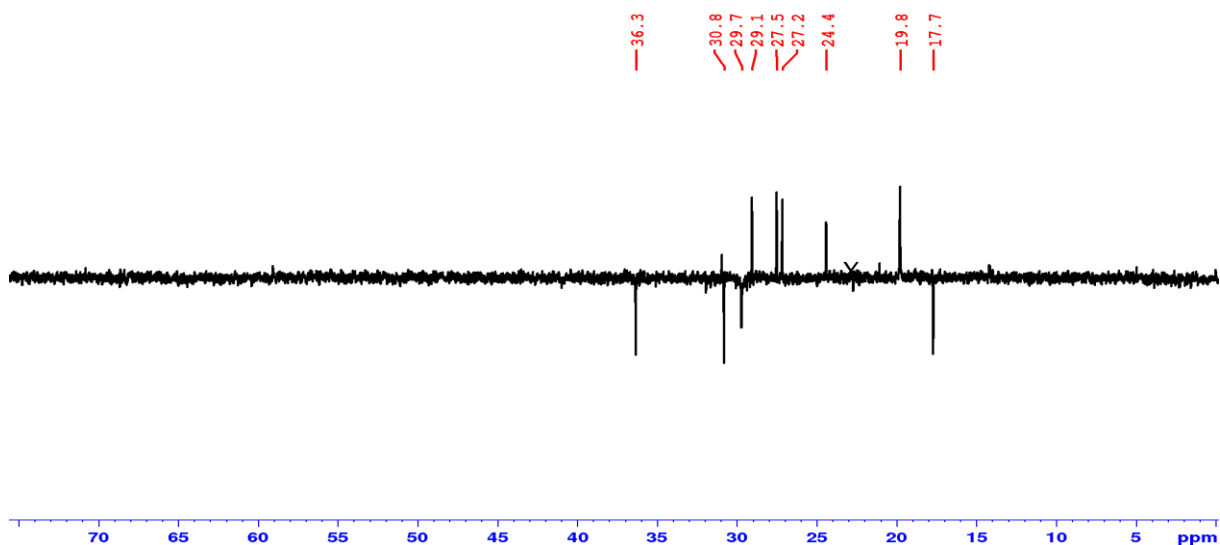


Figure 4.22:  $^{13}\text{C}$  NMR spectrum of coleon U quinone (IV)



X: Impurity

**Figure 4.23:** DEPT-135 NMR spectrum of coleon U quinone (**IV**)

The above-mentioned data were identical to the coleon U quinone isolated by Alder et al. (1984) from *P. argentatus*

#### 4.6.5 Compound V (carnosolon)

The  $^1\text{H}$  NMR spectrum (Figure 4.23) showed signals of four methyl groups at  $\delta_{\text{H}}$  1.31 (s, Me-19); 1.06 (s, Me-18); 1.17 (d,  $J = 7.1$  Hz, Me-17); 1.16 (d,  $J = 7.1$  Hz, Me-16). It also showed a signal of a downfield proton attached to two methyls at  $\delta_{\text{H}}$  3.0 (septet,  $J = 7.1$  Hz, H-15). The  $^1\text{H}$  NMR signals showed a downfield proton attached to a benzene ring at  $\delta_{\text{H}}$  7.65 (s, H-14), indicating the presence of a penta-substituted benzene ring. Signals of two low field non-equivalent protons attached to an epoxy group at  $\delta_{\text{H}}$  3.37 (d,  $J = 7.5$  Hz,  $\text{H}_{\alpha}$ -20) and  $\delta_{\text{H}}$  4.29 (d,  $J = 7.5$  Hz,  $\text{H}_{\beta}$ -20); in addition to a cluster of proton signals between  $\delta_{\text{H}}$  1.20 to  $\delta_{\text{H}}$  1.80 were identified (see Table 4.6 for more details).

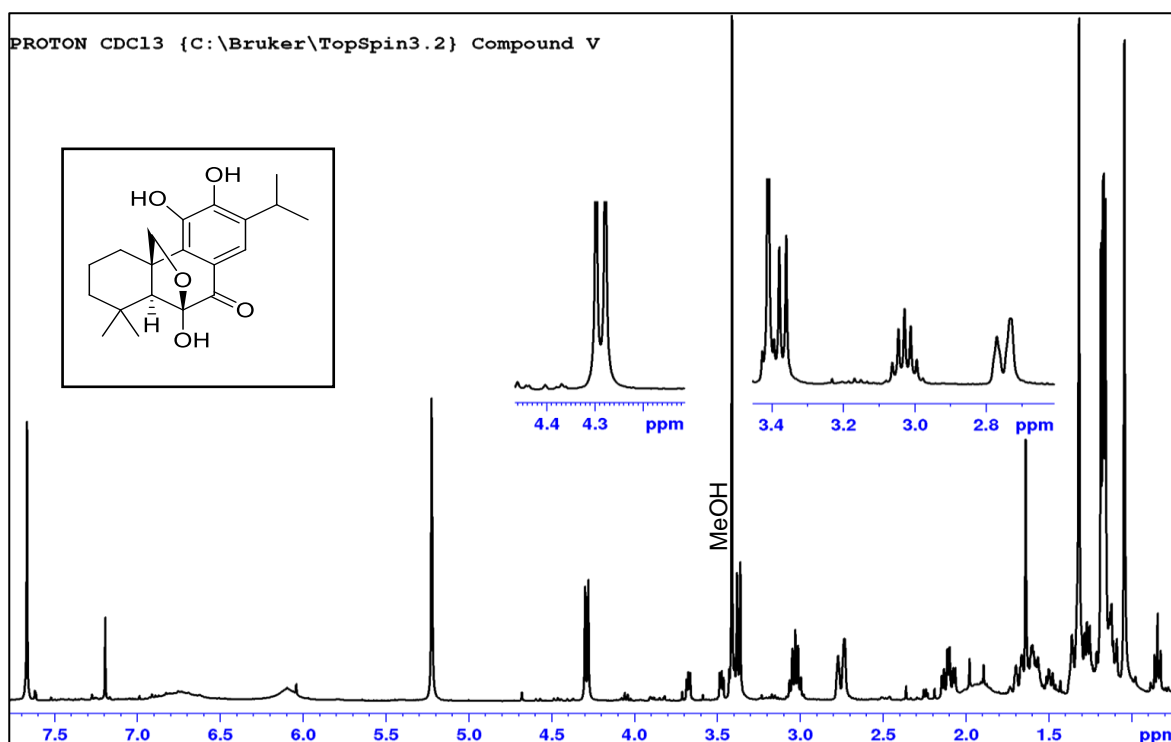


Figure 4.24:  $^1\text{H}$  NMR spectrum of carnosolon (V)

The  $^{13}\text{C}$  NMR spectrum (Figure 4.24) showed twenty signals and could be classified according to DEPT-135 (Figure 4.25) to four methyls, four methylenes; three methines and nine quaternary carbons with six of them forming the benzene structure (ring C), at  $\delta_{\text{C}}$  121.4 (C-8), 137.8 (C-9), 140.5 (C-11), 148.3 (C-12), 133.3 (C-13), and 120.1 (C-14). Furthermore, two oxygenated carbon forming an epoxy group was observed on the  $^{13}\text{C}$  NMR data at  $\delta_{\text{C}}$  105.2 (C-6) and 72.3 (C-20), while the chemical shift of the C-6 (105.2) indicated the dioxygenated carbon present.

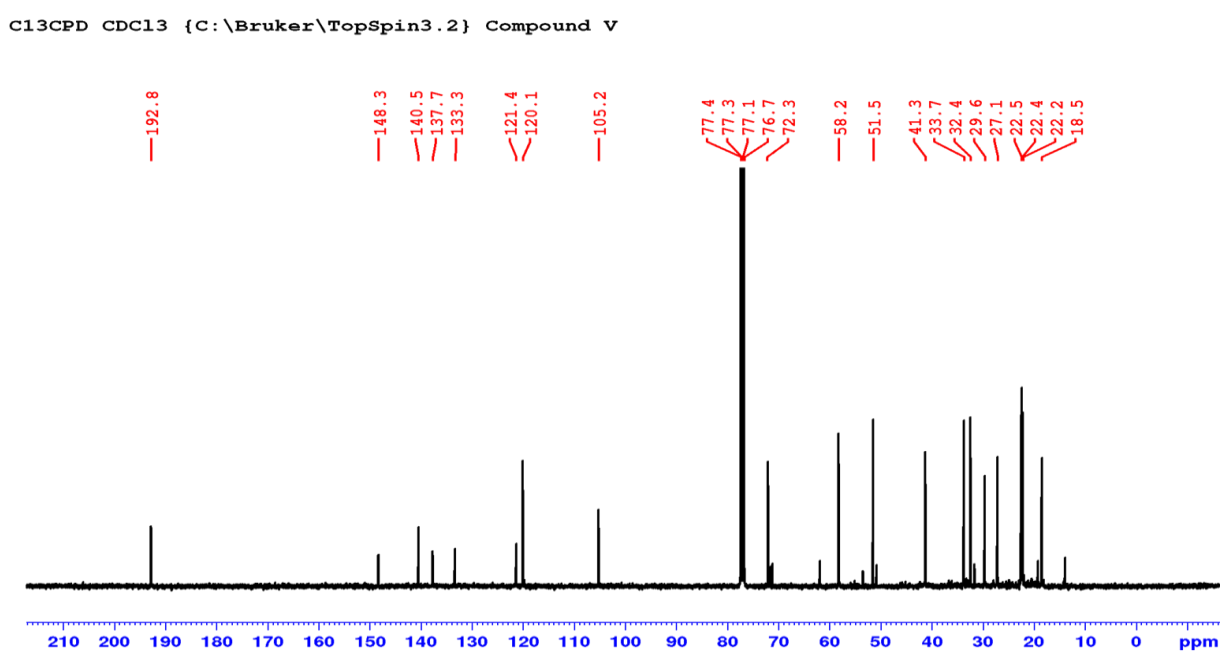
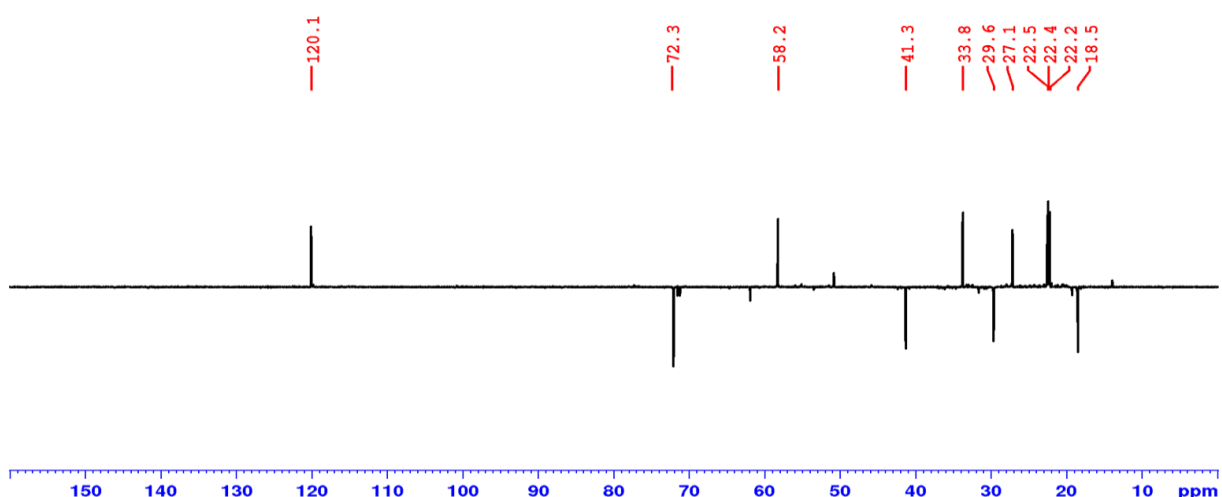


Figure 4.25:  $^{13}\text{C}$  NMR spectrum of carnosolon (V)



**Figure 4.26:** DEPT-135 NMR spectrum of carnosolon (V)

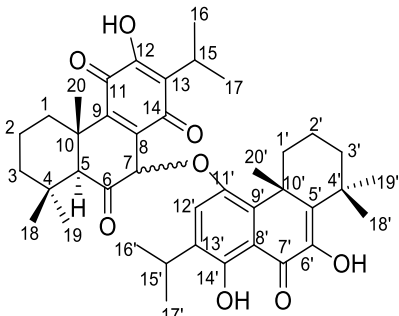
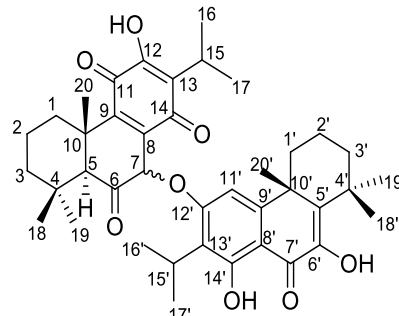
The above mentioned data were identical to carnosolon isolated by Horvath et al. (2004) from *P. cyaneus*.

#### 4.6.6 Compounds VI (grandidone A) and VII (7-epimer grandidone A)

The isolated compound showed a single spot on the TLC (see Figure 4.5), and complex NMR signals suggesting the compound is a mixture and many trials to purify it further has been conducted; however, the same NMR signal profile remained.

The  $^1\text{H}$  NMR spectrum (Figure 4.26) showed signals of two isopropyl group at  $\delta_{\text{H}}$  3.04 (m, H-15) and  $\delta_{\text{H}}$  3.47 (m, H-15') indicating the presence of a dimer. However, the  $^{13}\text{C}$  NMR spectrum (Figure 4.27) showed eighty signals which were classified according to DEPT-135 (Figure 4.28) to twenty methyls, twelve methylenes, six methines, and twenty quaternary carbons (Table 4.8). Furthermore, it was observed that each signal came in duplicate, implying that the sample might be a mixture of dimers. Additionally, the  $^{13}\text{C}$  NMR signals of the sample were compared to the  $^{13}\text{C}$  NMR signals of grandidone A and 7-epimer grandidone A isolated by Uchida et al. (1981) from *P. grandidentatus*. Grandidone A and 7-epimer grandidone A  $^{13}\text{C}$  NMR signals were similar to the sample  $^{13}\text{C}$  NMR signals, implying that the sample is a mixture of grandidone A and 7-epimeric grandidone A (**VI** & **VII**). The sample was also characterised using 2D NMR spectroscopy (Figure 4.29 and Figure 4.30) but because the dimers are epimers only the  $^{13}\text{C}$  NMR data was used to identify them as the only difference between the dimers  $^1\text{H}$  NMR signals lies in their C-11' and C-12'  $^1\text{H}$  NMR signals.

**Table 4.8:**  $^{13}\text{C}$  NMR data of compounds **VI** and **VII** in  $\text{CDCl}_3$

Chemical structures					
	Position	VI	Uchida et al., 1981 (VI)	VII	Uchida et al., 1981: (VII)
		$^{13}\text{C}$		$^{13}\text{C}$	
1	36.7	36.9	36.9		
2	17.2	17.3	17.4		
3	41.2	41.4	41.2		
4	36.1	36.2	36.1		
5	60.0	60.1	60.0		
6	196.6	196.6	196.1		
7	106.2	106.4	106.0		
8	137.1	137.4	135.2		
9	151.5	151.8	153.0		
10	39.9	40.0	39.8		
11	183.0	150.9, d	183.0		
12	150.7	183.2	150.6		
13	126.0	126.2	126.1		
14	183.3	183.4	183.2		
15	24.0	24.1	24.1		
16	19.6	19.7	19.7		
17	20.7	20.7	20.4		
18	32.0	32.0	32.2		
19	21.8	21.8	21.7		
20	28.5	28.6	30.0		
1'	29.7	29.9	30.7		
2'	18.5	18.5	18.5		
3'	35.9	36.1	35.9		
4'	44.3	44.4	44.1		
5'	142.2	142.3	142.1		
6'	141.9	142.1	141.3		
7'	182.5	182.7	182.3		
8'	105.9	106.0	105.3		
9'	130.5	130.0	130.6		
10'	32.4	32.4	32.5		
11'	133.7	133.9	133.6		
12'	150.7	150.9	150.6		
13'	116.3	116.4	116.3		
14'	158.2	158	158.7		
15'	24.3	24.1	24.3		
16'	19.8	19.8	19.8		
17'	20.7	20.7	20.4		
18'	27.3	27.5	27.2		
19'	21.0	21.0	21.1		
20'	27.9	28.0	27.9		

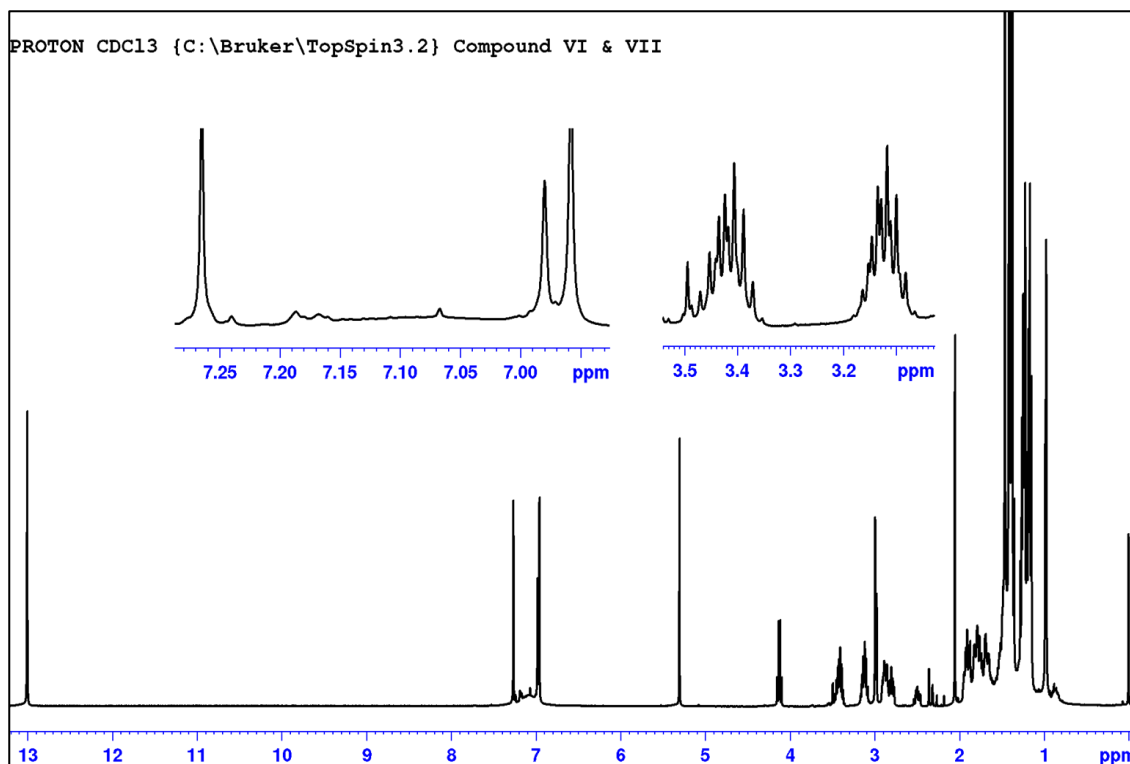


Figure 4.27:  $^1\text{H}$  NMR spectrum of grandidone A and 7-epimer grandidone A

C13CPD CDC13 {C:\Bruker\TopSpin3.2} Compound VI & VII

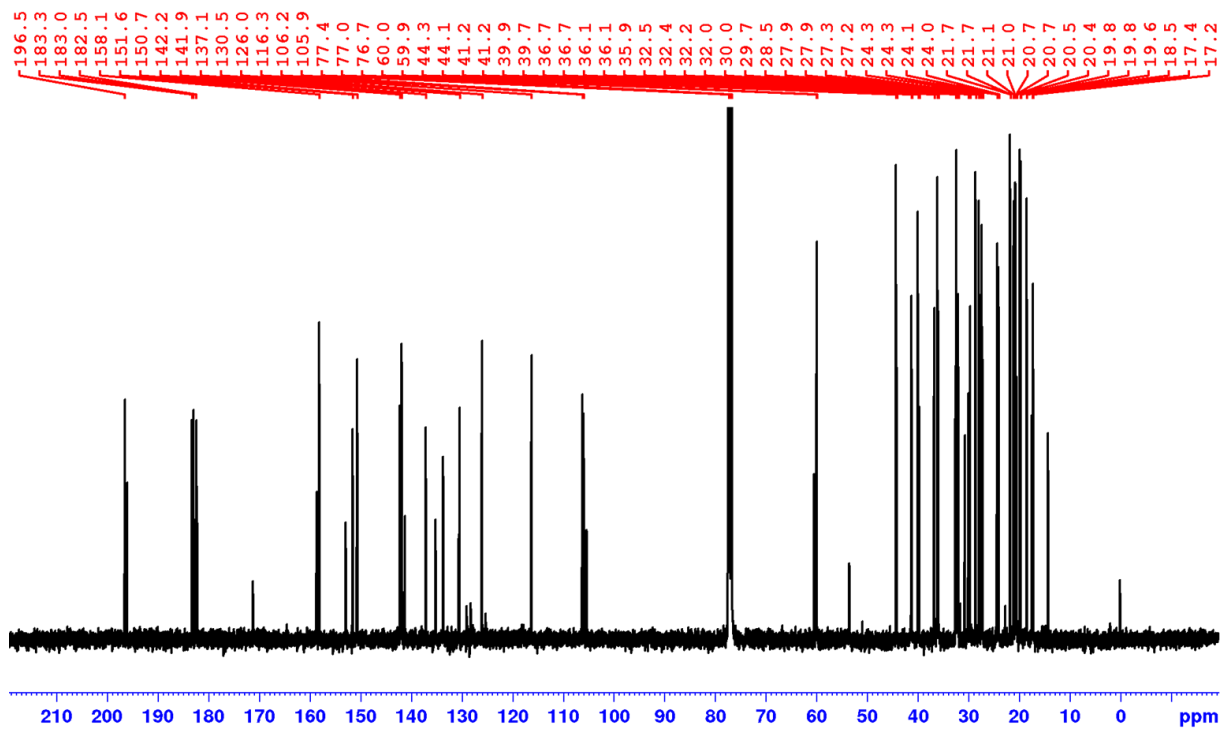
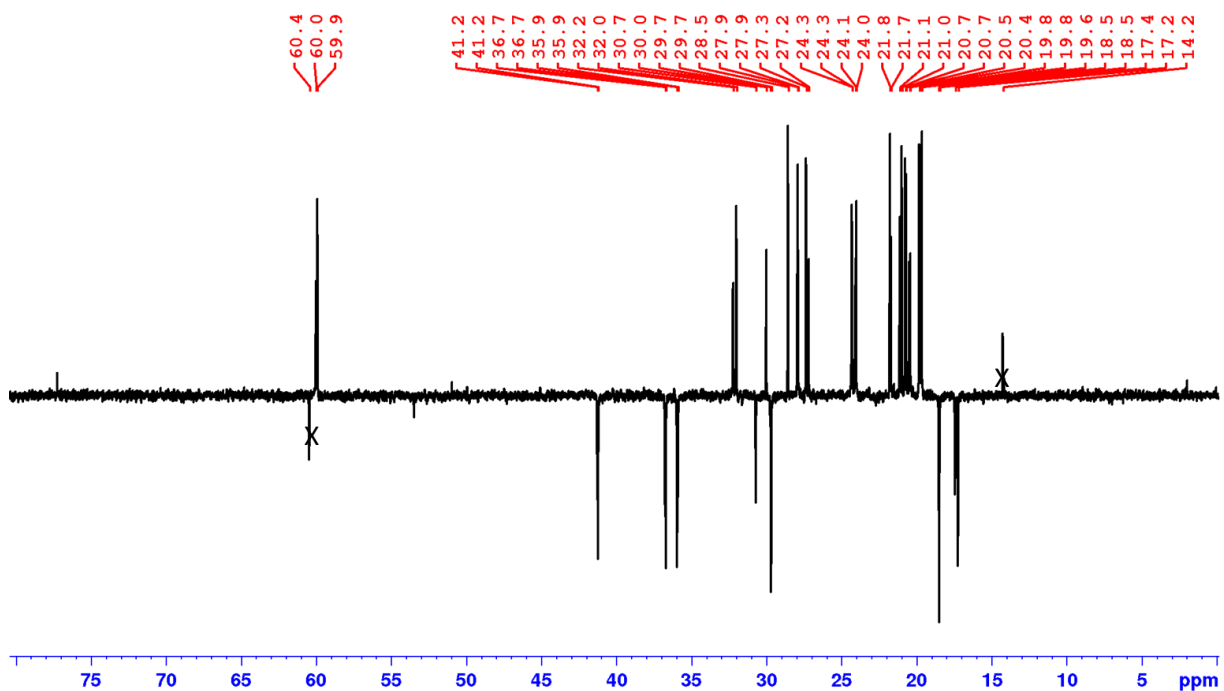


Figure 4.28:  $^{13}\text{C}$  NMR spectrum of grandidone A and 7-epimer grandidone A

C13DEPT135 CDC13 {C:\Bruker\TopSpin3.2} Compound VI & VII



X: Ethyl acetate solvent peaks

Figure 4.29: DEPT-135 NMR spectrum of grandidone A and 7-epimer grandidone A

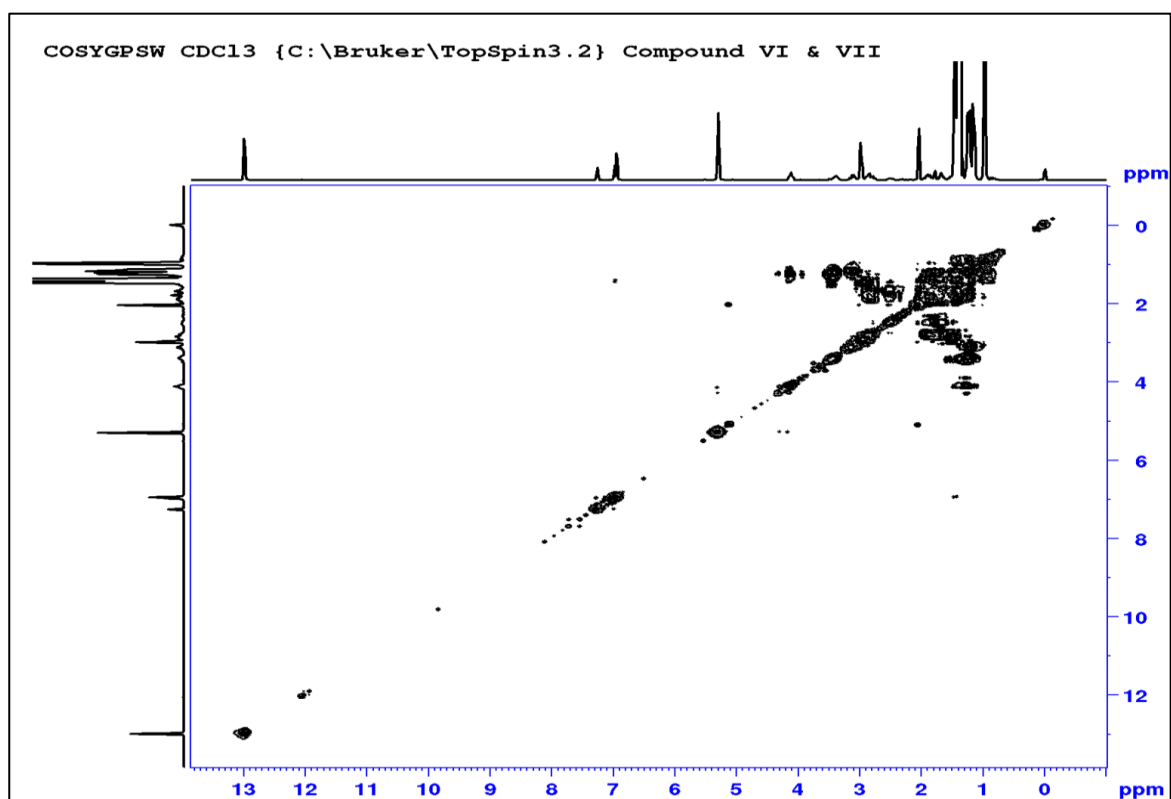


Figure 4.30: COSY NMR spectrum of grandidone A and 7-epimer grandidone A

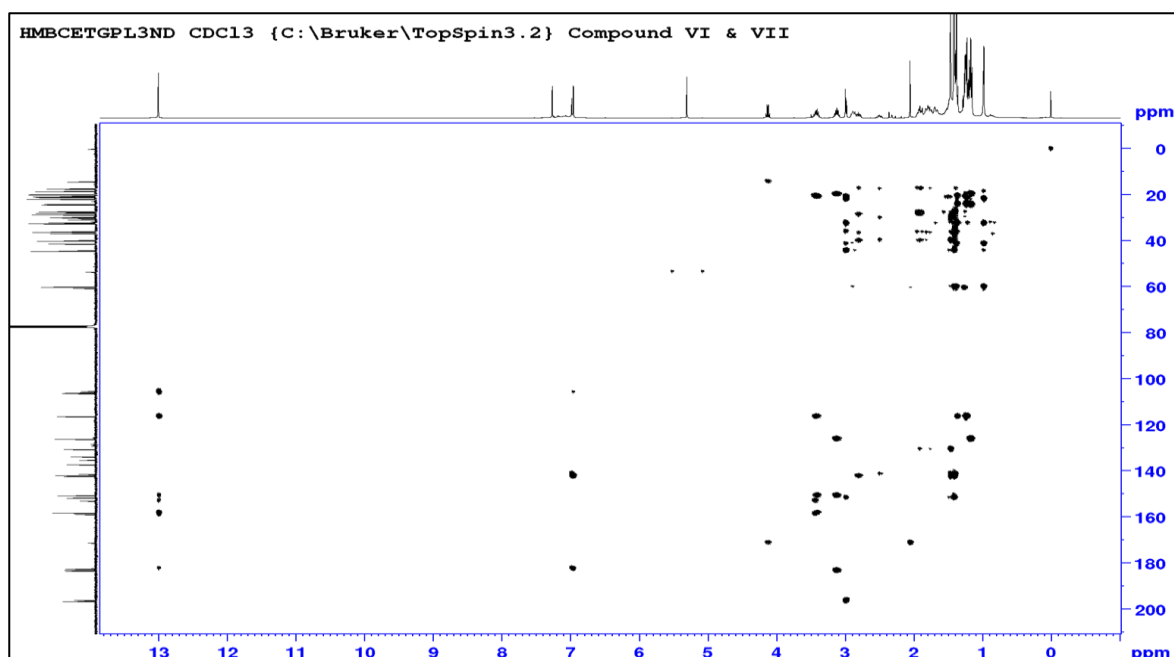


Figure 4.31: HMBC NMR spectrum of grandidone A and 7-epimer grandidone A

#### 4.7 Spectroscopic data of the isolated compounds

**6 $\beta$ ,7 $\alpha$ -dihydroxyroyleanone (C<sub>20</sub>H<sub>28</sub>O<sub>5</sub>):** Yellow crystal; melting point: 200°C;  $[\alpha]_D^{20} = -53$ ; IR: 3326 cm<sup>-1</sup> (OH), 2938 cm<sup>-1</sup> (CH), 1649 cm<sup>-1</sup> (C=O), 1422 cm<sup>-1</sup> (C=C), 1117 cm<sup>-1</sup> (C-O); UV: 270 nm and 400 nm; <sup>1</sup>H NMR (CDCl<sub>3</sub>) and <sup>13</sup>C NMR (CDCl<sub>3</sub>): see Table 4.6.

**7 $\alpha$ -acetoxy, 6 $\beta$ -hydroroyleanone (C<sub>22</sub>H<sub>30</sub>O<sub>6</sub>):** Yellow crystal, melting Point: 209°C;  $[\alpha]_D^{20} = +24$ ; IR: 3292 cm<sup>-1</sup> (OH), 2938 cm<sup>-1</sup> (CH), 1674 cm<sup>-1</sup> (C=O), 1457 cm<sup>-1</sup> (C=C), 1209cm<sup>-1</sup> (C-O); UV: 264 nm and 408 nm; <sup>1</sup>H NMR (CDCl<sub>3</sub>) and <sup>13</sup>C NMR (CDCl<sub>3</sub>): see Table 4.6.

**Horminone (C<sub>20</sub>H<sub>27</sub>O<sub>4</sub>):** Yellow crystal, melting point: 180 °C;  $[\alpha]_D^{20} = -130$ ; IR : 3301 cm<sup>-1</sup> (OH), 2947 cm<sup>-1</sup> (CH), 1451 cm<sup>-1</sup> (C=C), 1016 cm<sup>-1</sup> (C-O); UV: 262 nm and 410 nm; <sup>1</sup>H NMR (CDCl<sub>3</sub>) and <sup>13</sup>C NMR (CDCl<sub>3</sub>): see Table 4.6.

**Coleon U quinone (C<sub>20</sub>H<sub>24</sub>O<sub>5</sub>):** Yellow orange solid; IR: 3324 cm<sup>-1</sup> (OH), 2946 cm<sup>-1</sup> (C-H), 1649 cm<sup>-1</sup> (C=O), 1000 cm<sup>-1</sup> (C-O); UV: 260 nm and 424 nm; <sup>1</sup>H NMR (CDCl<sub>3</sub>) and <sup>13</sup>C NMR (CDCl<sub>3</sub>): see Table 4.6.

**Carnosolon (C<sub>20</sub>H<sub>26</sub>O<sub>5</sub>):** Green solid yellow crystal;  $[\alpha]_D^{20} = +62$ ; IR: 3339 cm<sup>-1</sup> (OH), 2934 cm<sup>-1</sup> (C-H), 1594 cm<sup>-1</sup> (C=O), 1440 cm<sup>-1</sup> (C=C), 1299 cm<sup>-1</sup> (C-O); UV: 278 nm, 404 nm <sup>1</sup>H NMR (CDCl<sub>3</sub>) and <sup>13</sup>C NMR (CDCl<sub>3</sub>): see Table 4.6.



**Grandidone A (C<sub>40</sub>H<sub>48</sub>O<sub>9</sub>) and 7-epimer grandidone A (C<sub>40</sub>H<sub>28</sub>O<sub>9</sub>):** Brown solid;  $[\alpha]_D^{20} = +81$ ; IR: 3318 cm<sup>-1</sup> (OH), 2947 cm<sup>-1</sup> (CH), 1657 cm<sup>-1</sup> (C=O), 1420 cm<sup>-1</sup> (C=C), 1117 cm<sup>-1</sup> (C-O); UV: 258 nm and 402 nm; <sup>1</sup>H NMR (CDCl<sub>3</sub>) and <sup>13</sup>C NMR (CDCl<sub>3</sub>): see Table 4.10.

#### 4.8 Conclusion

The sequential chromatographic methods and techniques used on the main fractions K4-3-III & IV, K4-3-VI, K4-3-VIII, K4-3-XI, and K4-3-XIII & XIV resulted in the isolation of five pure known royleanone type abietane diterpenoids viz 6 $\beta$ ,7 $\alpha$ -dihydroxyroyleanone (**I**), 7 $\alpha$ -acetoxy, 6 $\beta$ -hydroxyroyleanone (**II**), horminone (**III**), coleon U quinone (**IV**) and carnosolon (**V**). In addition to the isolated pure compounds, a mixture of epimeric dimers, namely grandidone A and 7-epimer grandidone A (**VI** & **VII**) was also isolated from the plant's extract, as illustrated in Figure 4.31. The weights of the compounds isolated from the main fractions (K4-3-III & IV, K4-3-VI, K4-3-VIII, K4-3-XI, and K4-3-XIII & XIV) is shown in Table 4.9. The structure elucidation and characterization of the isolated compounds were done by <sup>1</sup>H NMR, <sup>13</sup>C NMR, IR, UV, and optical rotation spectroscopic techniques, and the NMR data were compared with literature values. The X-ray crystallographic analysis of compound **II** and the 3D structure of compound **I** established the stereochemistry of compounds **I** and **II** as  $\beta$  and  $\alpha$  at C-6 and C-7 positions respectively.

**Table 4.9:** Compounds isolated from main fractions (K4-3-III & IV, K4-3-VI, K4-3-VIII, K4-3-XI, and K4-3-XIII & XIV) and their weight

Main fractions	Isolated compounds and code	Weight of compounds (mg)
K4-3-III & IV	Horminone ( <b>III</b> )	13.5
K4-3-VI	7 $\alpha$ -acetoxy-6 $\beta$ -hydroxyroyleanone ( <b>II</b> )	61.9
	Grandidone A and 7-epimer-grandidone A ( <b>VI</b> & <b>VII</b> )	16.9
K4-3-VIII	6 $\beta$ ,7 $\alpha$ -dihydroxyroyleanone ( <b>I</b> )	25.7
K4-3-XI	Coleon U quinone ( <b>IV</b> )	6.0
K4-3-XIII & XIV	Carnosolon ( <b>V</b> )	26.7

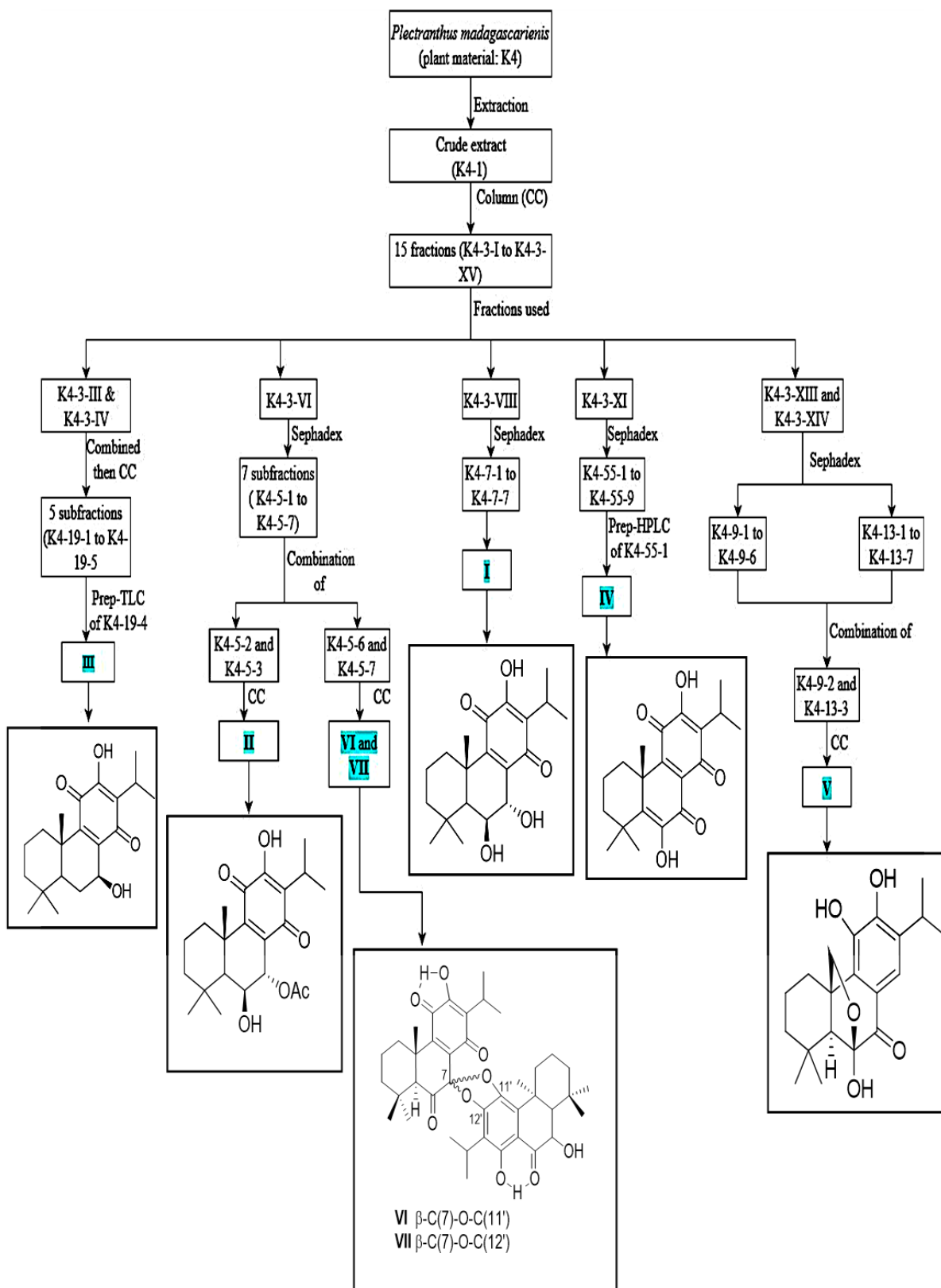


Figure 4.32: Methodology steps used in the isolation of bioactive compounds

## CHAPTER FIVE

### BIOLOGICAL EVALUATION

#### 5.1 Introduction

*P. madagascariensis* total extract and natural products were tested for their anti-diabetics, anti-tuberculosis, anti-psoriasis, and antioxidant activities. Some of the isolated compounds such as 6 $\beta$ ,7 $\alpha$ -dihydroxyroyleanone (I), 7 $\alpha$ -acetoxy-6 $\beta$ -hydroxyroyleanone (II), and horminone (III) previously isolated from *P. grandidentatus* showed activity against *Mycobacterium tuberculosis* H<sub>37</sub>Rv (Rijo et al., 2010). The 7 $\beta$  isomers of compound I and II, as well as coleon U quinone (IV) isolated from the study plant by Kubínová et al. (2014: 749-752), showed moderate to poor activity against  $\alpha$ -glucosidase inhibitor. Compounds I-VII were never evaluated for their anti-psoriasis activity. However, compounds I-IV were found to possess cytotoxic activities against NCI-H460 (lung cancer), NCI-H460/R (lung cancer), MCR-5 (healthy lung) and MCF-7 (breast cancer) cell lines. Moreover, the epimeric dimers grandidone A (VI) and 7-epimer grandidone A (VII) previously isolated from *P. grandidentatus* are known for their cytotoxicity properties against human cancer cell lines TK-10, MCF-7, UACC-62, NCI-H460, and SF-268 (Gaspar-Marques et al., 2002: 839-840; Cerqueira et al., 2004: 217-223). Compound V (carnosolon) isolated before from *P. cyanus* is an efficient antioxidant agent and is the only compound amongst those isolated which has been assessed for its antioxidant activity (Naman, 2015: 93-97). To our knowledge, the cytotoxicity activity of the isolated compounds against HaCaT cells was evaluated for the first time. Moreover, compounds V, VI & VII were also assessed for their  $\alpha$ -glucosidase and antimycobacterial activities for the first time.

In this chapter, the chemicals used during the biological studies are listed in section 5.2. Sections 5.3 to 5.6 describes the bioassays experimental procedures, cell cultures, data analysis, and interpretations of results. A conclusion about the tested compounds antituberculosis, antidiabetics, antioxidant, and anti-psoriasis inhibitory effects are given in section 5.7.

#### 5.2 Chemicals

The chemicals used for the different bioassays are tabulated in Table 5.1

**Table 5.1:** Bioassays chemicals reagents

Chemicals	Suppliers
$\alpha$ -Glucosidase ( <i>Saccharomyces cerevisiae</i> )	Sigma, Aldrich Cape Town, SA
<i>P</i> -nitro-phenyl- $\alpha$ -glucopyranoside	Sigma, Aldrich Cape Town, SA
Sodium carbonate	Kimix, Cape Town, SA

Sodium dihydrogen phosphate	Kimix, Cape Town, SA
Dimethyl sulfoxide	Kimix, Cape Town, SA
Green fluorescent protein	Sigma, Aldrich Cape Town, SA
Tyloxapol	Sigma, Aldrich Cape Town, SA
Albumin-Dextrose Complex	Sigma, Aldrich Cape Town, SA
D-glucose	Sigma, Aldrich Cape Town, SA
Casitone	Sigma, Aldrich Cape Town, SA
Tween 80	Sigma, Aldrich Cape Town, SA
7H9 broth medium	Sigma, Aldrich Cape Town, SA
Dibasic sodium phosphate	Sigma, Aldrich Cape Town, SA
Monobasic sodium phosphate	Sigma, Aldrich Cape Town, SA
Trypsin-EDTA	Sigma, Aldrich Cape Town, SA
Dulbecco's Modified Eagle Medium	Sigma, Aldrich Cape Town, SA
Fetal bovine serum	Sigma, Aldrich Cape Town, SA
Penicillin-streptomycin solution	Sigma, Aldrich Cape Town, SA
2,2'-azobis(2-amidinopropane) dihydrochloride	Sigma, Aldrich Cape Town, SA
Trolox	Sigma, Aldrich Cape Town, SA
L-ascorbic	Sigma, Aldrich Cape Town, SA

### 5.3 Antimycobacterial assay

The in vitro antimycobacterial activities of *P. madagascariensis* secondary metabolites, main fractions, and total extract against the green fluorescent protein (GFP) tagged *Mtb* H<sub>37</sub>Rv strain were carried out according to the standard broth microdilution method developed by Collins and Franzblau (1997), and Collins et al. (1998). In this assay, the mycobacterial strain H<sub>37</sub>Rv was cultured in the Middlebrook 7H9 broth medium supplemented with either Albumin-Dextrose complex, D-glucose, and tween 80 (7H9/ADC/Glu/Tw) or casitone, D-glucose, and tyloxapol (7H9/CAS/Glu/Tx). The minimum inhibition concentration at 90% (MIC<sub>90</sub>) of the tested samples were scored visually at one week and two weeks' post-inoculation using the microplate Alamar blue dye assay (MABA) and expressed in µg/mL. The media (7H9/ADC/Glu/Tw and 7H9/CAS/ Glu/Tx), as well as 5% dimethyl sulfoxide (DMSO) were used as a negative control, and rifampicin was used as a positive control.

#### 5.3.1 Cells culture

10 mL culture of *Mtb* H<sub>37</sub>Rv was grown to an optical density of 0.6-0.7 at 600nm (OD 600) at 37 °C. The culture was then diluted with either 7H9/ADC/Glu/Tw or 7H9/CAS/Glu/Tx medium to a ratio of 1:100.

### 5.3.2 Experimental procedure

12.8 mM of stock solutions were prepared in DMSO and diluted to 640 mM in two 7H9 mediums (7H9/ADC/Glu/Tw and 7H9/CAS/Glu/Tx). In a 96-well microtiter plate, 100  $\mu$ L of the diluted stock solution was added in duplicate to the wells in row 1 while 50  $\mu$ L of 7H9 medium supplemented with ADC/Glu/Tw or with CAS/Glu/Tx was added to the wells in rows 2-12. Afterward, a two-fold serial dilution was done by transferring 50  $\mu$ L of the solution in row 1 to row 2 using a multichannel pipette and aspirated to mix. The two-fold serial dilution procedure was replicated until row 12 was reached, from which 50  $\mu$ L was discarded in order to bring the final volume in all the wells to 50  $\mu$ L. Then, 50  $\mu$ L of the 1:100 diluted *Mtb* culture is added to all wells in rows 2-12, except row 1, as this serves as a contamination control evaporation. The microtiter plate was sealed in a zip lock bag and incubated at 37 °C alongside a humidifier to prevent liquid evaporation.

### 5.3.3 Data analysis

The MIC<sub>90</sub> values of the tested samples were determined using the dose-response curve (% inhibition) analysis of the relative fluorescence (excitation wavelength at 485 nm and emission wavelength at 520 nm) which were measured on the FLUOstar OPTIMA microplate reader. The dose-response curve was obtained by normalizing data to the minimum and maximum inhibition controls using the Levenberg-Marquardt algorithm method, from which the MIC<sub>90</sub> was calculated.

### 5.3.4 Results and discussions

The MIC<sub>90</sub> values of the tested substances after 7 and 14 days of post inoculation are tabulated in Table 5.2 and classified according to their potency.

Compounds and extracts with MIC<sub>90</sub>  $\leq$  10  $\mu$ g/mL were stratified as active; those with MIC<sub>90</sub> varying between 10-20  $\mu$ g/mL were indicated as having moderate activity, and those with MIC<sub>90</sub> between 20-125  $\mu$ g/mL were indicated with poor activity. Any MIC<sub>90</sub> values >125  $\mu$ g/mL were considered as inactive.

**Table 5.2:** The antimycobacterial activities of the isolated compounds, main fractions, and total extract at 90% inhibition in 7H9/ADC/Glu/Tw and 7H9/CAS/ Glu/Tx media.

	Identification code of samples	7H9/CAS/ Glu/Tx ( $\mu$ g/mL)		7H9/ADC/Glu/Tw ( $\mu$ g/mL)	
		7 days	14 days	7 days	14 days
Isolated compounds	I	62.5	60.62	>125	>125
	II	15.22	15.63	14.36	14.64
	III	14.34	3.96	>125	>125
	IV	15.62	1.93	>125	>125
	V	>125	>125	>125	>125
	VI & VII	>125	>125	>125	>125

Positive Control	Rifampin	0.015	0.035	0.001	0.002
Main fractions	K4-3-III & IV	>125	>125	>125	>125
	K4-3-VI	31,25	31,864	63,095	>125
	K4-3-VIII	16,189	14.71	>125	>125
	K4-3-XI	16,043	7.318	>125	>125
	K4-3-XIII & XIV	64,241	14.375	>125	>125
Total extract	K4-1-Hex	31.42	16.04	>125	>125

The antimycobacterial evaluation of the isolated compounds against *Mtb* H<sub>37</sub>Rv showed that the media in which the cells were cultured impinged on the potency of the tested substances. As observed, the isolated compounds showed activities only in the presence of 7H9/CAS/Glu/Tx medium except for compound **II** and main fraction K4-3-VI that displayed moderate activities in both medium (7H9/ADC/Glu/Tw and 7H9/CAS/Glu/Tx) from 7-14 days. This result may imply that the acetate group at the position 7 $\alpha$  in ring B of compound **II** is liable to the inhibitory activity in 7H9/ADC/Glu/Tw medium. This statement is verified as only the main fraction (K4-3-VI) containing compound **II** showed little activity against *Mtb* H<sub>37</sub>Rv in 7H9/ADC/Glu/Tw media at 7 days. Moreover, it was observed that the antimycobacterial potency of the isolated compounds increased from 7-14 days especially for compounds **III** and **IV** with MIC<sub>90</sub> values varying from 15.62-1.93  $\mu$ g/mL and 14.34-3.93  $\mu$ g/mL, respectively. Considering that the structure of the compounds **I** differs from that of compound **II** only by the presence of  $\beta$ -hydroxy group at C-6 and compound **I** (60.62  $\mu$ g/mL) had a poor antimycobacterial activity than compound **III** (3.96  $\mu$ g/mL), it was inferred that the 6 $\beta$ -hydroxy group reduces the compound's antimycobacterial potency. This observation can imply that *p*-benzoquinone ring C responsible for the antimycobacterial activities of several quinone compounds, as well as the substituents at C-6 and C-7 in ring B influence considerably the activity (Rijo et al., 2010). Compounds **V** and **VI** & **VII** did not show activity against the *Mtb* H<sub>37</sub>Rv in both mediums with MIC<sub>90</sub> values higher than 125  $\mu$ g/mL. However, main fractions K4-3-XIII & XIV and K4-3-VI comprising these bioactive compounds (**V** and **VI** & **VII**) showed weak to moderate activities between 7-14 days. This suggests that the isolated compounds are not responsible for the main fractions' inhibitory effects. The total extract antituberculosis activity went from poor to moderate activity with an MIC<sub>90</sub> that was reduced by half from 7-14 days showing the synergy between the bioactive compounds present in the total extract.

#### 5.4 *In vitro* $\alpha$ -glucosidase assay

The *in vitro*  $\alpha$ -glucosidase inhibition assay was conducted according to Telagari and Hullatti (2015) method with acarbose as a positive control. However, the half maximal inhibition concentration (IC<sub>50</sub>) of acarbose was above 610.4  $\mu$ g/mL. In this assay, the IC<sub>50</sub> of the tested substances was determined by measuring the release of *p*-nitrophenol from the *p*-

nitrophenyl- $\alpha$ -glucopyranoside (*p*-NPG) substrate. This method helps in determining the compounds and extracts capable of slowing down and regulate glucose absorption (Li et al., 2018).

#### 5.4.1 Phosphate buffer

20.209 g of dibasic sodium phosphate and 3.394 g of monobasic sodium phosphate were mixed and added to 800 mL of deionised water. The pH of the solution was adjusted to 6.8 using sodium hydroxide and topped up to 1L with distilled water.

#### 5.4.2 Experimental procedure

The isolated compounds and total extract were dissolved in MeOH to produce a stock solution of 1 mg/mL, while the total extract was dissolved in MeOH to make a stock solution of 2 mg/mL. In 96 well plates, 50  $\mu$ l phosphate buffer (100mM), 10  $\mu$ l alpha-glucosidase (1 U/mL), and 20  $\mu$ L of the tested samples were added and pre-incubated at 37 °C for 15 min. Different concentrations of the isolated compounds (500-3.25 $\mu$ g/mL), and total extract (1000-100  $\mu$ g/mL) were tested. The enzyme reaction was started by quickly adding 20  $\mu$ L of the substrate *p*-NPG (5 mM) before incubation at 37 °C for 20 min. Then, the enzyme reaction was ceased by adding 50  $\mu$ L of sodium carbonate (0.1 M). The change of absorbance was measured at wavelength 405 nm using a microplate reader.

#### 5.4.3 Data analysis

The inhibitory effect of the isolated compounds, main fractions, and total extract were calculated according to the following formula:

$\frac{A_s - A_c}{A_c} \times 100$ ; where  $A_s$  is the absorbance of the tested samples and  $A_c$  is the absorbance of the positive control.

The IC<sub>50</sub> of each sample was obtained by performing a nonlinear regression using GraphPad Prism 8 software (GraphPad Software, La Jolla, CA, USA).

#### 5.4.4 Results and discussions

The inhibitory effects of *P. madagascariensis* total extract and isolated compounds against the intestinal enzyme  $\alpha$ -glucosidase are summarized in Table 5.3. The positive control acarbose (IC<sub>50</sub> = 610.4  $\mu$ g/mL) had the lowest IC<sub>50</sub> among the tested samples implying that all the tested compounds have inhibitory effects against the enzyme  $\alpha$ -glucosidase (Table 5.3).

**Table 5.3:** Activity profile of the IC<sub>50</sub> values of *P. madagascariensis* isolated compounds and total extract against  $\alpha$ -glucosidase

	Identification code of samples	IC <sub>50</sub> ( $\mu$ g/mL)
Isolated compounds	I	128.50 $\pm$ 7.6
	II	94.06 $\pm$ 2.4
	III	280.6 $\pm$ 3.5
	IV	72.58 $\pm$ 0.8
	V	208.3 $\pm$ 6.5
	VI & VII	4.22 $\pm$ 0.4
Positive Control	Acarbose	610.4
Total extract	K4-1-Hex	156.4 $\pm$ 1.3

The inhibitory activities of the bioactive compounds viz 6 $\beta$ ,7 $\alpha$ -dihydroxyroyleanone (I), 7 $\alpha$ -acetoxy-6 $\beta$ -hydroxyroyleanone (II) and coleon U quinone (IV) against the enzyme  $\alpha$ -glucosidase were similar to the one obtained by Kubínová et al. (2014) except for compound IV which showed greater activity with an IC<sub>50</sub> of 72.58  $\mu$ g/mL. The epimeric dimers grandidone A and 7-epimer grandidone A (VI & VII) as well as compounds II and IV showed significant inhibition potencies against  $\alpha$ -glucosidase with IC<sub>50</sub> of 4.22  $\mu$ g/mL (VI & VII), 94.06  $\mu$ g/mL (II) and 72.58  $\mu$ g/mL (IV) respectively. Based on these results, these two pure compounds (II and IV) and the epimeric dimers (VI & VII) can slow down the hydrolysis or digestion of the starch by  $\alpha$ -glucosidase enzymes which will result in a suppression of hyperglycaemia and better regulation of blood glucose level (Figure 5.1 and Figure 5.2). Furthermore, the mixture of dimers which was never reported as  $\alpha$ -glucosidase inhibitors, displayed a strong inhibitory effect against  $\alpha$ -glucosidase. Compounds I, III and V showed activity with an IC<sub>50</sub> of 128.50  $\mu$ g/mL, 280.6  $\mu$ g/mL, and 208.3  $\mu$ g/mL respectively. The total extract K4-1-Hex showed moderate activity against  $\alpha$ -glucosidase with IC<sub>50</sub> of 156.4  $\mu$ g/mL.

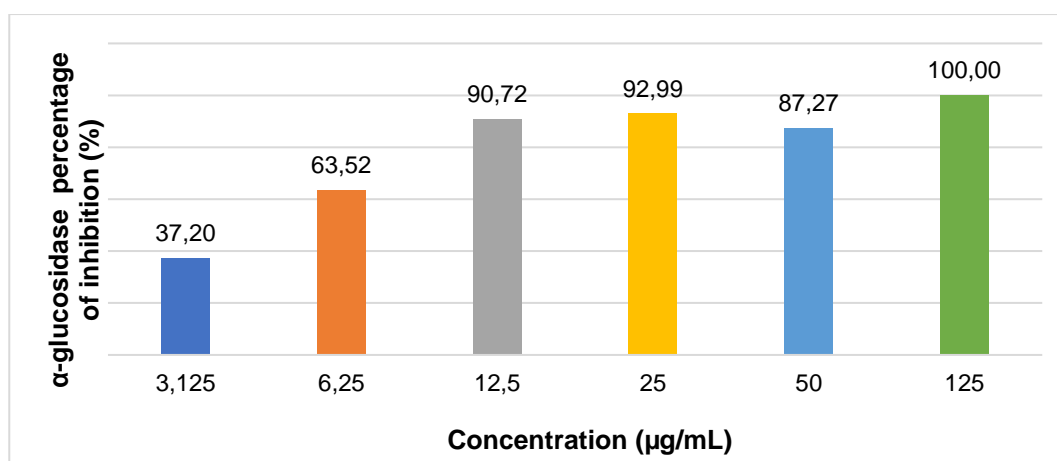


**Figure 5.1:**  $\alpha$ -glucosidase percentage inhibition of the grandidone A and 7-epimer grandidone A (VI & VII).



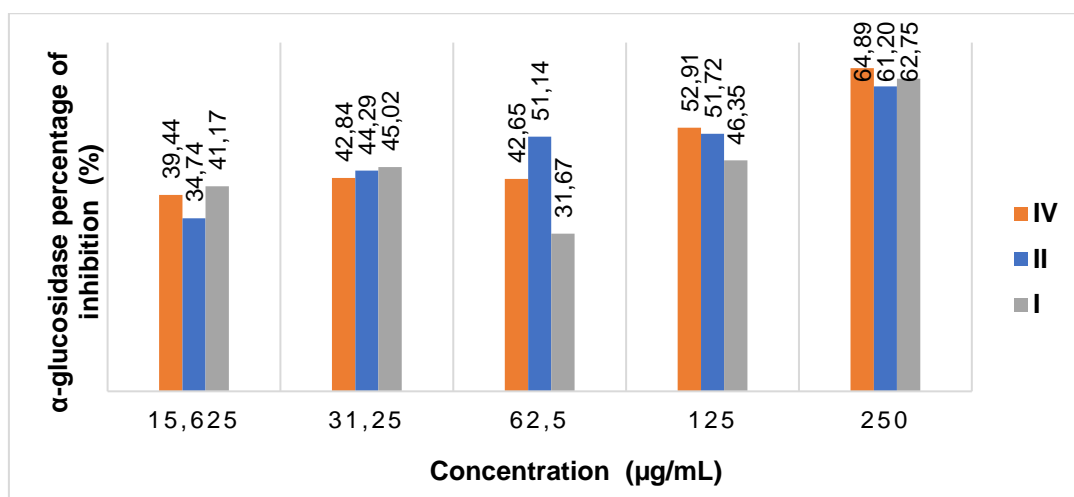


Figure 5.2:  $\alpha$ -glucosidase percentage of inhibition of compounds I, II, and IV.

## 5.5 *In vitro* Cytotoxicity Assay

The immortalized human skin epithelial keratinocytes (HaCaT) cell proliferation after treatment with *P. madagascariensis* total extract and isolated compounds was determined using the 3-(4,5-dimethylthiazol-2-yl)-2,5-diphenyltetrazolium bromide (MTT) assay reported by Mossmann (1983). The assay was used to determine the *in vitro* cytotoxicity activity of the isolated abietane diterpenoids and total extract against the HaCaT cells with tamoxifen as a positive control.

### 5.5.1 Cells Culture

HaCaT cells were cultured in Dulbecco's modified eagle medium (DMEM), which was supplemented with 10% fetal bovine serum (FBS) and 1% penicillin-streptomycin solution (penstrep). The HaCaT cells were grown for 4-5 days at 37 °C in a 5% carbon dioxide atmosphere. The cells were removed from the culture using trypsin-ethylenediaminetetraacetic acid solution (trypsin-EDTA) and transferred into a 96 well plate.

### 5.5.2 Experimental procedure

Stock solutions of 1 mg/mL of each sample were prepared in 10% DMSO and diluted to 100 µg/mL in the complete DMEN medium. It was followed by ten-fold serial dilution (100-0.001 µg/mL) and two-fold serial dilution (100-25 µg/mL) of the stock solutions. The positive control tamoxifen was also subjected to comparable dilutions process. The tested samples were applied to the cells and incubated at 37 °C for 24 hours. Thiazolyl blue (MTT, SIGMA) dissolved in phosphate buffered saline solution (PBS) at a final concentration of 0.8 mg/mL, was added to the cells that were exposed to the isolated compounds and total extract before incubation at 37°C in the dark for 4 hours. After observing the MTT change of colour (blue to purple), the media was separated and washed with PBS. The produced formazan

salts were dissolved with DMSO, and their concentrations were obtained by measuring their absorbance at 570 nm in a spectrophotometer.

### 5.5.3 Data analysis

All experiments were performed in triplicate, and recorded absorbances were used to determine the compounds (**I-VII**) and total extract cytotoxic activities against HaCaT cells. The  $IC_{50}$  values of the tested compounds were determined using GraphPad Prism 8 software (GraphPad Software, La Jolla, CA, USA). The dose-response curve (Figure 5.3) was obtained by normalizing data to the minimum and maximum inhibition controls using the Levenberg-Marquardt algorithm method, from which the  $IC_{50}$  was calculated.

### 5.5.4 Results and discussions

The percentage of proliferation of the isolated compounds and total extract against HaCaT cells is presented in terms of the log dose-response curve (Figure 5.3) with their  $IC_{50}$  values summarised in Table 5.4.

From the results obtained, the total extract and isolated compounds inhibit HaCaT cells in a dose-response dependent manner. Compounds **IV** and **V**, as well as the total extract (K4-1-Hex), were the most active test substances with  $IC_{50}$  of 33.88  $\mu\text{g/mL}$ , 27.52  $\mu\text{g/mL}$ , and 28.18  $\mu\text{g/mL}$ , respectively. The royleanone 7 $\alpha$ -acetoxy-6 $\beta$ -hydroxyroyleanone, 6 $\beta$ ,7 $\alpha$ -dihydroxyroyleanone, and horminone were moderately active against HaCaT cells whereas the dimers grandidone A and 7-epimer grandidone A showed poor antiproliferation inhibitory effect. The total extract ( $IC_{50} = 28.18 \mu\text{g/mL}$ ) which contains all the isolated compounds showed a good inhibitory effect as well as the synergetic effect of the bioactive compounds to suppress HaCaT cells. Furthermore, Diogo et al. (2019) stated that the difference between the cytotoxicity effect of royleanone type abietane lies on the polarity and lipophilicity of the substituent at 7 $\alpha$  position as well as on the presence of an electron-donating group at position 6. It was clearly proven by the  $IC_{50}$  values of compounds **I-III** which demonstrated that compound **II** is more potent than compounds **I** and **III** because the acetate group at position 7 $\alpha$  of compound **II** is more polar than the hydroxyl group at position 7 $\alpha$  of compounds **I** and **III**. It was also observed that compound **III** is more active than compound **I**, which implies that the substituents at position 6 of royleanones type abietane does not really affect the compounds cytotoxicity effects against HaCaT. González (2014) stated that aromatic abietane diterpenoids with catechol containing molecules and a carbonyl group at C-7 as well as coleons type abietane with diosphenol moiety in ring B displayed significant cytotoxicity activity. This statement was corroborated by compounds **IV** and **V** which were found to be the most active isolated compounds with an  $IC_{50}$  of 33.88  $\mu\text{g/mL}$  and 27.52  $\mu\text{g/mL}$ . Grandidone A, which was reported to have cytotoxicity activity showed weak antiproliferation activity when combined with 7-epimer

grandidone A. It can be suggested the combination of these epimeric dimers can barely reduce the proliferation of lymphocyte apoptosis in HaCaT cells or they have antagonistic effect when combined.

**Table 5.4:** The cytotoxicity activities of the *P. madagascariensis* isolated compounds and total extract against HaCaT cells.

Samples	IC <sub>50</sub> (µg/mL)
I	28.18 ± 2.42
II	60.25 ± 3.95
III	42.66 ± 1.22
IV	53.70 ± 0.67
V	33.88 ± 1.43
VI & VII	75.86 ± 1.31
K4-1-Hex	28.18 ± 0.84
Positive control (Tamoxifen)	22.00

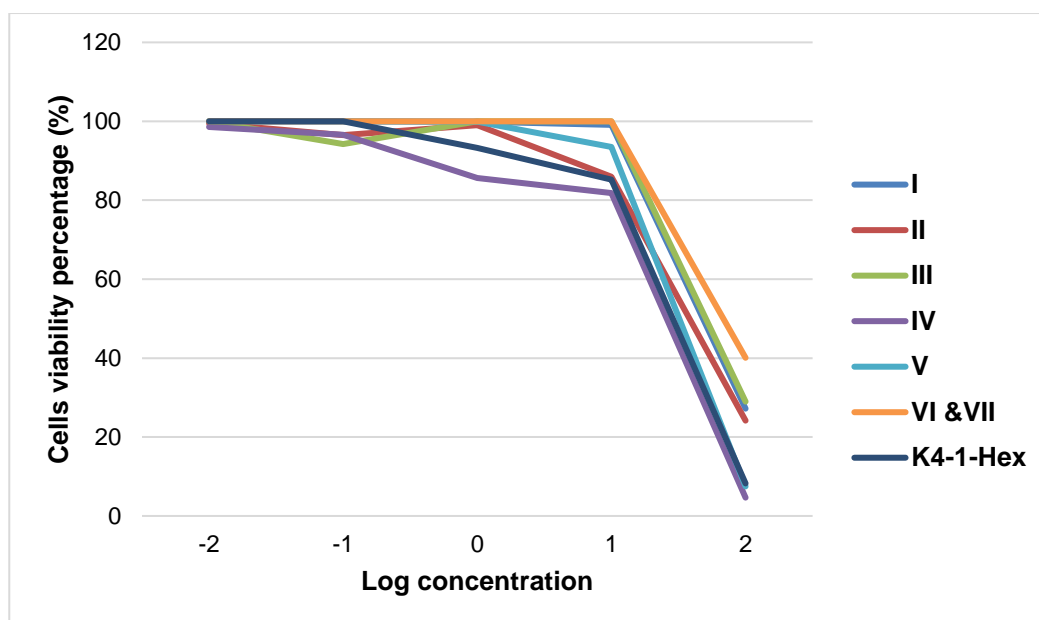


**Figure 5.3:** Dose-response curve of *P. madagascariensis* constituents and total extract against HaCaT cells

## 5.6 Antioxidant assay

The antioxidant activities of compound I-VII was assessed using three different free radical scavenging assays, namely ferric ion reducing antioxidant power (FRAP), automated oxygen radical absorbance capacity (ORAC), and Trolox equivalent absorbance capacity (TEAC).

The FRAP assay was conducted according to Benzie and Strain's (1996) method, which consists of finding the compounds' antioxidant potential in terms of µM ascorbic acid equivalents per milligram dry weight (µM AAE/g).

The ORAC assay was conducted according to Prior et al. (2003) method, which is a modified version of the original ORAC assay developed by Cao and Prior (1998: 50-62). In this assay, 2,2'-azobis(2-amidinopropane) dihydrochloride (AAPH) underwent thermal decomposition to generate peroxy radicals resulting in the reduction of fluorescent from fluorescein. The antioxidant potential of the isolated compounds was measured by their ability to prevent any loss of fluorescent from fluorescein by neutralizing peroxy radicals and assessing the sample's fluorescence area under the curve (AUC). ORAC values were expressed as  $\mu\text{M}$  Trolox equivalents (TE) per milligram of test samples ( $\mu\text{M TE/L}$ ).

The TEAC assay was done according to the method developed by Pellegrini et al. (1999), which consists of determining the activities of the isolated compounds in terms of  $\mu\text{M}$  Trolox equivalents per milligram dry weight ( $\mu\text{M TE/g}$ ) of the test samples.

L-ascorbic was used as a standard in FRAP assay with concentrations varying between 0 and 1000  $\mu\text{M}$  (Figure 5.4). On the other hand, Trolox was used as the standard for ORAC and TEAC assays with concentrations ranging from 0-500  $\mu\text{M}$  (Figure 5.5). The antioxidant epigallocatechingallate (EGCG) was used as a positive control.

#### **5.6.1 FRAP assay**

In a 96 well plate, 10  $\mu\text{L}$  of the 100  $\mu\text{g/mL}$  of the isolated compounds (**I-VII**) and total extract (K4-1-Hex) stock solutions were added to 300  $\mu\text{L}$  of FRAP reagent. The FRAP reagent was prepared by mixing 30 mL of acetate buffer (300 mM, pH 3.6), 3mL of tripyridyl triazine (TPTZ) (10 mM in 40 mM HCl) and 3mL of  $\text{FeCl}_3 \cdot 6\text{H}_2\text{O}$  (20 mM) in a 50 mL conical tube. After the addition of the samples' stock solutions to the FRAP reagent, the 96 well plate was incubated at room temperature for 30 minutes. The antioxidant potential was read at a wavelength of 593 nm in a Multiskan (Thermo Fisher Scientific) spectrum plate reader.

#### **5.6.2 ORAC assay**

An illuminated 96 well plate was used to mix 12  $\mu\text{L}$  of 100  $\mu\text{g/mL}$  of each sample and 138  $\mu\text{L}$  of a fluorescein working solution. This was followed by the addition of 50  $\mu\text{L}$  of AAPH prepared by adding 6 mL phosphate buffer to 150 mg of AAPH. The Fluoroskan spectrum plate reader was programmed to record fluorescein's fluorescence every 2 minutes after the addition of AAPH with the excitation wavelength at 485 nm and the emission wavelength at 530 nm. The Trolox stock solution was used as standard with concentration varying between 0-417  $\mu\text{M}$ . The ORAC values were calculated using a regression equation ( $Y = mx + c$ ) between Trolox concentration (Y in  $\mu\text{M}$ ) and the net area under the fluorescence decay curve (X).

### 5.6.3 TEAC assay

The stock solution used is a mixture of 88  $\mu\text{L}$  of 140mM of potassium peroxodisulphate ( $\text{K}_2\text{S}_2\text{O}_8$ ) and 5 mL of 7 mM of 2,2'-azino-bis (3-ethylbenzothiazoline-6-sulfonic acid (ABTS) in a 15 mL screw cap. The prepared ABTS solution was kept in a dark place at room temperature for 24 hours before use. The following day the prepared ABTS solution was diluted with ethanol (about 1 mL of ABTS solution mixed with 20 mL of ethanol) to be able to read the absorbance of approximately 2.0 ( $\pm 0.1$ ). Trolox was used as the standard with concentrations ranging between 0-500  $\mu\text{M}$ . In a 96 well plate, 25  $\mu\text{L}$  of the standards and isolated compounds were added to 300  $\mu\text{L}$  of ABTS mixture and incubated at room temperature for 30 minutes. The absorbance was recorded by a Multiskan spectrometer plate reader at wavelength 734 nm.

### 5.6.4 Results and discussions

The antioxidant activities of compounds **I-VII** were assessed using different free radical scavenging assays, namely ORAC, TEAC, and FRAP as summarised in Table 5.5.

**Table 5.5:** Antioxidant activity of the isolated compounds

Compounds	TEAC ( $\mu\text{M TE/g}$ )	FRAP ( $\mu\text{M AAE/g}$ )	ORAC ( $\mu\text{M TE/L}$ )
<b>I</b>	5080.8 $\pm$ 0.04	541.5 $\pm$ 1.59	23625 $\pm$ 1.64
<b>II</b>	3700.8 $\pm$ 1.50	345.5 $\pm$ 0.77	21404.1 $\pm$ 4.35
<b>III</b>	Inactive	296.5 $\pm$ 6.72	12443.3 $\pm$ 3.61
<b>IV</b>	225.5 $\pm$ 1.47	2109.6 $\pm$ 2.78	21857.8 $\pm$ 5.85
<b>V</b>	4876.3 $\pm$ 0.49	13772.2 $\pm$ 2.76	29287.4 $\pm$ 4.75
<b>VI &amp; VII</b>	3981.9 $\pm$ 0.16	1154.1 $\pm$ 2.60	11803.2 $\pm$ 1.50
<b>Positive control (EGCG)</b>	4722.5 $\pm$ 2.22	10455.1 $\pm$ 0.81	14970 $\pm$ 5.53

Based on the results obtained, compound **V** is the most potent antioxidant compound as it displayed a remarkable antioxidant inhibitory effect in all assays. Compound **V** ability to suppress radicals chain reactions via hydrogen atom transfer (HAT) and single electron transfer (SET) mechanisms is due to the catechol groups in the benzene ring. Compound **I** showed very little activity in FRAP assay. However, in TEAC and ORAC assays, compound **I** displayed good antioxidant activities suggesting that compound **I** neutralize the radical cation generated by ABTS as well as the peroxy radicals generated from the thermal decomposition of AAPH by HAT mechanism (Zhong & Shadidi, 2015). Compounds **II** and **IV** showed good activity in ORAC assay and weak antioxidant activities in TEAC and FRAP assays. At last, none of the isolated compounds showed significant activity in the FRAP assays classifies as SET methods except for compound **V**.

## 5.7 Conclusions

The antimycobacterial, anti-psoriasis, antidiabetic and antioxidant evaluation of the isolated compounds showed that compound **IV** is the most remarkable one due to its ability to inhibit *Mtb* H<sub>37</sub>Rv in 7H9/CAS/Glu/Tx medium as well as HaCaT cells. Moreover, compound **IV** can prevent peroxy free radical formation by the HAT mechanism as well as slowing down glucose hydrolysis by the intestinal enzyme  $\alpha$ -glucosidase.

Compounds **I** showed little activity in all assays except for the antioxidant assay TEAC and ORAC. This implies that compound **I** is an antioxidant agent that can only suppress free radicals by HAT mechanisms. Compound **II** displayed mild activity against *Mtb* H<sub>37</sub>Rv in both medium (7H9/CAS/Glu/Tx and 7H9/ADC/Glu/Tw). Like compound **I**, the antioxidant activity of compound **II** is pronounced only in assays that suppress free radicals by the HAT mechanism. Compound **II** also showed moderate inhibitory effects against the enzyme  $\alpha$ -glucosidase and HaCaT cells. Compound **III** exhibited good antimycobacterial property in 7H9/CAS/Glu/Tx media, but it has a poor antioxidant and cytotoxicity properties. Compound **V** is the most potent antioxidant and cytotoxic agents among the isolated compounds. Furthermore, compound **V** can stop the free radical chain reaction by SET and HAT mechanisms. The mixture of dimers (**VI** & **VII**) displayed strong  $\alpha$ -glucosidase inhibitory effect and mild antioxidant activity in assays classified as HAT methods. However, the mixture (**VI** & **VII**) cytotoxic inhibitory effect against HaCaT cells is weak.

## CHAPTER SIX

### CONCLUSION AND RECOMMENDATIONS

#### 6.1 Conclusions

This research study aimed to extract, isolate, characterize, and evaluate the antitubercular, antidiabetic, and anti-psoriasis properties of the phytochemical constituents of the aerial parts of *P. madagascariensis*. Through the phytochemical screening of *P. madagascariensis* semi-polar extract via chromatographic methods, it was found that the plant is rich in abietane diterpenoids, but it also possesses triterpenoids and caffeic acids. The bioactive compounds of this medicinal plant were isolated from the plant extract using chromatographic techniques such as column chromatography, prep-TLC, Sephadex LH-20, and semi-prep HPLC. The chemical study of *P. madagascariensis* led to the isolation of seven compounds consisting of five pure compounds and a mixture of two dimers. The structural elucidation of the seven bioactive compounds isolated from *P. madagascariensis* was done using the spectroscopic techniques namely NMR, X-ray, UV, and FTIR. From the NMR, X-ray, UV and FTIR spectrums, compounds **I**, **II**, **III**, **IV**, **V** were determined to be royleanone type abietane diterpenoids, whereas compounds **VI** and **VII** are abietane dimers. The royleanones 6 $\beta$ ,7 $\alpha$ -dihydroxyroyleanone (**I**), 7 $\alpha$ -acetoxy-6 $\beta$ -hydroxyroyleanone (**II**), horminone (**III**) and coleon U quinone (**IV**) and carnosolon (**V**), as well as the dimers grandidone A and 7-epimer grandidone A (**VI** & **VII**), were evaluated for their antitubercular, antidiabetic, antioxidant and cytotoxic activities. The X-ray crystallography of compound **II** showed that compound **I** and compound **II** have the 6 $\beta$ , 7 $\alpha$  stereochemical configurations

The antitubercular activity of compounds **I-V** and the mixture **VI** & **VII** showed that the medium, in which the *Mtb* bacillus is cultured, affects the percentage of inhibition of the compounds. Moreover, the *p*-benzoquinone ring C responsible for the antimycobacterial activities of several quinone compounds, as well as the substituents at C-6 and C-7 in ring B, influence the activity considerably. The royleanone 7 $\alpha$ -acetoxy-6 $\beta$ -hydroxyroyleanone is the only isolated compound to show activity against *Mtb* H<sub>37</sub>Rv in 7H9/ADC/Glu/Tw media due to the acetate group at position 7 $\alpha$  in ring B. Coleon U quinone and horminone effectively inhibit the *Mtb* H<sub>37</sub>Rv in the 7H9/CAS/Glu/Tx medium, after 14 days with MIC<sub>90</sub> values of 1.93  $\mu$ g/mL and 3.96  $\mu$ g/mL respectively. The MIC<sub>90</sub> values of compound **I-III** demonstrated that the hydroxy group at position 6 $\beta$  reduced the compound's antimycobacterial activities. Carnosolon and the epimeric dimers grandidone A and 7-epimer grandidone A are inactive against *Mtb* H<sub>37</sub>Rv in both mediums with MIC<sub>90</sub> values higher than 125  $\mu$ g/mL.

The cytotoxicity activity of the isolated natural products showed that compounds **IV** and **V** are good cytotoxicity agents against HaCaT cells with IC<sub>50</sub> of 33.88  $\mu$ g/mL and 27.52

µg/mL. Compounds **I-III** displayed moderate activity against HaCaT cells, whereas the mixture **VI & VII** showed poor antiproliferation activities. The epimeric dimers (**VI & VII**) showed little to no activity in antioxidant, antituberculosis, and cytotoxicity assays. However, they exhibited a strong inhibitory effect against the intestinal enzyme α-glucosidase with IC<sub>50</sub> 4.22 µg/mL. The roylenaone **I, II, and IV** showed mild activity with IC<sub>50</sub> of 128.50 µg/ml, 94.06 µg/mL, 72.58 µg/mL respectively. Compound **I, III, and V** exhibited weak (**II**) to no activity (**III and V**) against the enzyme α-glucosidase.

The free radical scavenging assays (ORAC, TEAC, and FRAP) done on *P. madagascariensis* natural products showed that the isolated compounds suppress free radicals' formation or chain reactions by HAT mechanism except for compound **V** which operate by the SET and HAT mechanisms. Compounds with the ability to inhibit free radicals by both mechanisms showed strong antioxidant activity compared to the ones that operate by HAT or SET only.

Furthermore, it was also noticed that compounds with good cytotoxicity activity like compounds **II, IV, and V** are good antioxidant agents. Moreover, compounds **II and IV** are the only isolated abietane diterpenoids that displayed good to moderate activities in all assays.

The findings of this research study establish *P. madagascariensis* as an important medicinal plant rich in diterpenoids which may be useful for the treatment of tuberculosis, diabetes, and psoriasis. It is envisaged that this study will contribute to a better understanding of the phytochemistry of *P. madagascariensis* and contribute to the development of potential antitubercular, antidiabetic, and anti-psoriasis compounds with improved activities.

## 6.2 Recommendation

The recommendations that can be made are to derivatize the isolated compounds and re-assess their antitubercular, antidiabetic, and cytotoxicity properties to study the structure-activity relationship in order to improve the biological activities.



## References

- Abdel-Mogib, M., Albar, H. & Batterjee, S.M. 2002. Chemistry of the Genus *Plectranthus*. *Molecules*, 7: 271-301.
- Ahmad, I. & Beg, A.Z. 2001. Antimicrobial and phytochemical studies on 45 Indian medicinal plants against multi-drug resistant human pathogens. *Journal of Ethnopharmacology*, 74: 113-123.
- Ahmadi, S., Marino, T., Prejan, M., Russo, N. & Toscano, M. 2018. Antioxidant Properties of the Vam3 Derivative of Resveratrol. *Molecules*, 23: 1-12.
- Alasbahi, R.H. and Melzig, M.F. 2010. *Plectranthus barbatus*: A Review of Phytochemistry, Ethnobotanical Uses and Pharmacology – Part 1. *Planta Medica*, 76: 653-661.
- Alder, A.C., Ruedi, P. & Eugster, C.H. 1984. Drusenfarbstoffe aus Labiaten: Identifizierung von 17 Abietanoiden aus *Plectranthus sanguineus* BRITTEN. *Helv. Chim. Acta*, 70: 975-983.
- Ali, A.M., Mackeen, M.M., Sharkawy, E.S.H., Hamid, J.A., Ismail, N.H., Ahmad, F.B.H. & Lajis, N.H. 1996. Antiviral and cytotoxic activities of some plants used in Malaysian indigenous medicine. *Pertanika J. Trop. Agric. Sci.*, 19: 129-136.
- Amoa Onguéné, P., Ntie-Kang, F., Likowo Lifongo, L., Ndom, J.C., Sippl, W. & Meva'a Mbaze, L. 2013. The potential of anti-malarial compounds derived from African medicinal plants, part I: a pharmacological evaluation of alkaloids and terpenoids. *Malaria Journal*, 12(1): 449.
- Arihara, S., Ruedi, P. & Eugster, C.H. 1977. Diterpenoid leaf-gland pigments: coleons S and T from *Plectranthus caninus* Roth (Labiatae), a new diosphenol-trans- A/B-6,7-diketone pair of the abietane series. *Helvetica Chimica Acta*, 60: 1443-1447.
- Arihara, S., Ruedi, P. & Eugster, C.H. 1983. Spirocoleone: Synthese und Charakterisierung von vier diastereomeren Spiro (methylcyclopropan)-Substrukturen; Revision der Konfiguration an C (12) und C (15) von Coleon P und Derivaten sowie von Coleon-Z-Derivaten; Röntgenstrukturanalysen von Lanugon J und weiteren Spirocoleonen. *Helv. Chim. Acta*, 66: 429-449.
- Arumugam, G., Swamy, M.K. & Sinniah, U.R. 2016. *Plectranthus amboinicus* (Lour.) Spreng: Botanical, Phytochemical, Pharmacological and Nutritional Significance. *Molecules*, 21: 1-26.
- Ascensao, L., Figueiredo, A.C., Barroso, J.G., Pedro, L.G., Schripsema, J., Deans, S.G. & Scheffer, J.J.C. 1998. *Plectranthus madagascariensis*: morphology of the glandular trichomes, essential oil composition and its biological activity. *International Journal of Plant Science*, 159: 31-38.
- Ascensao, Arumugam, G., Swamy, M.K. & Sinniah, U.R. 2016. *Plectranthus amboinicus* (Lour.) Spreng: Botanical, Phytochemical, Pharmacological and Nutritional Significance. *Molecules*, 21: 1-26.
- Aston, L.E., Makunga, N.P., Platten, S.J. 2018. Local Medicinal Plant Knowledge in South Africa Preserved by Apartheid. *Human Ecology*, 39(2): 203-216.
- Aswal, B.S., Bhakuni, D.S., Goel, A.K., Kar, K., Mehrotra, B.N. & Mukherjee, K.C. 1984. Screening of Indian plants for biological activity: Part X. *Indian J of Exp Bio.*, 22: 312-332.
- Ávila, F. N., Pinto, F.C.L., Sousa, T.S., Torres, M.C.M., Costa-Lotufo, L.V., Rocha, D.D., De Vasconcelos, M.A., Cardoso-Sá, N., Teixeira, E.H., Albuquerque, M.R.J.R., Silveira, E.R. & Pessoa, O.D.L. 2017. Miscellaneous diterpenes from the aerial parts of *Plectranthus ornatus* Codd. *Journal of the Brazilian Chemical Society*, 28(6): 1014-1022.

- Balick, M.J. & Cox, P.A. 1997. Plants, People, and Culture: Science of Ethnobotany. *Scientific American Library*.1: 1.
- Balunas, M.J. & Kinghorn, A.D. 2005. Drug discovery from medicinal plants. *Life Sciences*, 78: 431-441.
- Baranitharan, M. & Dhanasekaran, S. 2014. Mosquitocidal efficacies of medicinal plant of *Coleus aromaticus* Benth (Lamiaceae) leaf extracts Chikungunya vector, *Aedes aegypti* (Linn.) (Diptera: Culicidae). *Int. J. Curr. Res.Chem. Pharm. Sci.*, 1: 61–67.
- Barbour, L. J. 2001. X-Seed — A Software Tool for Supramolecular Crystallography. *J. Supramol. Chem.*, 1: 189-191.
- Batista, O., Simões, F.M., Duarte, A., Valdeira, L.M., De La Torre, M.C. & Rodríguez, B. 1995. An antimicrobial abietane from the root of *Plectranthus hereroensis*. *Phytochemistry*, 38(1): 167-169.
- Batista, O., Simoes, M.F., Nascimento, J., Riberio, S., Duarte, A., Rodriguez, B. & De La Torre, M.C. 1996. A rearranged abietane diterpenoid from *Plectranthus hereroensis*. *Phytochemistry*, 41: 571-573.
- Benzie, I.F.F. & Strain, J.J. 1996. Ferric reducing ability of plasma as measure of antioxidant power: The FRAP assay. *Analytical Biochemistry*, 238: 70-76.
- Bernardes, C.E.S., Garcia, C., Pereira, F., Mota, J., Pereira, P.C., Cebola, M.J., Reis, C.P., Correia, I., Da Piedade, F.M., Da Piedade, M.E.M. & Rijo, P. 2018. Extraction optimization, structural and thermal characterization of the antimicrobial abietane 7#-acetoxy-6#-hydroxyroyleanone. *Mol. Pharmaceutics*, 1:1-20.
- Bero, J. & Fre, M. 2009. Antimalarial compounds isolated from plants used in traditional medicine. *Journal of Pharmacy and Pharmacology*, 61: 1401-1433.
- Bhatt, A., Naidoo, Y. & Nicholas, A. 2010. The foliar trichomes of *Plectranthus laxiflorus* Benth [Lamiaceae]: An important medicinal plant. *New Zealand Journal of Botany*, 48(2): 55-56.
- Bordignon, V., Bultrini, S., Prignano, G., Sperduti, I., Piperno, G., Bonifati, C., Filippetti, M., Toma, L., Latini, A., Di Cecio, M., Giuliani, A., Vocaturo, A., Trento, E., D' Agosto, G., Francesconi, F., Cataldo, A., Vento, A., Cilenti, V., Berardesca, E., Ameglio, F., Cordiali, F. P. & Ensoli, F. 2011. High prevalence of latent tuberculosis infection in autoimmune disorders such as psoriasis and in chronic respiratory diseases, including lung cancer. *J Biol Regul Homeost Agents*, 25: 213-220.
- Brasileiro, B.G., Pizziolo, V.R., Raslan, D.S., Jamal, C.M. & Silveira, D. 2006. Antimicrobial and cytotoxic activities screening of some Brazilian medicinal plants used in Governador Valadares district. *Braz J Pharm Sci*, 42: 195-202.
- Brito, E., Gomes, E., Falé, P.L., Borges, C., Pacheco, R. & Teixeira, V. 2018. Bioactivities of decoctions from *Plectranthus* species related to their traditional use on the treatment of digestive problems and alcohol intoxication. *Journal of Ethnopharmacology*, 220: 147-154.
- Bruker. 1997. *AXS Inc. XPREP, Release 5.1/NT; X-Ray Data Preparation and Reciprocal Space Exploration Program*. Madison, Wisconsin, USA.
- Bruker. 2005. *AXS Inc. Program SAINT, Version 7.60a*. Madison, Wisconsin, USA.
- Byarugaba, D.K. 2004. A View on Antimicrobial Resistance in Developing Countries and

- Responsible Risk Factors. *International Journal of Antimicrobial Agents*, 24: 105-110.
- Caulfield, A.J. & Wengenack, N.L. 2016. Diagnosis of active tuberculosis disease: From microscopy to molecular techniques. *Journal of Clinical Tuberculosis and Other Mycobacterial Diseases*, 4: 33-43.
- Cao, G. & Prior, R.L. 1998. Measurement of oxygen radical absorbance capacity in biological samples. *Methods in Enzymology*, 229: 50-62.
- Cerqueira, F., Cordeira-Da-Silva, A., Gaspar-Marques, C., Simoes, F.M, Pinto, M.M.M. & Nascimento, M.S.J. 2004. Effect of abietane diterpenes from *Plectranthus grandidentatus* on T- and B-lymphocyte proliferation. *Bioorganic and Medicinal Chemistry*, 12: 217-223.
- Chandra, H., Bishnoi, P., Yadav, A., Patni, B., Mishra, A.P. & Nautiyal, A.R. 2017. Antimicrobial Resistance and the Alternative Resources with Special Emphasis on Plant-Based Antimicrobials—A Review. *Plants*, 6(2): 1-3.
- Chartone-Souza, E. 1998. Bactérias ultra-resistentes: uma guerra quase perdida. *Cienc Hoje*, 23(138): 27-35.
- Chiu, Y.J., Huang, T.H., Chiu, C.S., Lu, T.C. , Chen, Y.W., Peng, W.H. & Chen, C.Y. 2012. Analgesic and antiinflammatory activities of the aqueous extract from *Plectranthus amboinicus* (Lour.) Spreng. both in vitro and in vivo, Evid. *Based Complement. Altern. Med*, 2012: 1-11.
- Churchyard, G.J., Mametja, L.D., Mvusi, L., Ndjeka, N., Hesselning, A.C., Reid, A., Babatunde, S. & Pillay, Y. 2014. Tuberculosis control in South Africa: Successes, challenges and recommendations. *South African Medical Journal*, 104(3): 244-248.
- Codd, L.E. 1985. *Plectranthus* (Lamiaceae). *Flora of Southern Africa*, 28: 137-172.
- Collins, L. & Franzblau, S.G. 1997. Microplate almar blue assay versus BACTEC 460 system for high throughput screening of compounds against *Mycobacterium tuberculosis* and *Mycobacterium avium*. *Antimicrob. Agents Chemother.*, 41: 1004-1009.
- Collins, L., Torrero, M.N. & Franzblau, S.G. 1998. Green Fluorescent Protein Reporter Microplate Assay for High-Throughput Screening of Compounds against *Mycobacterium tuberculosis*. *Antimicrob. Agents Chemother.*, 42: 344-347.
- Colombo, I., Sangiovanni, E., Maggio, R., Mattozzi, C., Zava, S., Corbett, Y., Fumagalli, M., Carlino, C., Corsetto, P.A., Scaccabarozzi, D., Calvieri, S., Gismondi, A., Taramelli, D. & Dell'Agli, M. 2017. HaCaT Cells as a reliable in vitro differentiation model to dissect the inflammatory/repair response of human keratinocytes. *Mediators of Inflammation*, 2017: 1-12.
- Corsini, E. & Galli, C.L. 1998. Cytokines and irritant contact dermatitis. *Toxicology Letters*, 102-103: 277-282.
- Declercq, S.D. & Pouliot, R. 2013. Promising new treatments for psoriasis. *The Scientific World Journal*, 1: 1-7.
- De Luca, M.A., Solinas, M., Bimpisidis, Z., Goldberg, S.R. & DiChiara, G. 2012. Cannabinoid facilitation of behavioral and biochemical hedonic taste responses. *Neuropharmacology*, 63: 1658-1661.
- De Sousa, I.P., Sousa Teixeira, M.V. & Jacometti Cardoso Furtado, N.A. 2018. An overview of biotransformation and toxicity of diterpenes. *Molecules*, 23(6): 1-3.
- Dekker, T.G., Fourie, T.G., Elmare, M., Snyckers, F.O. & Van Der Schyf, C.J. 1988. Studies of South African medicinal plants. Part 7: rhinocer- otinoic acid, a labdane diterpene with anti-

- inflammatory properties from *Elytropappus rhinocerotis*. *S. Afr. J. Chem.*, 41: 33-35.
- Dellar, J.E., Cole, M.D. & Waterman, P.G. 1996. Antimicrobial abietane diterpenoids from *Plectranthus elegans*. *Phytochemistry*, 41(3): 735-738.
- Devendra, D., Liu, E. & Eisenbarth, G.S. 2004. Type 1 diabetes: recent developments. *BMJ*, 328: 750-754.
- Dewick, P.M. 2002. *Medicinal Natural Products: A Biosynthetic Approach*. 2<sup>nd</sup> Edition. Nottingham: John Wiley.
- Diogo, M., Nicolai, M., Saraiva, L., Pinheiro, R., Faustino, C., Diaz Lanza, A., Reis, C.P., Stankovic, T., Dinic, J., Pesic, M. & Rijo, P. 2019. Cytotoxic activity of royleanone diterpenes from *Plectranthus madagascariensis* (Benth). *ACS Omega*, 4(5): 8094-8103.
- Dukhea, S. 2010. *The isolation, structure elucidation and biological testing of compounds from Plectranthus hadiensis*. Msc Thesis, University of Kwazulu-Natal, Faculty of Science and Agriculture, Kwazulu-Natal.
- Duraipandiyar, V., Ayyanar, M. & Ignacimuthu, S. 2006. Antimicrobial activity of some ethnomedicinal plants used by Paliyar tribe from Tamil Nadu, India. *BMC Complementary Altern Med*, 6: 35-41.
- Engler, D., Chezuba, H. & Masuku, P. 2017. Psoriasis. *South African Pharmaceutical Journal*, 84(5): 38-42.
- Fabricant, D.S & Farnsworth, N.R. 2001. The value of plants used in traditional medicine for drug discovery. *Environ Health Perspect*, 109: 69-75.
- Falé, P.L., Borges, C., Madeira, P.J.A., Ascensão, L., Araújo, M.E.M., Florêncio, M.H. & Serralheiro, M.L.M. 2009. Rosmarinic acid, scutellarein 4'-methyl ether 7-O-glucuronide and (16S)-coleon E are the main compounds responsible for the antiacetylcholinesterase and antioxidant activity in herbal tea of *Plectranthus barbatus* ("falso boldo"). *Food Chemistry*, 114(3): 798-805.
- Farnsworth, N.R & Soejarto, D.D. 1991. Global importance of medicinal plants. In: akerele, Heywood & Syngé (eds). *Conservation of medicinal plants*. Cambridge: Cambridge University Press: 2-10.
- Figueiredo, N.L., De Aguiar, S.R.M.M., Fale, P.L., Ascensao, L., Serralheiro, M.L.M. & Lino, A.R.L. 2010. The inhibitory effect of *Plectranthus barbatus* and *Plectranthus ecklonii* leaves on the viability, glucosyltransferase activity and biofilm formation of *Streptococcus sobrinus* and *Streptococcus mutans*. *Food Chemistry*, 119: 664-668.
- Fleurentin, J., Mazars, G. & Pelt, J.M. 1983. Cultural background of the medicinal plants of Yemen. *Journal of Ethnopharmacology*, 7: 183-203.
- Fournier, G., Paris, M., Dumitresco, S. M., Pages, N. & Boudene, C. 1986 Contribution to the study of *Plectranthus fruticosus* leaf essential oil. *Planta Med.*, 52(6): 486-488.
- Frame, A.D., Riosolivares, E., De Jesus, L., Ortiz, D., Pagan, J. & Mendez, S. 1998. Plants from Puerto Rico with anti-*Mycobacterium tuberculosis* properties. *P. R. Health Sci. J.*, 17: 243-253.
- Gaspar-Marques, C., Pedro, M., Simoes, M.F.A., Nascimento, M.S.J., Pinto, M.M.M. &

- Rodríguez, B. 2002. Effect of abietane diterpenes from *Plectranthus grandidentatus* on the growth of human cancer cell lines. *Planta Medica*, 68: 839-840.
- Gaspar-marques, C., Simões, F.M., Duarte, A., Valdeira, L.M. & Rodríguez, B. 2003. Labdane and kaurane diterpenoids from *Plectranthus fruticosus*. *Journal of Natural Products*, 66(4): 491-496.
- Gaspar-Marques, C., Simões, M. F. & Rodríguez, B. 2004 'Further Labdane and Kaurane Diterpenoids and Other Constituents from *Plectranthus fruticosus*. *Journal of Natural Products*, 67(4): 614-621.
- Gaspar-Marques, C., Simoes, M.F., Valdeira, M.L. & Rodriguez, B. 2008. Terpenoids and phenolics from *Plectranthus strigosus*, bioactivity screening. *Natural Product Research, Part A: Structure and Synthesis*, 22: 167-177 [abstract in Scifinder Scholar database]
- Gaspari, A.A. 2006. Innate and adaptive immunity and the pathophysiology of psoriasis. *J Am Acad Dermatol.*, 54: 67-80.
- González, M. A. 2014. Aromatic abietane diterpenoids: Their biological activity and synthesis. *Natural Product Reports*, 32(5): 684-704.
- Grayer, R.J., Eckert, M.R., Veitch, N.C., Kite, G.C., Marin, P.D., Kokubun, T., Simmonds, M.S.J. & Paton, A.J. 2003. The chemotaxonomic significance of two bioactive caffeic acid esters, nepetoidins A and B, in the Lamiaceae. *Phytochemistry*, 64: 519-528.
- Gurgel, A.P.A.D., Da Silva, J.G., Grangeiro, A.R.S., Oliveira, D.C., Lima, C. M.P., Da Silva, A.C.P., Oliveira, R.A.G. & Souza, I.A. 2009. In vivo study of the anti-inflammatory and antitumor activities of leaves from *Plectranthus amboinicus* (Lour.) Spreng (Lamiaceae). *J. Ethnopharmacol*, 125: 361-363.
- Hanel, K. H., Cornelissen, C., Luscher, B. & Baron, J.M. 2013. Cytokines and the skin barrier. *International Journal of Molecular Sciences*, 14(4): 6720-6745.
- Harrower, A. 2014. *Plectranthus madagascariensis* Plantz Africa. Available at: <http://pza.sanbi.org/plectranthus-madagascariensis>. [14 May 2018].
- Hattori, M., Nakabayashi, T., Lim, Y.A., Miyashiro, H., Kurokawa, M., Shiraki, K., Gupta, M. P., Correa, M. & Pilapitiya, U. 1995. Inhibitory effects of various Ayurvedic and Panamanian medicinal plants on the infection of Herpes Simplex Virus-1 in vitro and in vivo. *Phytother. Res.*, 9: 270-276.
- Helwa, I., Patel, R., Karempelis, P., Kaddour-Djebbar, I., Choudhary, V. & and Bollag, W.B 2015. The antipsoriatic agent monomethylfumarate has antiproliferative, prodifferentiative, and anti-inflammatory effects on keratinocytes. *Journal of Pharmacology and Experimental Therapeutics*, 352: 90-97.
- Hemmelin, A., Harwood, J.L. & Bach, T.J. 2012. A raison d'être two distinct pathways in the early steps of plants isoprenoids biosynthesis?. *Prog. Lipid Res.*, 51: 95-148.
- Horvath, T., Linden, A., Yoshizaki, F., Eugster, C.H. & Ruedi, P. 2004. Abietanes and a novel 20-norabietanoid from *Plectranthus cyaneus* (Lamiaceae). *Helvetica Chimica Acta*, 87(9): 2346-2353.
- Huang, T., Lin, C.F., Alalaiwe, A., Yang, S.H. & Fang, J.Y. 2019. Apoptotic or antiproliferative activity of natural products against keratinocytes for the treatment of psoriasis. *International*

*Journal of Molecular Science*, 20: 1-9.

Hulme, M.M. 1954. *Wild Flowers of Natal*. Pietermaritzburg: Shulter & Shooter.

Hutchings, A., Scott, A.H., Lewis, G. & Cunningham, A. 1996. *Zulu medicinal plants: An inventory*. Pietermaritzburg: University of Natal Press.

Holm, J.G. & Thomsen, S.F. 2019. Type 2 diabetes and psoriasis: Links and risks. *Psoriasis Targets and Therapy*, 9: 1-6.

Jayakar, T. & Kumar, P. 2016. Treating pediatric plaque psoriasis: Challenges and solutions. *Dove Press Journal*, 7: 25-38.

International Diabetes Federation (IDF). 2017. *IDF Diabetes Atlas*. 8th Ed. Brussels: IDF. Available at: <http://www.diabetesatlas.org/resources/2017-atlas.html> [Accessed 5<sup>th</sup> october 2018].

IUPAC. 1999. Commission on nomenclature of organic chemistry revised section F : Natural products and related compounds (IUPAC recommendations 1999). *Pure application chemistry*, 71(4): 587-643.

Joubert, J., Norman, R., Bradshaw, D. 2007. Estimating the burden of disease attributable to excess body weight in South Africa in 2000. *S. Afr. Med. J.*, 97: 683-690.

Kana, B. & Churchyard, G. 2013. Tuberculosis: The global killer. *South African Journal of Science*, 109(9/10): 1-2.

Kharroubi, A.T. & Darwish, H.M. 2015. Diabetes mellitus : The epidemic of the century. *World Journal of Diabetes*, 6(6): 850-853.

Kinouchi, Y., Ohtsu, H., Tokuda, H., Nishino, H., Matsunaga, S. & Tanaka, R. 2000. Potential antitumor-promoting diterpenoids from the stem bark of *Picea glehni*. *J. Natl. Prod.*, 63: 817.

Koch, A., Mizrahi, V. & Warner, D.F. 2014. The impact of drug resistance on *Mycobacterium tuberculosis* physiology: What can we learn from rifampicin?. *Emerging Microbes and Infections*, 3(1): 1-8.

Kokwaro, J.O. 1993. *Medicinal Plants of East Africa*. 2nd ed. Nairobi: Kenya Literature Bureau.

Kubínová, R., Pořízková, R., Navrátilová, A., Farsa, O., Hanáková, Z., Bačinská, A., Čížek, A., & Valentová, M. 2014. Antimicrobial and enzyme inhibitory activities of the constituents of *Plectranthus madagascariensis* (Pers.) Benth. *Journal of Enzyme Inhibition and Medicinal Chemistry*, 29(5): 749-752.

Kusumoto, I.T., Nakabayashi, T., Kida, H., Miyashiro, H., Hattori, M., Namba, T. & Shimotohno, K. 1995. Screening of various plant extracts used in ayurvedic medicine for inhibitory effects on Human Immunodeficiency Virus-type 1 (HIV-1) protease. *Phytother. Res.*, 9: 180-184.

Kuzuyama, T. 2002. Mevalonate and non-mevalonate pathways for the Biosynthesis of Isoprene Units. *Bioscience, Biotechnology, and Biochemistry*, 66(8): 1619-1627.

Laing, M.D., Drewes, S.E. & Gurlal, P. 2006). Extracts of *Plectranthus hadiensis*, *P. argentatus* or *P. myrianthus* for the treatment of microbial infection. WO/2008/001: 10.

Li, K., Yao, F., Xue, Q., Fan, H., Yang, L., Li, X., Sun, L. & Liu, Y. 2018. Inhibitory effects

against  $\alpha$ -glucosidase and  $\alpha$ -amylase of the flavonoids-rich extract from *Scutellaria baicalensis* shoots and interpretation of structure–activity relationship of its eight flavonoids by a refined assign-score method. *Chemistry Central Journal*, 12(1): 1-11.

Liu, G. & Ruedi, P. 1996. Phyllocladanes (13 $\beta$ -kauranes) from *Plectranthus ambiguous*. *Phytochemistry*, 41: 1563-1568.

Lokhande, P.D., Gawai, K.R., Kodam, K.M., Kuchekar, B.S., Chabukswar, A.R. & Jagdale, S.C. (2007). Antibacterial activity of isolated constituents and extracts of roots of *Inula racemosa*. *Res. J. Medicinal Plant*, 1: 7-12.

Lukhoba, C.W., Simmonds, M. S.J. & Paton, A.J. 2006. *Plectranthus*: A review of ethnobotanical uses. *Journal of ethnopharmacology*, 103: 1–24.

Maistry, K. 2007. *The antimicrobial properties and chemical composition of leaf extracts and essential oils of indigenous Pteronia species*. Msc thesis, University of the Witwatersrand, Pretoria.

Maree, J.E. Khondkar, P., Kwapong, A.A., Oyedemi, B.M., Aljarba, T.M., Stapleton, P., Viljoen, A.M. & Gibbons, S. 2014. Bioactive acetophenones from *Plectranthus venteri*. *Phytochemistry Letters*. 10: 1-4.

Marie, N.G., Fleming, T., Robinson, M., Thomson, B., Graetz, N., Margono, C., Mvllany, E.C., Biryvkov, S., Abbafati, C., Abera, S.F., PAbraharn, J., Abu-Rrneileh, M.E., Achok, T., AlBuhairan, F.S., Alernu, A., Alfonso, R., Ali, M.K., Alit, R., Gvzrnan, N.A., Arnrnar, W., Anwari, P., Banerjee, A., Barquera, S., Basv, S., Bennett, D. & Gakidout, E. 2014. Global, regional, and national prevalence of overweight and obesity in children and adults during 1980-2013: a systematic analysis for the Global Burden of Disease Study 2013. *Lancet*, 384:766-781.

Marwah, R.G., Fatope, M.O., Deadman, M.L., Ochei, J.E. & Al-Saidi, S.H. 2007. Antimicrobial activity and the major components of the essential oil of *Plectranthus cylindraceus*. *Journal of Applied Microbiology*, 103: 1220-1226.

Masika, P.J. & Afolayan, A.J. 2003. An ethnobotanical study of plants used for the treatment of livestock diseases in the Eastern Cape province, South Africa. *Pharmaceutical Biology*, 41: 16-21.

Matias, D., Roque,L., Simões, M.F., Diaz-Lanza, A., Rijo, P& Reis, C.P. 2015. *Plectranthus madagascariensis* phytosomes : formulation optimization. *Biomed Biopharm Res.* , 2 (12): 223-231.

Mehrotra, R., Vishwakarma, R.A. & Thakur, R.S. 1989. Abietane diterpenoids from *Coleus zeylanicus*. *Phytochemistry*, 28: 3135.

Mei, S.X., Jiang, B., Niu, X.M., Li, M. L., Yang, H., Na, Z., Lin, Z. W., Li, C. M. & Sun, H.D. 2002. Abietane diterpenoids from *Coleus xanthanthus*. *J. Nat. Prod.*, 65: 633-637.

Mendelsohn, R. & Balick, M.J. 1995. The value of undiscovered pharmaceuticals in tropical forests. *Econ Bot.*, 49(2): 223-228.

Moharram, H.A. & Youssef, M.M. 2014. Methods for Determining the Antioxidant Activity : A Review. *Journal of Food Science & Technology*, 11(1): 31-42.

Morton, J.F., 1992. Country borage (*Coleus amboinicus* Lour.): a potent flavoring and medicinal plant. *Journal of Herbs, Spices Medicinal Plants*, 1: 77-90.

Mossman, T. 1983. Rapid colorimetric assay for cellular growth and survival: application to proliferation and cytotoxicity assay. *J. Immunol. Methods*, 65: 55.

Mustafa, G., Arif, R., Atta, A., Sharif, A. & Jamil, A. 2017. Bioactive Compounds from Medicinal Plants and Their Importance in Drug Discovery. *Matrix Science Pharma*, 1: 17-26.

Muthukumarana, R. & Dharmadasa, R.M. 2014. Pharmacognostical investigation of *Plectranthus hadiensis* (Forssk.) Schweinf. ex Sprenger. and *Plectranthus amboinicus* (Lour.). *World Journal of Agricultural Research*, 2(5): 240-246.

Naman, C. B. (2015). *Phytochemical Investigation of the Medicinal Plant Taxodium distichum and Library Screening of Thalictrum Alkaloids for New Antileishmanial Drug Leads*. PhD Thesis, Ohio State University, Ohio.

Nedoszytko, B., Sokołowska-Wojdyło, M., Ruckemann-Dziurdzińska, K. 2014. Chemokines and cytokines network in the pathogenesis of the inflammatory skin diseases: atopic dermatitis, psoriasis and skin mastocytosis. *Postep Derm Alergol*, 2: 84-91.

Newman, D.J. & Cragg, G.M. 2016. Natural Products as Sources of New Drugs from 1981 to 2014. *J. Nat. Prod.*, 79: 629-661.

Njaria, P.M. 2017. *Antimycobacterial 2-aminoquinazolinones and benzoxazole-based oximes: synthesis, biological evaluation, physicochemical profiling and supramolecular derivatization*. PhD thesis. University of Cape Town. Cape Town.

Nyila, M.A., Leonard, C.M., Hussein, A.A. & Lall, N. 2009. Bioactivities of *Plectranthus ecklonii* constituents. *Natural Product Communications*, 4: 1177-1180.

Okur, M.E., Karantas, I.D. & Siafaka, P.I. 2017. Diabetes mellitus: A review on pathophysiology, current status of oral medications and future perspectives. *Acta Pharmaceutica Scientia*, 55(1): 61-65.

Oliveira, P.M., Ferreira, A.A., Silveira, D., Alves, R.B., Rodrigues, G.V., Emerenciano, V.P. & Raslan, D.S. 2005. Diterpenoids from the Aerial Parts of *Plectranthus ornatus*. *Journal of Natural Products*, 68(4): 588-591.

Pages, N., Fournier, G., Chamorro, G. & Salazar, M. 1991. Teratogenic effects of *Plectranthus fruticosus* essential oil in mice. *Phytotherapy Research*, 5(2): 94-96.

Painuly, P. & Tandon, J.S. 1983. Triterpenes and Flavones From *Coleus spicatus*. *J. Nat. Prod.*, 46(2): 285.

Paton, A.J., Springate, D., Suddee, S., Otieno, D., Grayer, R.J., Harley, M.M., Willis, F., Simmonds, M.S., Powell, M.P. & Savolainen, V. 2004. Phylogeny and evolution of basilis and allies (Ocimeae, Labiatae) based on three plastid DNA regions. *Molecular Phylogenetics and Evolution*, 31: 277-299.

Paton, A.J., Bramley, G., Ryding, O., Polhill, R.M., Harvey, Y.B., Iwarsson, M., Willis, F., Phillipson, P.B., Balkwill, K., Lukhoba, C.W., Oteino, D. & Harley, R.M. 2009. Lamiaceae (Labiatae). In: Beentje HJ, Ghazanfar SA, Polhill RM, eds. *Flora of Tropical East Africa. Lamiaceae (Labiatae)*. Kew: Royal Botanic Gardens: 1–413.

Paton, A.J., Bramley, G., Ryding, O., Polhill, R.M., Harvey, Y.B., Iwarsson, M., Willis, F., Phillipson, P.B., Balkwill, K., Oteino, D. & Harley, R.M. 2013. Lamiaceae. In: Timberlake J, ed.



Flora Zambesiaca. Kew: Royal Botanic Gardens: 1–331.

Pellegrini, N., Re, R., Yang, M. & Rice-Evans, C.A. 1999. Screening of dietary carotenoid rich fruit extracts for antioxidant activities applying ABTS radical cation decolorisation assay. *Methods in Enzymology*, 229: 379-389.

Pheiffer, C. Pillay-Van Wyk, V., Joubert, J.D., Levitt, N., Nglazi, M.D. & Bradshaw, D. 2018. The prevalence of type 2 diabetes in South Africa: A systematic review protocol. *BMJ Open*, 8(7): 2-5.

Potgieter, C.J., Edwards, T.J., Miller, R.M. & Van Staden, J., 1999. Pollination of seven *Plectranthus* spp. (Lamiaceae) in southern Natal, South Africa. *Plant Systematics and Evolution*, 218: 99-112

Prior, R.L., Hoang, H., Gu, L., Wu, X., Bacchiocca, M., Howard, L., Hampsch-Woodill, M., Huang, D., Ou, B. & Jacob, R. 2003. Assays for hydrophilic and lipophilic antioxidant capacity of plasma and other biological and food samples. *Journal of Analytical and Food Chemistry*, 51: 3273-3279.

Prudent, D., Perineau, F., Bessiere, J.M., Michel, G.M. & Baccou, J.C. 1995. Analysis of the essential oil of wild oregano from Martinique (*Coleus aromaticus* Benth.): Evaluation of its bacteriostatic and fungistatic properties. *J. Essent. Oil Res.*, 7: 165-173.

Quan, D., Nagalingama, G., Payne, R. & Triccas, J.A. 2016. New tuberculosis drug leads from naturally occurring compounds. *International Journal of Infectious Diseases*, 56: 212-220.

Rabe, T. & Staden, J.V. 1998. Screening of *Plectranthus* species for antibacterial activity. *South African Journal of Botany*, 64(1): 62-65.

Raboobee, N., Aboobaker, J., Jordaan, H.F., Sinclair, W., Smith, J.M. Todd, G., Weiss, R. & Whitaker, D. 2010. Guideline on the management of psoriasis in South Africa. *South African Medical Journal*, 100(4): 257-282.

Rasikari, H. 2007. *Phytochemistry and arthropod bioactivity of Australian Lamiaceae*. PhD Thesis, Southern Cross University, Lismore.

Rasool, H.B.A. 2012. Pharmaceutica Medicinal Plants (Importance and Uses). *Pharmaceut Anal Acta*, 3(10): 4172.

Restrepo, B. I. 2017. Diabetes and tuberculosis. *Microbiol. Spectr*, 4(6): 1-9.

Rijo, P. 2010. *Phytochemical Study and Biological Activities of Diterpenes and Derivatives From Plectranthus Species*. PhD thesis. Universidade De Lisboa. Faculdade De Farmácia. Lisboa. Lisboa.

Rice, L.J., Brits, G.J., Potgieter, C.J. & Van Staden, J. 2011. *Plectranthus*: A plant for the future. *South African Journal of Botany*, 77(4): 947-959.

Rijo, P., Gaspar-Marques, C., Simoes, M.F., Duarte, A., Apreda-Rojas, M.C., Cano, F.H. & Rodriguez, B. 2002. Neoclerodane and labdane diterpenoids from *Plectranthus ornatus*. *J. Nat. Prod*, 65:1387-1390.

Rijo, P., Gaspar-Marques, C., Simões, M.F., Jimeno, M.L. & Rodríguez, B. 2007. Further diterpenoids from *Plectranthus ornatus* and *P. grandidentatus*. *Biochemical Systematics and Ecology*, 35(4): 215-221.

Rijo, P., Simões, M.F., Francisco, A.P., Rojas, R., Gilman, R.H., Vaisberg, A.J., Rodríguez, B. & Moiteiro, C. 2010. Antimycobacterial metabolites from *Plectranthus*: Royleanone derivatives against *Mycobacterium tuberculosis* strains. *Chemistry and Biodiversity*, 7: 922-932.

Rijo P., Rodríguez B., Duarte A. & Simões M.F. 2011. Antimicrobial properties of *Plectranthus ornatus* extracts, 11-acetoxyhalima-5,13-dien-15-oic acid metabolite and its derivatives. *Nat. Prod. J.*, 1: 57.

Roberts, M., 1990. *Indigenous Healing Plants*. Southern Book Publishers.

Roshan, P., Naveen, M., Manjul, P.S., Gulzar, A., Anita, S. & Sudarshan, S. 2014. *Plectranthus amboinicus* (Lour) spreng: An overview. *The Pharma Research*, 4: 1-15.

Salim, A.A., Chin, Y. & Kinghorn, A.D. 2008. Drug Discovery from Plants from: Bioactive Molecules and Medicinal Plants Chapter. In : Ramawat & Mérillon (eds.). *Springer*, 1: 1-20.

Samuelsson, G. 2004. *Drugs of Natural Origin: a Textbook of Pharmacognosy*. 5<sup>th</sup> Ed. Stockholm: Swedish Pharmaceutical Press.

Santos, F.A.V., Serra, C.G., Bezerra, J.A.C.R., Figueredo, F.G., Matias, F.F.E., Menezes, R. A.I., Costa, G.M.J. & Coutinho, D.M.E. 2016. Antibacterial activity of *Plectranthus amboinicus* Lour (Lamiaceae) essential oil against *Streptococcus mutans*. *European Journal of Integrative Medicine*, 8(3): 293-297.

Sasidharan, S., Chen, Y., Saravanan, D., Sundram, K.M. & Yoga Latha, L. 2011. Extraction, isolation and characterization of bioactive compounds from plants'extracts. *Journal of Molecular Medicine*, 8: 1-10.

Seo, M.D., Kang, T.J., Lee, C.H., Lee, A.Y. & Noh. M. 2012. HaCaT keratinocytes and primary epidermal keratinocytes have different transcriptional profiles of cornified envelope-associated genes to T helper cell cytokines. *Biomolecules and Therapeutics*, 20(2): 171-176.

Shaikha, S.A., Mansour, K. & Riad, H. 2012. Reactivation of tuberculosis in three cases of psoriasis after initiation of anti-TNF therapy. *Case Reports in Dermatology*, 4: 41-46.

Sheldrick, G. M. 1997. *SADABS, Program for empirical absorption correction of area detector data*. Göttingen, Germany: University of Göttingen.

Sheldrick, G. M. 2008. A Short History of SHELX. *Acta Crystallogr.*, 64: 112-122.

Sheldrick, G. M. 2015. Crystal Structure Refinement with SHELXL. *Acta Crystallogr. Crystallogr. Sect. C Struct. Chem.*, 71: 3-8.

Silva, N.C. & Fernandes, J.A. 2010. Biological properties of medicinal plants: A review of their antimicrobial activity. *Journal Venom Anim Toxins*, 16(3): 402-413.

Silva, M.G.D.V., Lima, L.B., Oliveira, M.D.C., Mattos, M.C. & Mafezoli, J. 2017. Quantification of barbatusin and 3  $\beta$ -hydroxy-3-deoxybarbatusin in *Plectranthus* Species by HPLC-DAD. *International Journal of Analytical Chemistry*, 1: 1-2.

Simões, M.F., Rijo, P., Duarte, A., Barbosa, D., Diogo, M., Delgado, J., Cirilo, N. & Rodríguez, B. 2010. Two new diterpenoids from *Plectranthus* species. *Phytochemistry Letters*, 3(4): 221-225.

Singh, R., 2015. Medicinal plants : A review. *Journal of Plants Sciences*, 3(1): 50-55.

- Soni, H. & Singhai, A.K. 2012. Recent updates on the genus *Coleus*: A review. *Asian J Pharm Clin Res.*, 5(1): 12-17.
- Srivastava, V., Rouanet, C., Srivastava, R., Ramalingam, B., Loch, C. & Srivastava, B.S. 2007. Macrophage-specific *Mycobacterium tuberculosis* genes: Identification by green fluorescent protein and kanamycin resistance selection. *Microbiology*, 153(3): 659-666.
- Statistics South Africa. 2016. Mortality and causes of death in South Africa: Findings from death notification. *Statistical release*, 1: 1-127.
- Stavri, M., Paton, A., Skelton, B.W. & Gibbons, S. 2009. Antibacterial diterpenes from *Plectranthus ernstii*. *Journal of Natural Products*, 72: 1191-1194.
- Tadesse, S., Mazumder, A., Bucar, F., Veeresham, C. & Asres, K. 2011. Chemical composition and biological activities of the essential oil of *Plectranthus caninus* Roth. *Pharmacognosy Journal*, 3(67): 571-579.
- Takehita, J., Grewal, S., Langan, S.M., Mehta, N.N., Ogdie, A., Van Voorhees, A.S. & Gelfand, J.M. 2017. Psoriasis and comorbid diseases: Epidemiology. *J. Am. Acad. Dermatol.*, 76: 377-390.
- Teixeira, A.P., Batista, O., Simões, M.F., Nascimento, J., Duarte, A., Torre, C.M. & Rodríguez, B. 1997. Abietane diterpenoids from *Plectranthus grandidentatus*. *Phytochemistry*, 44(2): 325-327
- Telagari, M. & Hullatti, K. 2015. In-vitro  $\alpha$ -amylase and  $\alpha$ -glucosidase inhibitory activity of *Adiantum caudatum* Linn. And *Celosia aegentea* Linn. Extracts and fractions. *Indian Journal of Pharmacology*, 47(4): 425-429.
- Uchida, M., Miyase, T., Yoshizaki, F., Bieri, J.H., Ruedi, P. & Eugster, C.H. 1981. 14-Hydroxytaxodione as major diterpenoid in *Plectranthus grandidentatus* Gurke; isolation of seven new dimeric diterpenoids from *P. grandidentatus*, *P. myrianthus* Briq. and *Coleus carnosus* Hassk.: Structures of grandidones A, 7-epi-A, B, 7-epi-B, C, D and 7-epi-D. *Helvetica Chimica Acta*, 64: 2227-2250.
- Udensi, K.U., Graham-Evans, B.E., Rogers, C. & Isokpehi, R.D. 2011. Cytotoxicity patterns of arsenic trioxide exposure on HaCaT keratinocytes. *Clinical Cosmetic and Investigational Dermatology*, 4: 183-190.
- Van Jaarsveld, E. 1987. *The Plectranthus Handbook*. National Botanical Institute. 1<sup>st</sup> ed. Cape Town: 1-6.
- Van Wyk, A.E., & Smith, G.F. 2001. *Regions of Floristic Endemism in Southern Africa: A review with Emphasis on Succulents*. Umdaus Press. Pretoria: Hatfield.
- Van Zyl, R.L., Khan, F., Edwards, T.J. & Drewes, S.E. 2008. Antiplasmodial activities of some abietane diterpenes from the leaves of five *Plectranthus* species. *South African Journal of Science*, 104: 62-65.
- Verma, S. & Singh, S.P. 2008. Current and future status of herbal medicines. *Vet. World*, 1(11): 347-350.
- Wade, M.M. & Zhang, Y. 2004. Mechanisms of drug resistance in *Mycobacterium tuberculosis*. *Molecular Microbiology*, 1(3): 1136-1156.
- Wagner, H.M., Bladt, S. & Zgainski, E.M. 1984. *Plant drug analysis*. New York: Springer-

Verlag: 320.

Wakkee, M., De-Vries, E., Van Den Haak, P. & Nijsten, T. 2011. Increased risk of infectious disease requiring hospitalization among patients with psoriasis: A population-based cohort. *Journal of American Dermatology*, 65(6): 1135-1144.

Waldiaa, S. 2008. *Chemical investigation on Plectranthus coesta*. M.Sc. Thesis. L.S.M. GOVT. P.G. College Pithoragarh. Uttarakhand.

Waldiaa, S., Joshi, B., Pathaka, U. & Joshi, M. 2011. The Genus *Plectranthus* in India and Its Chemistry: Review. *Chemistry & Biodiversity*, 8: 244-252.

Wellsow, J., Grayer, R.J., Veitch, N.C., Kokubun, T., Lelli, R., Kite, G.C. & Simmonds, M.S.J. 2006. Insect-antifeedant and antibacterial activity of diterpenoids from species of *Plectranthus*. *Phytochemistry*, 67(16): 1818-1825.

WHO. 2014. Tuberculosis & Diabetes. Available from: [https://www.who.int/tb/publications/diabetes\\_tb.pdf](https://www.who.int/tb/publications/diabetes_tb.pdf) [4<sup>th</sup> September 2018].

WHO. 2016. *Global report on psoriasis*. Available at: [https://apps.who.int/iris/bitstream/handle/10665/204417/9789241565189\\_eng.pdf](https://apps.who.int/iris/bitstream/handle/10665/204417/9789241565189_eng.pdf) [5<sup>th</sup> June 2018].

WHO. 2016. *Diabetes*. Available at: <https://www.who.int/news-room/fact-sheets/detail/diabetes> [4<sup>th</sup> september 2018].

WHO. 2018. Global WHO report on tuberculosis 2018. Available at: [https://www.who.int/tb/publications/global\\_report/en/](https://www.who.int/tb/publications/global_report/en/). [10<sup>th</sup> February 2019].

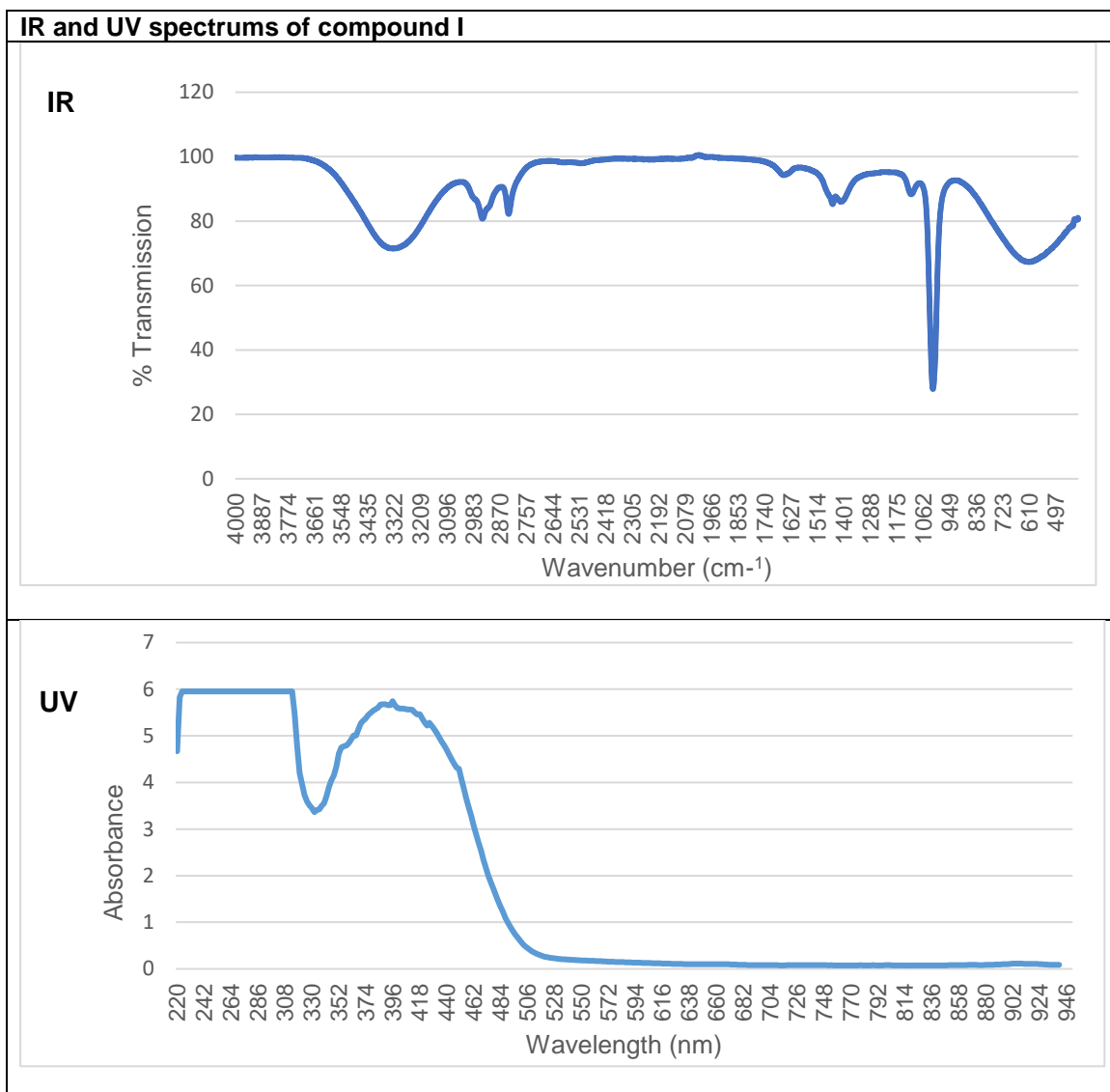
Yeon, J. J. & Lee, K. S. 2008. Pulmonary tuberculosis: Up-to-date imaging and management. *American Journal of Roentgenology*, 191(3): 834.

Yilmazer-Musa, M., Griffith, A.M., Michels, A.J., Schneider, E. & Frei, B. 2012. Grape seed and tea extracts and catechin 3-gallates are potent inhibitors of  $\alpha$ -amylase and  $\alpha$ -glucosidase activity. *Journal of Agricultural and Food Chemistry*, 60(36): 8924-8929.

Yulianto, W., Andarwulan, N., Giriwono, P.E. & Pamungkas, J. 2016. HPLC-based metabolomics to identify cytotoxic compounds from *Plectranthus amboinicus* (Lour.) Spreng against human breast cancer MCF-7 cells. *Journal of Chromatography*, 1039: 28-34.

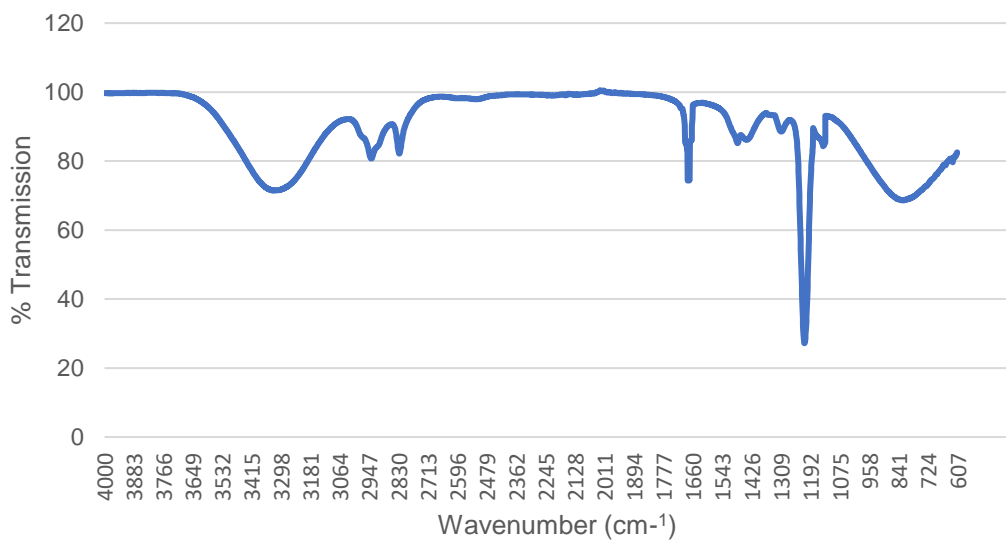
Zhong, Y. & Shahidi, F. 2015. Methods for the assessment of antioxidant activity in foods: In Shahidi, F. (ed). *Handbook of Antioxidants for Food Preservation*. London: Woodhead Publishing: 287-333.

Appendix A: IR and UV spectrum of *P. madagascariensis* Isolated natural products

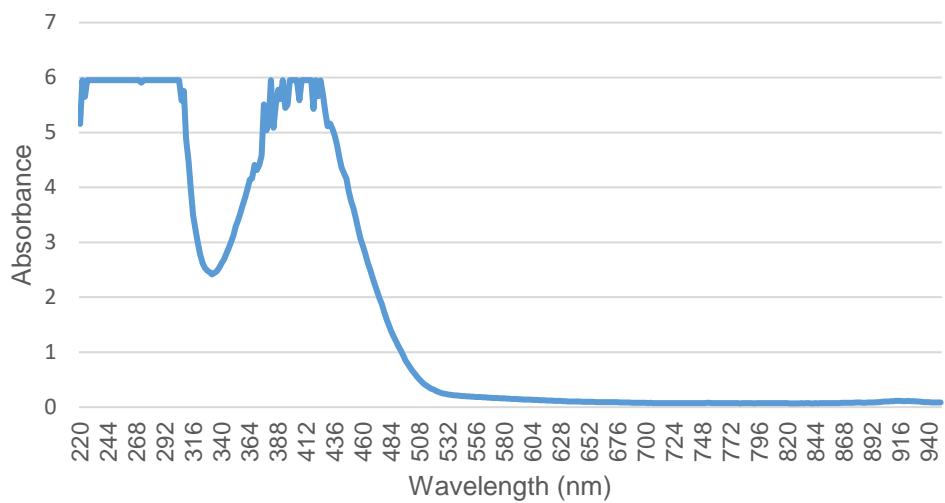


### IR and UV spectrums of compound II

IR

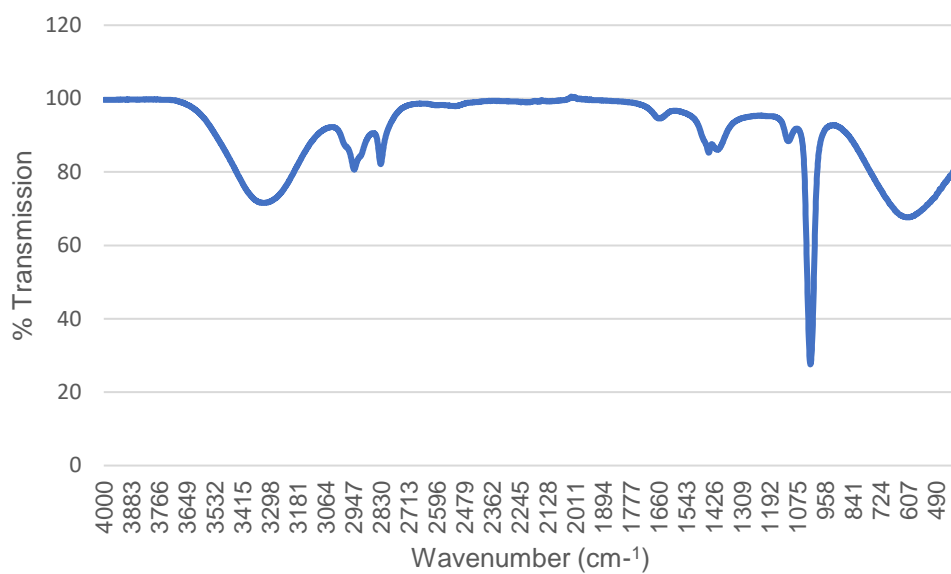


UV

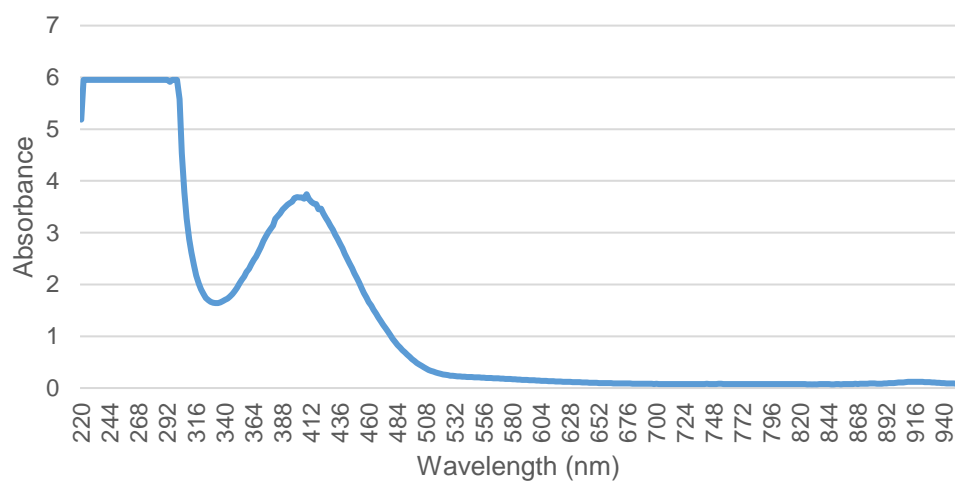


### IR and UV spectrums of compound III

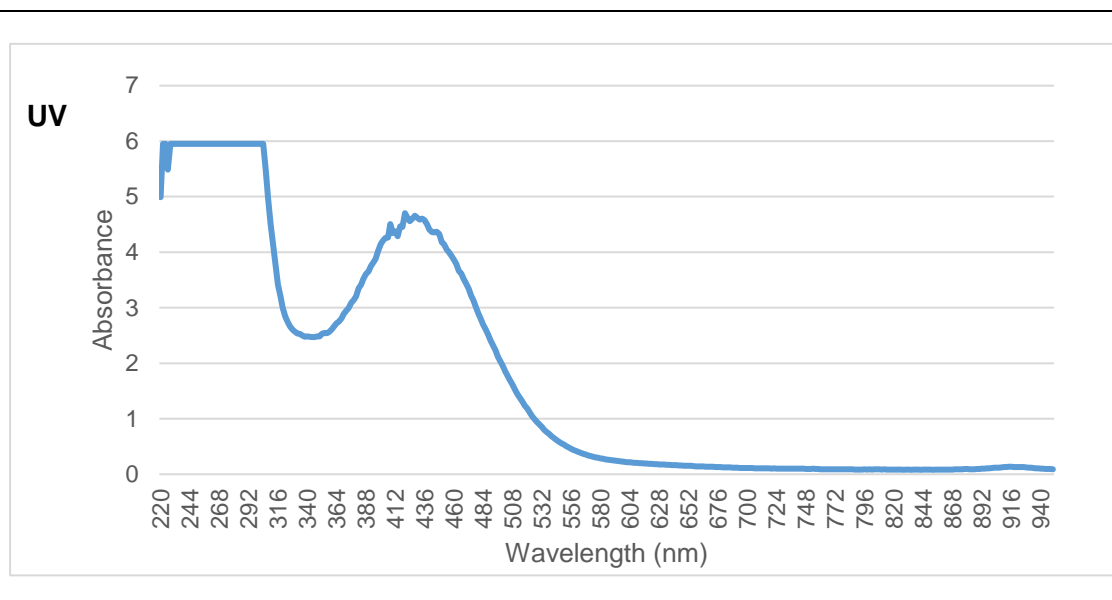
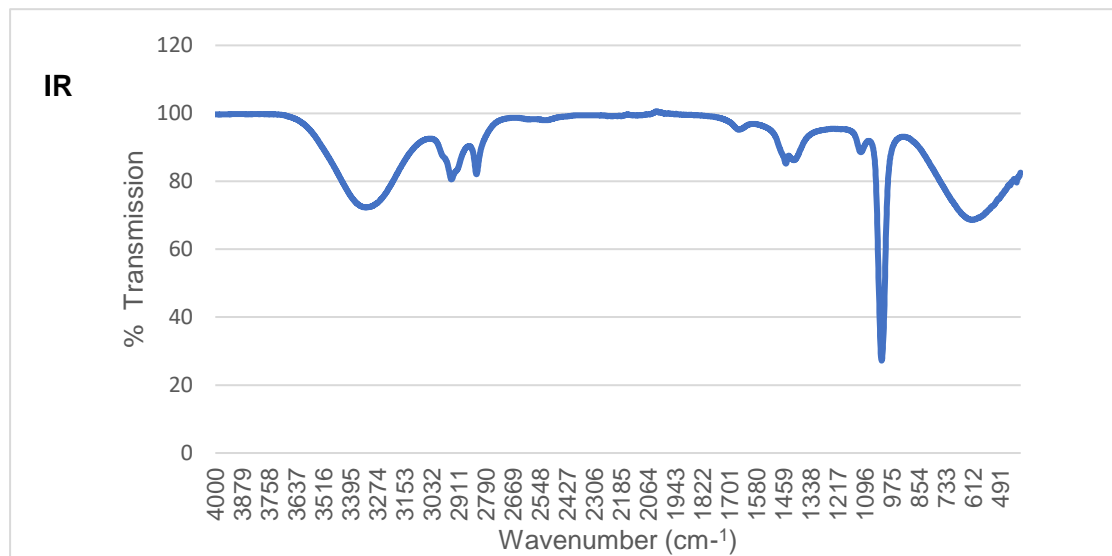
**IR**



**UV**



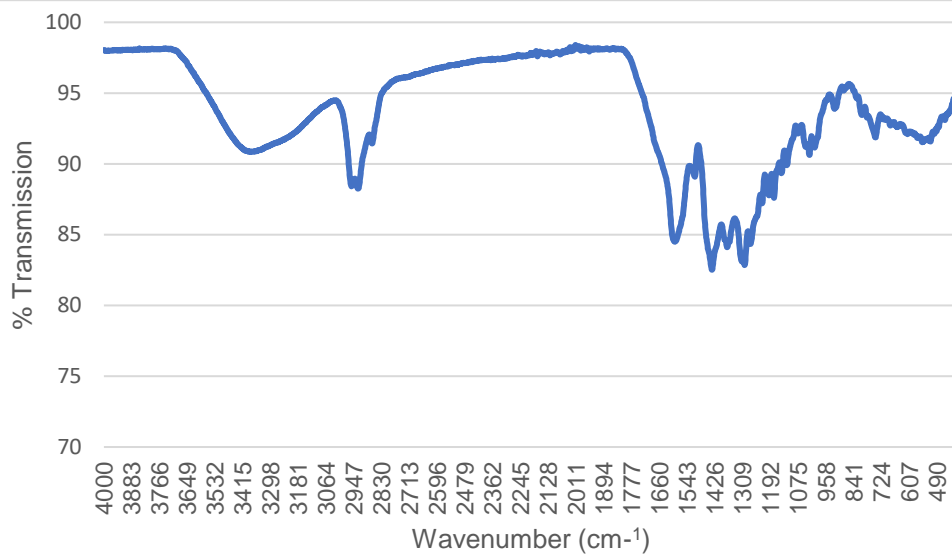
### IR and UV spectrums of compound IV



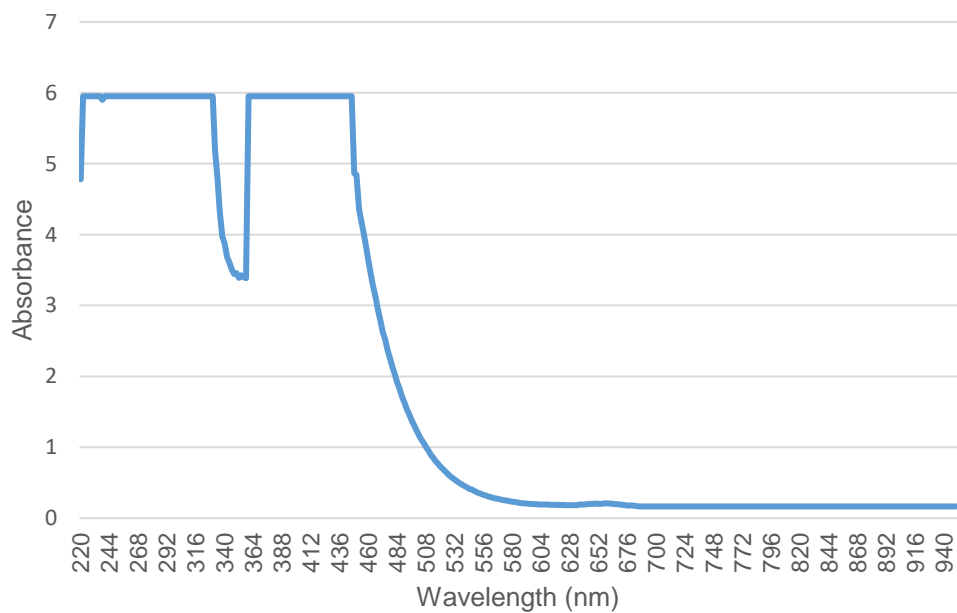


### IR and UV spectrums of compound V

IR

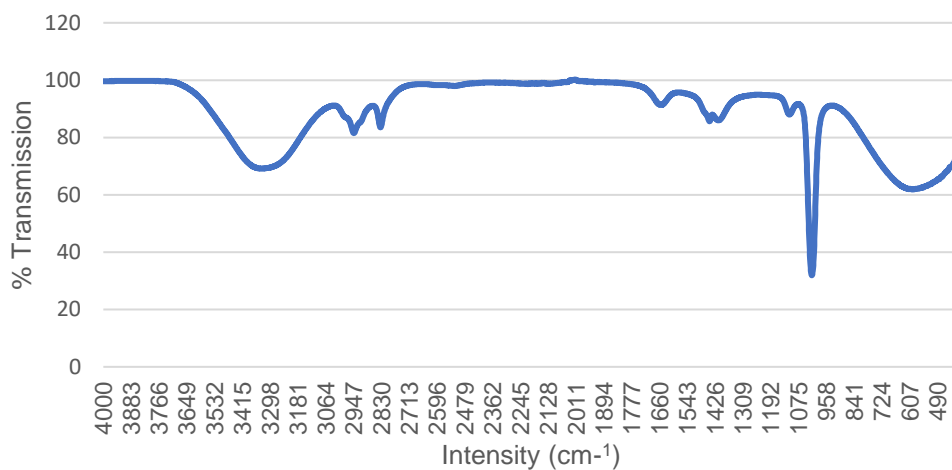


UV

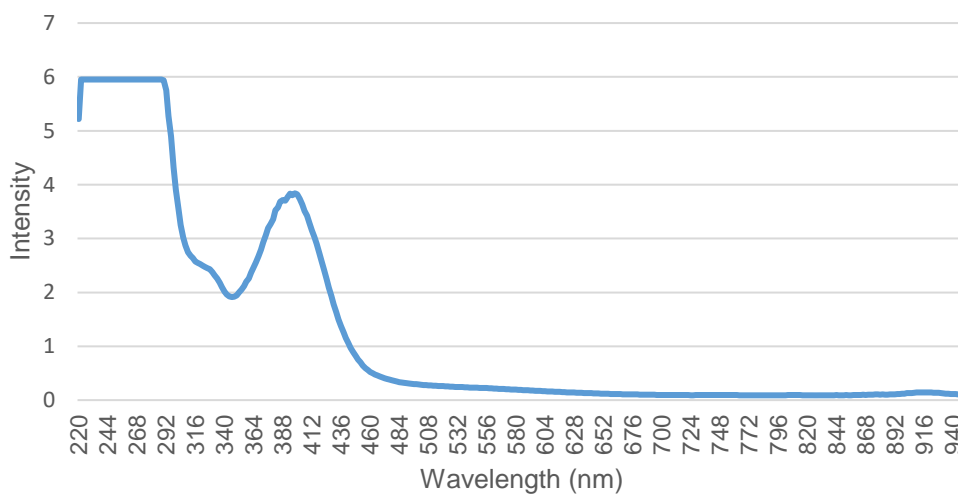


### IR and UV spectrums of compound VI & VII

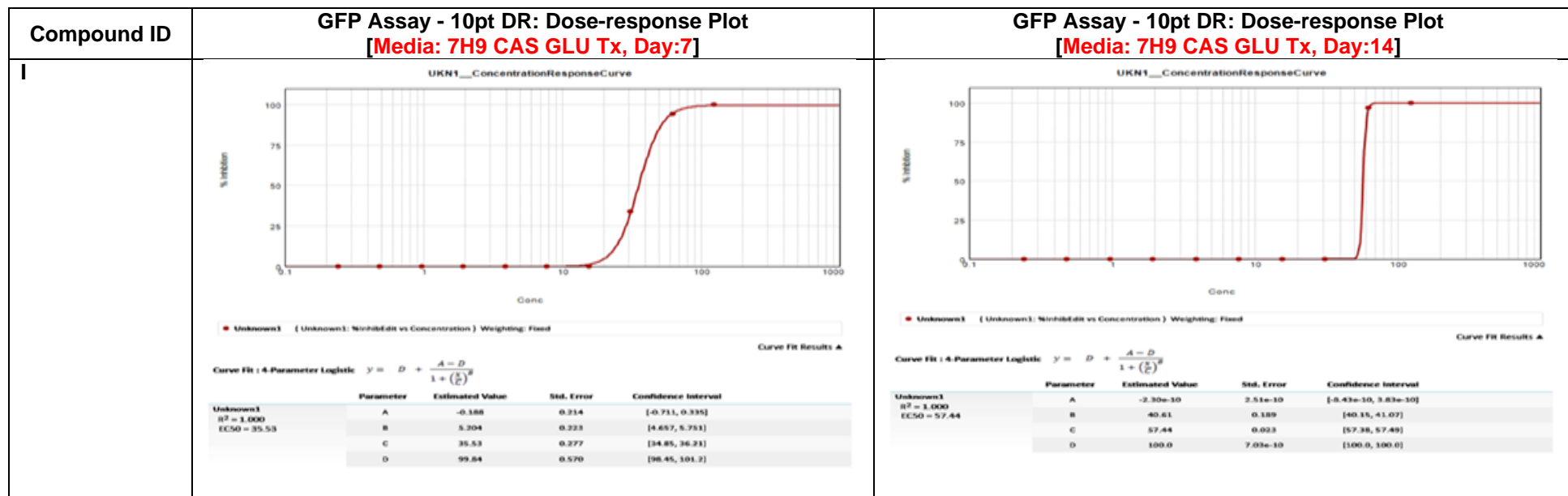
IR



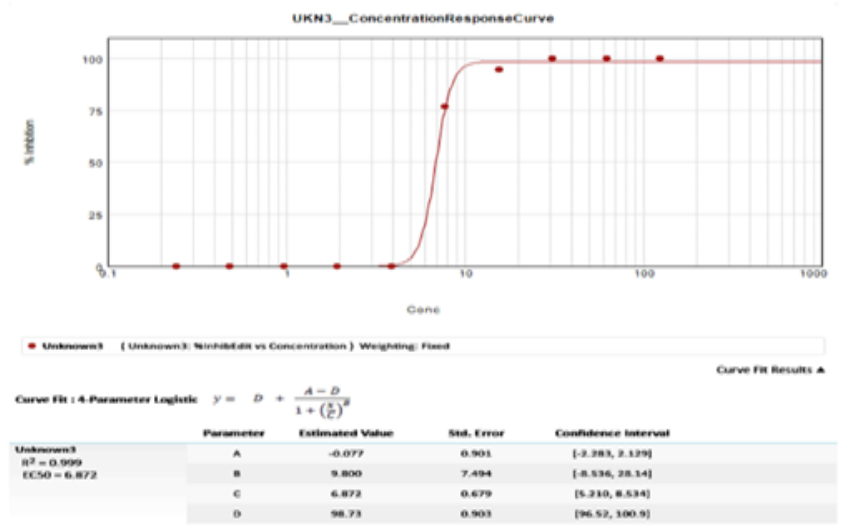
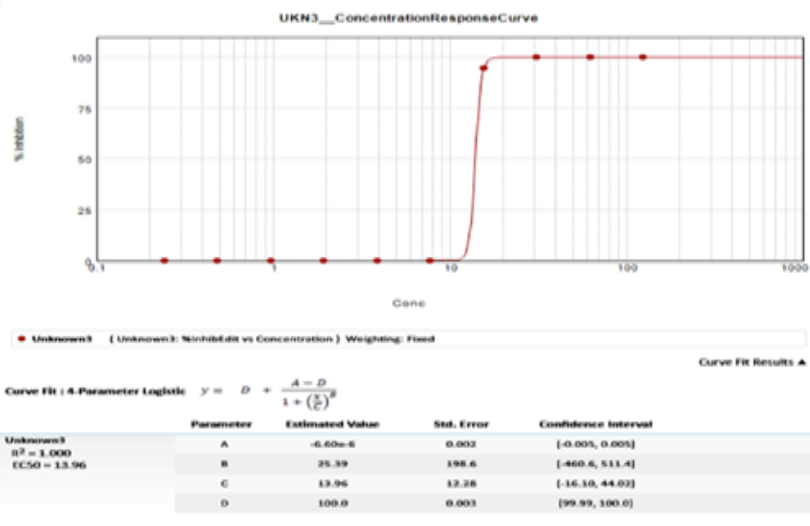
UV



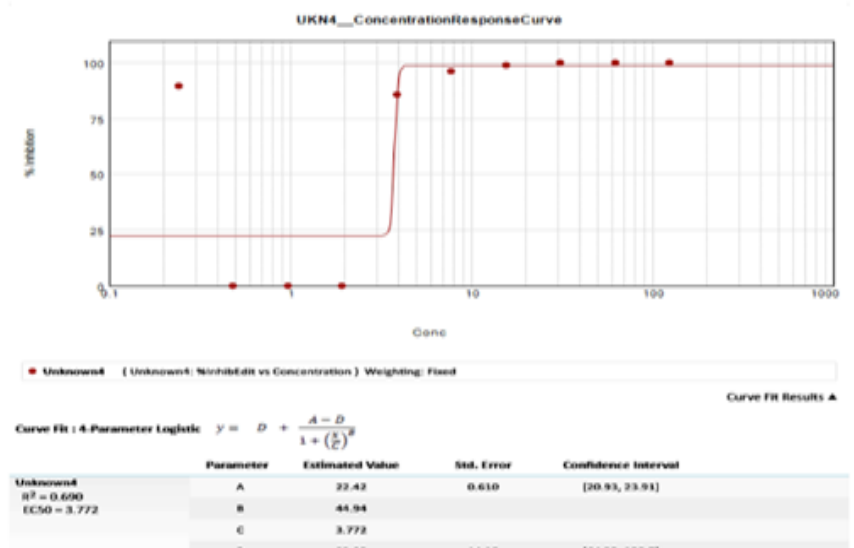
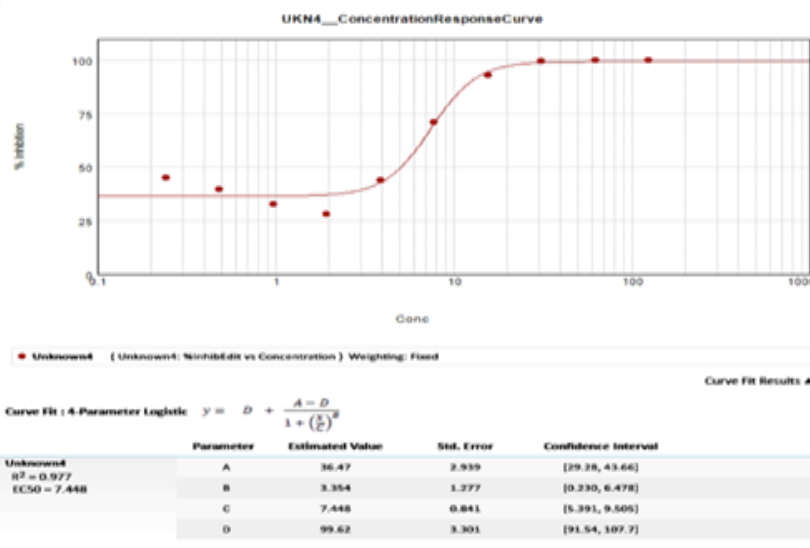
**Appendix B:** GFP tagged *Mtb* Assay - 10pt DR: Dose-response Plot of *P. madagascariensis* isolated compounds, main fractions and total extract



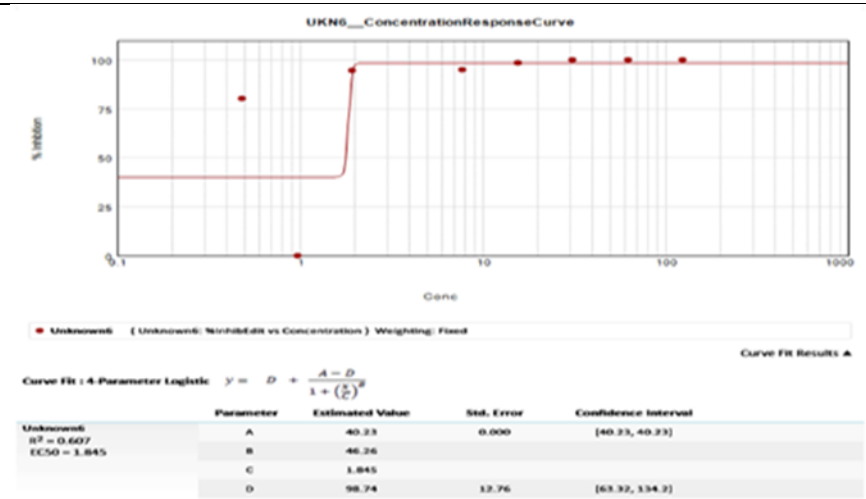
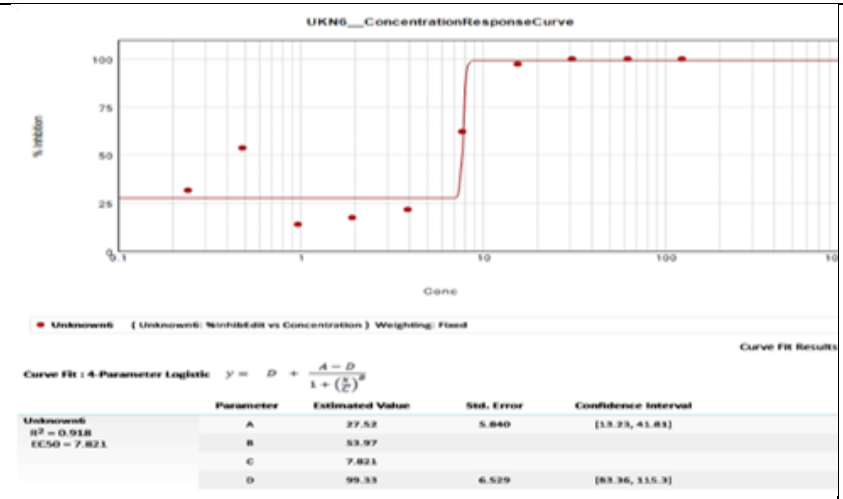
II



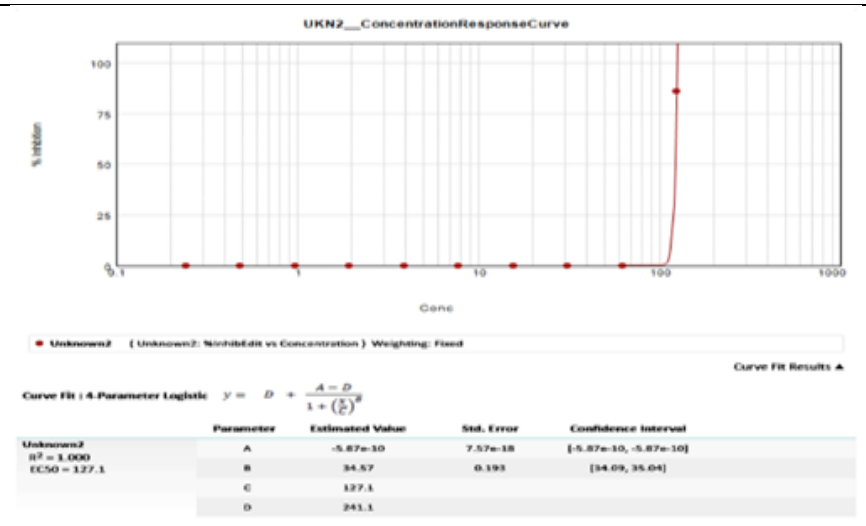
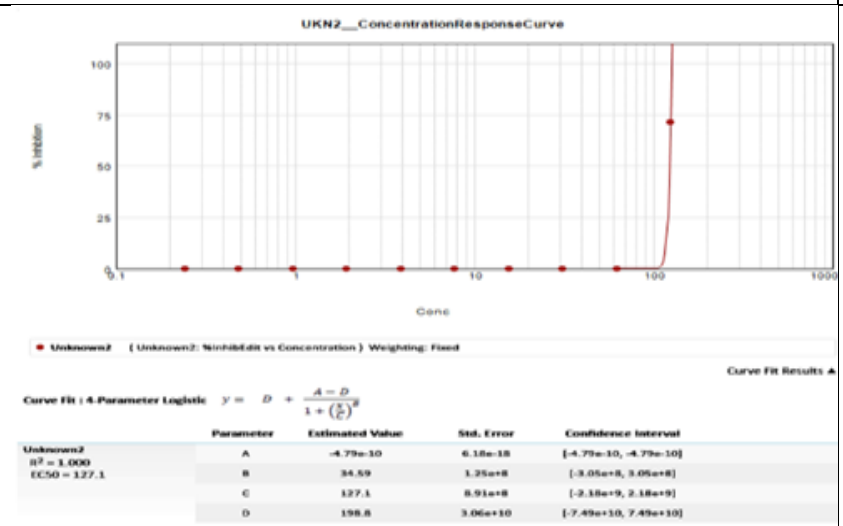
III



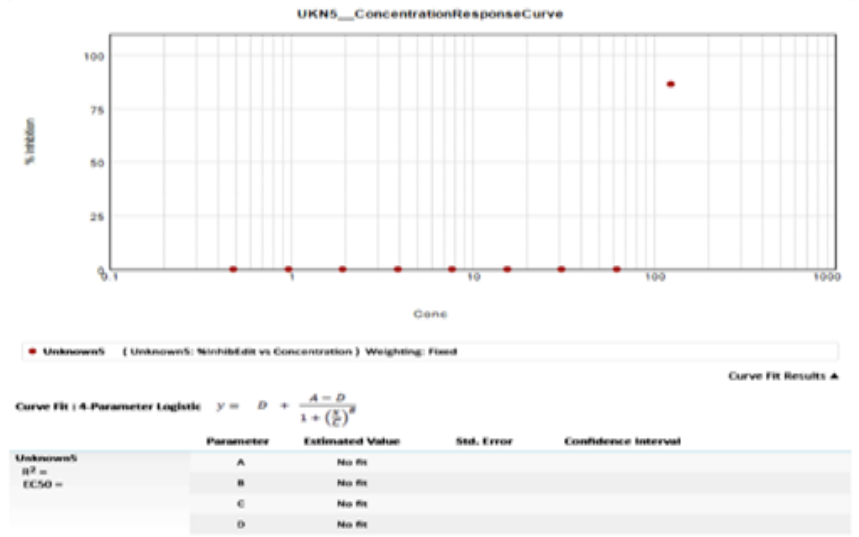
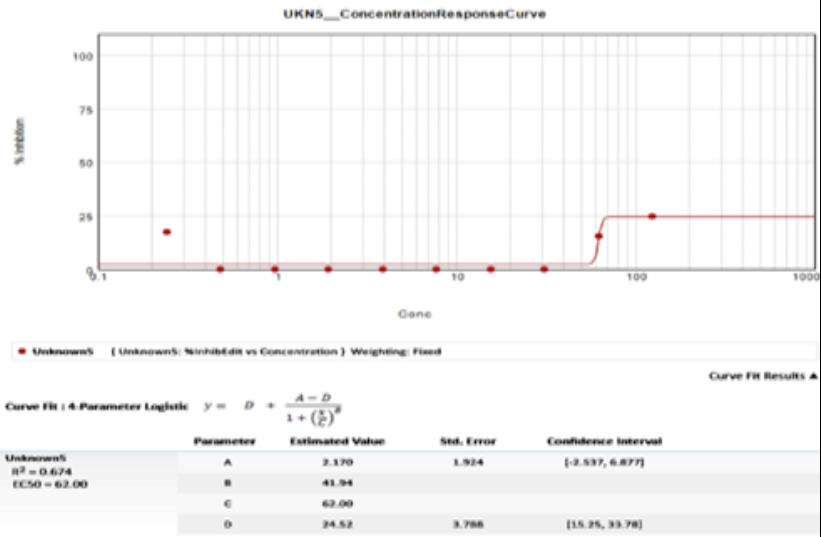
IV



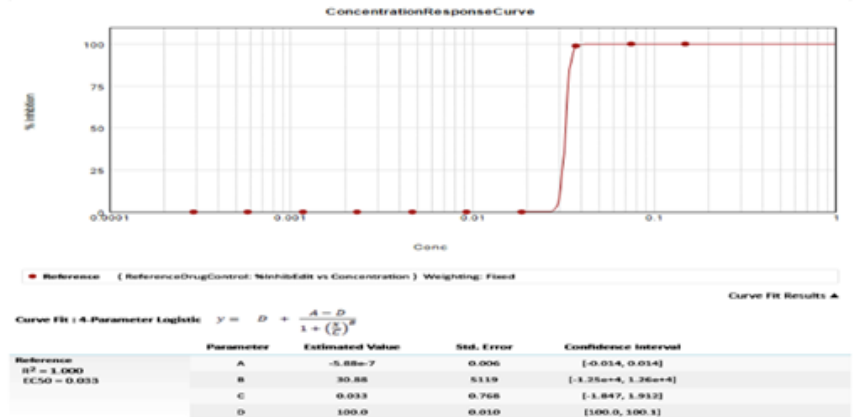
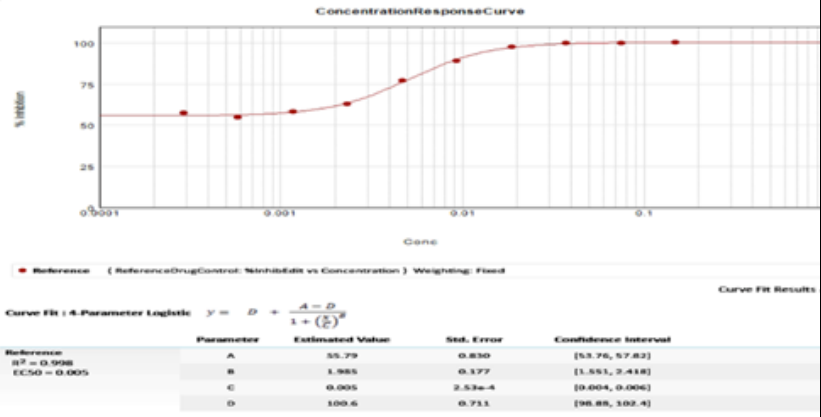
V



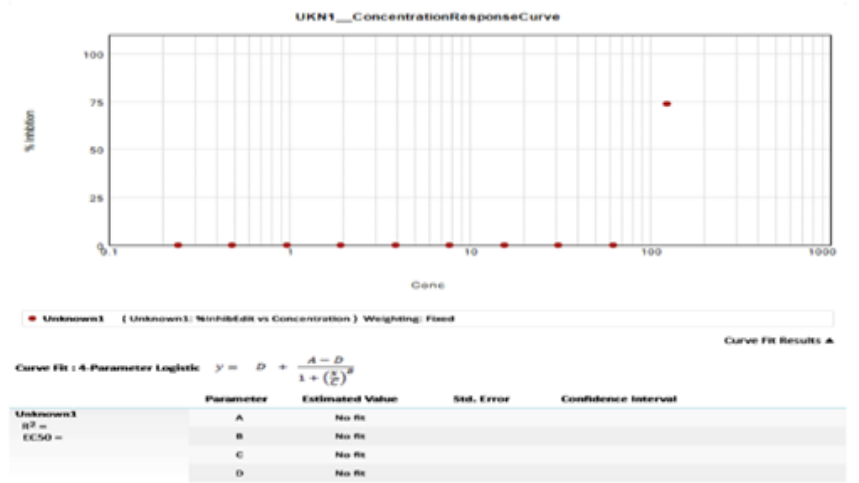
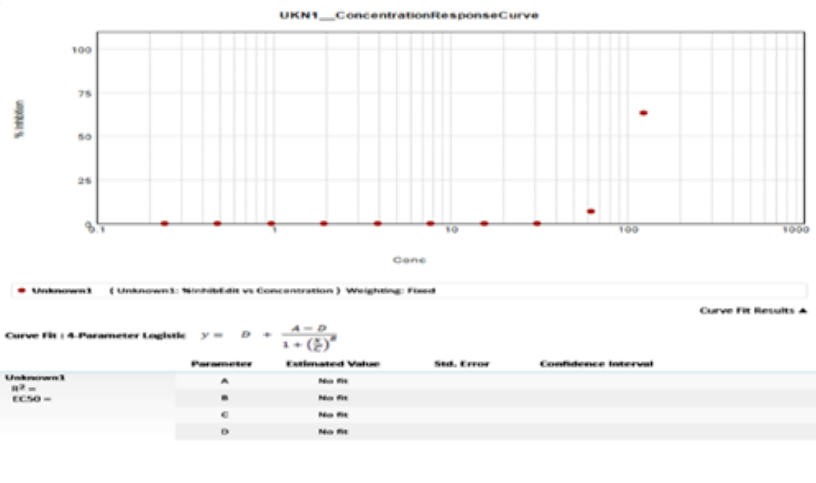
VI & VII



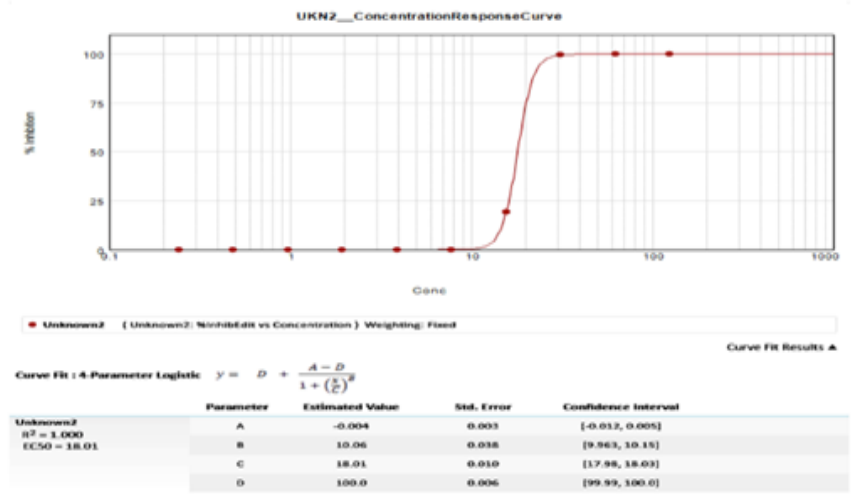
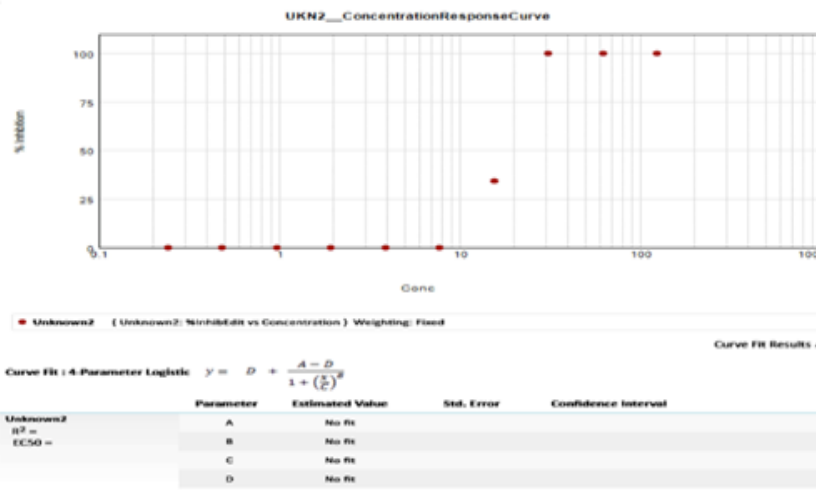
Rifampicin



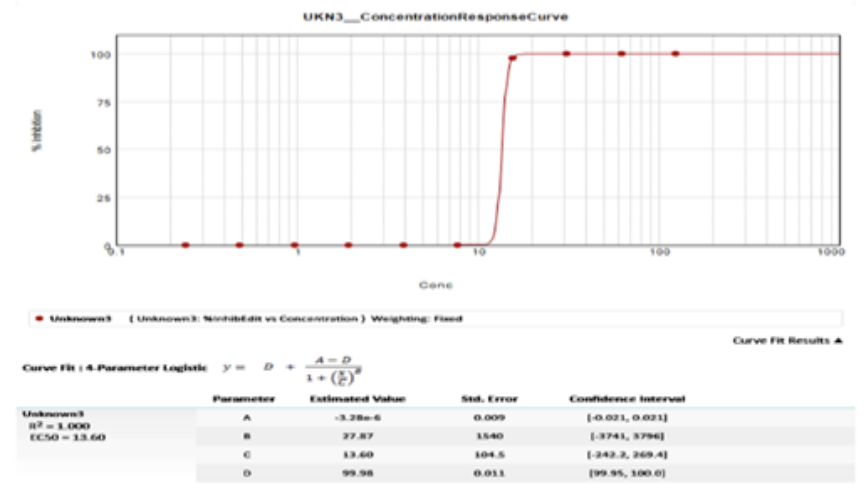
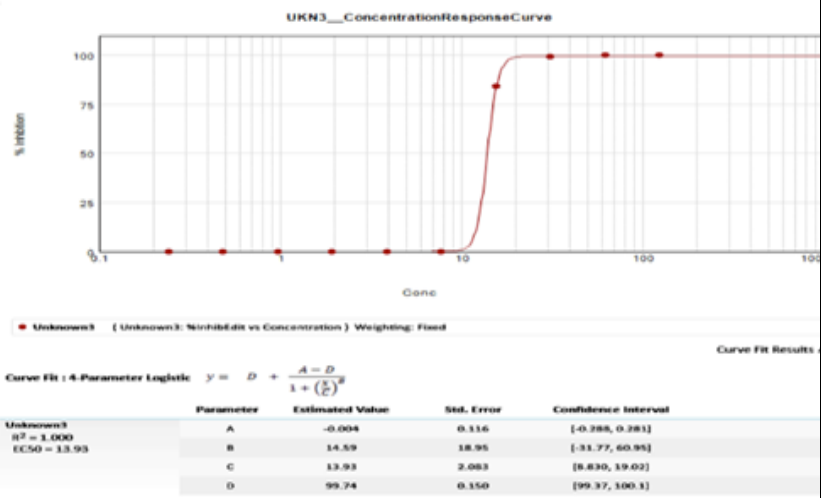
K4-3-III & IV



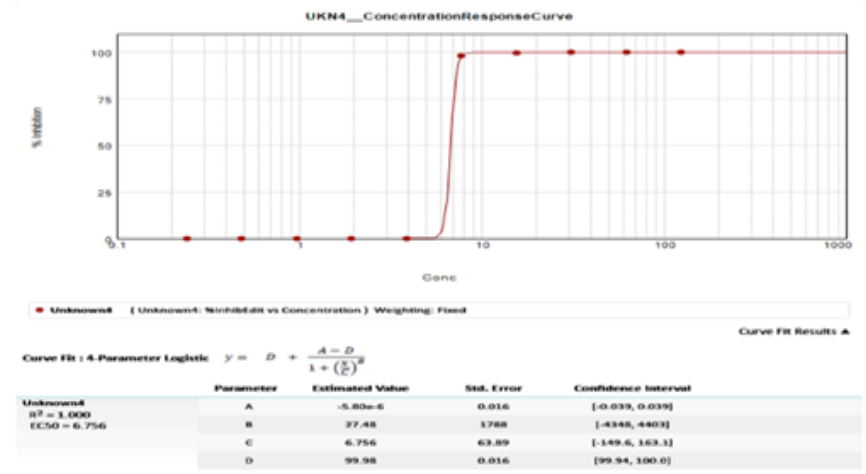
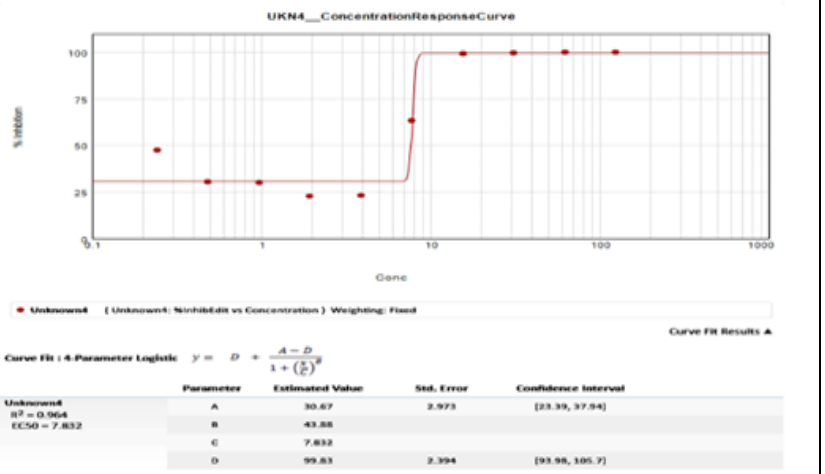
K4-3-VI



K4-3-VIII

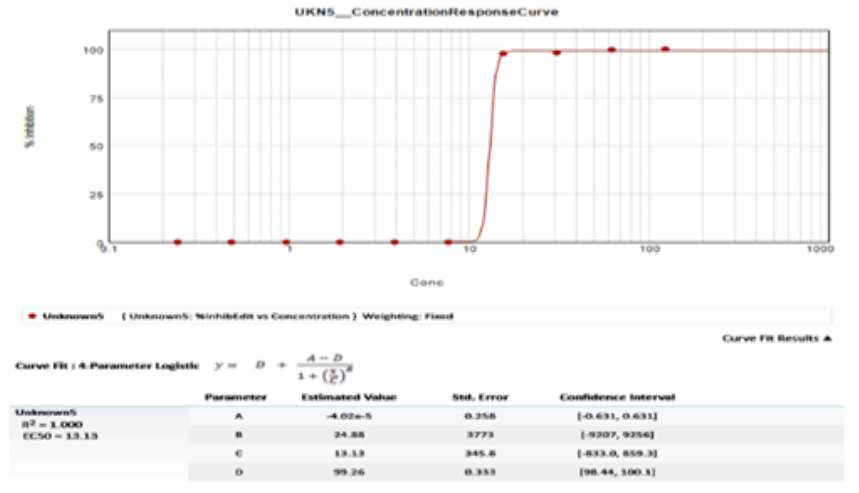
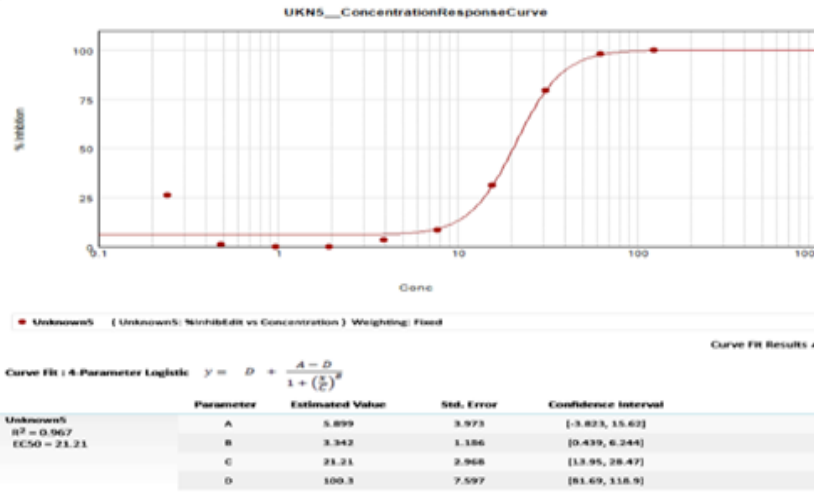


K4-3-XI

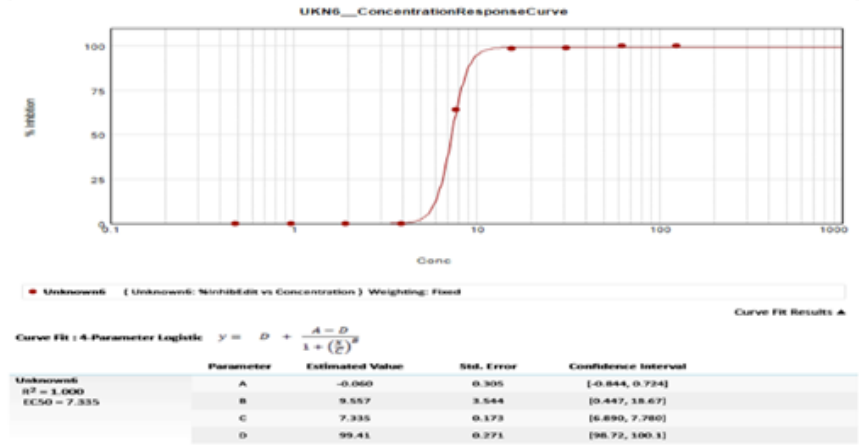
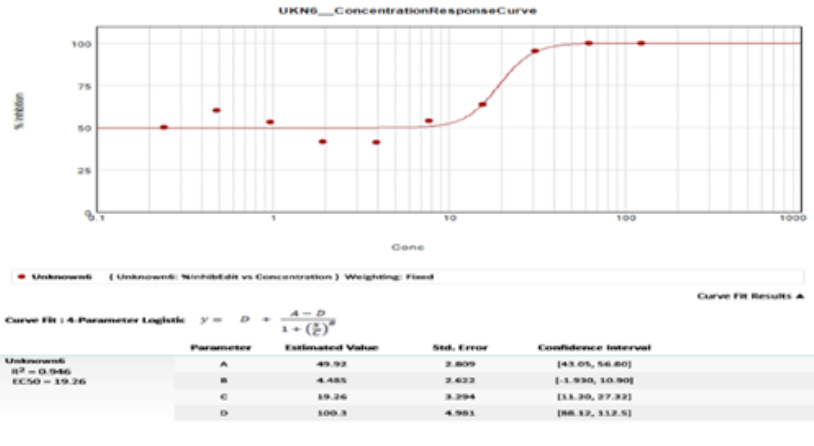


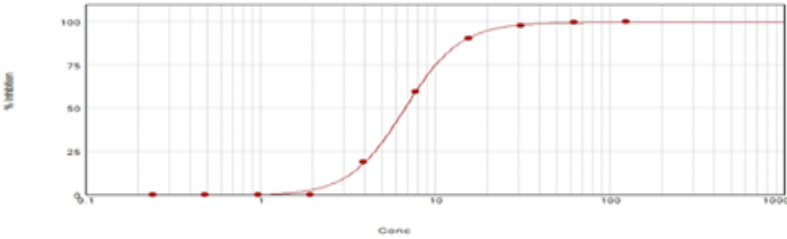
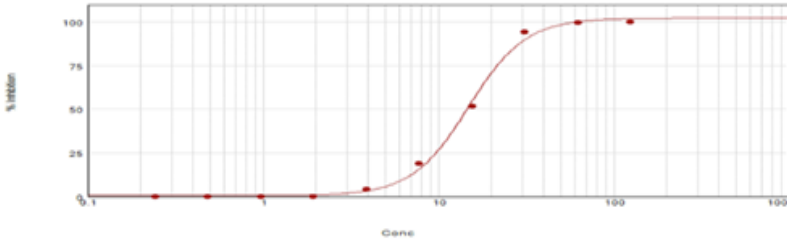
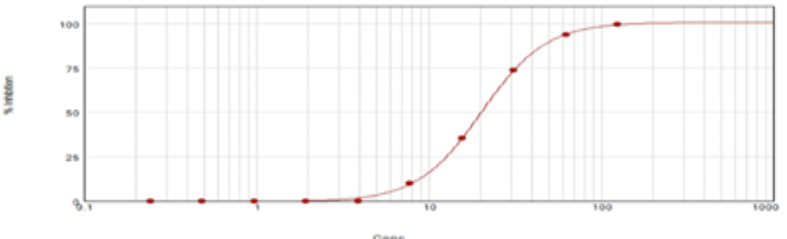
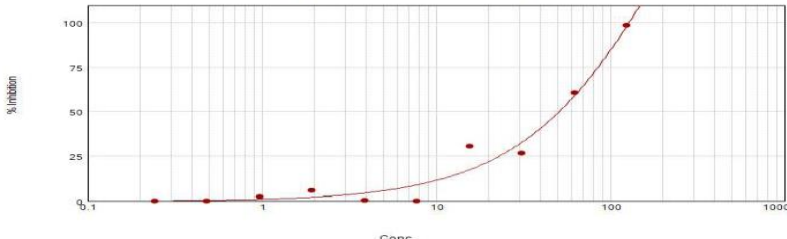


K4-3-XIII & XIV



K4-1-Hex



Compound ID	GFP Assay - 10pt DR: Dose-response Plot [Media: ADC GLU Tw, Day:7]	GFP Assay - 10pt DR: Dose-response Plot [Media: ADC GLU Tw, Day:14]																																																		
II	<p style="text-align: center;">UKN3__ConcentrationResponseCurve</p>  <p style="text-align: center;">Curve Fit Results ▲</p> <p>Curve Fit: 4-Parameter Logistic <math>y = D + \frac{A-D}{1 + (\frac{x}{EC50})^B}</math></p> <table border="1" data-bbox="392 670 1198 758"> <thead> <tr> <th></th> <th>Parameter</th> <th>Estimated Value</th> <th>Std. Error</th> <th>Confidence Interval</th> </tr> </thead> <tbody> <tr> <td>Unknown3</td> <td>A</td> <td>-0.796</td> <td>0.664</td> <td>[-2.421, 0.828]</td> </tr> <tr> <td>R<sup>2</sup> = 1.000</td> <td>B</td> <td>3.739</td> <td>0.118</td> <td>[3.450, 3.028]</td> </tr> <tr> <td>EC50 = 6.706</td> <td>C</td> <td>6.706</td> <td>0.119</td> <td>[6.414, 6.998]</td> </tr> <tr> <td></td> <td>D</td> <td>99.70</td> <td>0.720</td> <td>[97.94, 101.5]</td> </tr> </tbody> </table>		Parameter	Estimated Value	Std. Error	Confidence Interval	Unknown3	A	-0.796	0.664	[-2.421, 0.828]	R <sup>2</sup> = 1.000	B	3.739	0.118	[3.450, 3.028]	EC50 = 6.706	C	6.706	0.119	[6.414, 6.998]		D	99.70	0.720	[97.94, 101.5]	<p style="text-align: center;">UKN3__ConcentrationResponseCurve</p>  <p style="text-align: center;">Curve Fit Results ▲</p> <p>Curve Fit: 4-Parameter Logistic <math>y = D + \frac{A-D}{1 + (\frac{x}{EC50})^B}</math></p> <table border="1" data-bbox="1238 670 2045 758"> <thead> <tr> <th></th> <th>Parameter</th> <th>Estimated Value</th> <th>Std. Error</th> <th>Confidence Interval</th> </tr> </thead> <tbody> <tr> <td>Unknown3</td> <td>A</td> <td>0.409</td> <td>1.288</td> <td>[-2.742, 3.560]</td> </tr> <tr> <td>R<sup>2</sup> = 0.998</td> <td>B</td> <td>2.683</td> <td>0.269</td> <td>[2.025, 3.341]</td> </tr> <tr> <td>EC50 = 14.84</td> <td>C</td> <td>14.84</td> <td>0.610</td> <td>[13.34, 16.33]</td> </tr> <tr> <td></td> <td>D</td> <td>102.3</td> <td>2.121</td> <td>[97.14, 107.5]</td> </tr> </tbody> </table>		Parameter	Estimated Value	Std. Error	Confidence Interval	Unknown3	A	0.409	1.288	[-2.742, 3.560]	R <sup>2</sup> = 0.998	B	2.683	0.269	[2.025, 3.341]	EC50 = 14.84	C	14.84	0.610	[13.34, 16.33]		D	102.3	2.121	[97.14, 107.5]
	Parameter	Estimated Value	Std. Error	Confidence Interval																																																
Unknown3	A	-0.796	0.664	[-2.421, 0.828]																																																
R <sup>2</sup> = 1.000	B	3.739	0.118	[3.450, 3.028]																																																
EC50 = 6.706	C	6.706	0.119	[6.414, 6.998]																																																
	D	99.70	0.720	[97.94, 101.5]																																																
	Parameter	Estimated Value	Std. Error	Confidence Interval																																																
Unknown3	A	0.409	1.288	[-2.742, 3.560]																																																
R <sup>2</sup> = 0.998	B	2.683	0.269	[2.025, 3.341]																																																
EC50 = 14.84	C	14.84	0.610	[13.34, 16.33]																																																
	D	102.3	2.121	[97.14, 107.5]																																																
K4-3-VI	<p style="text-align: center;">UKN2__ConcentrationResponseCurve</p>  <p style="text-align: center;">Curve Fit Results ▲</p> <p>Curve Fit: 4-Parameter Logistic <math>y = D + \frac{A-D}{1 + (\frac{x}{EC50})^B}</math></p> <table border="1" data-bbox="392 1121 1198 1209"> <thead> <tr> <th></th> <th>Parameter</th> <th>Estimated Value</th> <th>Std. Error</th> <th>Confidence Interval</th> </tr> </thead> <tbody> <tr> <td>Unknown2</td> <td>A</td> <td>-0.438</td> <td>0.368</td> <td>[-1.340, 0.463]</td> </tr> <tr> <td>R<sup>2</sup> = 1.000</td> <td>B</td> <td>2.334</td> <td>0.068</td> <td>[2.168, 2.500]</td> </tr> <tr> <td>EC50 = 20.22</td> <td>C</td> <td>20.22</td> <td>0.295</td> <td>[19.50, 20.95]</td> </tr> <tr> <td></td> <td>D</td> <td>101.0</td> <td>0.798</td> <td>[99.00, 102.9]</td> </tr> </tbody> </table>		Parameter	Estimated Value	Std. Error	Confidence Interval	Unknown2	A	-0.438	0.368	[-1.340, 0.463]	R <sup>2</sup> = 1.000	B	2.334	0.068	[2.168, 2.500]	EC50 = 20.22	C	20.22	0.295	[19.50, 20.95]		D	101.0	0.798	[99.00, 102.9]	<p style="text-align: center;">UKN2__ConcentrationResponseCurve</p>  <p style="text-align: center;">Curve Fit Results ▲</p> <p>Curve Fit: 4-Parameter Logistic <math>y = D + \frac{A-D}{1 + (\frac{x}{EC50})^B}</math></p> <table border="1" data-bbox="1238 1121 2045 1209"> <thead> <tr> <th></th> <th>Parameter</th> <th>Estimated Value</th> <th>Std. Error</th> <th>Confidence Interval</th> </tr> </thead> <tbody> <tr> <td>Unknown2</td> <td>A</td> <td>-0.393</td> <td>4.824</td> <td>[-12.20, 11.41]</td> </tr> <tr> <td>R<sup>2</sup> = 0.967</td> <td>B</td> <td>0.990</td> <td>0.560</td> <td>[-0.380, 2.360]</td> </tr> <tr> <td>EC50 = 257.2</td> <td>C</td> <td>257.2</td> <td>862.6</td> <td>[-1854, 2368]</td> </tr> <tr> <td></td> <td>D</td> <td>300.8</td> <td>605.7</td> <td>[-1181, 1783]</td> </tr> </tbody> </table>		Parameter	Estimated Value	Std. Error	Confidence Interval	Unknown2	A	-0.393	4.824	[-12.20, 11.41]	R <sup>2</sup> = 0.967	B	0.990	0.560	[-0.380, 2.360]	EC50 = 257.2	C	257.2	862.6	[-1854, 2368]		D	300.8	605.7	[-1181, 1783]
	Parameter	Estimated Value	Std. Error	Confidence Interval																																																
Unknown2	A	-0.438	0.368	[-1.340, 0.463]																																																
R <sup>2</sup> = 1.000	B	2.334	0.068	[2.168, 2.500]																																																
EC50 = 20.22	C	20.22	0.295	[19.50, 20.95]																																																
	D	101.0	0.798	[99.00, 102.9]																																																
	Parameter	Estimated Value	Std. Error	Confidence Interval																																																
Unknown2	A	-0.393	4.824	[-12.20, 11.41]																																																
R <sup>2</sup> = 0.967	B	0.990	0.560	[-0.380, 2.360]																																																
EC50 = 257.2	C	257.2	862.6	[-1854, 2368]																																																
	D	300.8	605.7	[-1181, 1783]																																																

# Rifampicin

